ENZYMATIC HYDROLYSIS OF CELLULOSE - A KINETIC STUDY

by

Bingham H. Van Dyke, Jr.

B.S., University of Pennsylvania
(1966)

Submitted in Partial Fulfillment

of the Requirements for the

Degree of Doctor of Science

at the

MASSACHUSETTS INSTITUTE OF TECHNOLOGY

September, 1972

Signature of Author _____
Department of Chemical Engineering

Certified by _____
R. F. Baddour, Thesis Supervisor

_____
S. W. Bodman, III, Thesis Supervisor

_____
C. K. Colton, Thesis Supervisor

Accepted by _____
G. C. Williams, Chairman,
Departmental Committee on
Graduate Theses

ABSTRACT

ENZYMATIC HYDROLYSIS OF CELLULOSE - A KINETIC STUDY

by Bingham H. Van Dyke, Jr.

Submitted to the Department of Chemical Engineering in September, 1972, in partial fulfillment of the requirements for the degree of Doctor of Science

Assay procedures were developed to quantify and differentiate among the products of hydrolysis and to determine the concentrations of the different enzymes in solution. A solute exclusion technique to determine the pore structure of water swollen cellulose was studied and developed.

The hydrolysis reaction was not influenced by bulk mass transfer of enzyme to or of carbohydrate from the cellulose particles, provided the particles were suspended in solution. The hydrolysis of wood pulps appeared to be the result of simultaneous reactions of an amorphous and crystalline cellulose fractions. A much less digestible material thought to be a mixture of amorphous and crystalline cellulose inaccessible to the enzyme was observed at extended stages of hydrolysis.

The rate of hydrolysis increased with initial cellulose concentrations until an optimum concentration, C_{opt}, whereupon it decreased. A "dual adsorption" theory was proposed to explain this phenomenon. C_{opt} was dependent on the endoglucanase concentration. The overall rate of hydrolysis was dependent on the C_1 concentration at cellulose concentrations less than or equal to C_{opt}. A kinetic model was developed to predict the hydrolysis reaction as expressed by carbohydrate liberated from the cellulose.

A study of cellulose pore structure indicated that 15% of the pore volume was possibly accessible to a molecule the size of an enzyme molecule. External surface of the particles was 2% of the accessible internal area. Nearly all of the accessible pore area was required for the amount of enzyme adsorption observed.

Thesis Supervisors: Raymond F. Baddour
Professor of Chemical Engineering

Samuel W. Bodman, III
Associate Professor of
Chemical Engineering

Clark K. Colton
Assistant Professor of
Chemical Engineering

Department of Chemical Engineering
Massachusetts Institute of Technology
Cambridge, Massachusetts 02139
September, 1972

Professor David B. Ralston
Secretary of the Faculty
Massachusetts Institute of Technology
Cambridge, Massachusetts 02139

Dear Professor Ralston:

In accordance with the regulations of the Faculty, I herewith submit a thesis, entitled "Enzymatic Hydrolysis of Cellulose - a Kinetic Study," in partial fulfillment of the requirements for the degree of Doctor of Science in Chemical Engineering at the Massachusetts Institute of Technology.

Respectfully submitted,

Bingham H. Van Dyke, Jr.

ACKNOWLEDGEMENTS

The author wishes to express his gratitude to Professor R. F. Baddour for suggesting the topic and for his unselfish financial support. Professor S. W. Bodman provided encouragement when expecially needed and was particularly generous with his time and technical assistance in finalizing the thesis. Professor C. K. Colton was always available for consultation; his technical assistance was very much appreciated.

The author is grateful to Dr. M. C. Molstad of the University of Pennsylvania for his guidence during the author's undergraduate education. His suggestion that the author preceed his graduate education with practical experience was invaluable.

Financial support by the Eastman Kodak Company, the Proctor and Gamble Company, the Dow Chemical Company, and the Department of Chemical engineering, M.I.T. is greatfully acknowledged.

Dr. Mary Mandels of the U.S. Army Research Laboratory, Natick, Massachusetts, was generous with her advice and provided the fungus culture used for enzyme production as well as some of the enzyme used. The polyethylene glycols used in the solute exclusion technique were donated by the Dow Chemical Company. The CMC used in the assays was donated by the Hercules Powder Company.

The author wishes to thank Irenee Dupont, III for his assistance in establishing the laboratory and for his exploratory studies. Philip C. Lewellen was untiring in developing the solute exclusion technique. His mature responsible approach to the project was commendable.

The author is indebted to his parents for their encouragement and especially to his father, who as a chemical engineer himself, was mainly responsible for instilling in the author a sense of professionalism and intuition. Most important of all the author is indebted to his wife, Janice, who truly deserves co-authorship. She not only provided love, inspiration and understanding, but was lab assistant, typist and critic.

TO

JANICE

TABLE OF CONTENTS

LIST OF FIGURES

LIST OF TABLES

I. SUMMARY

A. Introduction

Cellulose is an abundant, annually renewed source of carbon. In industrially developed countries it poses a major waste disposal problem (30, 141). The advantages of changing waste cellulose into a usable raw material are obvious. The process under consideration here is to hydrolyze enzymatically the cellulose to glucose which can be utilized as a high energy human nutrient, as a carbon source for the production of single cell protein (235), or as an industrial raw material.

Much of the research effort to date has been expended in three major areas. The first has been the elucidation of the hydrolytic mechanism and in particular the enzyme complex involved (53, 101, 108, 128, 142, 195, 216, 227). The second area has been to define the accessibility of the cellulose to the enzyme molecules and especially to increase enzyme-cellulose contact (38, 75, 125, 189, 191, 194, 242, 246, 254). The third research effort has been to increase the strength of the enzyme complex (148, 149, 194).

Little previous effort had been expended in elaborating the mass transfer resistances encountered in the diffusion of the enzyme molecule from the bulk solution to the site of hydrolysis. Further, no researcher had con-

clusively proved if the enzyme molecules diffuse into the cellulose pore structure.

Although hydrolysis kinetics have been discussed, especially in regard to the mechanism of enzyme action, no general model existed until now to describe the overall reaction. In fact the order of the reaction with respect to enzyme and cellulose concentrations had not been clearly defined.

Finally, the rate controlling step in the hydrolysis reaction was thought to be proportional to the C_1 concentration. Little data, however, were available to verify this hypothesis. Published hydrolysis data were scarce and in general difficult to use for determining kinetic rate constants.

The purpose of this thesis was four fold: first to elucidate the mass transfer resistances involved in hydrolysis; second to develop a kinetic model for the hydrolysis reaction; third to verify that C_1 is the rate controlling enzyme; and fourth to determine if the enzyme diffuses into the cellulose pore structure. Accomplishment of these objectives required specialized assay procedures and refinement of a solute exclusion technique to study cellulose pore structure.

B. Literature Review

1. Introduction

Cellulose is a linear glucose polymer that is stabilized by interchain and intrachain hydrogen bonds (130). Crystalline cellulose is formed when many cellulose fibrils align themselves into a bundle allowing the maximum number of interchain hydrogen bonds to form. Amorphous cellulose is considered a disruption of this rigid structure. Because the fibrils of amorphous cellulose participate in fewer interchain hydrogen bonds, it is more easily hydrolyzed than crystalline cellulose (177).

2. Enzyme Source

The term cellulase refers to a family of related enzymes that can hydrolyze crystalline cellulose. These enzymes are produced by fermentation of earth fungi which release them into the fermentation broth (148). The enzyme families produced by different fungi can differ in the chemical composition of the individual enzymes, in the specific activity of the enzymes, and in the ratio of their individual concentrations. In addition, the batches can vary from one fermentation to the next. The enzymes used for the following studies were produced by fermentation of Trichoderma viride obtained as a culture from the U.S. Army Research Laboratory, Natick, Massachusetts. The enzyme molecule was assumed to be a prolate ellipsoid 35 Å by 210 Å (272).

3. Enzyme Complex

The enzyme family consists of C_1 , endo- and exo-β-1→4 glucanase, and β-glucosidase enzymes (108). The C_1 is thought to initiate hydrolysis by breaking interchain hydrogen bonds, making the individual cellulose chains more accessible to the actual hydrolysis enzymes, the β-glucanases (227). Endo-β-1→4 glucanase is most active on long cellulose chains having little activity on chains of less than four glucose units. It is thought to bind to a pair of glucose residues and to hydrolyze an adjacent bond (193). Endoglucanase, preferring interior to terminal linkages, hydrolyzes the chain in a random manner and produces the glucose dimer, cellobiose, as its final product.

Exo-β-1→4 glucanase acts by removing the terminal glucose residue from the nonreducing end of the chain. The optumum chain length for exoglucanase action is four or five glucose residues, cellobiose being only 3% as active a substrate as cellotetrose. Endoglucanase is only 2% as active on cellotetrose as exoglucanase and is only 10% as active on cellobiose as is exoglucanase. β-Glucosidase is the enzyme mainly responsible for hydrolyzing cellobiose to glucose. T. viride, the enzyme used in the present hydrolysis studies, porduces little if any β-glucosidase. Both C_1 and endoglucanase must be present for hydrolysis of crystalline cellulose (216).

4. The Relationship of Substrate to Enzyme Action

The fine structure of cellulose greatly influences the rate, extent and uniformity of chemical reactions in which it participates. Accessibility is believed to be the major factor while other structurally related properties such as fiber dimension, crystalline form and hydrogen bonding have lesser effects (169).

Cowling and Brown, (38) have reviewed six structural features of cellulose substrates that directly affect susceptibility to enzyme hydrolysis. These are: (1) the moisture content of the fiber; (2) the size and diffusivity of the enzyme molecules involved in relation to the size and surface properties of the gross capillaries; (3) the degree of crystallinity of the cellulose; (4) the conformation and steric rigidity of the anhydroglucose units; (5) the nature of the substances with which the cellulose is associated.

Moisture swells the fiber, provides a diffusion path for the enzyme and the hydrolysis products, aids in the formation of inter- and intrachain hydrogen bonds and provides an essential reactant (H-OH) that must be added to the cellulose fragments during hydrolysis. The fiber saturation point is a measure of the maximum water content.

The influence of crystallinity on the susceptibility of cellulose to enzymatic hydrolysis has been studied by Norkans (172), Walseth (265) and Reese et al. (199). Some

enzymes, including the ones used in the present study, degrade amorphous cellulose faster than crystalline cellulose, while others degrade both at the same rate. The rate of hydrolysis in this latter situation is probably controlled by the rate at which the enzyme can gain access to the cellulose molecules rather than by intrinsic kinetics which are dependent on the type of cellulose present.

The internal matrix of the cellulose particles is also a major factor in the hydrolysis mechanism. The enzyme must have access to the cellulose molecules. If the initial pores are too small the enzyme will be confined to the gross capillaries which account for only 0.03% of the available surface (38). Pulping and acid swelling increase the average pore size, thus improving accessibility.

Data by Selby presented in the discussion of Ranby (189) indicated that the hydrolysis of cotton was first order with respect to cellulose concentration for the initial 35% of hydrolysis. At later stages of hydrolysis the rate was slower than that predicted by a first order approximation. Ranby rebutted these data by stating that in the hydrolysis by acid, 10% of the cellulose was hydrolyzed much more rapidly than the remaining material. Similar behavior was reported by Cowling and Brown (38) for the enzymatic hydrolysis of wood. The data of Ghose (74, 75) on Solka Floc seemed to indicate a very rapid initial hydrolysis followed by a slower rate. These data, and the

work of Norkans and Walseth who found that the crystallinity index increases with reaction, form one of the main hypotheses of the kinetic model discussed later.

Studies in agitated vessels showed significantly faster hydrolysis than comparable studies in test tubes. This indicated the possibility that the overall kinetics might be limited by the bulk mass transfer of the enzyme to or of the reaction products from the particles.

C. Assay Procedures

Assay procedures were developed to quantify and differentiate among the products of reaction, long chain polyglucose fragments, cellobiose and glucose, and to determine the concentrations of the different enzymes in solution. The procedures were designed to facilitate concurrent determinations on numerous samples. In addition the enzyme assay procedures based in part on those of Mandels and Weber (148) closely duplicated the actual temperature and pH of the hydrolysis studies. All of the procedures ultimately required a spectrophotometric analysis, yielding a measured optical density (O.D.).

1. Products of Reaction

The phenol sulfuric acid technique developed by Dubois et al. (45) and modified by Reese (93) was chosen for determination of all soluble carbohydrate. PSOD, the result-

ing optical density, was translated into PCARB, the carbohydrate concentration, by means of a standard curve. The Glucostat procedure of Worthington Biochemical Corporation (78) was modified to determine concentrations of glucose and cellobiose (a glucose dimer).

Samples were also incubated with buffered solutions of β-glucosidase to hydrolyze cellobiose to glucose to yield a "total" carbohydrate optical density (TCOD); TCARB was the sum of the cellobiose and glucose concentrations. The optical density from hydrolyzed cellobiose was an order of magnitude greater than that from unconverted cellobiose.

2. Enzyme Assays

Enzyme activity was measured as the production of cellobiose and glucose (TCARB) by the enzyme in the sample during incubation with various substrates at pH 4.9 and 50°C. The incubation period, 30 or 60 min, was short and the enzyme concentration dilute to minimize effects caused by extensive substrate hydrolysis. Optical densities determined on the samples after incubation were corrected for the carbohydrate initially present by blanks based on concurrent TCARB determinations.

C_1 activity (FPACT) measured the ability of the enzyme to hydrolyze crystalline cellulose. Filter paper was chosen as a substrate because it is as nearly susceptible as the sulfite pulps actually employed in the hydrolysis

studies (148). Endoglucanase activity (ENACT) measured the ability to hydrolyze soluble cellulose. Carboxymethylcellulose (CMC), a substituted cellulose derivative, was chosen as a substrate because of its solubility and susceptibility to hydrolysis by endoglucanase.

A method for determining protein concentration in solution was employed as a check on the enzyme assays. The technique of Lowry et al. (139) was chosen because of its sensitivity. The method suffered one serious disadvantage; carbohydrate interfered with the analysis, enhancing the measured optical density. A series of standard curves at increasing carbohydrate concentrations was produced to correct for this effect.

D. Experimental Apparatus and Procedure

1. Apparatus

The hydrolysis apparatus consisted of a stirred tank reactor, a constant speed agitator and a temperature bath. Peripheral equipment consisted of sampling apparatus, reagent addition equipment, a water bath and a spectrophotometer.

The reactor was a 200 ml pyrex jar covered with a plexiglas top. Two standpipes were fitted in the top to furnish access for the propeller shaft and for a sample port. Samples were removed from the reactor with a modified pipet and filtered to remove cellulose. The filtrates

were collected, covered, and set aside for later assay.

Samples (0.1 ml) were withdrawn from every filtrate for each different assay. This was accomplished with a BBL pipetor equipped with disposable tips. Reagents were added with Cornwall syringes. These were supplied with check valves and rubber hoses for continuous operation.

2. Procedure

The cellulose employed for the hydrolysis studies was a ball milled Spruce wood pulp, Solka Floc BW-300 obtained from Brown Company, Berlin, New Hampshire. The cellulose was swollen overnight in 0.05 M, pH 4.9 phosphate buffer (hereafter referred to as buffer). The enzyme was a Trichoderma viride fermentation broth.

Dry cellulose was weighed into a reactor and the desired amount of buffer added. After complete mixing the baffles and propeller were added and the cover screwed tight. After standing overnight the reactor was placed in a constant temperature water bath and the agitator adjusted to the desired RPM. At time zero enzyme was added to the reactor through the sample standpipe. Figure 6-1 is a schematic treatment of the reactor samples.

E. Results and Discussion

A series of hydrolysis studies was employed to elucidate the kinetic resistances in order to model the hydrol-

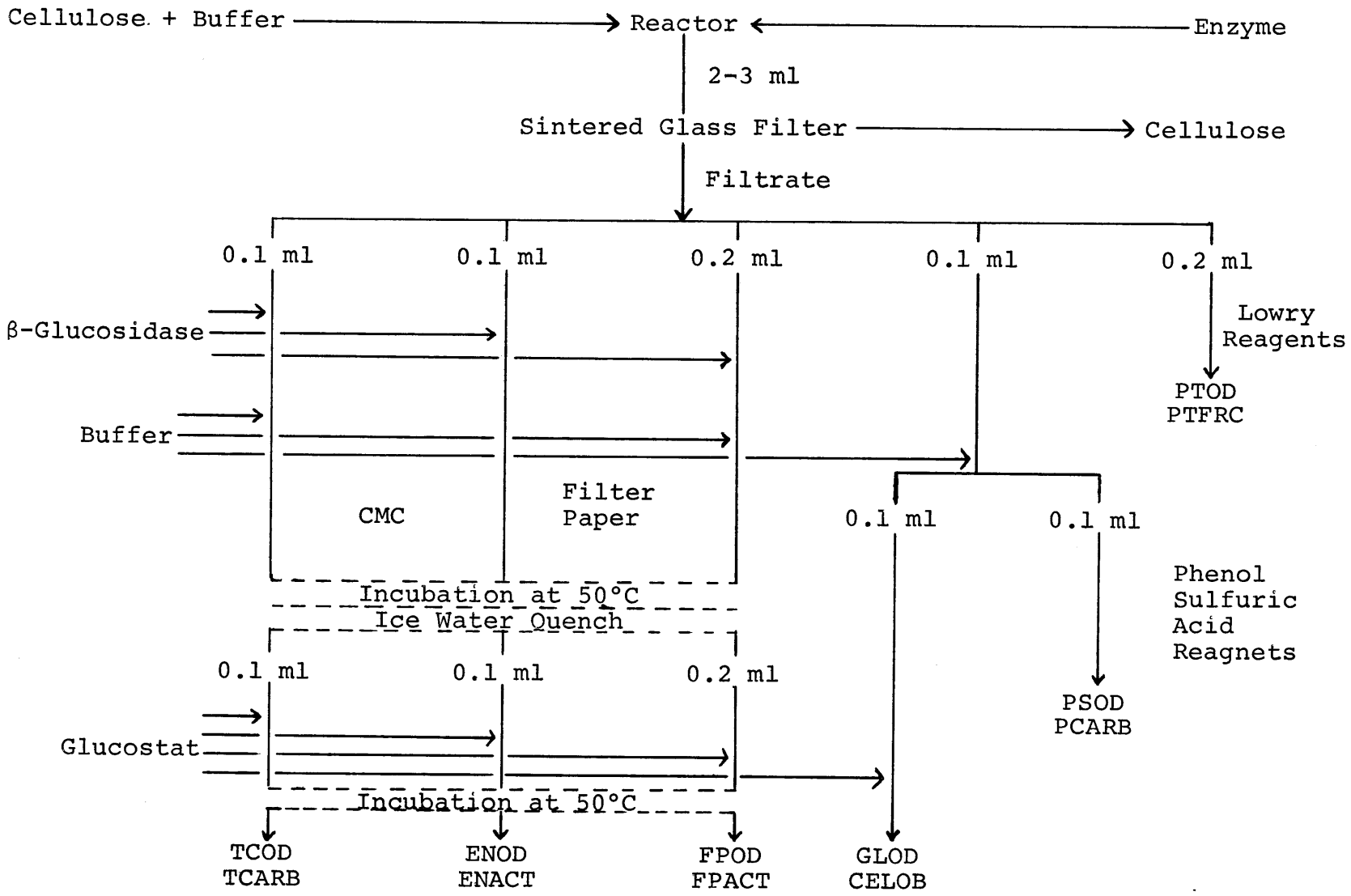

Figure 6-1. Schematic Diagram of Sample Analysis

ysis reaction. Agitator speed and substrate and enzyme concentrations were the primary variables.

The enzyme concentration was quantified as "adsorbable protein" since "total" protein included material that would not adsorb. Cellulose concentration was in weight per cent (1 wt% is equivalent to 10 mg/ml cellulose or 11 mg/ml equivalent glucose). During most of the runs the reaction was maintained at 51°C, the optimum as determined by Ghose (75).

1. Bulk Mass Transfer Studies

The purpose of the first series of hydrolysis runs was to determine the magnitude of the bulk mass transfer resistance. As can be seen from Figure 7-2, agitation intensity appeared to have little or no effect on the hydrolysis provided the particles were suspended. The minimum RPM to suspend 8 wt% cellulose with the geometry employed was 100, corresponding to a Reynolds number of 1200. The Reynolds number corresponding to transition from a laminar to a turbulent flow pattern for a three-bladed propeller in a baffled reactor is 1000 (154). Since this geometry is similar to that employed in the hydrolysis studies, 200 RPM (N_{Re} = 2400) is, therefore, close to the minimum turbulent agitator speed and well within the range of commercial Reynolds numbers (100 - 20,000).

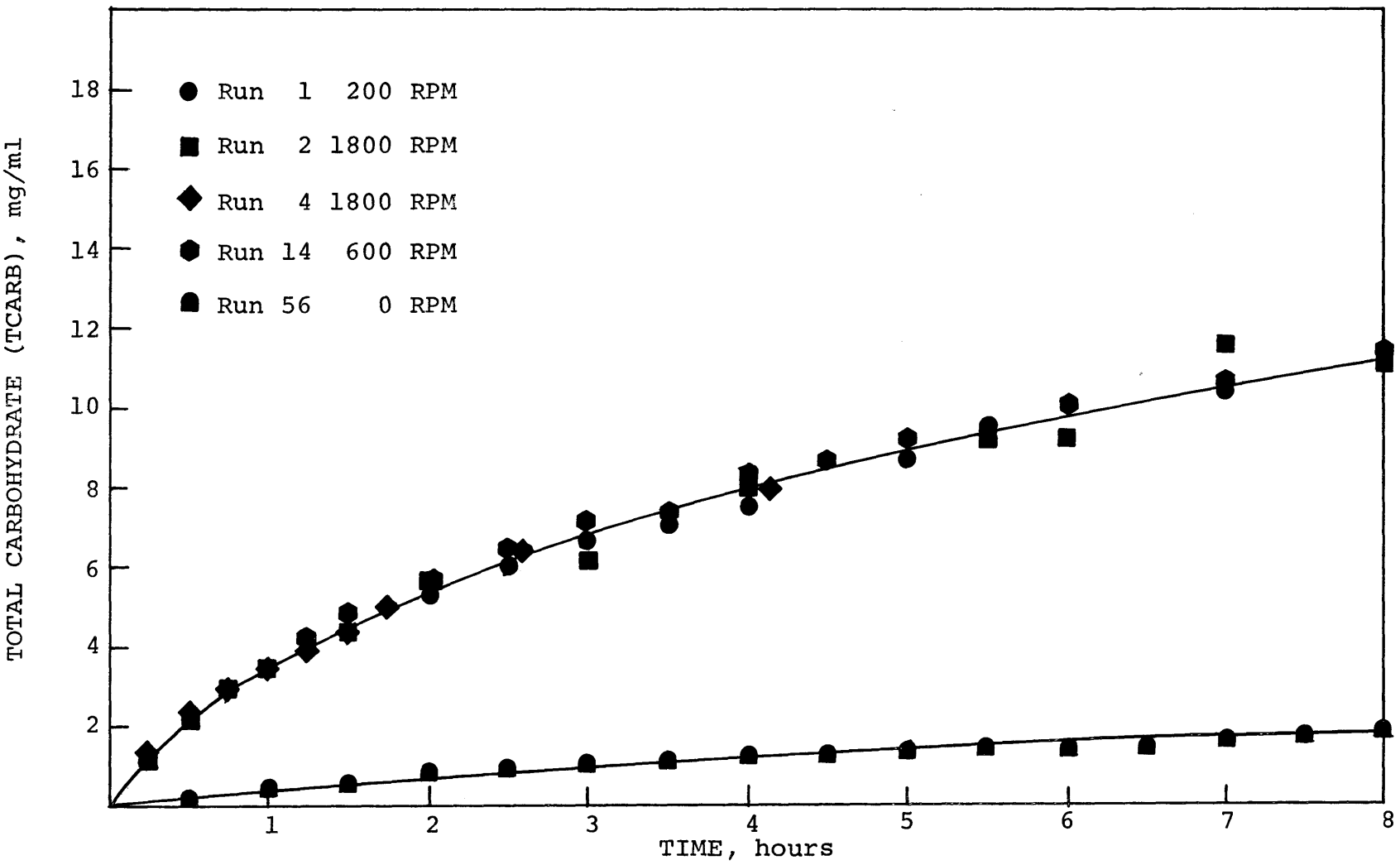

Figure 7-2. Effect of Agitation on Hydrolysis

It should be noted that the data sets shown in Figure 7-2 were taken over a time span of six weeks. The near superposition of the data points is indicative of the high level of reproducibility found during the present study.

2. The Effect of Enzyme and Substrate Concentration

The effect of varying the enzyme concentration for a fixed cellulose concentration is presented in Figures 7-3 and 7-4. The enzyme was diluted with buffer to obtain the different concentrations. A reaction time curve with a rapid initial rate followed by a nearly constant rate may be indicative of a two component reaction in which one component is more reactive than the other. The "constant" rate plateau appears to occur when the more reactive species is exhausted and is usually proportional to the quantity of resistant reactant remaining.

The carbohydrate (PCARB) production curves were indicative of this multi-substrate behavior. The nearly constant rate plateaus in Figure 7-3 evidenced by Runs 14 and 15 occurred after all of the easily hydrolyzed amorphous cellulose had been reacted. The plateaus resulted from hydrolysis of resistant crystalline cellulose. Extrapolation to the zero time axis yielded carbohydrate production curves (dashed lines) that would have resulted had there been no amorphous cellulose. The intercept (2.8 mg/ml or 3.2 wt%) gave the carbohydrate resulting from the rapid

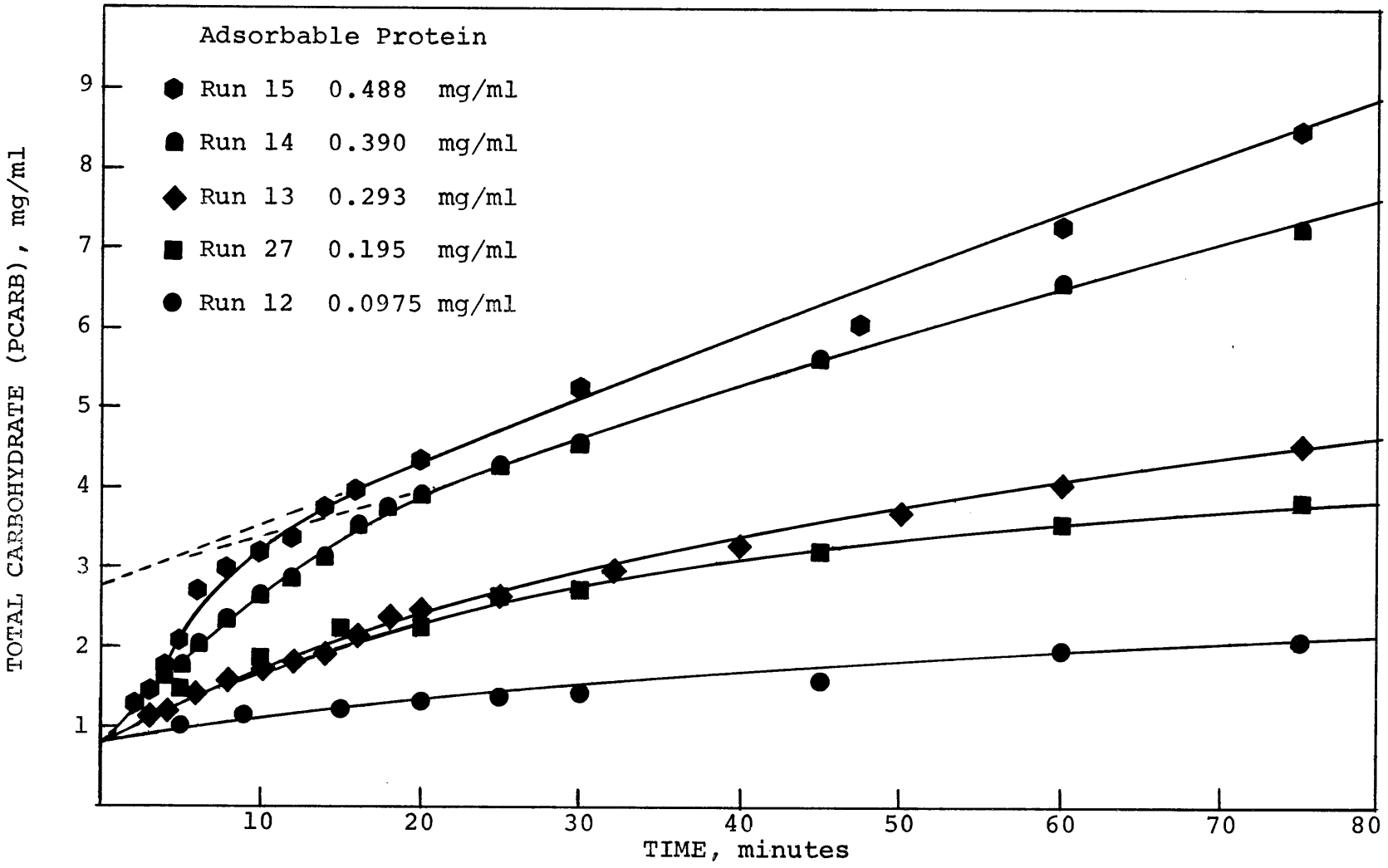

Figure 7-3. Production of Total Soluble Carbohydrate - Short Term

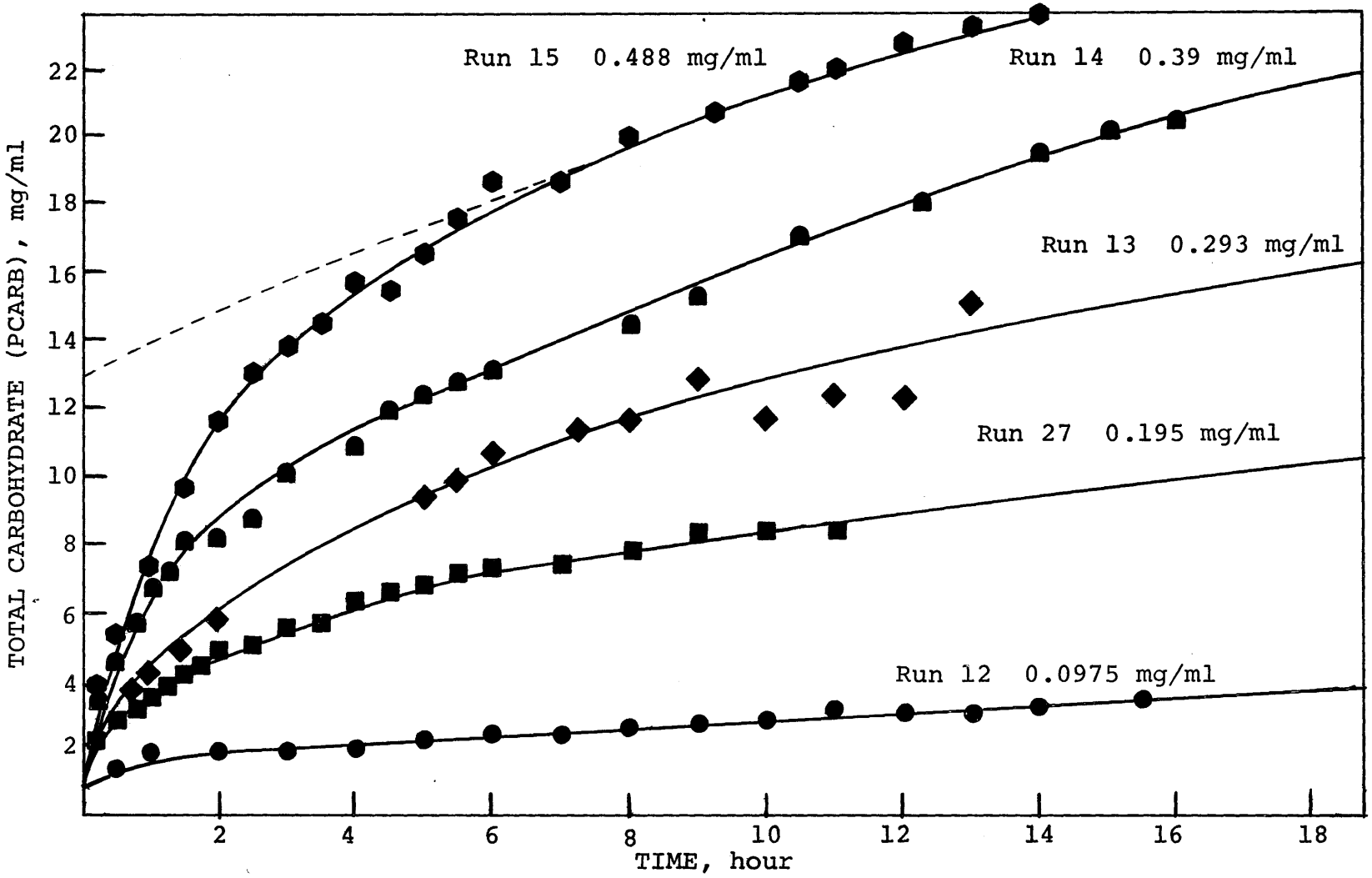

Figure 7-4. Production of Total Carbohydrate - Moderate Time

hydrolysis of amorphous cellulose. Since PCARB was not zero at zero time, part of this easily hydrolyzed cellulose must have been initially soluble. This cellulose, C_a (0.8 mg/ml or 0.91 wt%), was probably moderate length cellulose chains (5<DP<200) fragmented during milling. The other portion (2.0 mg/ml or 2.28 wt%) was considered insoluble amorphous cellulose, C_b .

The resistant material could probably have been considered one substrate. The Run 15 curve in Figure 7-4 however, showed a change in curvature at 6 to 8 hours. The resistant material was consequently subdivided into crystalline cellulose, C_c , and inaccessible cellulose, C_d .

The present study suggests that the cellulose particle may be considered a spheroid. A fairly porous casing of amorphous and crystalline cellulose surrounds a highly crystalline core containing few, if any, pores large enough to admit an enzyme molecule. The casing is much more accessible to the enzyme than is the core; thus, it is hydrolyzed first. Since the enzyme has access to cellulose molecules in the casing, the rate of carbohydrate production is proportional to the intrinsic kinetics of the hydrolysis of the amorphous and crystalline fractions. Although the core could contain amorphous cellulose, the overall kinetics are probably limited by the rate at which enzyme molecules can gain access to new cellulose chains rather than by the

hydrolysis itself.

The observed rate coefficient k_d was calculated from the data for Run 15 at 10 hours. Integration of the rate expression (equation 1-3) permitted determination of C_d at time zero (75.2 mg/ml or 85.4 wt% of the initial cellulose). This in turn permitted computation of C_c (10.0 mg/ml or 11.4 wt%) since the other three fractions and the initial cellulose concentration were then established. Calculation of C_d, and hence C_c, was based on Run 15. This was the only experiment to have hydrolyzed completely the accessible amorphous and crystalline fractions during the time period studied without so reducing the surface that enzyme diffused back into the bulk solution.

The major assumptions in the above argument are supported by the latter sections of the Literature Review. Ghose's data tend to support the present findings that Solka Floc contains amorphous and crystalline cellulose. The work of Norkans and Walseth supports the hypothesis of a crystalline core. The inaccessible nature of the core is supported by the small fraction of pore volume accessible to an enzyme molecule (see F. Diffusion of Enzyme into the Cellulose). The absence of a rapid initial rate occurring with Selby's data is understandable when one realizes that cotton has a median pore diameter one-half that of wood pulp (38). The rapid initial rate

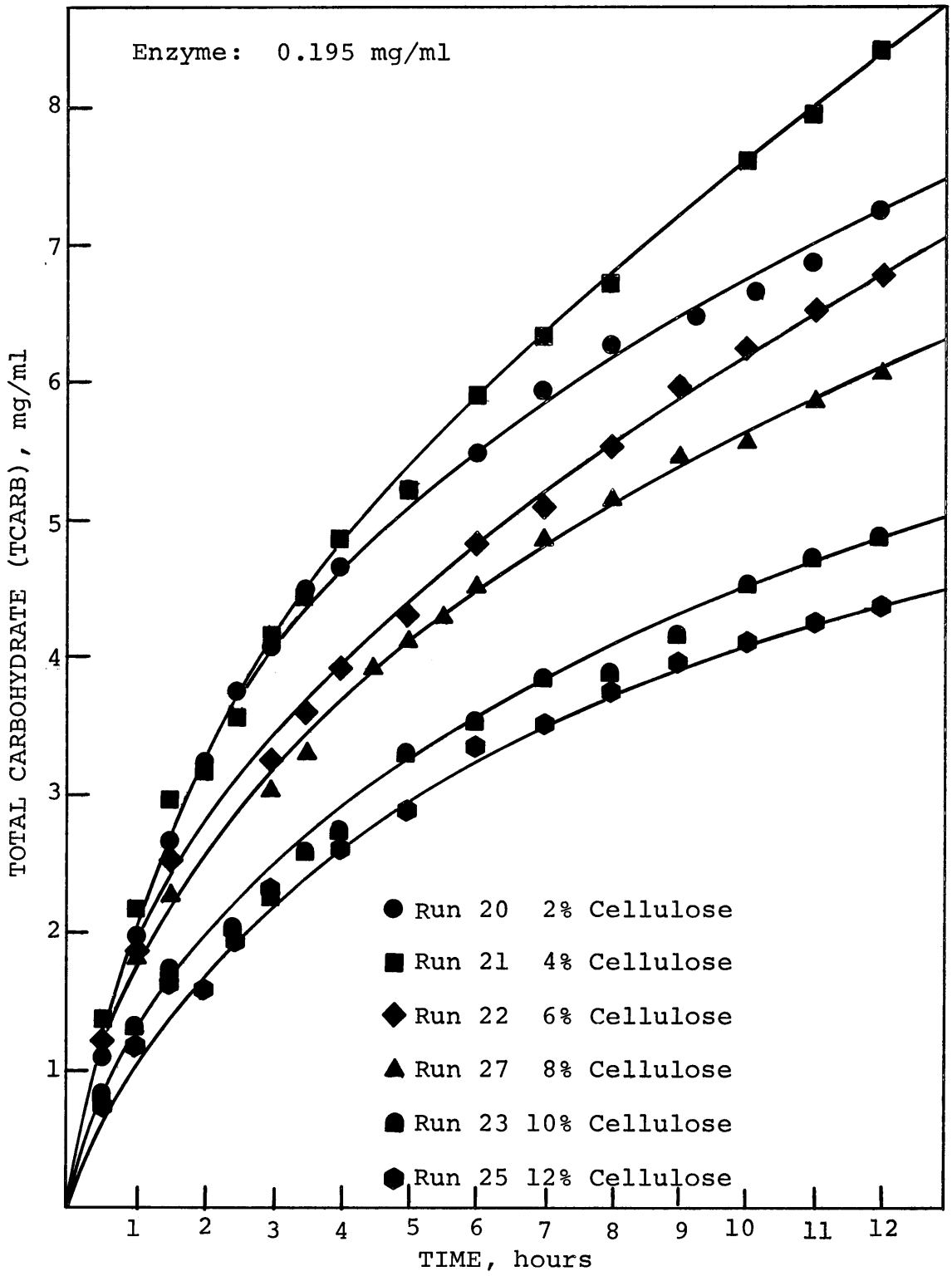

Figure 7-10. Effect of Initial Cellulose Concentration

is absent because most of the amorphous cellulose is inaccessible to the enzyme.

The rate of carbohydrate production was expected to increase with an increase in initial cellulose, C_o , until all of the enzyme was adsorbed and participating in hydrolysis. At this point further increase in C_o was not expected to effect the rate of hydrolysis. TCARB was chosen to portray this effect because initilaly there is no cellobiose or glucose present , whereas the varying $PCARB_o$ values would obscure the effect. The results differed significantly from those expected. As can be seen in Figure 7-10 the rate of hydrolysis did increase as the cellulose increased from 2 wt% to 4 wt%. The rate of hydrolysis then decreased as C_o was increased. Similar behavior was exhibited for other enzyme concentrations.

The optimum cellulose concentration, C_{opt} , was defined as that C_o yielding the maximum hydrolysis for a given enzyme concentration. The cellulose concentration is given as weight per cent of the total solution because it is the dimension most often found in the literature and to differentiate it from C , the glucose equivalent of the cellulose concentration (mg/ml). C_{opt} , plotted as a function of the enzyme concentration in Figure 8-2, can be expressed

$$C_{opt} = 14.1[E] \qquad (1\text{-}1)$$

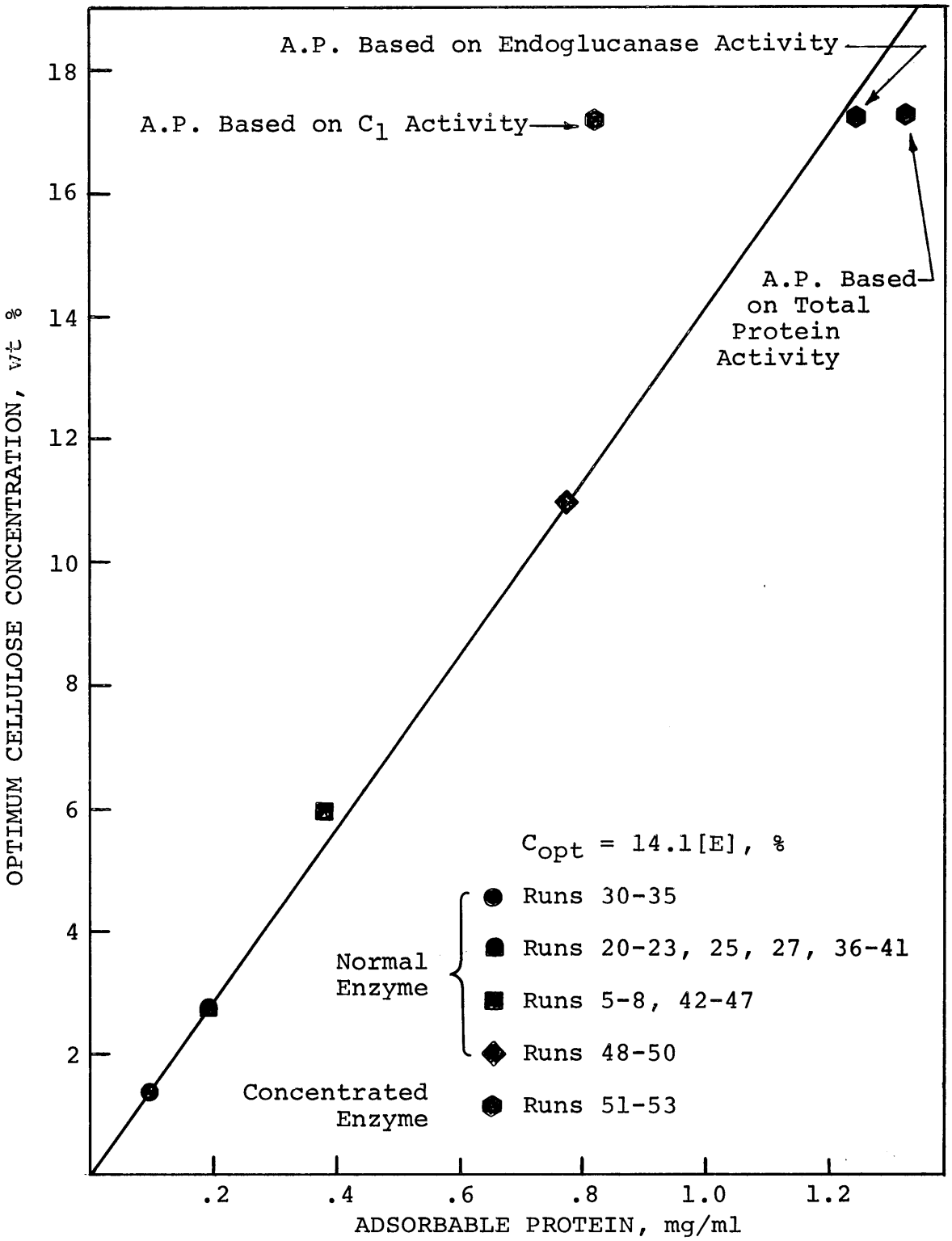

Figure 8-2. Optimum Cellulose Concentration

where [E] is the adsorbable enzyme protein (mg/ml). The data up to and including [E] of 0.78 mg/ml were obtained with the normal enzyme mixture (see section D, Experimental Apparatus and Procedure).

A special batch of enzyme was prepared which was more concentrated than the enzyme used during most of this study. This allowed extension of equation (1-1) to high enzyme levels. The concentrated T. viride enzyme was obtained from Dr. Mary Mandels of the U.S. Army Research Laboratory, Natick, Massachusetts. This was originally a fermentation broth similar to that used for most of the hydrolysis studies. It was concentrated by passage through an ultrafiltration unit that deactivated some of the endoglucanase and nearly one-half of the C_1 . The concentrate, therefore, had a ratio of C_1 : endoglucanase : total protein different from the standard T. viride mixture. This difference in enzyme adtivities between the standard enzyme and the concentrated batch was important in determining which enzyme governed the optimum cellulose concentration.

Since the maximum stirrable cellulose concentration was 20 wt%, the concentrated enzyme was diluted 1:2 with buffer so that the expected optimum cellulose concentration would be below 20 wt%. This dilution gave a protein, endoglucanase activity, and C_1 activity of 1.7, 1.6, and 1.05 times the corresponding values of the normal enzyme mixture used in most of the studies. The optimum cellulose concen-

tration for the diluted concentrate was 17.2 wt%. Multiplication of adsorbable protein value of the standard mixture by the various activity ratios resulted in abscissa values of 0.82 mg/ml, 1.25 mg/ml, or 1.33 mg/ml based on C_1 activity, endoglucanase activity, or total protein respectively. It is evident from Figure 8-2 that the abscissa value based on comparative endoglucanase activity yields the best correlation.

The "adsorbable protein" calculated from the total protein ratio above assumed that 64% of the concentrate's total protein was adsorbable. Since some of the special enzyme was deactivated during concentration, the adsorbable protein of the concentrate was probably less than that of the standard mixture although this was not substantiated by data.

An intellectually more satisfying hypothesis for C_{opt} would be, therefore, that it corresponds to complete saturation of the cellulose surface by the enzyme molecules. C_{opt} would provide the maximum surface concentration of the enzyme. It would, therefore, be preferable to consider C_{opt} proportional to adsorbable protein rather than to the endoglucanase concentration.

The effective enzyme concentration on the surface can be expressed as a dimensionless group, θ , the enzyme adsorbed per unit cellulose

$$\theta = \frac{[E]}{10.0\ C_o} \tag{1-2}$$

At the optimum cellulose concentration this group would be

$$\theta_{opt} = \frac{[E]}{10.0\ C_{opt}} = 0.0071 \tag{1-3}$$

A similar θ group could be formed for any adsorbing system. A θ_{opt} probably exists for other enzyme-cellulose systems, and possibly even for noncellulosic systems. It should be pointed out that this group is similar to catalyst loading factors employed with heterogeneous catalysis.

3. Development of the Kinetic Expression

A kinetic expression was developed to relate the initial enzyme and cellulose concentration to the observed rate coefficient, k_i , and hence to the intrinsic kinetic constant, k_i^* . The model was based on the division of the substrate into the four fractions, i . The carbohydrate produced, PCARB, was assumed to be the sum of that resulting from the hydrolysis of each fraction. The hydrolysis of each substrate was considered first order with respect to the amount of that material remaining according to

$$-\frac{dC_i}{dt} = k_i C_i \tag{1-4}$$

The composite hydrolysis expression was then

$$-\frac{dC}{dt} = \frac{dPCARB}{dt} = \Sigma k_i C_i \qquad (1\text{-}5)$$

Since the rate of hydrolysis appeared to depend on the initial concentration of enzyme and cellulose, the observed rate coefficient in equation (1-5) was assumed

$$k_i = k_i^* [E]^{\sigma} C_o^{\rho_i} \qquad (1\text{-}6)$$

These units (mg/ml enzyme, and per cent cellulose) were again chosen because of their prevalence in the literature.

The observed rate coefficients were determined from the instantaneous slopes of the hydrolysis curves by equation (1-4). (The cellulose remaining was the difference between the initial cellulose and PCARB.) The data from Runs 20-23, 25 and 27, given in Table 8-1, were used to determine the effect of the initial cellulose concentration on the observed rate coefficient shown in Figure 8-3. The slopes of the curves are the exponents ρ_i (also given in Table 8-1).

The effect of C_o on k_i is both physical and apparent. The physical effect exhibited by a decrease in the rate of hydrolysis is caused by a decrease in θ as C_o is increased above C_{opt}. The apparent effect is noticed with the observed rate coefficient, but not with the hydrol-

TABLE 8-1. FIRST ORDER KINETIC RATE CONSTANTS

Run	C_o	[E] mg/ml	k_b hr^{-1}	k_c hr^{-1}	k_d hr^{-1}
Opt A	8	0.566	7.35	0.675	0.0140
12	8	0.0975	0.55	0.049	
27	8	0.195	1.49	0.136	
13	8	0.293	2.9	0.26	
14	8	0.390	4.35	0.39	
15	8	0.488	6.25	0.55	0.01125
Opt B	2.75	0.195	4.50	1.45	
21	4	0.195	2.90	0.63	
22	6	0.195	2.13	0.25	
27	8	0.195	1.49	0.136	
23	10	0.195	1.21	0.088	
25	12	0.195	1.07	0.059	

Intrinsic Rate Constants, k_i^* :

$k_b^* = 144\ (mg/ml)^{-1.5} hr^{-1}$ $\quad \rho_b = -1.0$

$k_c^* = 102\ (mg/ml)^{-1.5} hr^{-1}$ $\quad \rho_c = -2.5$

$k_d^* = 2.1\ (mg/ml)^{-1.5} hr^{-1}$ $\quad \rho_d = -2.5$

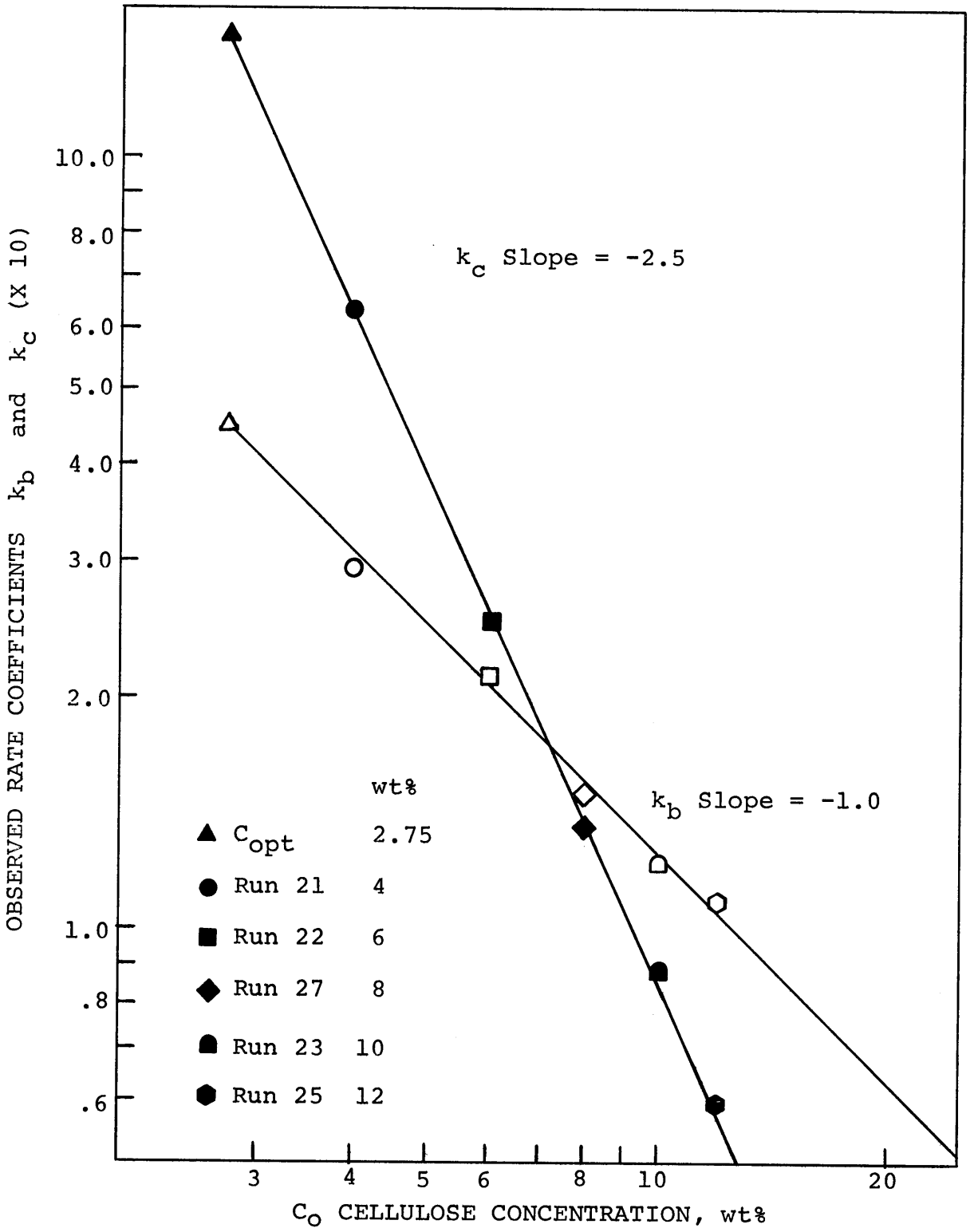

Figure 8-3. Effect of Initial Cellulose Concentration on Rate Coefficients

ysis rate itself. From the difinition of the observed coefficient (see equation 1-4), and since C_{i_o} is proportional to C_o, k_i would have to be inversely proportional to C_o for the reaction rate to remain unaffected. This apparent effect can be eliminated by normalizing C_i

$$- \frac{dC}{dt} = k_i \frac{C_i}{C_o} \qquad (1\text{-}7)$$

where C_i/C_o is proportional to the fraction of C_i remaining.

Assuming that the rate of hydrolysis requires concurrent action on the same chain by an endoglucanase molecule and a C_1 molecule (a hypothesis supported by the literature), a "dual adsorption" theory provides a possible explanation. (Note that C_1 is considered a hydrogenbondase (227). It is thought to break interchain hydrogen bonds, thus increasing the ability of the chain to orient to the endoglucanase molecule which causes the actual hydrolysis or chain scission. All of the hydrogen bonds of a fragment must be broken for the fragment to diffuse into solution.) Surface in excess of that proportional to C_{opt} would decrease the effective enzyme concentration on the surface thus decreasing θ. Since θ is a measure of the probability of an endoglucanase - C_1 interaction, a decrease in θ would decrease the overall rate of reaction.

As hydrolysis proceeds the overall hydrolysis is in-

fluenced by two opposing phenomena. The reacting species C_i decreases directly reducing the hydrolysis rate. The total surface also decreases, thus increasing θ and thereby tending to increase the rate. The effective surface is proportional to all of the cellulose present, mainly C_d, which hydrolyzes much more slowly than C_b and C_c. The concentrations of amorphous and crystalline cellulose thus decrease faster than θ increases. The overall rate, therefore, appears to decrease. At extended hydrolysis ($C = C_d$) it is possible that the effects could cancel or that the rate could increase. When C is less than C_{opt} the surface is saturated and θ becomes equal to θ_{sat} which should be independent of further reduction in surface.

As can be seen in Figure 8-3 C_o has a much greater influence on k_c than on k_b. Since the apparent effect can be considered proportional to C_o^{-1} from equation (1-7), the decrease in k_b is apparent, not physical. The physical effect of C_o on k_c, however, is proportional to $C_o^{-1.5}$. The hydrolysis of amorphous cellulose, therefore, appears relatively independent of θ, being proportional to the total enzyme adsorbed and to the C_b remaining. The hydrolysis of crystalline cellulose, on the other hand, is very much dependent on θ. The difference in θ dependence is reasonable because amorphous cellulose has fewer interchain hydrogen bonds than crystalline cellulose. The release of an amorphous chain should require

fewer C_1 - endoglucanase interactions than a similar length crystalline chain, and the hydrolysis of C_b should be less dependent on θ than C_c .

The next step in refining the kinetic model was to determine the effect of [E] on the apparent rate coefficient. Figure 8-4, a logarithmic plot of k_i versus [E], was constructed from the data for Runs 12-15 and 27. The curves can be expressed

$$k_i \alpha [E]^{\sigma} \tag{1-8}$$

where σ (=1.5) is the slope of the curves. Since the function f(E) is the same for both b and c , amorphous and crystalline celluloses are probably hydrolyzed by the same mechanism.

Incorporating the effects of [E] and C_o , the complete expression for the observed rate coefficient is therefore

$$k_i = k_i * [E]^{1.5} C_o^{\rho i} \tag{1-9}$$

The hydrolysis of each component is

$$\text{Hydrolysis Rate} = \begin{bmatrix}\text{Intrinsic} \\ \text{Rate} \\ \text{Constant}\end{bmatrix} \begin{bmatrix}\text{Effective} \\ \text{Enzyme} \\ \text{Conc.}\end{bmatrix} \begin{bmatrix}\text{Fraction} \\ C_i \\ \text{Remaining}\end{bmatrix} \tag{1-10}$$

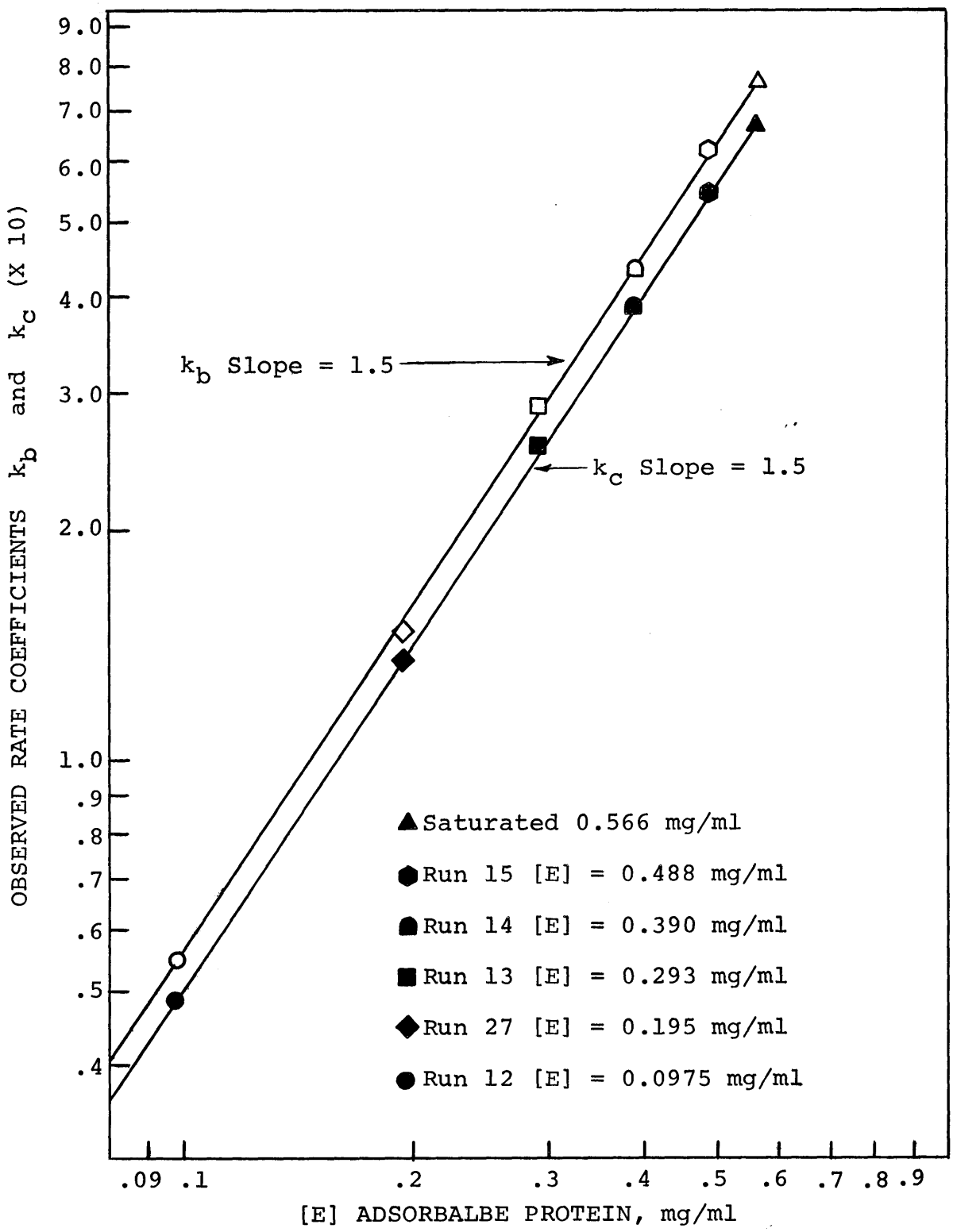

Figure 8-4. Effect of Enzyme Concentration

$$- \frac{dC_b}{dt} = k_b * [E]^{1.5} \frac{C_b}{C_o} \qquad (1\text{-}11)$$

$$- \frac{dC_c}{dt} = k_c * \left(\frac{[E]}{C_o}\right)^{1.5} \frac{C_c}{C_o} \qquad (1\text{-}12)$$

$$- \frac{dC_d}{dt} = k_d * \left(\frac{[E]}{C_o}\right)^{1.5} \frac{C_d}{C_o} \qquad (1\text{-}13)$$

The complete rate equation is

$$- \frac{dC}{dt} = \frac{dPCARB}{dt} = - \sum_{i=b}^{d} \frac{dC_i}{dt} \qquad (1\text{-}14)$$

$$= - \sum_{i=b}^{d} k_i * [E]^{1.5} \, C_o^{\rho_i} \, C_i \qquad (1\text{-}15)$$

Note that the form of equation (1-13) was assumed from the similarity of C_d with C_c. Substitution of θ for $[E]/(10C_o)$ results in

$$- \frac{dC_c}{dt} = k_c * (10\theta)^{1.5} \frac{C_c}{C_o} \qquad (1\text{-}16)$$

$$- \frac{dC_d}{dt} = k_d * (10\theta)^{1.5} \frac{C_d}{C_o} \qquad (1\text{-}17)$$

The hydrolysis of crystalline cellulose is, therefore, proportional to the (enzyme per unit cellulose)$^{1.5}$ and to the crystalline cellulose concentration. An enzyme exponent

of unity would have been indicative of monatomic reaction; an exponent of two would have indicated a diatomic (enzyme-enzyme) interaction. A power of 1.5 is somewhere in between; i.e., one C_1 interaction with two endoglucanase molecules could possibly liberate two soluble fragments.

The intrinsic rate coefficient k_i^* is a composite of surface diffusion of the enzyme molecules and a true intrinsic constant. These equations (1-8 to 1-17) hold only as long as C is greater than C_{opt} so that all of the enzyme is adsorbed and participating in hydrolysis. When C is less than C_{opt} there will be insufficient surface for total enzyme adsorption. The enzyme initially participating in the reaction can be calculated from equations (1-1) and (1-2). As hydrolysis proceeds the enzyme participating in hydrolysis becomes limited by the available surface. Assuming that the enzyme loading factor θ is constant at saturation, equation (1-17) becomes

$$- \frac{dC}{dt} = k_d^*(10\theta)^{1.5} C_d^{\,n} \qquad (1\text{-}18)$$

where n is the order of the reaction. Data for the later stage of Runs 15 and 20 indicated that n = 0.78. An n of 0.67 would imply that the reacting cellulose was on the external surface of a decreasing sphere rather than throughout the sphere (n=1.0)

The data for Runs 14 and 15 are presented along with

the curves predicted by equation (1-15) in Figure 8-6. The equation tends to predict slightly high values in the initial stages of hydrolysis because it assumes hydrolysis of all three substrates (C_b , C_c , and C_d) from time zero. In reality there is probably a slight time lag that the equation does not consider; this time lag is evident in Figures 7-3 and 7-5.

Total carbohydrate production both measured and predicted by equation (1-15) and solution enzyme concentrations are plotted in Figure 8-7. Protein appears to adsorb much faster than enzyme activity decreases. This is caused by adsorption to soluble long chain fragments. The enzyme adsorbed on these fragments can still participate in hydrolysis and, hence, show activity. In this adsorbed state, however, the enzyme protein can not react with the Lowry reagent to yield protein optical density. As these fragments are hydrolyzed the enzyme adsorbs onto the solid cellulose particle.

At high enzyme concentrations the external surface of these particles is rapidly saturated forcing the remaining unadsorbed enzyme to diffuse into the pore structure to find surface on which to adsorb. The restricted diffusion into the "pores" is much slower than adsorption onto the surface as is evidenced by the slow reduction in enzyme activity shown in Figure 8-7. This behavior is only evident at high enzyme concentrations. Adsorption of enzyme

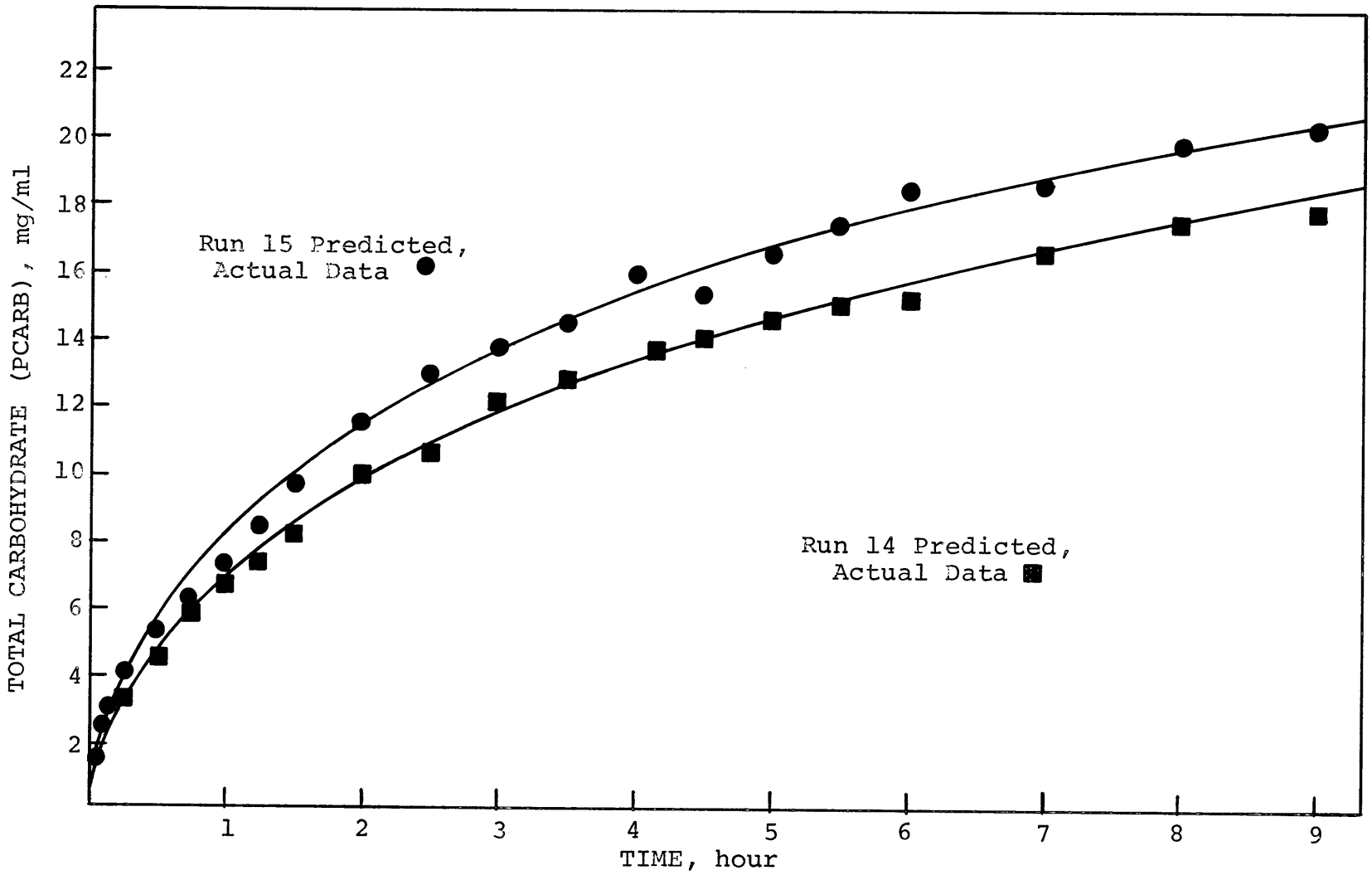

Figure 8-6. Comparison of Actual and Predicted Data

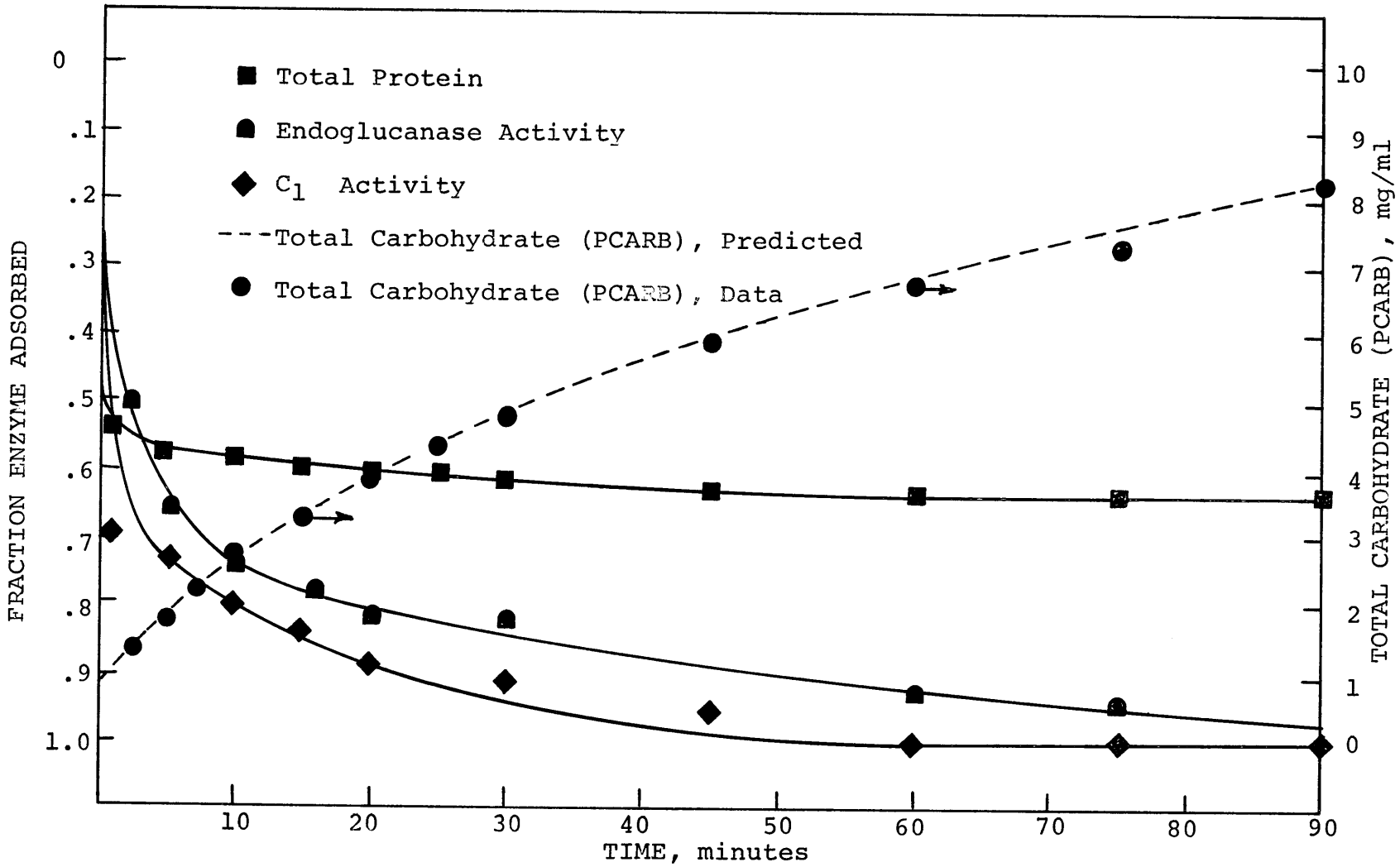

Figure 8-7. Reaction Progress Curves, Run 14

onto the external surface and onto the surface of the gross capillaries near the external surface is nearly instantaneous as long as this surface is in excess of that required for complete enzyme adsorption.

4. Evidence that C_1 is the Rate Controlling Enzyme

Development of the kinetic model and review of the hydrolysis studies have provided some evidence that C_1 is the rate controlling enzyme. As mentioned previously a special concentrated batch of T. viride enzyme was used for some of the hydrolysis studies (Runs 11, 51-53). Run 11 employed the concentrate diluted with buffer to allow comparison of the hydrolytic action of the concentrate as compared with runs employing various dilutions of the mixture. Since the rate of reaction is proportional to $[E]^{1.5}$, the hydrolysis of Run 11 should be predicted by the kinetic model with suitably chosen values of $[E]$.

The predicted behavior based on the C_1 and endoglucanase enzyme activities is presented in Figure 8-8 by the solid and dashed lines respectively. The C_1 activity yielded a much better prediction than did the endoglucanase activity. The kinetic model based on C_1 activity tended to underpredict the initial hydrolysis of amorphous cellulose, but not nearly as much as the model based on endoglucanase overpredicted hydrolysis. The amorphous cellulose C_b, therefore, requires some C_1 enzyme for hydrol-

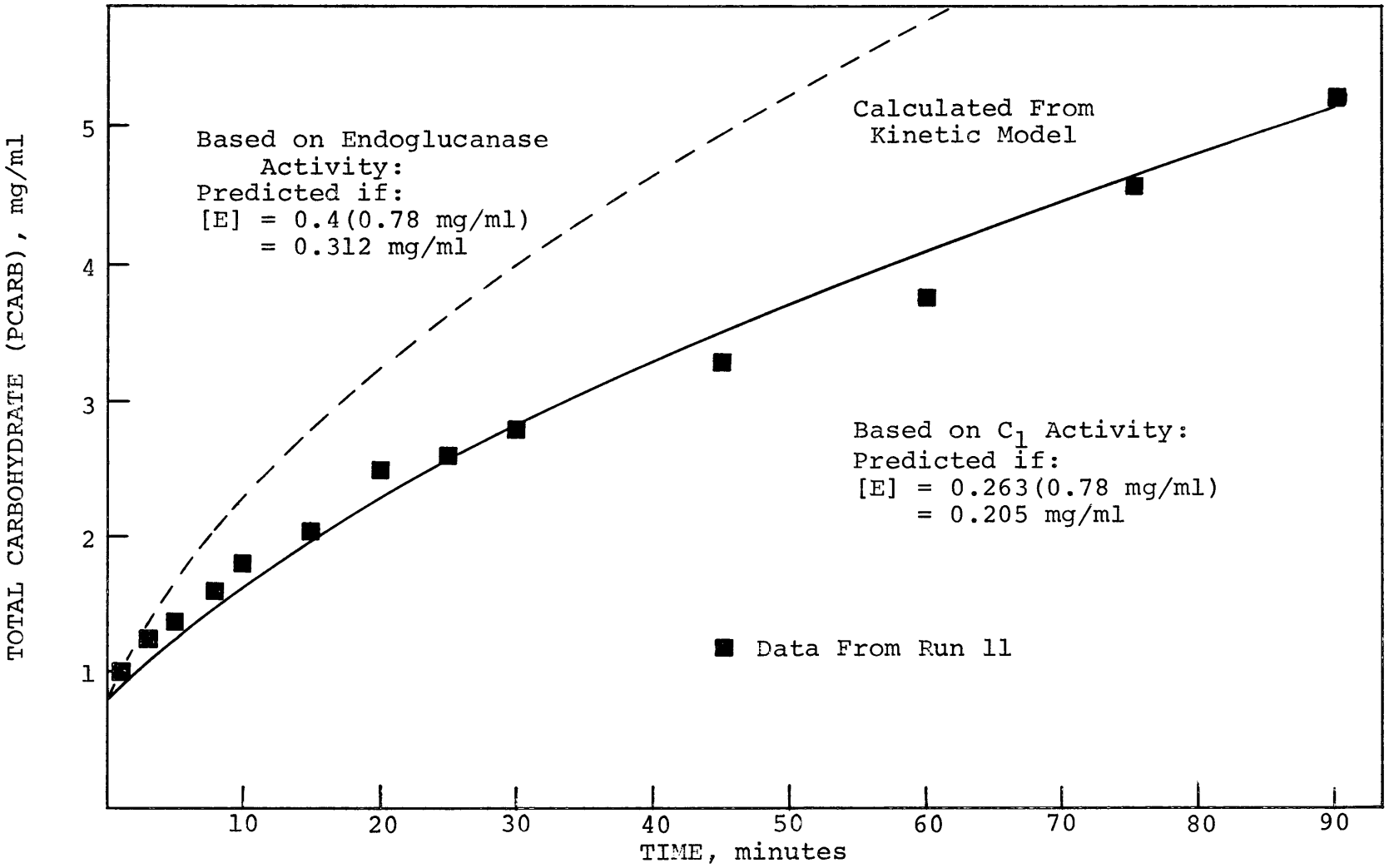

Figure 8-8. Verification That C_1 is the Rate Controlling Enzyme

ysis although it is not as dependent on C_1 as is the hydrolysis of cellulose C_c .

The initial time lag shown in Figure 7-3 is often observed in enzyme reactions requiring sequential action of two different enzymes (44). This further supports the hypothesis that the action of the enzyme complex is initiated by the C_1 enzyme providing a point of attachment for the glucanase enzymes, endoglucanase in particular.

F. Diffusion of Enzyme into the Cellulose

1. General

A solute exclusion technique was studied and developed into a procedure for investigating the porous structure of materials in an aqueous environment, specifically the cellulose employed in the hydrolysis studies. A similar technique was employed by Stone et al. (238-242) and Tarkow et al. (254,255) to obtain pore size distribution of water swollen cellulosic materials. Nelson and Oliver (169) employed the technique to characterize acetic acid swollen cellulose. None of the researchers, however, presented a clearly defined experimental procedure complete with caveats.

The technique is based on measuring the concentration change in a solution of macromolecular "probes" before and after addition to porous particles. A sequence of probe molecules of increasing molecular weights can be used to

develop a cumulative pore volume curve. Such a curve is a plot of "inaccessible water" versus probe molecular weight. Inaccessible water is a measure of the volume of pores inaccessible to the probe molecule. When no further increase in inaccessible water occurs with increasing probe molecular weight, the fiber saturation point has been reached. This is therefore the total water adsorbed by the particles. Accessible water is the difference between the fiber saturation point and the inaccessible water. It can be employed with an assumption of pore shape to compute the relative pore area accessible to the corresponding molecular probe. The calculations of the actual pore dimensions are relative to the molecular probes and are not definitive.

2. Results

A series of dextran and of polyethylene glycol molecules were employed to determine the pore volume distribution of the Solka Floc used in the hydrolysis studies. The results have been plotted in Figure 9-1.

The results of the dextran series were not used for further calculations because the shape of the dextran molecule in solution is very much in doubt. It is possible that it is a rod shaped molecule that increases in length with molecular weight. This would explain the relatively constant values obtained with the dextran series. The

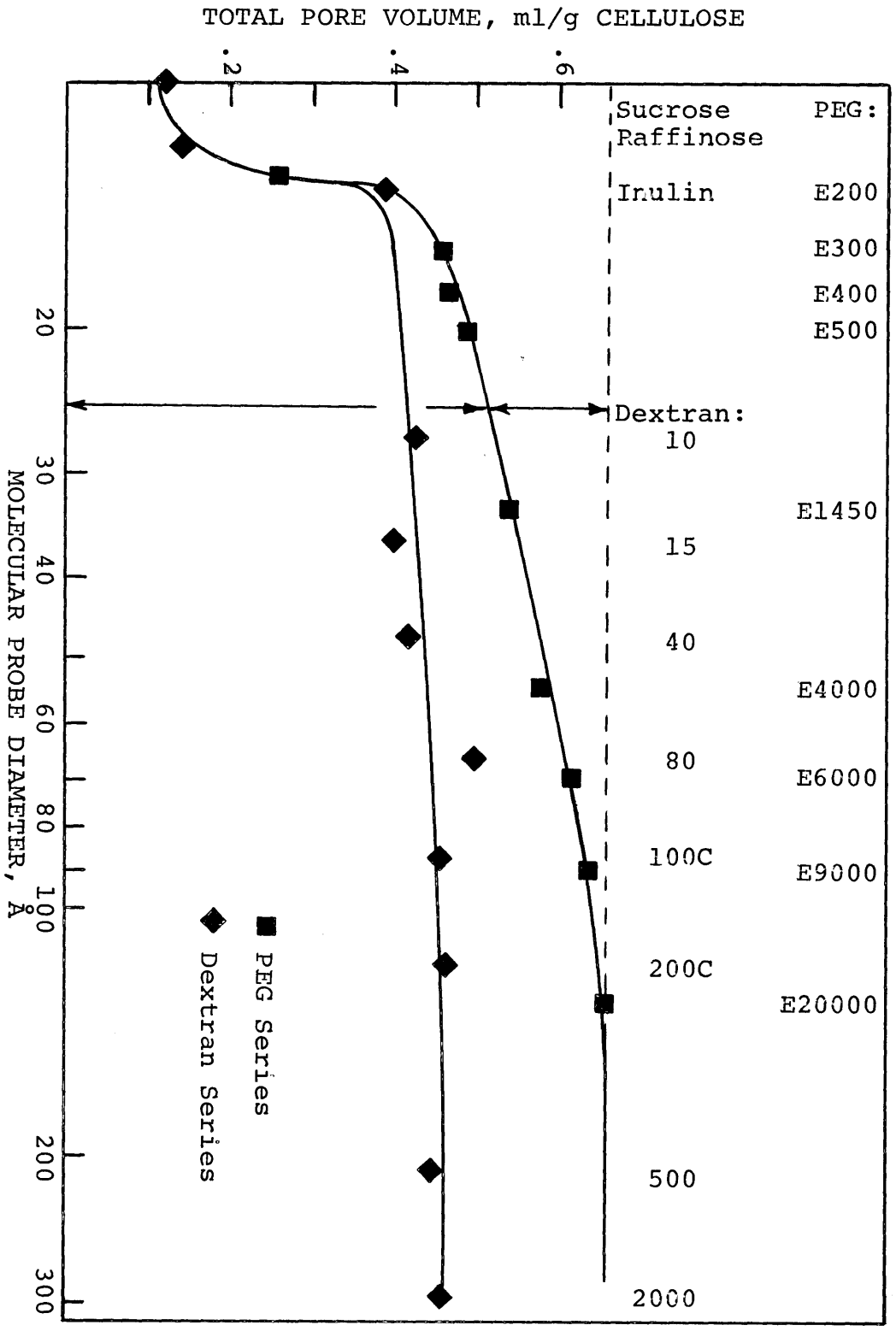

Figure 9-1. Cumulative Pore Volume Curve

characteristic diameter used for the dextran series was the minor axis of a prolate ellipsoid. These were calculated from equivalent sphere diameters (242) using an axial ratio of 6.9 which was considered adequate for Dextran 15 (33). The enzyme molecule, assumed a prolate ellipsoid 35 Å by 210 Å (272), was also characterized by its minor axis.

A pore size distribution curve was computed from the cumulative pore volume curve for the PEG series. The cumulative curve was differentiated by division into intervals of increasing pore diameters. The change in pore volume per angstrom, $\Delta V/\Delta pd$, was computed for each interval. This quantity was then plotted as a function of the median pore diameter in each interval to yield Figure 9-2. Eighty-five per cent of the pore volume was inaccessible to a molecule larger than 35 Å, the minimum enzyme dimension. The pore volume possibly accessible to an enzyme molecule was 0.1 cc/g cellulose. The unshaded area under the curve is the pore volume inaccessible to the enzyme, while the shaded area is the accessible volume.

Stone et al. (242) have reasoned that the most feasible intrafibrillar shape is that of lamellae or sheets of microfibrils. The pores would then be the slit-like spaces between these sheets. The characteristic pore width would be the space between the sheets w . The pore area for each characteristic "diameter" would then be

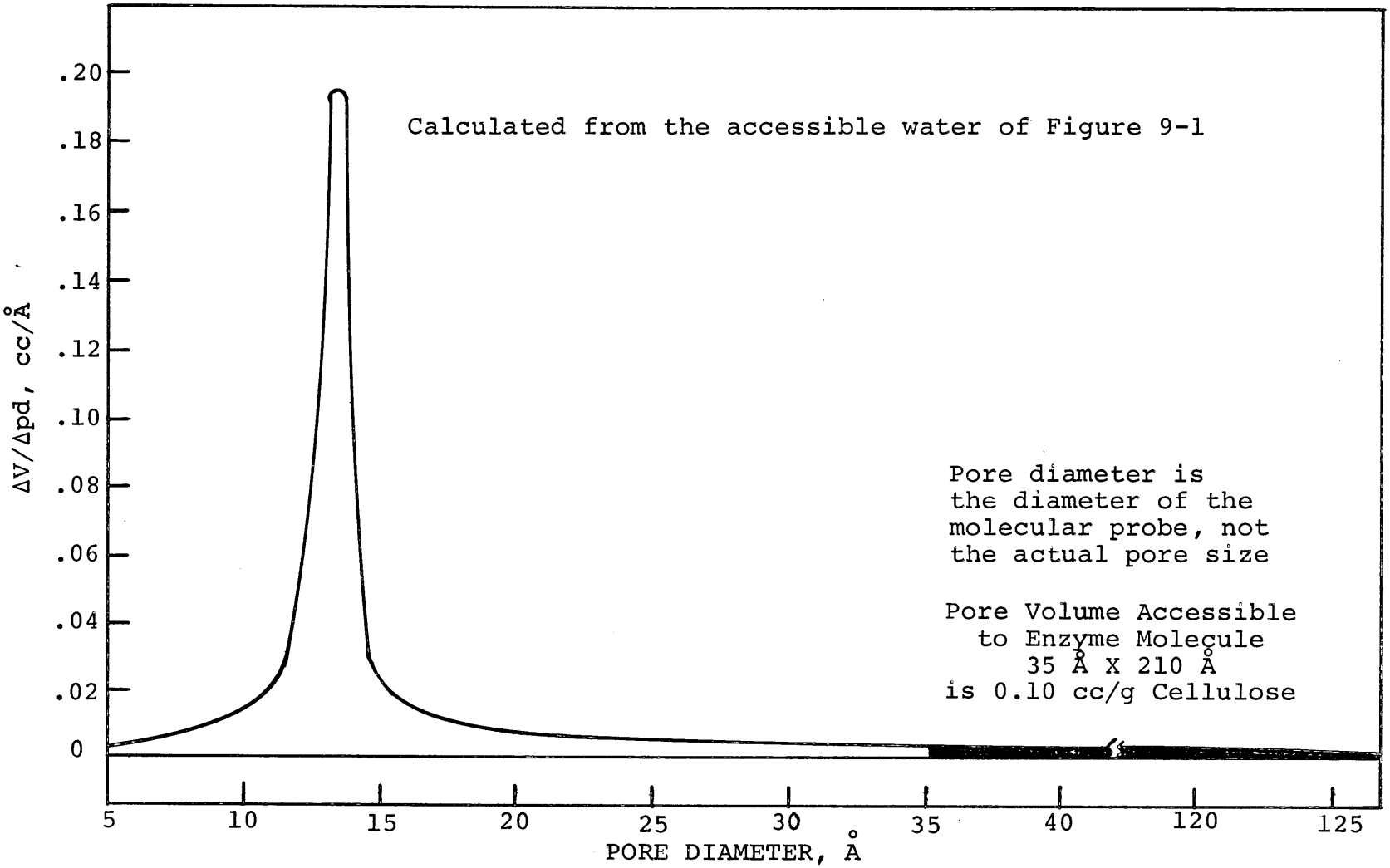

Figure 9-2. Pore Size Distribution Curve for Solka Floc

$$A = \frac{2\Delta V}{w} \qquad (1\text{-}19)$$

where ΔV is the differential volume associated with each median pore "diameter" w. (The actual pore width is greater than the molecular diameter because of the partition effect.)

The accessible area calculated from this equation was 35 m^2/g cellulose. The external surface area based on swollen 16μ spherical cellulose particles was only 0.5 m^2/g cellulose. The external surface is, therefore, only 2% of the total area accessible to the enzyme molecules. The surface required to adsorb the enzyme measured during the hydrolysis studies was calculated to be 25 m^2/g, which agreed with the total available surface and is 50 times greater than that available only from the external surface. Although the available pore surface is only 10% of the total pore area, it is extremely important to the hydrolysis reaction. It is upon this surface that most of the hydrolysis occurs. This accessible porous structure probably forms the "casing" around the core which contains 90% of the pore area, corresponding to pores smaller than the enzyme.

The adsorption data for Run 15 was used with classical solutions of the pore diffusion equation to approximate the effective diffusivity; a 100 fold reduction in diffusivity was apparent. Albeit rough, these calculations

also support the hypothesis that the enzyme can and does diffuse into the cellulose particle.

G. Conclusions and Recommendations

1. Conclusions

a. Bulk mass transfer of the enzyme to the cellulose surface, or of reaction products from the surface is not a controlling resistance provided the particles are at least suspended in solution.

b. The wood pulp employed as a substrate yielded a rapid initial rate followed by a slower rate implying the presence of both amorphous and crystalline cellulose.

c. At extended periods of hydrolysis the substrate became very resistant to hydrolysis as if it was inaccessible to the enzyme molecules.

d. The hydrolysis reaction was first order with respect to the amorphous, crystalline, and resistant substrates.

e. Increase in initial cellulose concentration with a fixed enzyme concentration caused the reaction rate to pass through a maximum occurring at an optimum cellulose concentration.

f. The optimum cellulose concentration appears to be proportional to the adsorbable protein.

g. The hydrolysis of amorphous cellulose and crystalline cellulose was proportional to the enzyme concen-

tration raised to the 1.5 power. In addition the studies with concentrated enzyme indicated that the overall hydrolysis of both crystalline and amorphous cellulose was proportional to C_1 activity. Both amorphous and crystalline cellulose, therefore, are probably hydrolyzed by the same mechanism.

h. At cellulose concentrations greater than the optimum the specific hydrolysis rate of amorphous cellulose was independent of the initial cellulose concentration; the hydrolysis rate of crystalline cellulose, however, was inversely proportional to the initial cellulose concentration.

i. At cellulose concentrations less than the optimum the enzyme concentration initially participating in hydrolysis was proportional to the initial cellulose concentration.

j. At extended hydrolysis with excess enzyme in solution the enzyme participating in hydrolysis appeared proportional to the remaining cellulose concentration raised to a fractional poser, possibly 0.67.

k. A kinetic model was developed that predicts the hydrolysis kinetics from knowledge of the initial enzyme and cellulose concentrations for conditions of excess cellulose.

l. The intrinsic rate coefficient, k_i^* , is probably a composite of the surface diffusion of the enzyme

molecules and a true intrinsic constant.

m. The solute exclusion results and the fact that the external particle surface is 50 times too meager for the observed enzyme adsorption indicate that the enzyme diffuses into the cellulose pores. These pores are about 15% of the total pore volume.

2. Recommendations

a. The effect of varying the C_1 : endoglucanase ratio should be explored.

b. The addition of exoglucanase and β-glucosidase and the use of these enzymes, possibly insolubilized, in an auxillary reactor should be studied.

c. The kinetic model should be extended into areas where cellulose concentration is definitely the limiting reagent.

d. Other substrates, specifically milled newspaper should be employed and the kinetic model modified.

The overall hydrolysis reaction appears to be a function of the accessible cellulose surface irrespective of the enzyme concentration. Research efforts should be expended in economically increasing this surface rather than increasing the enzyme concentration.

II. INTRODUCTION

Cellulose is an abundant, annually renewed source of carbon. In industrially developed countries it poses a major waste disposal problem. The advantages of changing waste cellulose into a usable raw material are obvious. The process under consideration here is to hydrolyze enzymatically the cellulose to glucose which can be utilized as a high energy human nutrient, as a carbon source for the production of singly cell protein, or as an industrial raw material.

Much of the research effort to date has been expended in three major areas. The first has been the elucidation of the hydrolytic mechanism and in particular the enzyme complex involved. The second area has been to define the accessibility of the cellulose to the enzyme molecules and especially to increase enzyme-cellulose contact. The third research effort has been to increase the strength of the enzyme complex.

Little effort had been expended in elaborating the mass transfer resistances encountered in the diffusion of the enzyme molecule from the bulk solution to the site of hydrolysis. Further, no researcher had conclusively proven if the enzyme molecules diffuse into the cellulose pore structure.

Although hydrolysis kinetics had been discussed, espe-

cially in regard to the mechanism of enzyme action, no general model existed to describe the overall reaction. In fact the order of the reaction with respect to enzyme and cellulose concentrations had not been clearly defined.

Finally, the rate controlling step in the hydrolysis reaction was thought to be proportional to the C_1 concentration. Little data, however, were available to verify this hypothesis. Published hydrolysis data were scarce and in general hard to utilize for determining kinetic rate constants.

The purpose of this thesis was four fold: first to elucidate the mass transfer resistances involved in hydrolysis; second to develop a kinetic model for the hydrolysis reaction; third to verify that C_1 is the rate controlling enzyme; and fourth to determine if the enzyme diffused into the cellulose pore structure. Accomplishment of these objectives required specialized assay procedures and refinement of a solute exclusion technique to study cellulose pore structure.

III. LITERATURE REVIEW

A. Introduction

The fine structure of cellulose greatly influences the rate, extent and uniformity of chemical reactions in which it participates. Accessibility is believed to be the major factor while other structurally related factors such as fiber dimensions, crystalline form and hydrogen bonding have lesser effects (169). As stated by Cowling and Brown (38):

> "The susceptibility of cellulose to enzymatic hydrolysis is determined largely by its accessibility to extracellular enzymes secreted by, or bound on the surface of cellulolytic microorganisms. Direct physical contact between these enzymes and the cellulosic substrate molecules is an essential prerequisite to hydrolysis. Since cellulose is an insoluble and structurally complex substrate, this contact can only be achieved by diffusion of the enzyme from the organism (or solution) into the complex structural matrix of the cellulose. Any structural feature that limits the accessibility of the cellulose to enzymes by diffusion within the fiber will diminish the susceptibility of the cellulose of that fiber to enzymatic degradation."

The reader is referred to Appendices A and B for a review of general cellulose structure and the enzyme complex.

B. The Relationship of Substrate to Enzyme Action

Cowling and Brown (38) have reviewed six structural features of cellulose substrates that directly affect susceptibility to enzyme hydrolysis. These are: (1) the moisture content of the fiber; (2) the size and diffusivity

of the enzyme molecules involved in relation to the size and surface properties of the gross capillaries; (3) the degree of crystallinity of the cellulose; (4) the conformation and steric rigidity of the anhydroglucose units; (5) the degree of polymerization of the cellulose; and (6) the nature of the substances with which the cellulose is associated.

Moisture plays four major roles in the degradation of cellulose. It swells the fiber by hydrating the cellulose molecules thus opening the fine structure and increasing accessibility to cellulolytic enzymes. It provides a diffusion path for the enzyme from the solution to the substrate and for the product from the substrate to the solution. Moisture aids in the formation of inter- and intrachain hydrogen bonds thus increasing crystallinity in amorphous areas. It also provides an essential reactant (H-OH) that must be added to the cellulose fragments during hydrolysis. The fiber saturation point is a measure of the water content of the fiber and is critical for enzyme action.

The size and diffusivity of cellulolytic enzymes in relation to the capillary structure of cellulose will be discussed in Section C: The Relationship of Substrate Capillary Structure to Hydrolysis.

The influence of the degree of crystallinity on the susceptibility of cellulose to enzymatic hydrolysis has been studied by Norkans (172), Walseth (265), and Reese et al. (199) among others. Using samples precipitated

after swelling in phosphoric acid, Walseth showed that the preparations with lower moisture-regain values (higher crystallinity) were more resistant to hydrolysis by isolated enzymes of Aspergillus niger than those with higher regain values. Norkans (172), using x-ray diffraction data, drew the same conclusion for cellulose regenerated from cupra-ammonium solution. She concluded that the enzymes were degrading the amorphous portions of the regenerated cellulose but not the crystalline portions.

Preferential attack of amorphous cellulose is indicated in some microorganisms, but not all. Cowling and Brown studied the attack of two wood rot fungi on wood (38). The brown rot fungus Poria monticola rapidly hydrolyzed about 10% of the wood; much slower hydrolysis then followed. The white rot fungus Polyporous versicolor attacked the wood in a more uniform manner. The amount of material rapidly hydrolyzed by P. monticola agreed with estimates of the proportion of amorphous cellulose in several similar woods as obtained from acid hydrolysis. The gradual decrease in DP in the case of P. versicolor indicated that amorphous and crystalline cellulose were degraded simultaneously. This conclusion was confirmed by x-ray diffraction and moisture regain analyses (27).

In Norkans' work the rate of hydrolysis was also followed by DP measurements. The rates were initially very rapid, but they were much slower at later stages to the

point of complete inhibition at a "leveling-off DP" analogous to that observed during acid hydrolysis. As with acid hydrolysis there was a significant increase in crystallinity during reaction. Walseth reported an increase of nearly 20%. As the more accessible portions of cellulose are hydrolyzed, the remainder becomes more resistant to enzymatic attack. From these observations it follows that any treatment which will reduce the crystalline to amorphous ratio will probalby increase the susceptibility to hydrolysis. Such treatments include reprecipitation from solution, mechanical disruption such as milling, or swelling with acid or base.

Conformation and steric rigidity of the anhydroglucose units within the crystalline region may also be a factor in its increased resistance to hydrolysis as compared to the amorphous region (104). In the crystalline regions the glucose units occur in the C_1 (chair) configuration, with alternate glucopyranose units oriented in opposite directions within the lattice. It is possible, although not necessarily likely, that the C_1 conformation and planer orientation of the glucose units is the one that fits best in the active site of the enzyme. It is also possible, but still more unlikely in terms of modern understanding of enzyme specificity, that the active site of the enzyme is so designed that cellulose chains on all sides of a crystallite are in a steric orientation equally

ideal for complex formation and subsequent hydrolysis. These considerations strongly suggest the possibility that an induced fit mechanism as described by Thoma and Koshland (256) for α-amylases may be involved in enzymatic hydrolysis of cellulose. The possibility for adjustments in configuration and respective orientations of the glucose rings in cellulose increases as the degree of crystallinity decreases and the degree of hydration increases. It is in exactly this way that cellulose susceptibility to enzymatic degradation also increases. Thus it seems highly probable that configuration and steric rigidity as well as accessibility may have a bearing on the resistance of crystalline cellulose to enzymatic hydrolysis (38).

The degree of polymerization of the cellulose molecules in a fiber varies over a wide range from γ-celluloses containing less than 15 glucose units to α-cellulose with as many as 14,000 units per molecule. This variation would be expected to affect the rate of hydrolysis considerably, since the number of chain ends per unit weight is inversely proportional to the degree of polymerization. The effect should be most pronounced with cellulases active in an endwise fashion (exoglucanases) as compared with the random acting endoglucanases.

The nature of the substances with which the cellulose is associated and the nature of that association should also have an important effect on hydrolysis by extracel-

lular enzymes. The extraneous materials in cotton and wood include a variety of organic substances that are soluble in such neutral solvents as acetone, ether, alcohol, benzene and water. The water insoluble substances are usually deposited within the gross capillary structure of the fibers; the water soluble materials are deposited in part in the fine capillary structure within the fiber walls. These materials influence the susceptibility of cellulose fibers to enzymatic hydrolysis in two major ways: (1) Various substances deposited within the fine capillary structure of the cell wall physically reduce the accessibility of the cellulose to extracellular enzymes. (2) Certain specific enzyme inhibitors act directly to reduce the rate or extent of an enzymatic hydrolysis of the cellulose.

The combination of lignin with the partially crystalline cellulose that occurs in wood forms one of the natural materials most resistant to enzymatic hydrolysis. Although the chemical nature of lignin has been investigated as discussed in Appendix A, the nature of the association between lignin and the wood polysaccharides is still obscure. A chemical bond between lignin and cellulose has been postulated. Present evidence suggests, however, that the association is largely physical in nature, the lignin and amorphous cellulose forming a mutually interpenetrating system of high polymers. Lignin apparently decreases the acces-

sibility of the wood fibers to the enzyme molecules diffusing into the fine pore structure. To degrade the cellulose in wood, an organism must possess not only the ability to degrade cellulose but also to degrade the lignin or to at least break down its association with the cellulose.

The lignin can be extracted by pulping, leaving a fairly easily digested substrate. Treatment such as milling will also break down the lignin-cellulose structure, increasing reactivity.

C. The Relationship of Substrate Capillary Structure to Hydrolysis

As discussed earlier and reviewed by Cowling and Brown (38), cellulose hydrolysis requires that the cellulase diffuse from the solution into the fiber. Accessible surface is that surface which can be reached by the enzyme. It is defined by the size, shape, and surface properties of the microscopic and submicroscopic capillaries within the fiber, as compared to the size, shape, and diffusivity of the enzyme molecules themselves. The influence of these relationships on the susceptibility and resistance of cellulose to enzymatic hydrolysis has not been verified experimentally in natural fibers, but the validity of the concepts that follow has been demonstrated by the work of Stone et al. (242), Nelson and Oliver (169), and Lee (125).

The capillary voids in wood and cotton can be divided into (1) gross capillaries such as the cellumina, pit apertures, and pit membrane pores that are visible in the light microscope and thus are between 2000 Å and 10 or more microns in diameter; and (2) cell wall capillaries such as the spaces between microfibrils and the cellulose molecules in the amorphous regions that are less than 200 Å in diameter. Most of the cell wall capillaries are closed when the cells are dry, but open again when moisture is absorbed, attaining their maximum dimensions when the cellulose is saturated with water. Some expand to 200 Å, but most are substantially smaller in diameter.

The total area represented by the gross capillaries is about 1.0 m^2 per gram, while the cell wall capillaries of swollen cellulose represent about 300 m^2 per gram. Thus, if cellulolytic enzymes can penetrate the cell wall capillaries, substantially faster hydrolysis will occur than if they are confined only to the gross capillaries. One square meter can adsorb about 1×10^{16} globular enzyme molecules approximately 200 Å by 35 Å. That is equivalent to approximately 1 mg of enzyme protein per square meter of accessible surface.

The dimensions of the swollen cell wall capillaries have been explored by Stone et al. (238-242) and by Tarkow et al. (254, 255) who adapted the "inaccessible water technique" of Aggerbrandt and Samuelson (3) to cel-

lulose fibers.

The approximate median and maximum diameters of the capillaries of water swollen wood, cotton and wood pulp were 10 and 35, 5 and 75, and 25 and 150 Å respectively (238). It should be emphasized that the dextran and polyethylene glycol molecules used to obtain these estimates had fairly broad molecular weight distributions and did not have the specific affinity for the substrate that a cellulolytic enzyme would have. The substantial increase in dimensions for the pulp resulted in part from the removal of lignin and hemicellulose from the cell wall capillaries. Only a small fraction of the water swollen capillaries were large enough to accomodate most of the cellulolytic enzymes.

D. The Effect of Substrate Pretreatment on Enzyme Action

Various factors affect the susceptibility of cellulose to enzymatic hydrolysis often called saccharification. Most of these factors impede the binding of the enzyme with its substrate. Several methods have been tried to break the interchain hydrogen bonding and hence, to improve the accessibility of the substrate, thereby increasing the rate of hydrolysis (198). Phosphoric acid swelling was the most effective method with milling a close second. Sodium hydroxide swelling, irradiation, and treatment with weak organic acids appeared of questionable value in in-

creasing susceptibility, although extended treatment caused improvement. Another, although impractical, method would be chemical modifications creating cellulose derivatives that are soluble. Both swollen and soluble moderately substituted celluloses can be rapidly saccharified and the former completely converted into sugar in a relatively short period of time. Unfortunately, the maximum concentration of substrate and product achievable with these methods is quite low. A 5% solution of cellulose will yield at best a 5.5% solution of glucose which would have to be concentrated. It would be desirable therefore, to reach a higher initial cellulose concentration. For example, the drying of a 5% glucose solution requires removal of nearly eight times as much water per unit glucose as does the drying of a 30% solution.

The object, then, is not only to make the interior of the substrate particles more accessible to the cellulolytic enzymes, but also to increase the bulk density of the substrate slurry. Krupnova and Sharkow (119, 120) found that a combination of milling and heating greatly increased susceptibility to hydrolysis. They showed that milling and heating to 210°C for 20 minutes resulted in a 105% yield of glucose, nearly complete hydrolysis. Katz and Reese (101) prepared samples of 50% (w/v) of ground and heat treated cellulose wood pulp (Solka Floc). Enzymatic hydrolysis of these samples was rapid and resulted

in glucose concentration in excess of 30%.

Ghose and Kostick (75) reported that infrared spectra and x-ray diffraction studies suggested that heating and milling oxidized the cellulose and partially destroyed its crystalline structure as previously reported by McBurney (Appendix A, 4. Degradation of Cellulose). The crystallinity index of the milled, and milled and heated cellulose was reduced from 83 for untreated Solka Floc to 41. As digestion proceeded, however, the material became more fibrillar and the crystallinity index increased. This implied that either amorphous cellulose was rapidly hydrolyzed leaving a more crystalline core, or that the cellulose chains were recrystallizing.

Ghose and Kostick used Solka Floc SW40A (Brown Company, Berlin, New Hampshire), a Spruce wood pulp, as cellulosic material for their susceptibility studies. The material was dry milled in a laboratory porcelain ball mill or in a Sweco Vibro Energy Mill. Some of the material was heated to 200°C for 25 minutes before or after milling in the presence of air. Preheated cellulose milled for 24 hours yielded a mixture 80% of which was below 53μ in size.

Better results were obtained if heating preceeded rather than followed milling. Over long hydrolysis periods the method of pretreatment and the pretreatment itself had little net effect on the rate of hydrolysis although heating followed by milling is particularly effective in in-

creasing the initial rate of hydrolysis. The removal of the lignin matrix greatly weakens the cellulose structure. As the pulp ages, however, the hydrogen bonds that were broken during pulping are reformed, causing an increase in crystallinity. Drying causes a significant increase in crystallinity as shown by the greater reactivity, fiber saturation point and median pore size of never-dried as compared to dried wood pulps (242).

E. Effect of Substrate and Enzyme Concentration on Saccharification

The rate of cellulose hydrolysis is dependent on the concentration of the enzyme. As the hydrolysis progresses its rate becomes less dependent upon the enzyme concentration, and eventually appears to stop. This is a result of complete utilization of substrate. The initial rate of hydrolysis is proportional to the enzyme concentration if the substrate is in excess.

A comparison of some of Ghose's data (78) indicated a discrepency between results obtained with agitated vessels and test tubes (presumed unagitated). Agitated vessels with one-half of the enzyme strength of the test tubes produced nearly twice the rate of hydrolysis. This indicated the possibility of bulk mass transfer effects on the rate of reaction.

The work of Selby presented in the discussion of Ranby

(189) indicated that the hydrolysis of cotton was first order with respect to the substrate up to about 35% solubilization. This first order relationship was not always apparent and was definitely not present during initial hydrolysis of wood pulp. Selby had no explanation for the departure from first order behavior at higher degrees of hydrolysis.

F. Cellulase Adsorption onto Cellulose

Ghose (73) and Selby (216) both reported that enzymes of the cellulase complex adsorb onto cellulose and other adsorbants. The enzyme is still active in its adsorbed form. Selby reported that neither C_1 nor C_x influences the adsorption of the other enzyme upon the cellulose. Neither researcher appears to have modeled the adsorption process or to have obtained adsorption isotherms.

Mandels (141, 142) performed an interesting experiment that illustrated the importance of the adsorption phenomenon. Parallel series of hydrolysis experiments were performed in shake flasks. After 1 hour the hydrolysis liquid in one set of flasks was removed from the cellulose by centrifugation and replaced by an equal volume of buffer. Cellulose was added to all flasks at various intervals to restore the cellulose concentration to the initial 10%. Both sets of flasks showed nearly equal

hydrolysis, despite the fact that 99% of the original enzyme liquid had been removed by centrifugation. This suggested that enough enzyme had adsorbed onto the cellulose to perform the hydrolysis. Since C_1 enzyme is inactive without C_x, both enzymes must have been adsorbed.

Further adsorption studies were carried out by Mandels to determine the effect of cellulose concentration, particle size, and pH on the amount of adsorption. The adsorption was measured as total protein adsorbed, C_1 enzyme adsorbed (filter paper activity), and as C_x adsorbed (carboxymethylcellulose activity). The amount of adsorption after 1 hour appeared to be a limited function of the cellulose surface present. At cellulose concentrations over 4% the adsorption appeared nearly independent of cellulose concentration. C_x adsorption lagged behind C_1 adsorption at lower cellulose concentrations. Whether this is peculiar to this data or is a characteristic of the adsorption of cellulases onto cellulose is a question that will have to be answered.

At longer time Mandels reported that enzyme began to diffuse back into solution. This effect was observed as an increase in total protein, C_1 activity and endoglucanase activity in the bulk solution. The hydrolysis at this point was about 35% of an initial 10% cellulose concentration.

G. Summary

The six structural features reviewed in section B are extremely important to understanding enzyme action. Cowling and Brown's work with the wood fungi provides a possible method of interpreting hydrolysis data. A rapid rate followed by a slower change is indicative of a two component hydrolysis. A constant rate of change is indicative of uniform hydrolysis. The influence of crystallinity on hydrolysis can not be overstated. Amorphous cellulose is far easier to digest than crystalline cellulose. Milling appears to reduce crystallinity. Even with milling, however, the rapid initial hydrolysis rate yields to a much slower rate typical of that for crystalline cellulose.

The internal matrix of the cellulose particles is also a major factor in the hydrolysis mechanism. The enzyme must have access to the cellulose molecules. If the initial pore structure is too small the enzyme will be confined to the gross capillaries which account for only 0.03% of the available surface. Pulping appears to increase the average pore size by removing lignin. Acid swelling also increases the average pore size.

In addition to the structure and type of substrate, the rate of hydrolysis is also dependent upon the concentration of the enzyme and the substrate. The functionality is in doubt although some evidence does support a first order relationship with respect to cellulose concen-

tration.

The difference between results obtained from agitated vessels and from test tubes indicated the possibility of a mass transfer limited system.

The main areas of investigation pursued in this thesis were therefore:

(1) to elucidate the mass transfer resistances involved;

(2) to determine the functionality of the hydrolysis reaction to the enzyme and cellulose concentrations;

(3) to develop a kinetic model of the hydrolysis reaction; and

(4) to determine whether or not the enzyme enters into the cellulose pore structure.

IV. ASSAY PROCEDURES

A. Introduction

The term cellulase refers to a complex of at least three enzymes: C_1 , β-glucanase, and β-glucosidase. The enzyme C_1 acts along with β-glucanase to hydrolyze crystalline cellulose to soluble long chain (DP<200) glucose polymers. These soluble chains are then hydrolyzed by the β-glucanases alone to the glucose dimer, cellobiose, and glucose. β-Glucosidase hydrolyzes the cellobiose to glucose. Assay procedures were established by the author to determine the products of reaction: long chain polyglucose fragments, cellobiose and glucose, and the concentrations of the different enzymes in solution. The latter was accomplished by determining both enzyme activity and protein concentration.

Action of the enzyme complex on different substrates, and differentiation of the products resulting thereby, provide means of assaying for the individual enzymes. The ideal assay should be simple and reproducible, and should closely duplicate the actual experimental conditions.

The first step in developing the assay procedures was to find methods for differentiating between glucose and cellobiose. Most possible methods ultimately required a spectrophotometric analysis in which the optical density at a characteristic wavelength is proportional to the con-

centration of the substrate being assayed. The second step was to develop reproducible procedures for determining enzyme activity in solution. The third area explored was to obtain a workable method for determining enzyme protein in solution.

1. Determination of Reaction Products

The method commonly employed in following the enzymatic hydrolysis of cellulose is to measure the increase of "reducing end groups" with time. A new "reducing end group" (the -O-CHOH- found only at the end of a glucose chain) should be formed at each point of chain scission. Miller (164) and Miller et al. (165) have refined the colorimetric dinitrosalicylic acid (DNS) method of Sumner (249) for determining reducing sugars, assuming that each sugar has only one "reducing end group". The method is convenient in that the finished assay can be diluted with distilled water to bring the original optical density into a readable range on the colorimeter. The major drawback of this method is that it measures neither molar concentration nor monosaccharide content. The reducing sugar determination for cellobiose gives only 85% of the result expected from its monosaccharide content.

Sulfuric acid based spectrophotometric techniques are superior to the DNS method in that they yield quantitative determination of monosaccharide content. The

orcinol and anthrone methods reviewed by Miller et al. (165) require heating in boiling water for color stability. The phenol sulfuric acid technique developed by Dubois et al. (45) and modified by Reese (93) is superior to the other two sulfuric acid methods. This procedure uses the heat of dilution resulting from the rapid addition of concentrated sulfurid acid to a dilute phenol solution containing the sugar sample to provide the reaction energy. This method is rapid, reproducible and simple, and is as sensitive as the orcinol and anthrone procedures.

The phenol sulfuric acid technique allows accurate determination of the total carbohydrate present in a solution. Differentiation between the long chain soluble cellulose fragments, cellobiose, and glucose is a difficult problem. Chromatography is often used to separate the various fractions. Worthington Biochemical Corporation (78) has developed an enzymatic "Glucostat" procedure that is relatively specific for glucose. Unfortunately no similar method exists for determining cellobiose concentrations.

2. Determination of Enzyme Concentration

Enzyme assays are based on the change of some solution property caused by the action of the enzyme on its substrate at standardized conditions of time, temperature, and pH. Several procedures for determining cellulase

concentrations are reviewed by Erikkson (48) and Mandels and Weber (148). Cellulose substrates include highly resistant crystalline forms such as cotton, sulfite pulps such as Solka Floc, and filter paper. More susceptible substrates include swollen or reprecipitated cellulose, cellophane, and ball milled cellulose. Most susceptible are the soluble cellulose derivatives of low degree of substitution (DS) such as carboxymethylcellulose (CMC). There are, therefore, many assay methods each differing in sensitivity and in cellulase component detected, depending on the substrate, the effect measured, and the duration and conditions of the assay.

Crystalline substrates are employed to assay for combined C_1 and β-glucanase activity. Cellulose derivatives, especially CMC, are employed for determining the activity of β-glucanase alone. Since substituent groups interfere with enzymatic hydrolysis, they must be kept small and to a minimum. Unfortunately this also limits the length of the derivative chain since solubility is proportional to the size and number of substituent groups. Cellobiose provides a good substrate for β-glucosidase activity since it is very resistant to hydrolysis by β-glucanase.

The following sections discuss the assay procedures developed. Detailed experimental procedures are reported in Appendix H. An error analysis is presented in Chpater VI.

B. Determination of Reaction Products

1. Phenol Sulfuric Acid Procedure

Glucose reacts with a dilute phenol solution in the presence of concentrated sulfuric acid to give a characteristic absorbance at 485 nm. The method, developed by Dubois et al. (45) and modified by Reese (93) is quick, easy and reproducible. Glucose polymers yield a result proportional to the number of glucose residues, corrected on a weight basis for the water lost in polymerization. The optical density of 1 mg/ml of cellulose, therefore, is the same as that of 1.1 mg/ml of glucose.

An appropriately diluted sample (0.1 ml) is placed with 1.9 ml of phenol solution (2.63 weight per cent phenol in distilled water) in a large test tube. Five ml of 95% sulfuric acid are then rapidly added from a buret. The acid must be added to the center of the liquid surface to promote rapid mixing. After acid addition the tube is mixed on a vortex mixer. The high heat of dilution promotes color development that is stable for several hours. After the tube has cooled to room temperature the phenol sulfuric optical density (PSOD) is read at 485 nm. The phenol sulfuric acid standard curve is shown in Figure 4-1. The curve can be expressed as

$$PCARB = (PSOD - 0.010)PSK \qquad (4\text{-}1)$$

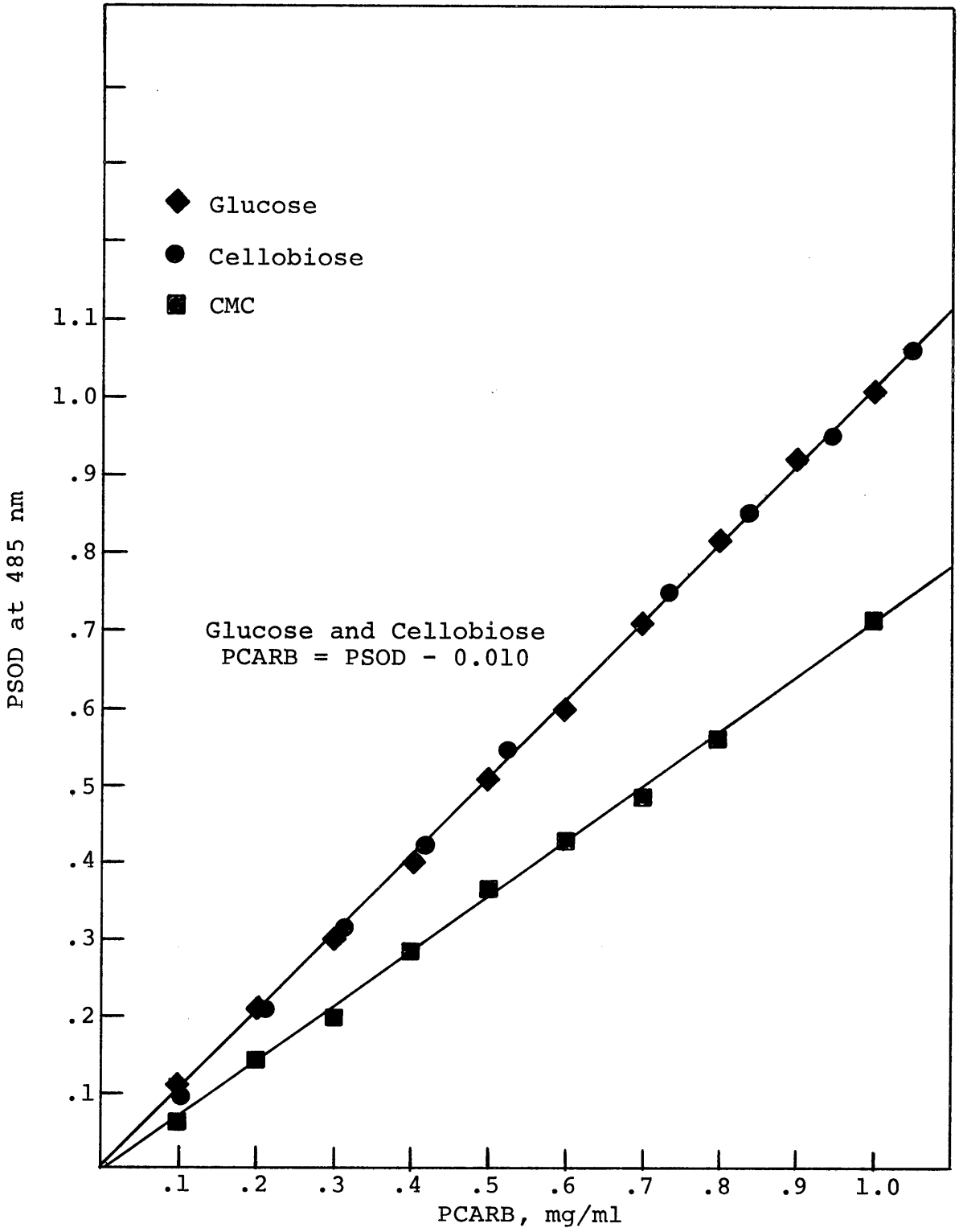

Figure 4-1. Phenol Sulfuric Acid Standard Curve

where PCARB is the carbohydrate concentration in mg/ml.

Cellobiose is converted to glucose equivalent by multiplying PCARB by 1.05. (The moleuclar weights of glucose and cellobiose are 180 and 342 respectively. Cellobiose is not equal to two glucose molecules because water is eliminated during dimerization.) Carboxymethylcellulose did not give a result equivalent to glucose because of interference of the substituent group with the colorimetric reaction. The CMC reacted sufficiently, however, so that the phenol sulfuric procedure could not be used to determine the amount of cellobiose produced by the enzymatic hydrolysis of CMC.

2. Glucostat Procedure

The enzyme glucose-oxidase converts glucose to glucuronic acid and hydrogen peroxide with a high degree of substrate (glucose) specificity. The hydrogen peroxide donates a proton to develop a chromogen with a characteristic absorbance at 415 nm. This reaction sequence has been developed by Worthington Biochemical Corporation into the Glucostat reagent (78). A small (0.1 ml) sample is placed in a test tube with 2.0 ml of pH 7.0 Tris buffer, and 2.0 ml of the Glucostat reagent are added. The tube is then incubated at 50°C for 45 min. Two drops of 4 N hydrochloric acid are then added to stabilize the color for several hours. The optical density is then read at

415 nm.

The glucose standard curve is shown in Figure 4-2. The 95% confidence limits are contained within the glucose symbol unless otherwise indicated by arrows. TCARB (glucose and cellobiose converted to glucose) and CELOB (unconverted cellobiose) are the carbohydrate concentrations in mg/ml that react with the Glucostat reagent. Note that glucose and converted cellobiose produce ten times the optical density as does unconverted cellobiose.

The Glucostat procedure is reproducible and has a high degree of specificity that enables it to measure glucose in the presence of other carbohydrates, specifically CMC; thus, this technique was used with the β-glucanase assay. Note: Glucostat is a lyophilized reagent that should be reconstituted immediately prior to addition to the assay tube because the solution tends to darken upon exposure to light.

3. Cellobiose Determination

Conversion of cellobiose to glucose prior to employing the Glucostat procedure increases the sensitivity of the cellobiose determination by an order of magnitude. This hydrolysis is accomplished by incubating a 0.1 ml sample with 0.2 ml of β-glucosidase solution (1% in pH 4.9 buffer) and 0.7 ml of additional buffer. High cellobiose concentrations required 0.4 ml of β-glucosidase solution

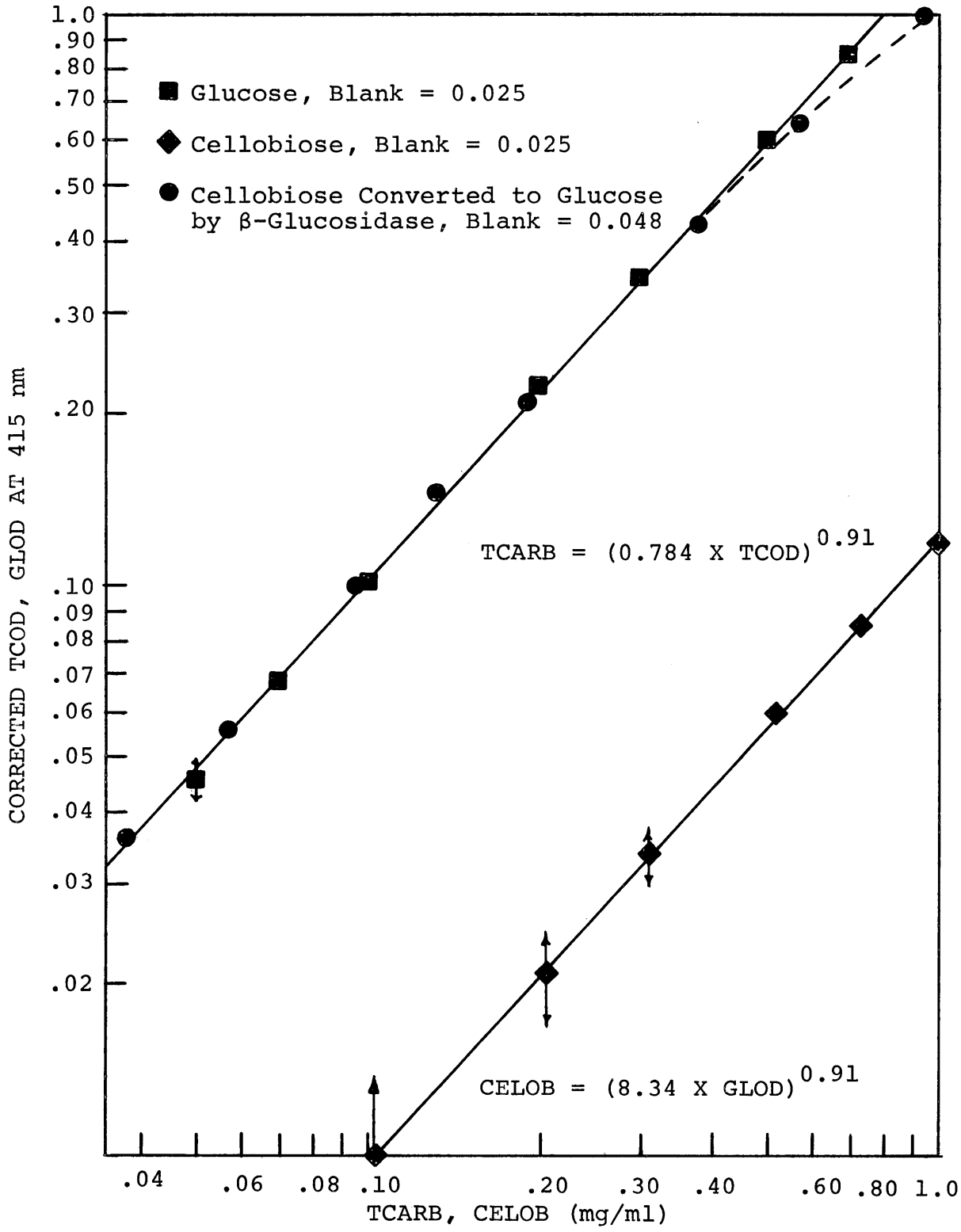

Figure 4-2. Glucostat Standard Curve

and 2.0 ml of buffer. (The additional buffer is added so that the final glucose concentration produced by the hydrolysis will be in the proper range for determination by the Glucostat procedure.) The test tube is then incubated for 1 hour at 50°C, quenched in an ice bath, and the glucose concentration determined.

Typical results are shown in the "Cellobiose as Glucose" points in Figure 4-2. At higher carbohydrate concentrations (0.6 mg/ml in the Glucostat sample) the relationship loses its linearity, probably because of equilibrium between the glucose and cellobiose. Additional β-glucosidase did not restore linearity. The total carbohydrate curve can be approximated by

$$TCARB = TCK[(TCOD - 0.048)/1.275]^{0.91} \qquad (4\text{-}2)$$

where TCOD is the measured optical density and TCARB is the converted cellobiose and/or glucose concentration in mg/ml. TCK is a dilution factor that converts the TCARB measured to that actually present in the original undiluted sample. The equation for the unconverted cellobiose curve is

$$CELOB = GLK[(GLOD - 0.025)/0.12]^{0.91} \qquad (4\text{-}3)$$

where GLK is a diltuion factor similar to TCK.

4. Differentiation Between Glucose and Cellobiose

A mixture of glucose and cellobiose concentrations was differentiated with the Glucostat technique. "Total" carbohydrate (TCARB) was determined by adding β-glucosidase to the sample to convert cellobiose to glucose. The "total" carbohydrate optical density (TCOD) was that resulting from converted cellobiose and from glucose. Similarly the cellobiose optical density (GLOD) reflected contributions from the glucose and from the unconverted cellobiose. A trial and error procedure (using the equations developed in Appendix J) permitted differentiation between the glucose and cellobiose concentrations.

This procedure predicts that the measured optical density of a mixture of glucose and cellobiose converted to glucose would be equal to the sum of the optical densities resulting from each component alone. Knowledge of the mixture optical density plus the concentration of one of the components would allow calculation of the concentration of the other component. To test this technique a trial "total" carbohydrate determination was accomplished. Mixtures of different concentrations of glucose and cellobiose were made. Microsamples of each mixture were incubated with β-glucosidase and buffer to convert the cellobiose to glucose. Samples of the incubations were used with the Glucostat procedure to determine measured total carbohydrate optical density, TCOD.

The data for this trial run are given in Table 4-1. The table is constructed in matrix format. Each set of four rows corresponds to a different glucose concentration while each column corresponds to a different cellobiose concentration. The intersection of a row set and a column contains the optical densities from a mixture of the cellobiose and glucose concentrations, the sum of which is TCARB. Optical density A (O.D. A) is the measured optical density for each mixture. Optical density B (O.D. B) is the optical density corresponding to the sum of the optical densities of the cellobiose and glucose concentrations incubated individually. These separate optical densities are distinguished by an astrisk. The optical density corresponding to the TCARB value for each of the 25 matrix intersections is recorded as O.D. C. These values were read from Figure 4-2 or calculated from equation (4-2). The agreement between the measured optical densities and those predicted from the individual cellobiose and glucose optical densities was within 2%. The measured values also agreed closely with the optical densities predicted from knowledge of the total carbohydrate concentration. The measured optical density, TCOD, is thus a good measure of the sum of the cellobiose and glucose concentrations.

A second trial determination was performed to test the hypothesis that the optical density of a mixture of glucose and unconverted cellobiose is equivalent to the

TABLE 4-1. OPTICAL DENSITIES RESULTING FROM MIXTURES OF GLUCOSE AND CONVERTED CELLOBIOSE

	Glucose mg/ml	Cellobiose as Glucose, mg/ml				
		0	0.087	0.175	0.346	0.489
		Optical Densities (TCOD) & TCARB, mg/ml				
TCARB	0	0	0.087	0.175	0.346	0.489
O.D. A		0	0.085	0.185	0.391	0.556
O.D. B	TCOD*→	0	0.086*	0.188*	0.400*	0.550*
O.D. C		0	0.085	0.185	0.391	0.556
TCARB	0.05	0.05	0.137	0.225	0.396	0.539
O.D. A		0.041	0.138	0.237	0.431	0.597
O.D. B		0.048*	0.134	0.236	0.448	0.598
O.D. C		0.048	0.145	0.248	0.450	0.600
TCARB	0.083	0.083	0.170	0.258	0.429	0.572
O.D. A		0.077	0.177	0.275	0.490	0.650
O.D. B		0.083*	0.169	0.271	0.483	0.633
O.D. C		0.083	0.185	0.285	0.490	0.645
TCARB	0.117	0.117	0.204	0.292	0.463	0.606
O.D. A		0.116	0.218	0.321	0.529	0.697
O.D. B		0.120*	0.206	0.308	0.520	0.670
O.D. C		0.120	0.224	0.330	0.530	0.675
TCARB	0.167	0.167	0.254	0.342	0.513	0.656
O.D. A		0.180	0.272	0.381	0.578	0.738
O.D. B		0.180*	0.266	0.368	0.580	0.730
O.D. C		0.180	0.280	0.390	0.580	0.720

O.D. A: Measured optical densities
O.D. B: Glucose O.D. (corrected to glucose concentration) + TCOD*
O.D. C: O.D. corresponding to TCARB from Figure 4-2

sum of the individual optical densities. The method employed was similar to the one just discussed except that the mixtures of cellobiose and glucose were not incubated with β-glucosidase. The cellobiose was, therefore not converted to glucose. The measured otpical densities were termed GLOD to differentiate them from TCOD which measures converted cellobiose. The data, presented in Table 4-2, follows a format similar to the TCARB determination.

Since the optical density is dependent upon the ratio of glucose to cellobiose as well as the carbohydrate concentration, an optical density can not be predicted just from knowledge of the latter. The total carbohydrate value, therefore, was not needed in the determination. Row A is the measured optical density for each mixture of glucose and cellobiose. Row B is the sum of the cellobiose and glucose optical densities measured individually. These individual optical densities are distinguished by astrisks. The optical densities in Row C are similar to Row B except that the individual optical densities were not measured. Instead they were predicted from Figure 4-2 for the corresponding glucose and unconverted cellobiose concentrations.

The measured individual optical densities for glucose concentrations of 0.125 and 0.225 mg/ml were much lower than predicted. At times a drop of sample would remain in

TABLE 4-2. OPTICAL DENSITIES RESULTING FROM MIXTURES OF GLUCOSE AND UNCONVERTED CELLOBIOSE

	Glucose mg/ml	Cellobiose, mg/ml				
		0	0.48	0.95	1.875	2.6
		Optical Density, Glucostat at 415 nm				
A	0	0	0.054**	0.112**	0.239**	0.341**
A	0.125	0.112*	0.184	0.246	0.367	0.472
B		0.112	0.166	0.224	0.351	0.453
C		0.130	0.184	0.242	0.369	0.471
A	0.225	0.223*	0.300	0.362	0.488	0.592
B		0.223	0.277	0.335	0.462	0.564
C		0.250	0.304	0.362	0.489	0.591
A	0.325	0.362*	0.419	0.485	0.604	0.712
B		0.362	0.416	0.474	0.601	0.703
C		0.370	0.424	0.482	0.609	0.711
A	0.500	0.598*	0.665	0.716	0.827	0.940
B		0.598	0.652	0.710	0.837	0.939
C		0.598	0.652	0.710	0.837	0.939

Row A: Measured values of optical density
B: Sum of glucose and cellobiose measured O.D.
C: Sum of theoretical glucose O.D. and cellobiose O.D.

the pipet that was used to transfer a 0.1 ml sample from the dilution tube to the Glucostat tube causing the resulting optical density to appear 10% low. This is evidently what happened to these two determinations. Agreement between the measured values of Row A and the predicted values of Rows B and C is exceptionally good. The agreement is, in fact, better than with the TCARB determination, probably because of the requirement to incubate the latter carbohydrate mixture with β-glucosidase. The incubation doubles the sample handling and hence the possibility of error.

5. Effect of Temperature on Glucostat Procedure

Since the total carbohydrate incubations and enzyme assays were to be at 50°C, it was desirable to perform the Glucostat procedure at this temperature, rather than the normal 37°C as recommended by Worthington Biochemical Corporation. Table 4-3 shows that the increase in temperature had no deleterious effect on the procedure. The reaction on cellobiose, however, doubled even with δ-gluconolactone present. Since lactone inhibits β-glucosidase, this indicated that some impurity other than β-glucosidase was present that reacted slightly with cellobiose. Note that 0.6% cellobiose corresponds to an equivalent glucose concentration of 6.3 mg/ml if hydrolyzed completely. The impurity was, therefore, present in very small amounts.

TABLE 4-3. EFFECT OF TEMPERATURE ON GLUCOSTAT REAGENT

Sample	Temp °C	Optical Density at 415 nm	
		a	b
.6% Cellobiose + 1 mg/ml Lactone	37	0.020	0.603
	50	0.041	0.039
Blank = 0.035			
.5 mg/ml Glucose	37	0.615	0.603
Blank = 0.028	50	0.620	0.620
.5 mg/ml Glucose + 1 mg/ml Lactone[a]	37	0.620	0.615
	50	0.620	0.620
Blank = 0.038			

All samples were initially in 0.05M pH 4.9 phosphate buffer. A 0.1 ml sample was added to 1.9 ml of 0.1M pH 7.0 tris buffer and 2.0 ml of Glucostat reagent was added.
Time in water bath was 45 min
[a]δ-gluconolactone inhibits β-glucosidase (195)

C. Enzyme Assays

After obtaining reproducible methods for cellobiose and glucose determinations, assay procedures for enzyme activity were developed. Enzyme activity was measured as the production of glucose and cellobiose by the enzyme incubated with various substrates in pH 4.9 phosphate buffer at 50°C for up to 1 hour. The incubation period was short, and the enzyme concentrations were dilute to minimize effects caused by extensive substrate hydrolysis. The enzyme concentration was high enough, however, that the reaction products were not overshadowed by residual carbohydrate.

The enzyme used for developing the assay procedures and hence the standard curves was the Trichoderma viride mixture discussed in Chapters VII and VIII and Appendix I. The enzyme concentration was catagorized as mg/ml of adsorbable protein. Undiluted enzyme was equivalent to 0.78 mg/ml of adsorbable protein. The enzyme mixture was diluted with phosphate buffer to vary the enzyme strength employed in the following assay procedures. The buffer used in the following procedures was phosphate, 0.05 M, pH 4.9.

1. C_1 Assay

C_1 activity (FPACT) measures the ability of the enzyme complex to hydrolyze crystalline cellulose. Filter

paper was chosen as a substrate because it is about as susceptible as the sulfite pulps actually employed in the hydrolysis studies. In addition, it can be cut into reproducible strips that can be easily added to or removed from the assay tube. Cotton is too resistant to be easily hydrolyzed. (Cotton swabs were tried but proved not only too resistant, but they varied considerably in susceptibility.) The temperature and pH employed in this assay are optimum and closely approximate the conditions of the kinetic studies.

C_1 activity or filter paper activity (FPACT) is the "total" carbohydrate (TCARB) liberated by hydrolysis of filter paper. The measured quantity is the filter paper optical density (FPOD*) which can be converted to C_1 activity by Figure 4-2 or equation (4-2). The assay curves in Figure 4-3 plot optical density directly as a function of the enzyme concentration.

The actual assay procedure is simple, but it does involve several sequential manipulations. A 0.2 ml sample of enzyme solution is placed in a small test tube with 0.2 ml of β-glucosidase solution. The β-glucosidase converts to glucose any cellobiose formed by the action of the enzyme on the substrate. The assay tube is placed in an ice bath and 2.0 ml of buffer are added. A 1 cm by 6 cm strip of Whatman No. 1 filter paper is rolled and added to the cold reactants in the assay tube. The ice bath reduces

the reaction rate sufficiently so that several assay tubes can be prepared simultaneously. After addition of the filter paper the assay tube is incubated at 50°C for 1 hour. The assay tube is transferred to an ice bath to halt the reaction until the filter paper can be removed. A microsample (0.2 ml) is then used with the Glucostat procedure to determine the total carbohydrate optical density, which in this case is termed FPOD.

Filter paper optical density is plotted as a function of adsorbable enzyme protein in Figure 4-3. The curve loses linearity at higher enzyme concentrations because of substrate limitations caused by depletion of the amorphous fraction of the filter paper cellulose. Assay of a strong enzyme solution should, therefore, use only a 0.1 ml sample, or be diluted prior to the C_1 assay.

Since the assay was developed to determine enzyme concentrations in a hydrolysis broth, provision had to be made to "blank out" the carbohydrate present in the solution at the time of the enzyme assay. To this effect a series of blanks were run along with the enzyme assays. These were handled similarly to the assay tubes except that no filter paper was added. These blank optical densities, FBOD, correct for the residual carbohydrate. The net carbohydrate optical density produced during the assay is

$$FPOD = FPOD^* - FBOD \qquad (4\text{-}4)$$

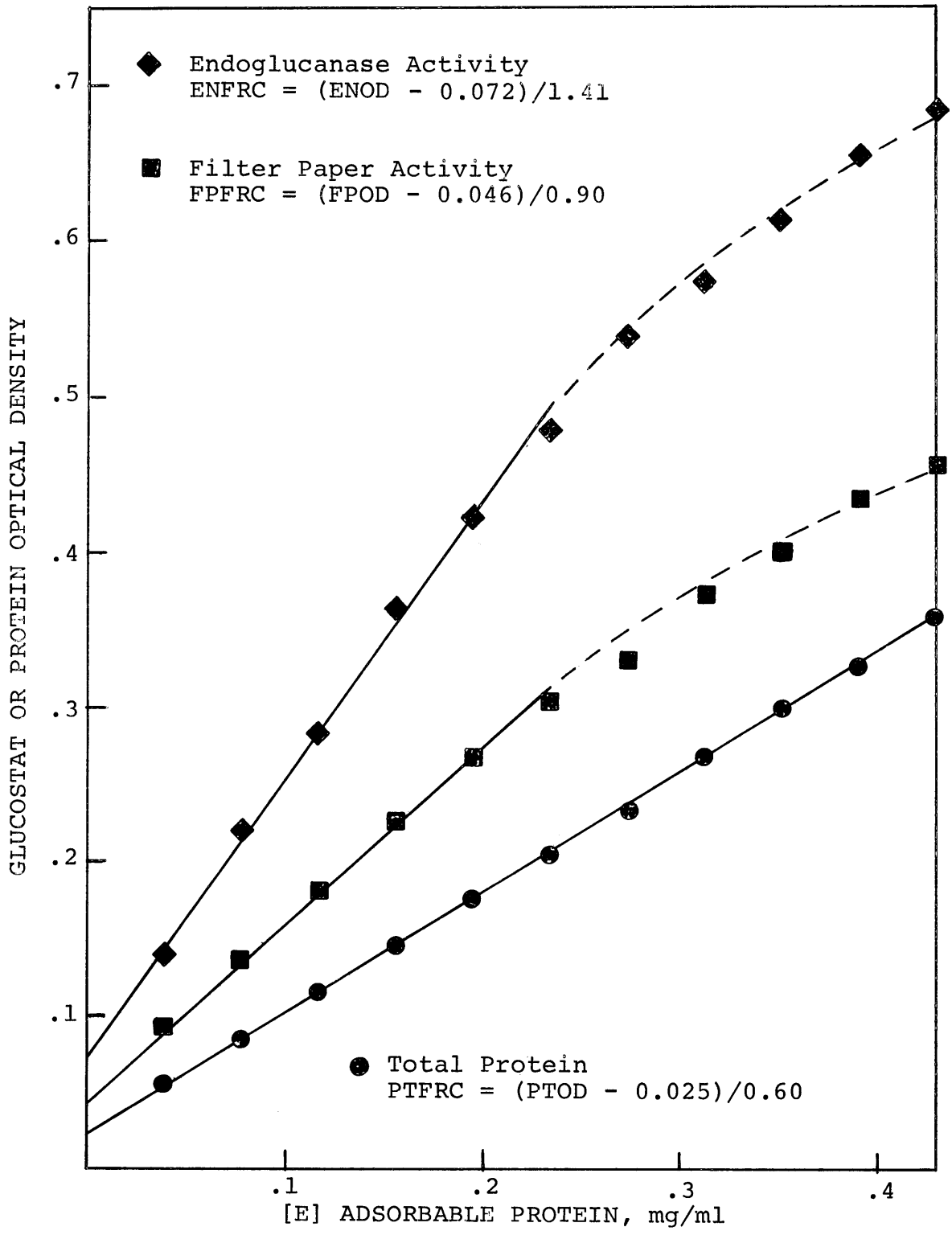

Figure 4-3. Assay Optical Densities

where FPOD* is the measured filter paper optical density.

Comparison of the filter paper blanks and the total carbohydrate values for the first eight hydrolysis runs indicated that the blank FBOD could be calculated from the corresponding TCOD value.

$$FBOD = (TCK/FPDIL)(FPK/0.05)(TCOD) + 0.035 \quad (4\text{-}5)$$

where TCK and FPDIL are the "total" carbohydrate and filter paper dilution factors respectively. FPK, usually 0.2, is the sample volume used in the filter paper assay. (Since TCOD utilizes a 0.1 ml sample for incubation and a similar sample for glucose determination, the resultant optical density is only 25% of the equivalent value had 0.2 ml samples been used as in the filter paper assay. The FPK/0.05 factor adjusts for this.) The net optical density, FPOD* - FBOD, determines the actual enzyme activity. This net optical density, FPOD, is related to the enzyme "mixture" fraction, FPFRC, by

$$FPFRC = [(FPOD - 0.046)/0.9](0.2/FPK) \quad (4\text{-}6)$$

This relationship is a linear approximation to the curve in Figure 4-3 and is accurate only below enzyme concentrations of 0.195 mg/ml adsorbable protein.

2. Endo-β-1→4 glucanase Assay

The endoglucanase assay measures the ability of the enzyme complex to hydrolyze soluble cellulose. Endoglucanase activity (ENACT) is the amount of "total" carbohydrate (cellobiose hydrolyzed to glucose by β-glucosidase) released by the enzyme during hydrolysis of carboxymethylcellulose. The CMC used was provided by the Hercules Powder Company and had a degree of substitution of 0.4.

The assay procedure is generally similar to the C_1 assay. A 0.1 ml sample is placed with 0.2 ml of β-glucosidase solution (see Cellobiose Determination) in a small test tube. The assay tube is then placed in an ice bath and 2.0 ml of cold CMC solution (1% in 0.05 M, pH 4.9 phosphate buffer) is added and mixed. The assay is then incubated at 50°C for 30 min followed by transfer to an ice bath. As quickly as possible a 0.1 ml sample is transferred to a test tube containing 2.0 ml of pH 7 Tris buffer (also in an ice bath) whereupon the Glucostat reagent is added and the optical density (ENOD*) determined. The combination of low temperature and neutral pH lowers the reaction velocity by a factor of 20 (see Appendix B: Effect of pH and Temperature) to enable the handling of multiple samples.

The net endoglucanase activity optical density (ENOD) versus enzyme concentration (ENFRC) curve is also shown in Figure 4-3. The loss of linearity at T.v. "mixture" con-

centrations greater than 0.195 mg/ml results from substrate limitations (a DS of 0.4 means 40% of the glucose residues are substituted, thus, at least 40% of the CMC is nonhydrolyzable) and from equilibrium between glucose and cellobiose (see Cellobiose Determination). The endoglucanase curve can be approximated by

$$ENFRC = ENK(ENOD - 0.072)/1.41 \qquad (4\text{-}7)$$

where ENK is the dilution factor employed at high enzyme concentrations. When the initial sample is undiluted ENK is 1.0. An enzyme solution of 0.78 mg/ml would require a 1:4 dilution so that the result would fall on the linear portion of the standard curve. ENK would therefore equal 4.0.

ENOD, the net endoglucanase optical density, is the difference between the measured optical density, ENOD*, and the optical density contributed by residual carbohydrate (NBOD). Unlike the filter paper blank, FBOD, NBOD can not be computed from TCOD and the proper dilution factors because the endoglucanase assay is incubated for only 30 min versus 60 min for TCOD. An actual blank had to be run with the first hydrolysis studies by replacing the CMC solution with buffer and performing the remainder of the endoglucanase assay. A comparison of corresponding NBOD and TCOD values enabled computation of the endoglu-

canase blank as

$$NBOD = 0.36(TCK/9.6)(TCOD)/ENK + 0.010 \qquad (4\text{-}8)$$

3. Lowry Protein Assay

A method for determining protein solution concentration was developed as a check on the enzyme assays. Two methods were explored: the modified biuret of Itzhaki and Gill (99) and the technique of Lowry et al. (139). The latter method was chosen because it is an order of magnitude more sensitive than the biuret technique. The biuret reaction depends upon the number of peptide bonds and, therefore, is independent of the amino acid residues. The Lowry reaction on the other hand, depends upon the few ring containing amino acids. The biuret method is useful in estimating protein when no standard is available. Both methods suffer one serious disadvantage: carbohydrate interferes with the analysis and enhances the apparent optical density due to protein as shown in Figure 4-4. PTOD, the actual protein optical density is determined by interpolating between the curves according to the total carbohydrate present (see Appendix J).

The measured protein optical density (PTOD*) is determined by placing 0.2 ml of sample in a test tube to which is added 3.0 ml of carbonate reagent (2.0% Na_2CO_3 in

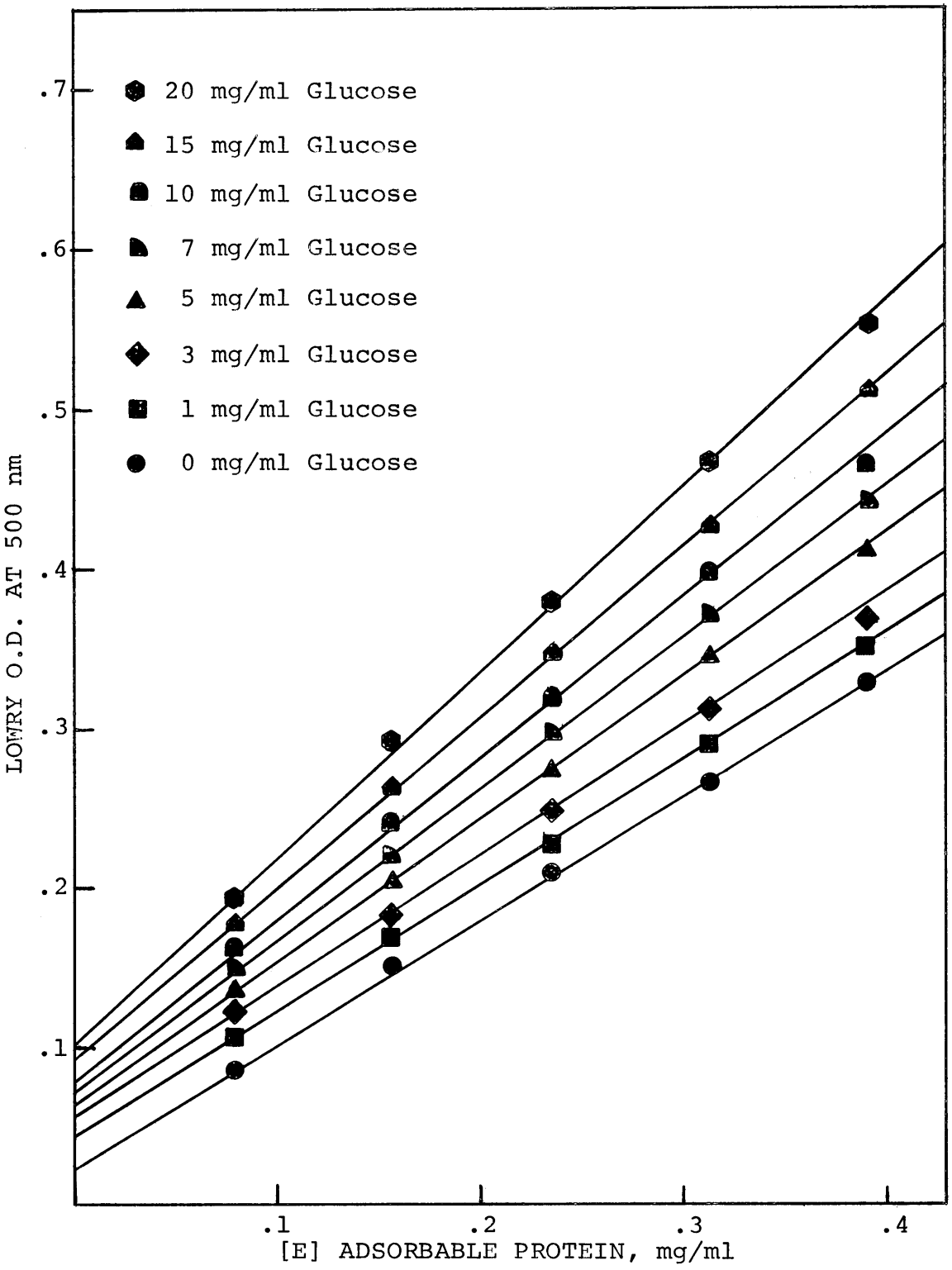

Figure 4-4. Effect of Glucose on Lowry Protein O.D.

0.1 N NaOH). After 30 min 0.3 ml of 1 N Folin Phenol Reagent (Fisher Scientific Inc.) is added to the test tube. The optical density (PTOD*) must be read at 500 nm 30 min later. The protein standard curve (at zero carbohydrate) also given in Figure 4-3 is

$$PTFRC = (PTOD - 0.025)/0.60 \qquad (4\text{-}9)$$

where PTOD is the measured optical density corrected for the carbohydrate present and PTFRC is the enzyme concentration.

A standard curve was constructed with bovine serum albumin (BSA). The enzyme PTOD is equated with the BSA O.D. to determine enzyme protein as BSA equivalent.

V. EXPERIMENTAL APPARATUS AND PROCEDURE

The hydrolysis apparatus consisted of a stirred tank reactor, a constant speed agitator and a temperature bath. Peripheral equipment consisted of sampling apparatus, reagent addition equipment, a water bath and a spectrophotometer.

A. Hydrolysis Equipment

The reactor itself is diagramed in Figure 5-1. It consisted of a 200 ml pyrex jar. A worm clamp was modified by soldering 4 screws at 90° intervals. The clamp was attached to the jar with the lugs projecting above the lip to provide a means of fastening the reactor cover. (A piece of tape was wrapped about the jar to increase friction between the clamp and the jar.) The reactor top was of plexiglas with holes corresponding to the lugs on the clamp. A 3/4 in. hole was bored in the center of the top. This was fitted with a piece of 3/4 in. plastic rod that had been bored to 3/8 in. ID. This standpipe provided for expansion of the material within the reactor without overflowing and hindered evaporation by reducing the opening around the propeller shaft. A similar standpipe of 1/2 in. rod with a 1/4 in. hole was offset to provide a sample port. This was stoppered except when samples were removed. A neoprene gasket was cut with holes matching

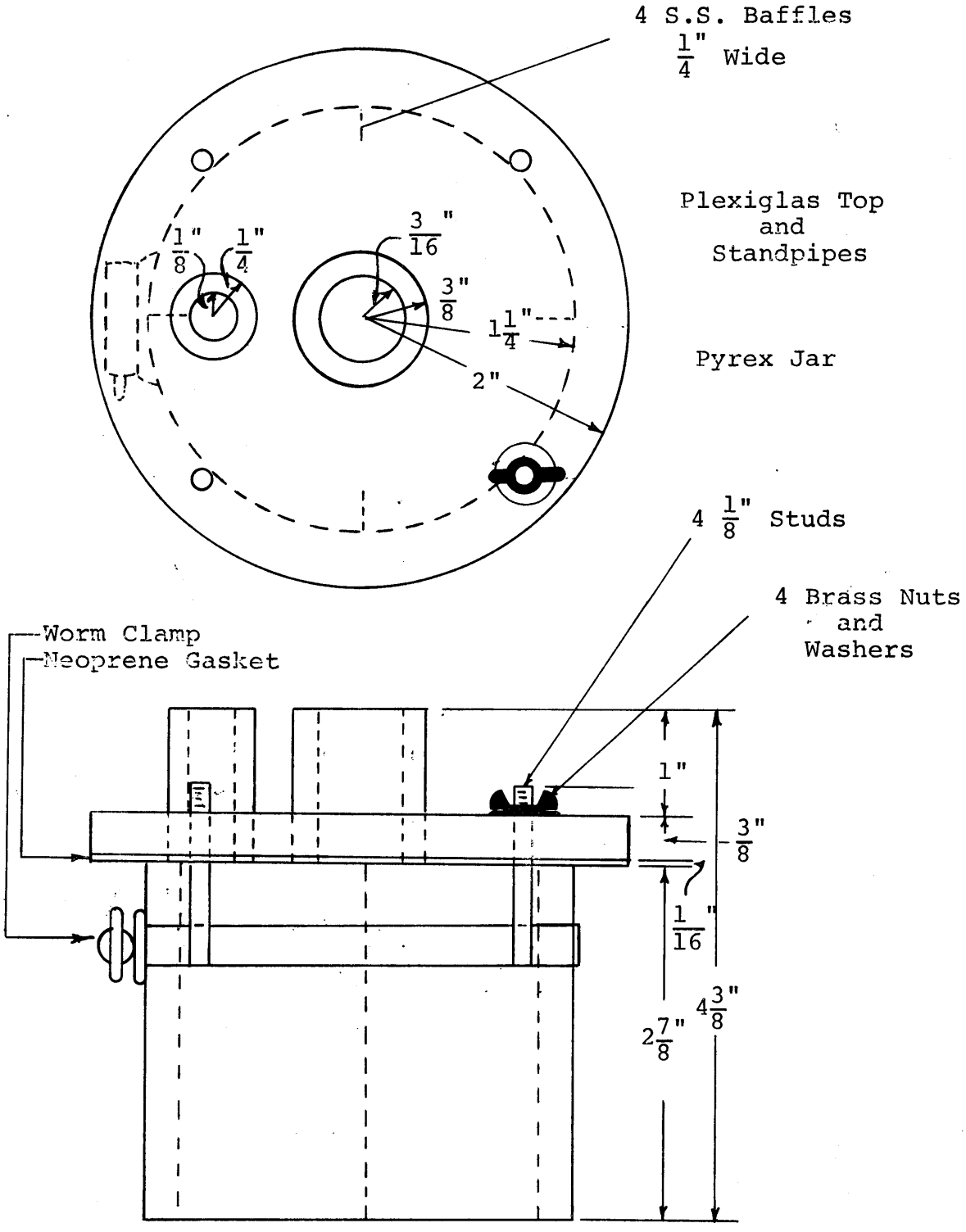

Figure 5-1. Detail of Hydrolysis Reactor

those in the top. The reactor was equipped with 4, 1/4 in. stainless steel baffles.

The agitator was a stainless stell 1 in., 4-bladed propeller on an 8 in. long, 1/4 in. diameter stainless steel shaft. This was fitted in the chuck of a Cole Parmer standard Servodyne agitator. This solid state unit controlled the agitator speed and provided constant RPM indication.

B. Peripheral Apparatus

The sampling apparatus consisted of a probe and a filtration unit. The probe was a 2 ml volumetric pipet from which the the tip had been removed. The probe was bent at an 80° angle above the volume bulb. Vacuum was applied to the probe by a rubber pipet filler. The probe was inserted into the sample standpipe and an aliquot removed. Since this was representative of the reactor mixture the cellulose had to be separated from the liquid to halt the reaction. For this reason the sample was released into a fine sintered glass Buchner funnel and vacuum applied. The filtration was collected in a test tube taking care that the vacuum was broken before the filtrate began to foam. The tube was covered and set aside for analysis as discussed in IV, Assay Procedures. The funnels were then rinsed with tap water to remove the cellulose. Dilute hydrochloric acid (1 N) solution fol-

lowed by distilled water was run through the funnels which were then dried.

Samples were withdrawn from the filtrate tubes for each different assay. This was accomplished with a BBL Pipetor equipped with disposable polyethylene tips. This apparatus could transfer either 0.1 ml or 0.2 ml samples. Sample size was reproducible to plus or minus 1% although material would occasionally remain in the tip causing as much as 10% error. Tips were reused or discarded at the discretion of the operator. This method appeared more accurate and reproducible than standard pipets or "Grunbaum" pipets which were more susceptible to operator error.

Reagents were initially added from three-way burets equipped for refilling from overhead reservoirs. These proved inadequate because of the variation in quantity caused by operator error. A superior method was found in Cornwall Syringes. These are standard syringes in a spring loaded holder that can be locked to deliver a fixed amount of reagent. A check valve chamber is located between the barrel of the syringe and the tip allowing continuous action. One valve is between the chamber and a rubber filling tube equipped with a weight. This tube is placed in a reagent reservoir. The check valve allows passage of reagent from the reservoir only into the chamber. A similar check valve allows passage of reagent from the chamber to the tip but prevents back flow. These

syringes are accurate to 1% and reproducible to plus or minus 0.5%. A Cornwall syringe was provided for each of the major reagents.

All of the assay procedures required the measurement of solution optical density. This was accomplished with a Coleman Model 111 UV-Visible Spectrophotometer. This instrument produced a wavelength accurate to plus or minus 0.5 nm and reproducible to plus or minus 0.1 nm. An aspirator was used to rapidly remove waste samples from the cuvets to increase operating speed. Under normal conditions approximately 150 to 200 samples could be read in an hour. Only three cuvets were used for samples as the fourth cuvet was a blank usually filled with distilled water. A separate aspirator bottle with a glass transfer tube and suction tip instead of rubber and metal was provided for use with the phenol sulfuric acid assays.

C. Procedure

The cellulose employed for the hydrolysis studies was a ball milled Spruce wood pulp, Solka Floc BW-300, obtained from Brown Company, Berlin, New Hampshire. The cellulose was swollen overnight in 0.05 M, pH 4.9 phosphate buffer (hereafter referred to as buffer). The enzyme was a Trichoderma viride fermentation broth as described in Appendix I: Enzyme Production.

Dry cellulose was weighed into a reactor and the

desired amount of buffer added. After complete mixing the baffles and propeller were added and the cover screwed tight. Vacuum grease was applied to the lip of the reactor and between the neoprene gasket and the cover to insure a complete seal.

After standing overnight the reactor was then placed in a constant temperature bath in a worm clamp holder that positioned the agitator directly beneath the motor. After placing the propeller shaft in the chuck and leveling the reactor the agitator was switched on to the desired RPM. At time zero enzyme was added to the reactor through the sample standpipe. A piece of glass tubing connected by tygon tubing to a glass funnel facilitated this operation. With extremely high cellulose concentrations the agitator speed was increased to 1800 RPM for a few seconds to completely mix the enzyme and cellulose solutions.

Samples were withdrawn at time t as discussed above. The initial rate was examined by taking samples every 30 sec for 4 min, then every minute until 6 min, at which time the interval between samples was extended to 2 min. The sample interval increased as the rate was expected to decrease to give reasonable changes in carbohydrate concentration between samples.

VI. REDUCTION OF HYDROLYSIS DATA

The various hydrolysis runs are discussed in Chapter VII. The complete sequence from raw sample to hydrolysis curve data point to rate constant, however, is a complicated one. This brief chapter outlines the procedure followed.

A. Transformation of Raw Sample to Usable Data

The original sample was the filtrate of the material removed from the hydrolysis reactor. This sample contained glucose, cellobiose, cellulose fragments, enzyme protein and residual protein. The assay procedures discussed in Chapter IV were developed to determine the concentrations of these various species. As shown in Figure 6-1, each of the diagnostic procedures required some or all of the following steps:

1. Transfer of a microsample of filtrate to a test tube;
2. Addition of reagents;
3. Incubation;
4. Transfer of a microsample from the incubated test tube to another tube;
5. Addition of a second set of reagents;
6. Incubation;
7. Determination of optical density.

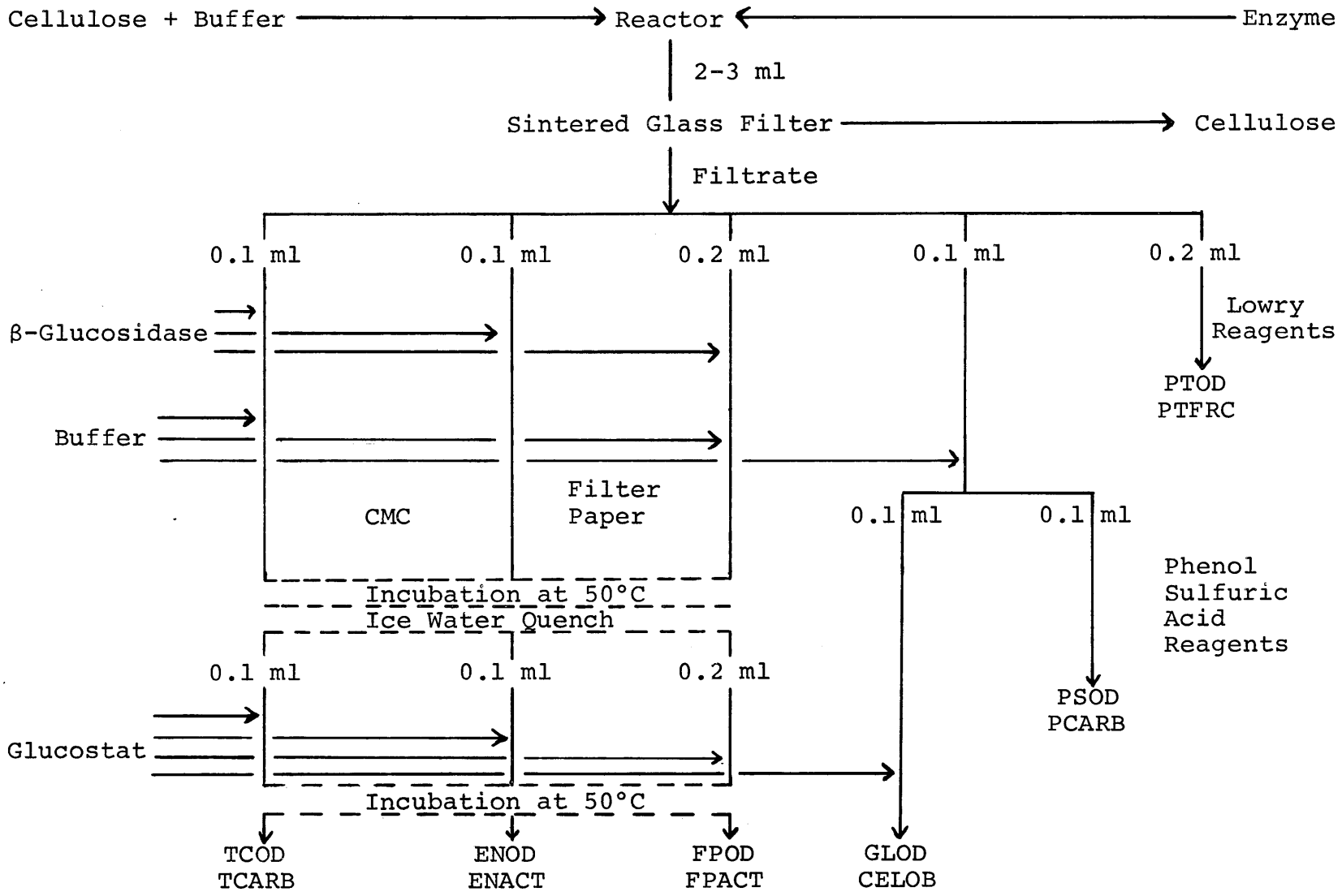

Figure 6-1. Schematic Diagram of Sample Analysis

All samples were, therefore, finally reduced to a series of optical densities. These were then converted to more usable quantities by the equations developed in Chapter IV as follows:

PSOD → PCARB, the total soluble carbohydrate

TCOD → TCARB, the total concentration of glucose and cellobiose converted to glucose

GLOD → GLUCO, the total concentration of glucose and unconverted cellobiose

PTOD → PTACT, the total protein as equivalent to bovine serum albumin (BSA)

ENOD → ENACT, the TCARB value produced by endoglucanase in the sample acting on soluble cellulose, carboxymethylcellulose (CMC)

FPOD → FPACT, the TCARB value produced by the enzyme complex acting on insoluble cellulose, filter paper; a measure of C_1 concentration

The PCARB and TCARB values were used to establish the hydrolysis curves discussed in Chapter VII. The GLUCO values were used with the corresponding TCARB values to calculate the individual cellobiose and glucose concentrations. PTACT was the concentration of total protein remaining in solution. This included enzyme protein and residual protein. The amount of protein adsorbed by the cellulose, the difference between the initial total protein and the total protein in solution, was considered adsorb-

able enzyme protein. This protein was approximately 64% of the total protein. The difference between the initial enzyme concentrations and those in solution at any time allowed determination of the enzyme participating in hydrolysis.

B. Logical Basis of the Kinetic Model

The shape of the hydrolysis curves indicated that more than one type of substrate was being hydrolyzed. The cellulose substrate was, therefore, divided into i fractions according to the ease of hydrolysis. The basis of the kinetic model was that the hydrolysis reaction could be described by a series of equations whereupon the hydrolysis rate of C_i would be proportional to the concentration of C_i remaining. The proportionality constants k_i would be the observed rate coefficients. As Will be discussed in Chapter VIII, this hypothesis can be expressed mathematically as

$$- \frac{dC_i}{dt} = k_i C_i \qquad (6-1)$$

or

$$- \frac{dC_i}{C_i} = - d \ln C_i = k_i dt \qquad (6-2)$$

The hypothesis predicts that a plot of $-\ln(C_i/C_{i_o})$ versus time should be linear in the region i where the majority of the carbohydrate produced results from hydrolysis of C_i . The slope of the plot would be the observed rate coefficient k_i . The hydrolysis of each cellulose fraction becomes controlling as the concentration of the immediately more reactive fraction is reduced through hydrolysis. Rate constants normally determined in this manner assume proportionality from time zero. In this case, however, the porportionality begins at various times after some of the material has been hydrolyzed. The amount of substrate i at any time t must therefore be known in order to calculate the observed rate coefficient from the instantaneous slopes of the hydrolysis curves.

C. Error Analysis

The kinetic model is only as accurate as the data itself. Since all of the data involved the use of a spectrophotometer, this instrument provided a common source of error. The instrument used was reproducible to better than 1%. The individual samples, however, were dependent upon addition of reagents, dilution errors, and sample transfer errors.

As can be seen in Tables 6-1 and 6-2, the Glucostat procedure for glucose and TCARB determinations, one standard deviation gives better than plus or minus 4% accuracy.

TABLE 6-1. REPRODUCIBILITY - GLUCOSE

Glucose mg/ml	Optical Censities at 415 nm.	Avg. O.D.	1 S.D. O.D.	95% Limit
.01	.007 .031 .006 .007 .010 .006 .004 .007 .009 .012	.008	.003	.002- .014
.02	.019 .014 .015 .018 .011 .018 .019 .017 .015 .017	.016	.002	.012- .020
.03	.020 .030 .023 .028 .026 .024 .023 .026 .027 .028	.026	.033	.020- .032
.05	.045 .044 .046 .045 .050 .049 .045 .044 .048 .049	.046	.002	.042- .050
.07	.068 .068 .068 .069 .067 .069 .069 .071 .064 .067	.068	.001	.066- .070
.10	.111 .104 .103 .098 .095 .106 .098 .101 .105 .103	.103	.004	.095-
.10	.099 .103 .107 .105 .104 .101 .098 .104 .105 .104 .105			.111
.20	.228 .221 .221 .214 .221 .219 .221 .226 .226 .214 .219	.221	.005	.211- .231
.30	.340 .342 .342 .342 .347 .349 .343 .343 .358 .337 .342	.346	.006	.334- .358
.50	.598 .594 .598 .600 .600 .590 .606 .608 .607 .585 .595	.598	.007	.584- .612
.70	.810 .806 .783 .790 .825 .805 .768 .793 .848 .830 .827	.810	.024	.757- .858
1.00	1.25 1.27 1.26 1.26 1.27 1.27 1.26 1.27 1.30 1.30 1.27	1.27	0.16	1.24- 1.30

TABLE 6-2. REPRODUCIBILITY - CELLOBIOSE

Cellobiose mg/ml	Optical Densities at 415 nm	Avg. O.D.	1 S.D. O.D.	95% Limit
0.104	.012 .009 .008 .011 .014 .008 .010 .011 .010 .009	.010	.002	.006- .014
0.208	.019 .020 .024 .021 .022 .023 .024 .021 .018 .022	.021	.002	.017- .025
0.312	.029 .034 .035 .035 .035 .037 .034 .034 .033 .035	.034	.002	.030- .038
0.52	.058 .060 .062 .060 .058 .054 .062 .059 .060 .061 .059	.060	.001	.058- .062
0.73	.084 .085 .086 .085 .086 .087 .086 .089 .083 .086	.086	.002	.082- .090
1.04	.125 .120 .124 .120 .122 .111 .125 .121 .122 .125 .115	.122	.002	.118- .126
1.04	.131 .129 .126 .122 .128 .113 .125 .131 .128 .128 .125	.127	.002	.123- .131
2.08	.245 .250 .244 .246 .245 .237 .250 .245 .248 .244 .245 .240	.246	.002	.242- .250
3.12	.348 .350 .350 .350 .352 .338 .358 .358 .360 .359 .360 .340	.355	.005	.345- .365
5.2	.532 .542 .535 .542 .538 .535 .538 .540 .540 .541	.538	.003	.529- .547
7.3	.705 .705 .710 .695 .700 .713 .695 .697 .695 .695	.701	.007	.687- .715
10.4	.910 .895 .912 .911 .883 .881 .920 .920 .912 .900	.904	.014	.876- .932

Most of the error was in the transfer of a measured sample from the dilution tube to the reaction tube.

Most of the data were within plus or minus 2% with occasional points much more inaccurate. These resulted from double sample addition or dilution, nonaddition of reagents, loss of material due to splashing, etc. The major cause of these "ridiculous" errors was the large number of samples run at any one time.

The average hydrolysis run required over 40 time samples. The determinations mentioned in the initial part of this chapter required at least six different procedures for each time sample. Five required transfer of the time sample to an intermediate tube for dilution and/or reaction, followed by transfer to a fresh tube for final reaction. The sequential sample transfer magnified possible errors. In addition, the necessity to manipulate 500 test tubes required speed and dexterity which occasionally resulted in a missed test tube.

VII. RESULTS OF HYDROLYSIS STUDIES

A. Introduction

The experimental effort was separated into three areas. The first was to develop procedures to measure the products of reaction and enzyme concentrations in solution as previously discussed in Chapter IV: Assay Procedures. The second area was the elucidation of the kinetic resistances in order to model the hydrolysis reaction. The vehicle employed was a series of hydrolysis studies using agitator speed, and substrate and enzyme concentrations as the primary variables. The results of this series are included below. The third area of investigation was the development of a technique to measure the pore size distribution of materials in an aqueous environment. This last area is discussed in Chapter IX.

The series of hydrolysis runs is listed in Table 7-1. In the following paragraphs the term buffer refers to 0.05 M, pH 4.9 phosphate buffer and the term mixture refers to the basic Trichoderma viride cellulase enzyme mixture as discussed in Appendix I. The total protein of the mixture was 1.22 mg/ml measured as protein equivalent to bovine serum albumin (BSA). Only 64% of this protein would adsorb onto cellulose. Since this adsorption paralleled enzyme activity in solution enzyme protein was designated as adsorbable protein, which for the mixture was 0.78 mg/ml.

TABLE 7-1. HYDROLYSIS STUDIES

Run No.	RPM	Temp. °C	ml. Buff.	ml. Enz.	Type Enz.	gm. Cell.	% Cell.
1	200	51	100	100	mix	17.4	8
2	1800	"	"	"	"	"	"
3	200	"	"	"	"	"	"
4	1800	"	"	"	"	"	"
5	600	"	"	"	"	4.08	2
6	"	"	"	"	"	8.33	4
7	"	"	"	"	"	12.77	6
8	"	"	"	"	"	17.4	8
9	"	"	"	"	conc	"	"
10	"	"	150	50	3019	"	"
11	"	"	175	25	conc	"	"
12	"	"	175	25	mix	"	"
13	"	"	125	75	"	"	"
14	"	"	100	100	"	"	"
15	"	"	75	125	"	"	"
16	"	"	150	50	"	"	"
17	"	"	"	"	"	"	"
18	"	"	"	"	"	"	"
19	"	"	100	100	P.w.	"	"
20	"	"	150	50	mix	4.08	2
21	"	"	"	"	"	8.33	4
22	"	"	"	"	"	12.77	6
23	"	"	"	"	"	22.22	10
24	"	"	"	"	"	24.86	11
25	"	"	"	"	"	27.27	12
26	"	20	"	"	"	17.4	8
27	200	51	"	"	"	"	"
28	1800	"	"	"	"	"	"
29	600	"	"	"	"	8.33	4
30	"	"	175	25	"	2.03	1
31	"	"	"	"	"	4.08	2
32	"	"	"	"	"	6.03	3
33	"	"	"	"	"	8.33	4
34	"	"	"	"	"	10.5	5
35	"	"	"	"	"	12.77	6

TABLE 7-1. CONTINUED

Run No.	RPM	Temp. °C	ml. Buff.	ml. Enz.	Type Enz.	gm. Cell.	% Cell.
36	600	51	150	50	mix	4.08	2
37	"	"	"	"	"	6.03	3
38	"	"	"	"	"	8.33	4
39	"	"	"	"	"	10.5	5
40	"	"	"	"	"	12.77	6
41	"	"	"	"	"	17.4	8
42	"	"	100	100	"	12.77	6
43	"	"	"	"	"	15.05	7
44	"	"	"	"	"	17.4	8
45	"	"	"	"	"	19.48	9
46	"	"	"	"	"	22.22	10
47	"	"	"	"	"	27.27	12
48	"	"	0	200	"	22.22	10
49	"	"	"	"	"	27.27	12
50	"	"	"	"	"	32.56	14
51	"	"	75	75	conc	28.57	16
52	"	"	"	"	"	32.93	18
53	"	"	"	"	"	37.5	20
54	"	30	150	50	mix	17.4	8
55	"	40	"	"	"	"	"
56	0	53	"	"	"	"	"
57	600	51	0	100	"	2.04	2
58	"	"	12.5	87.5	"	"	"
59	"	"	25	75	"	"	"
60	"	"	37.5	62.5	"	"	"
61	"	"	50	50	"	"	"
62	"	"	62.5	37.5	"	"	"
63	"	"	75	25	"	"	"
64	"	"	87.5	12.5	"	"	"

The cellulose concentration was given in wt % of the total solution. The temperature was 51°C, the optimum as determined by Ghose (75), and the agitator speed was 600 RPM.

The measured quantities for each run included some or all of the following:

Reaction Products in Solution (see Assay Procedures):

PCARB (mg/ml): total soluble carbohydrate, including long chain fragments, as measured by phenol sulfuric acid technique

TCARB (mg/ml): sum of cellobiose and glucose as measured by the total carbohydrate technique

Glucose (mg/ml): calculated from TCARB

Cellobiose (mg/ml): calculated from TCARB

Enzyme Concentration in Solution:

FPFRC: fraction of C_1 activity (activity on crystalline cellulose) as compared to the raw T.v. mixture having an FPFRC of 1.0

ENFRC: fraction of endoglucanase activity (activity on soluble cellulose) as compared to the raw T.v. mixture having an ENFRC of 1.0

PTFRC: fraction of total protein as compared to the raw T.v. mixture having a PTFRC of 1.0

The substrate was Solka Floc BW-300, a ball milled Spruce wood pulp (Brown Company, Berlin, New Hampshire).

The material had a fairly uniform distribution of particles between 5μ and 20μ. There were few very fine particles of large agglomerates. Optical microscopy suggested that the cellulose particles were rough 16μ spheroids. Since Cellulose is a glucose polymer formed by the elimination of a water molecule for each glucose residue (mw = 180 - 18), the glucose equivalent of cellulose is obtained by multiplying the cellulose weight by 1.10 or wt % by 11.0.

B. Bulk Mass Transfer Studies

The purpose of the first series of hydrolysis runs was to determine the magnitude of the bulk mass transfer resistance. The agitator RPM was 200 for Runs 1 and 3, 1800 RPM for Runs 2 and 4, and 600 RPM for Runs 8 and 14. In addition Run 56 was accomplished without any agitation. All runs employed an equal amount of buffer and mixture to yield an initial enzyme fraction of 0.5. The cellulose concentration was 8%.

Figures 7-1 and 7-2 present the short term and extended effects of mixing. If mass transfer of enzyme from the bulk solution to the cellulose particles was a rate controlling factor, carbohydrate production should have increased with RPM as discussed in Appendix G. Similarly, if diffusion of reaction products from the particles to the bulk solution had been a major factor, a similar increase in rate with RPM should have been observed during

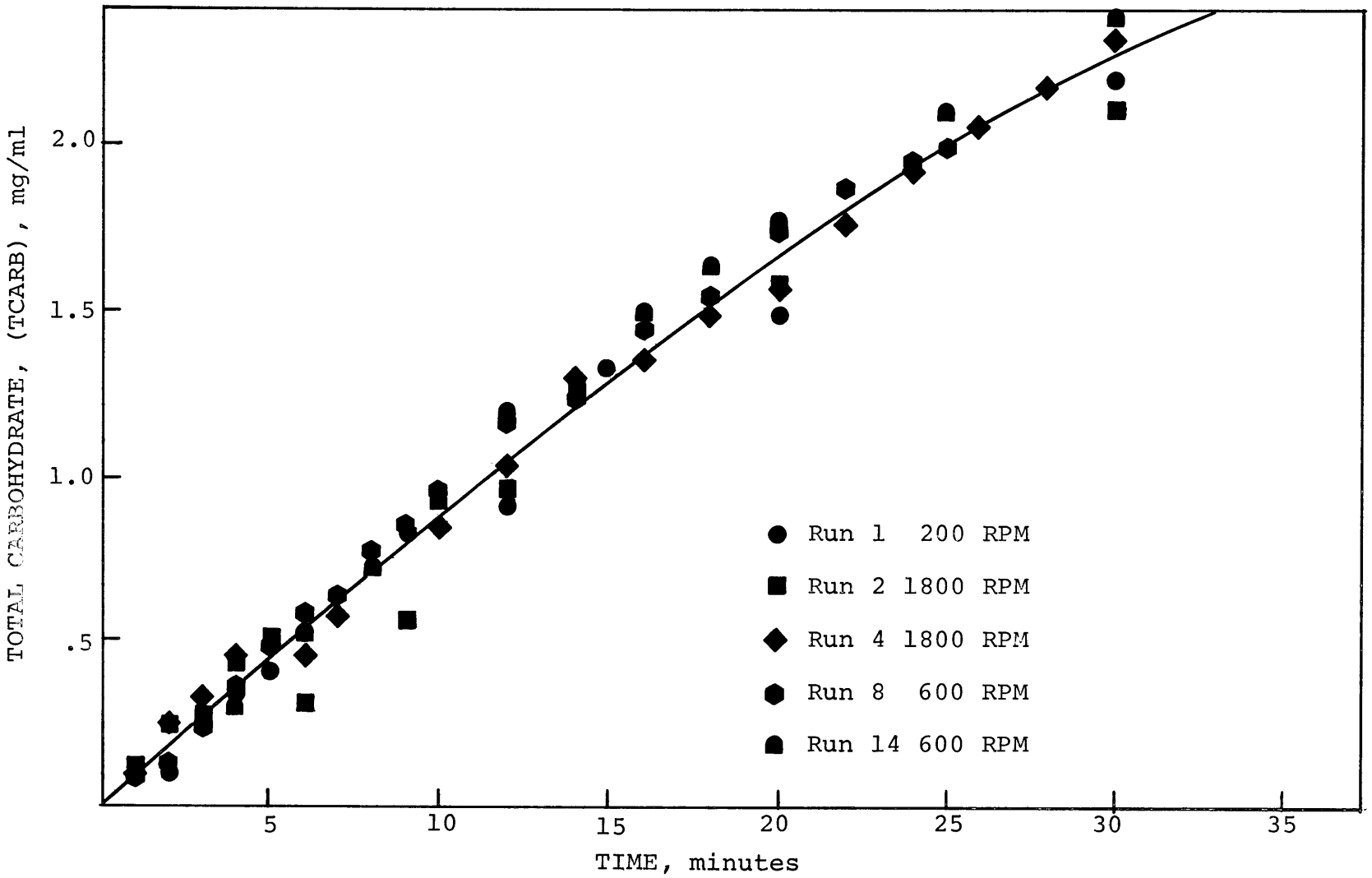

Figure 7-1. Effect of Agitation on Initial Rate of Hydrolysis

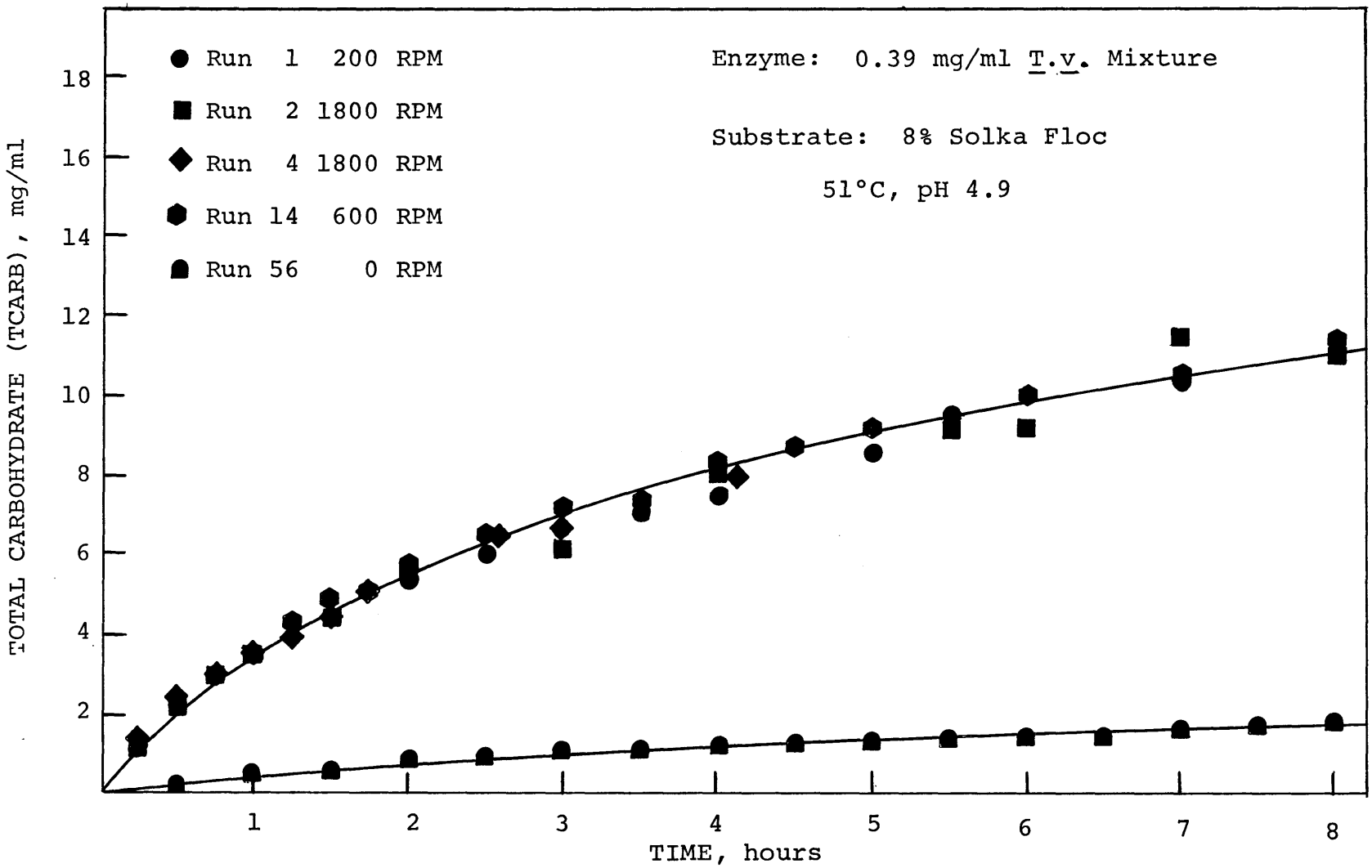

Figure 7-2. Effect of Agitation on Hydrolysis

extended hydrolysis. As can be seen from the Figures, diffusion of neither enzymes nor products appeared a controlling resistance to hydrolysis.

It should be noted that the data sets shown in Figure 7-2 were taken over a time span of six weeks. The near superposition of the data points is indicative of the high level of reproducibility found during the present study.

C. Effect of Enzyme Concentration

The second saccharification series, Runs 12 through 15 and 27, showed the overall effect of increasing enzyme concentration at a fixed cellulose concentration of 8%. The enzyme was the mixture diluted with different amounts of buffer to yield the various fractions indicated. Figure 7-3 is the total soluble carbohydrate (PCARB) produced as a function of time. Total hydrolysis would have resulted in a PCARB value of 88 mg/ml. An enzyme strength 5/8 of mixture, therefore, yielded 27% hydrolysis in 14 hours (Run 15).

The production of cellobiose and glucose (TCARB) for these same runs is shown in Figures 7-5 and 7-6. Note that TCARB is only one-half of the total soluble carbohydrate, indicating a significant concentration of polyglucose fragments longer than DP 5 (shorter fragments can be hydrolyzed to glucose by β-glucosidase). Calculations indicated that the cellobiose and glucose concentrations

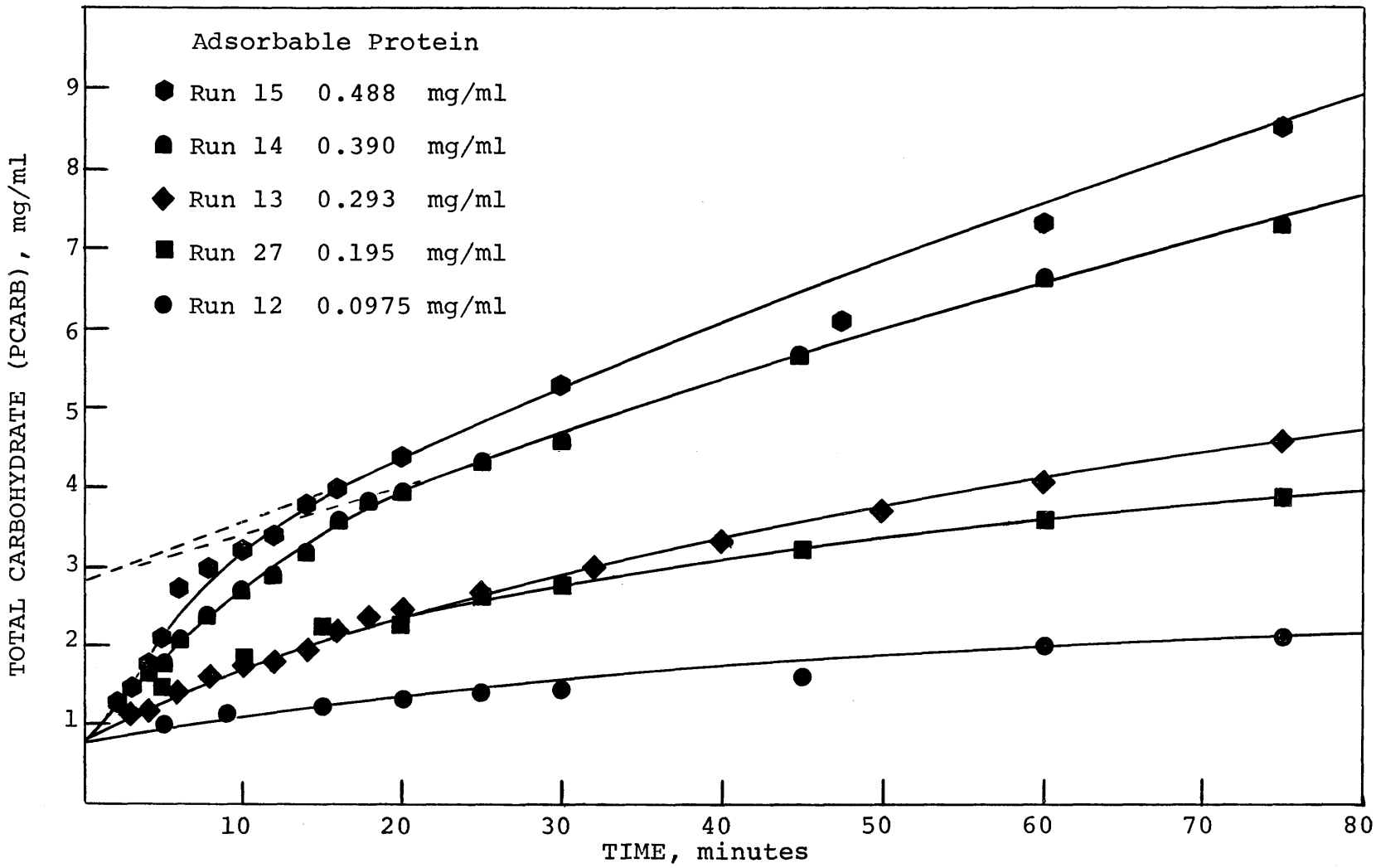

Figure 7-3. Production of Total Soluble Carbohydrate - Short Term

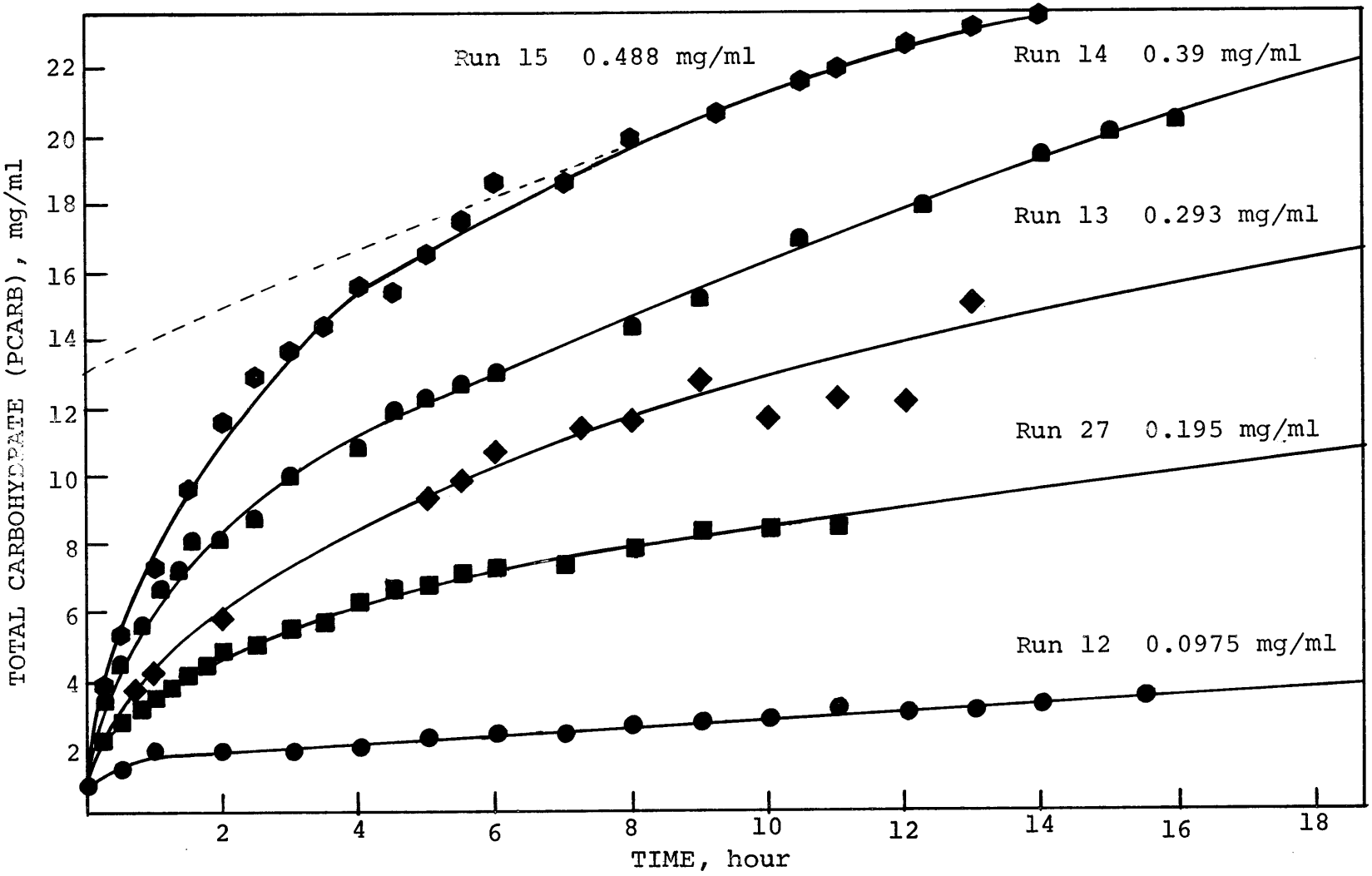

Figure 7-4. Production of Total Carbohydrate - Moderate Time

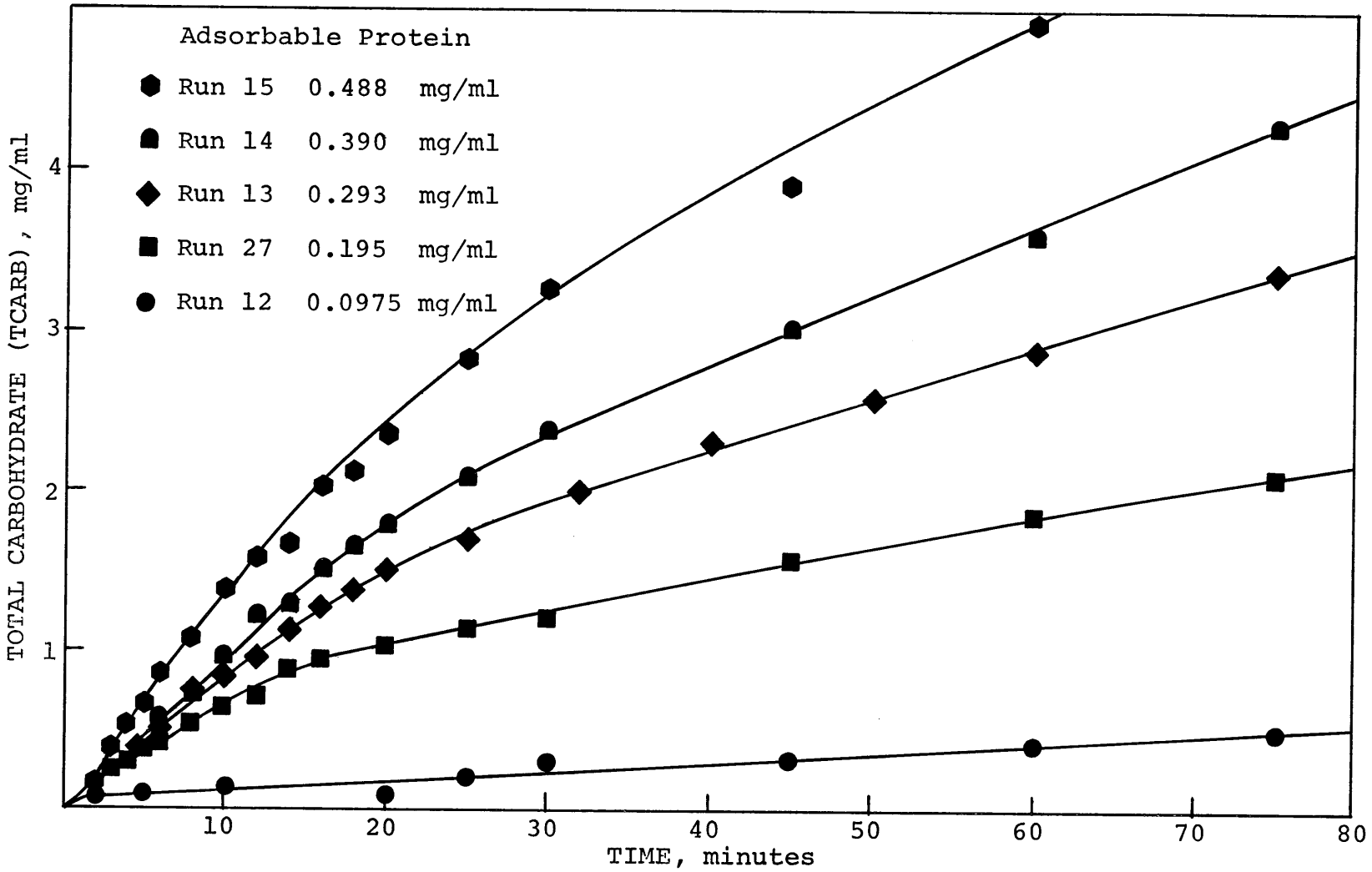

Figure 7-5. Production of Cellobiose and Glucose - Initial Hydrolysis

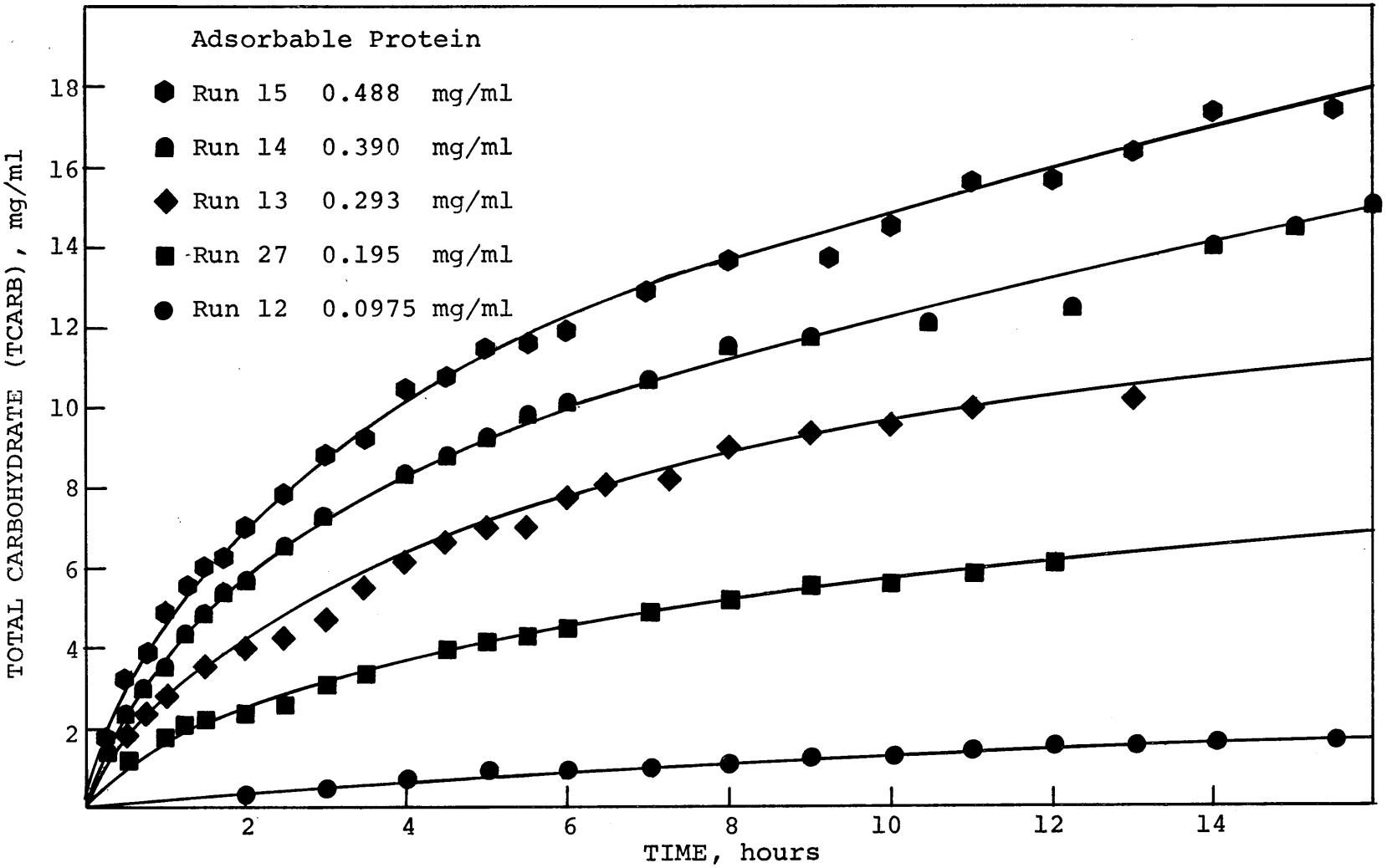

Figure 7-6. Production of Cellobiose and Glucose - Moderate Time

were approximately equal.

An initial time lag similar to that in Figures 7-3 and 7-5 is often observed in enzyme reactions requiring the action of two different enzymes in series. This supports the hypothesis that the action of the cellulase complex is initiated by the C_1 enzyme providing a point of attack for the glucanase enzymes, endoglucanase in particular. Note that the TCARB values were notably less than PCARB, but the shape of the curves was similar. This indicates a fairly constant ratio of glucose and cellobiose to total soluble carbohydrate.

D. Verification of the Kinetic Model

The kinetic model suggested in Chapter VI was based upon the hypothesis that the overall hydrolysis curve could be subdivided into three sections, b , c , and d , each first order with respect to cellulose C_b , C_c , and C_d respectively. (The determination of these fractions will be discussed in Chapter VIII.) This first order behavior should yield linear plots of $-\ln(C_i/C_{i_o})$ versus time for each Region i . As can be seen in Figures 7-7 to 7-9 such plots are indeed linear. The slopes of these curves yield the apparent rate coefficients k_i . Region d has been subdivided into Regions d_1 and d_2 for Run 15. Region d_1 is similar to b and c but proportional to cellulose C_d .

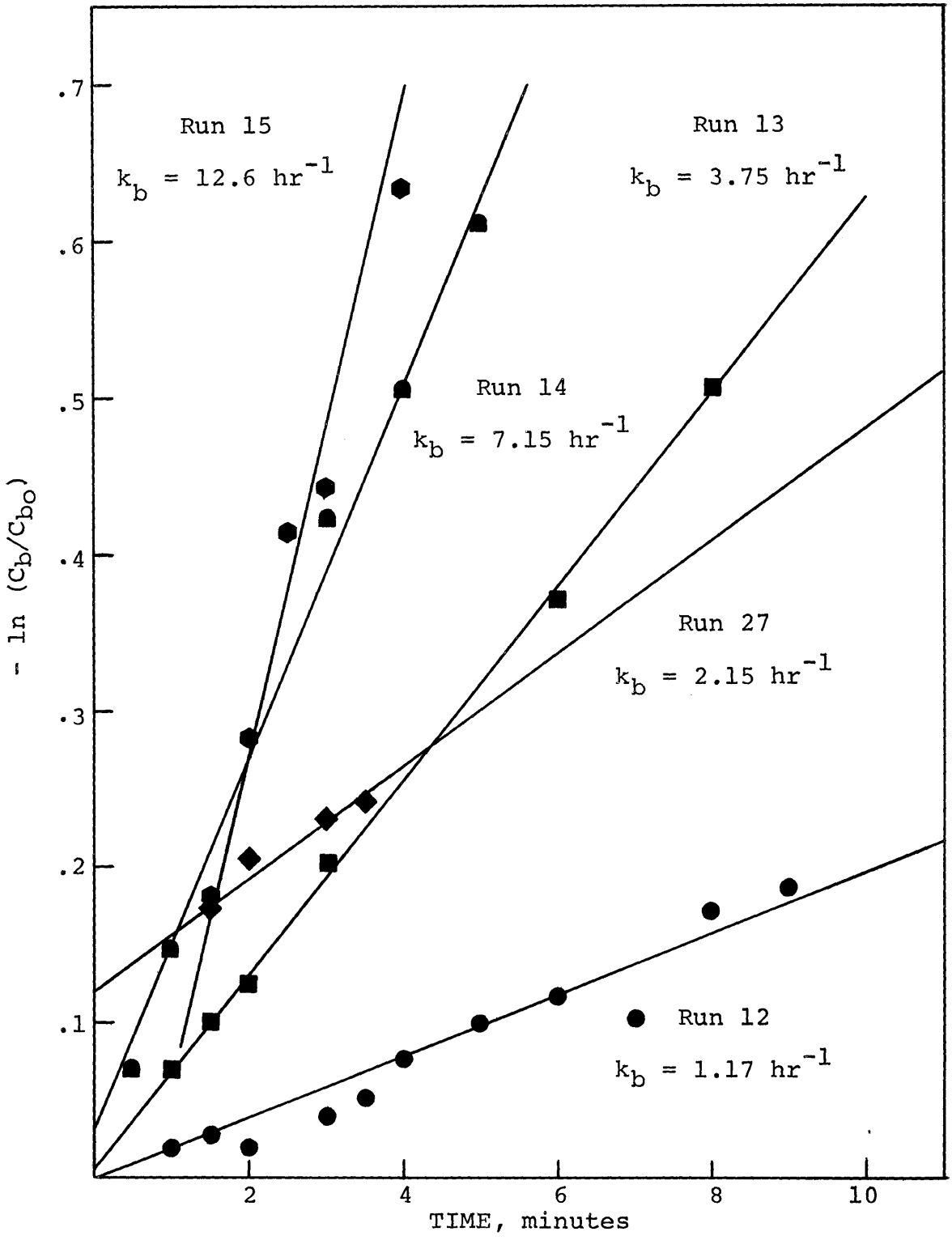

Figure 7-7. First Order Approximation for k_b

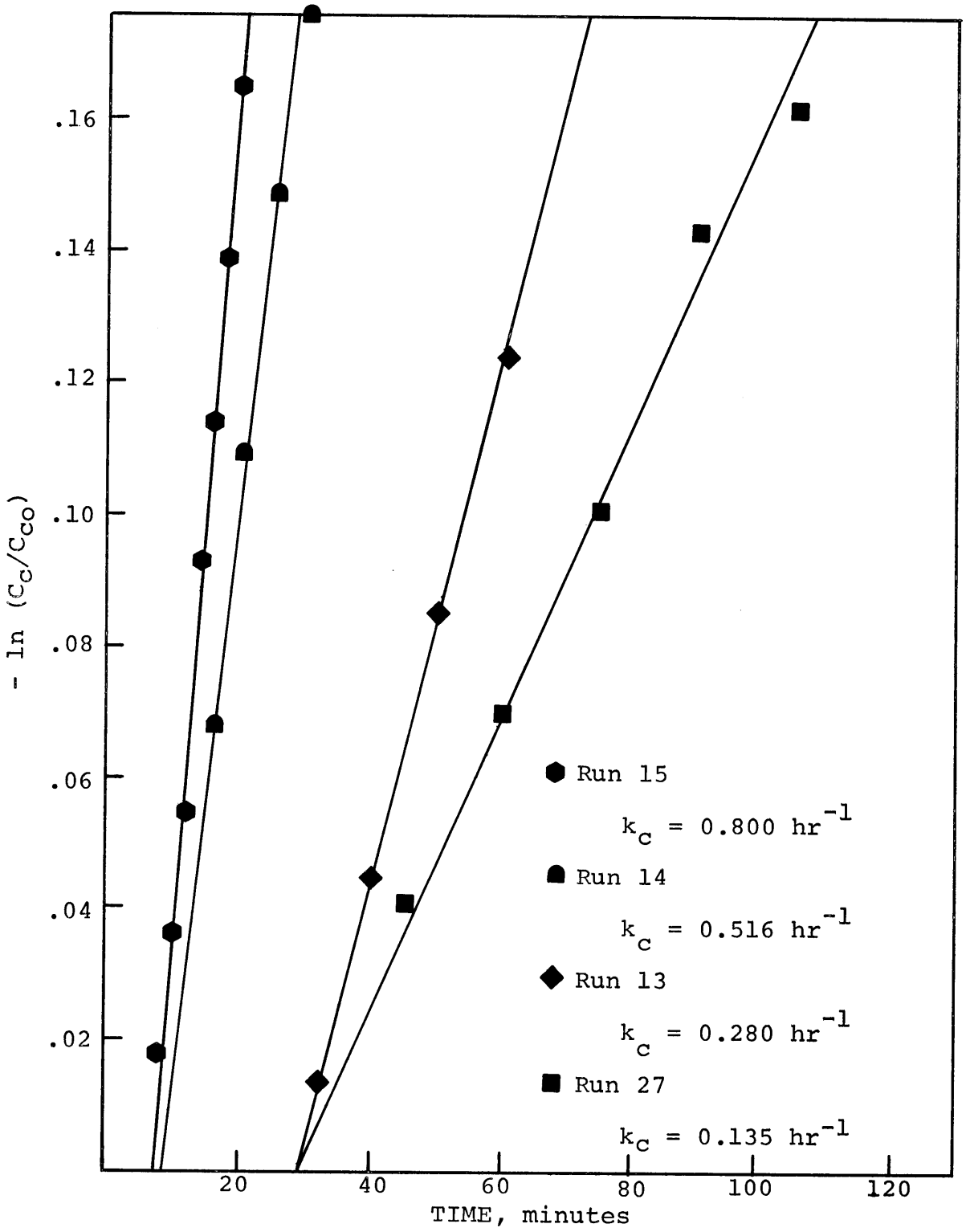

Figure 7-8. First Order Approximation for k_c

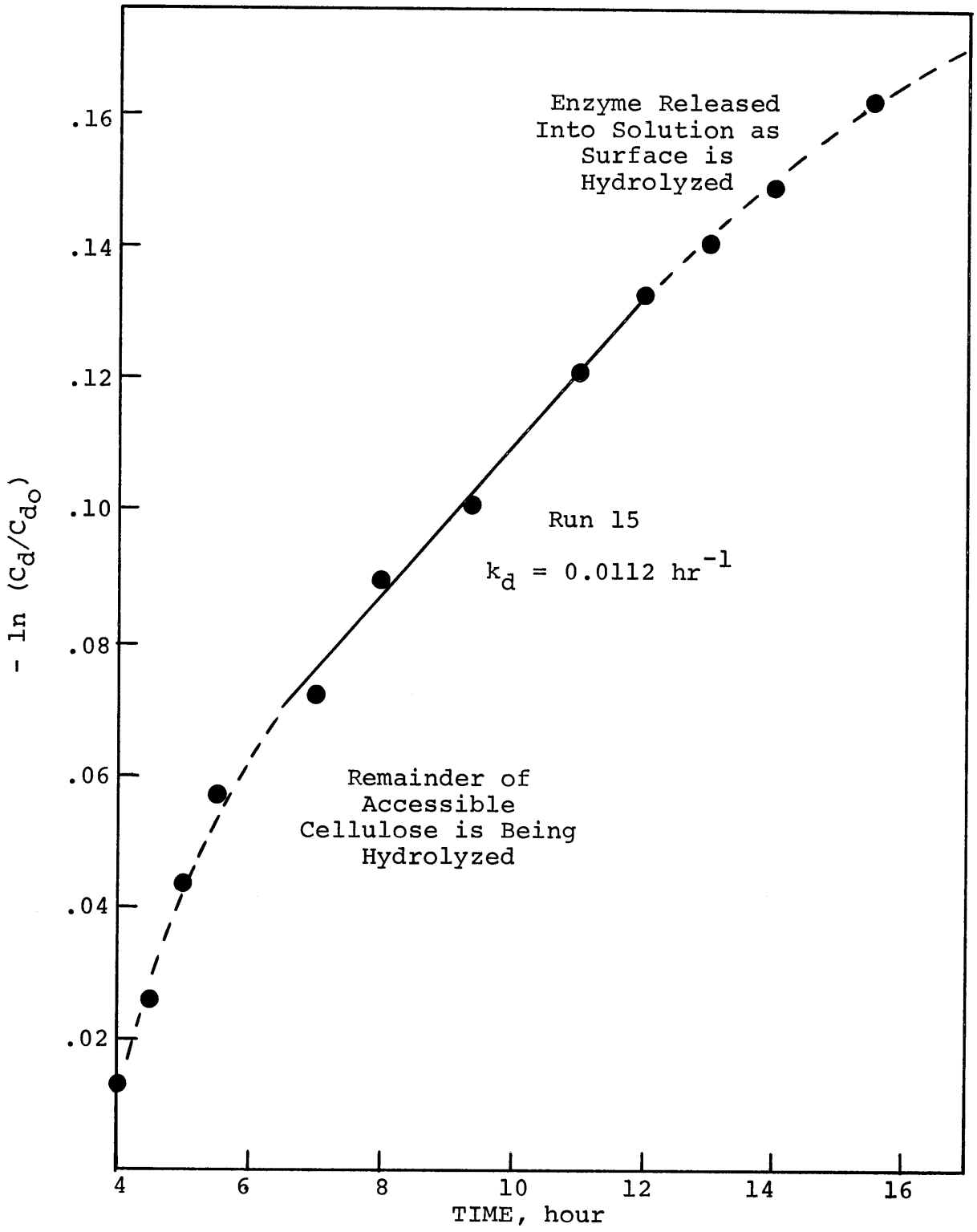

Figure 7-9. First Order Approximation for k_d

At some point, however, the amount of cellulose hydrolyzed has sufficiently reduced the surface so that all of the enzyme can not remain adsorbed, and therefore must begin diffusing into the bulk solution. With Run 15 this should happen at a PCARB value of 18 mg/ml or after about 10 hours. At this transition point, the enzyme concentration actually participating in the reaction becomes dependent upon the amount of cellulose remaining ($C_{d_2}{}^{n}$). Assuming a first order dependence of adsorbed enzyme with respect to cellulose remaining the overall proportionality would therefore go from first order (Regions b , c , and d_1) to $(1 + n)^{th}$ order with respect to cellulose.

As can be seen from Figure 7-9, Run 15 does exhibit transition points as shown by the dashed and solid lines. The slow hydrolysis rate after 10 hours resulted from the reduction in adsorbed enzyme as discussed above. Assuming that this latter hydrolysis can be considered first order with respect to the cellulose remaining, the rate coefficient should be the same as for the solid section, but adjusted for the lesser amount of enzyme present. This can be accomplished by multiplying the rate constant k_{d_1} by $[C_d/(C_{opt} \times 11.0)]$, the ratio of cellulose present to that required for complete adsorption of the enzyme. (The multiplication factor converts C_{opt} to its glucose equivalent.) At 12 hours 84% of the cellulose required for adsorption remained. The observed first order rate

coefficient, C_{d_2} , at 12 hours should have been 84% of k_{d_1} or 0.0118 hr^{-1} . The measured rate coefficient was 0.0111 hr^{-1}.

The steep rate shown by the initial dashed line is indicative of a more susceptible substrate rapidly nearing exhaustion. This material was designated C_c to differentiate it from cellulose C_d . Cellulose fractions C_a , C_b , and C_c are about 15% of the total cellulose (C_o) initially present. In Run 15 only 0.1% of the initial amount of C_c (C_{c_o}) remained after 6 hours. At 5 hours, however, enough crystalline cellulose remained so that hydrolysis of C_c yielded 25% of the carbohydrate produced. Run 15 was the only experiment in this series to undergo sufficient hydrolysis in the time period studied to exhibit this behavior.

E. Effect of Cellulose Concentration

The effect of increasing the initial cellulose concentration, C_o , while keeping the enzyme concentration constant was determined from the third hydrolysis series of experiments. The first group of this series, Runs 20-23, 25 and 27 used the enzyme mixture diluted to 0.195 mg/ml adsorbable protein (a fraction of 0.25) with buffer. The rate of carbohydrate production was expected to increase with an increase of initial cellulose, C_o , until all enzyme was adsorbed and participating in hydrolysis. At

this point further increase in the initial cellulose concentration was not expected to affect the rate of hydrolysis. TCARB was chosen to portray this effect because initially there is no cellobiose or glucose present (i.e., TCARB equals zero at time equals zero while PCARB equals C_a at time equals zero). The results differed significantly from those expected. As can be seen in Figure 7-10 for this first group, the rate of hydrolysis did increase as the cellulose concentration increased from 2 wt% to 4 wt%. The rate of hydrolysis then proceeded to fall drastically as C_o was increased from 4 wt% to 12 wt%. Similar behavior was exhibited for other enzyme concentrations and by PCARB.

Protein measurements indicated that a protein fraction (PTFRC) of 0.08 was adsorbed for each initial PTFRC of 0.125 as long as cellulose was in excess. This indicated that the adsorbable protein was 64% of the total protein. Since the mixture (PTFRC = 1.0) had an optical density equivalent to 1.22 mg/ml of bovine serum albumin, it was considered to have 0.78 mg/ml adsorbable protein (BSA equivalent). The decrease in adsorbable protein in the bulk solution was roughly paralleled by the decrease in C_1 and endoglucanase activities. Adsorbable protein was, therefore regarded as a fairly good measure of the enzyme protein.

The optimal cellulose concentration C_{opt} was defined

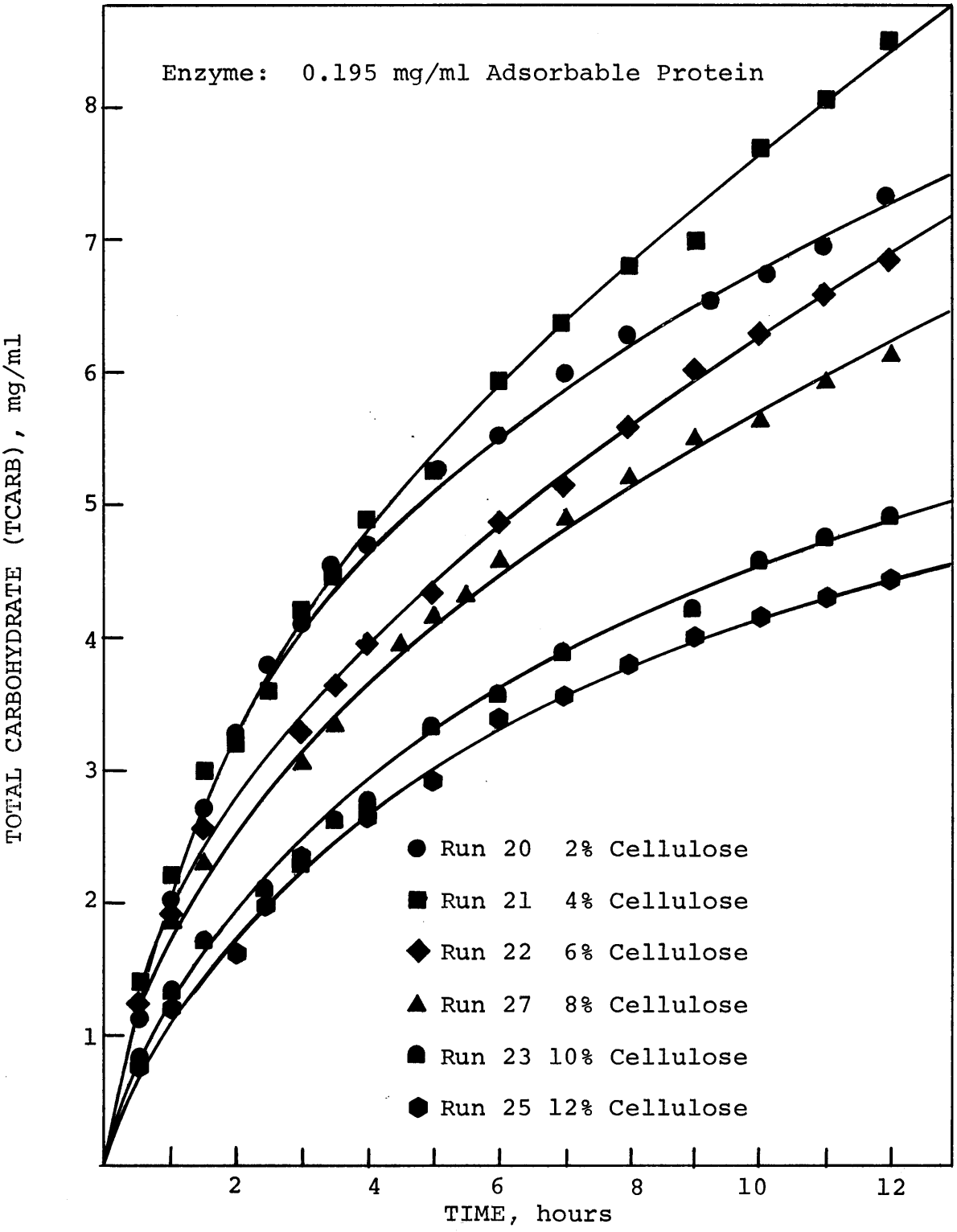

Figure 7-10. Effect of Initial Cellulose Concentration

as that C_o yielding the maximum hydrolysis rate for a given enzyme concentration. Subsequent runs were accomplished at various enzyme concentrations to determine the proportionality between adsorbable protein and optimal cellulose concentration. As expected the optimum cellulose concentration did increase with enzyme strength. This concentration is the minimum amount of cellulose required to adsorb all of the enzyme, 14.1 wt% cellulose for each mg/ml of adsorbed protein as equivalent BSA.

Figure 7-11 is similar to Figure 7-10 except that the enzyme concentration was only 0.0975 mg/ml and the time period was only 90 minutes. The initial time lag behavior was again indicative of sequential enzyme reactions. As expected the optimum cellulose concentration appeared to be one-half of the amount for the previous set of runs which had an enzyme concentration of 0.195 mg/ml.

Figure 7-12 is again similar to Figure 7-10 except that the enzyme was an equal mixture of buffer and a special concentrated T. viride enzyme. This concentrated enzyme had 3.4 times the total protein as the mixture. The endoglucanase and C_1 activities were 3.2 and 2.3 times as strong as the corresponding mixtures' enzyme activities. The optimum cellulose concentration appeared to be between 16% and 18%.

The optimum cellulose concentration was determined by assuming that the enzyme participating in hydrolysis at

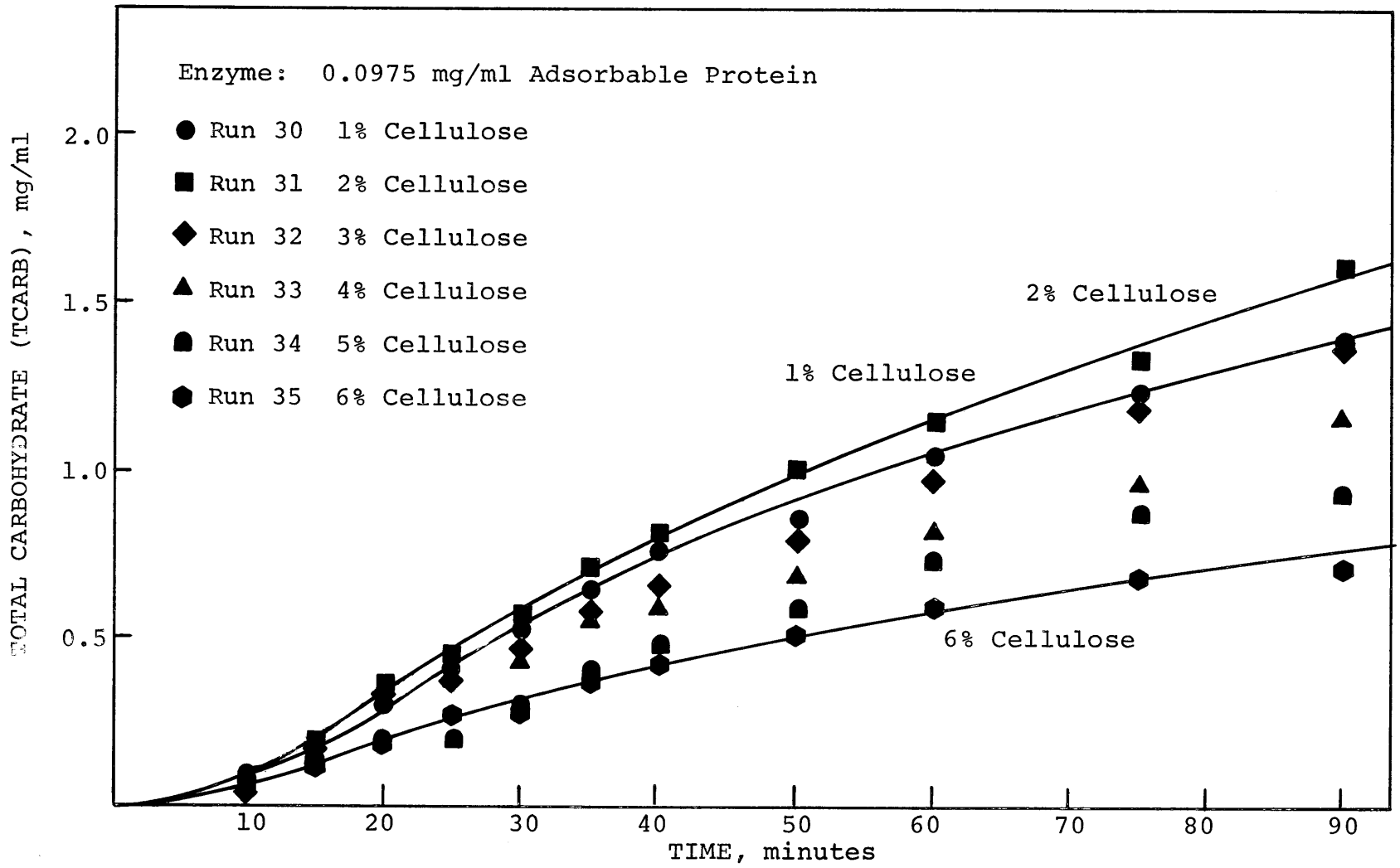

Figure 7-11. Effect of Cellulose Concentration (Low Enzyme Strength)

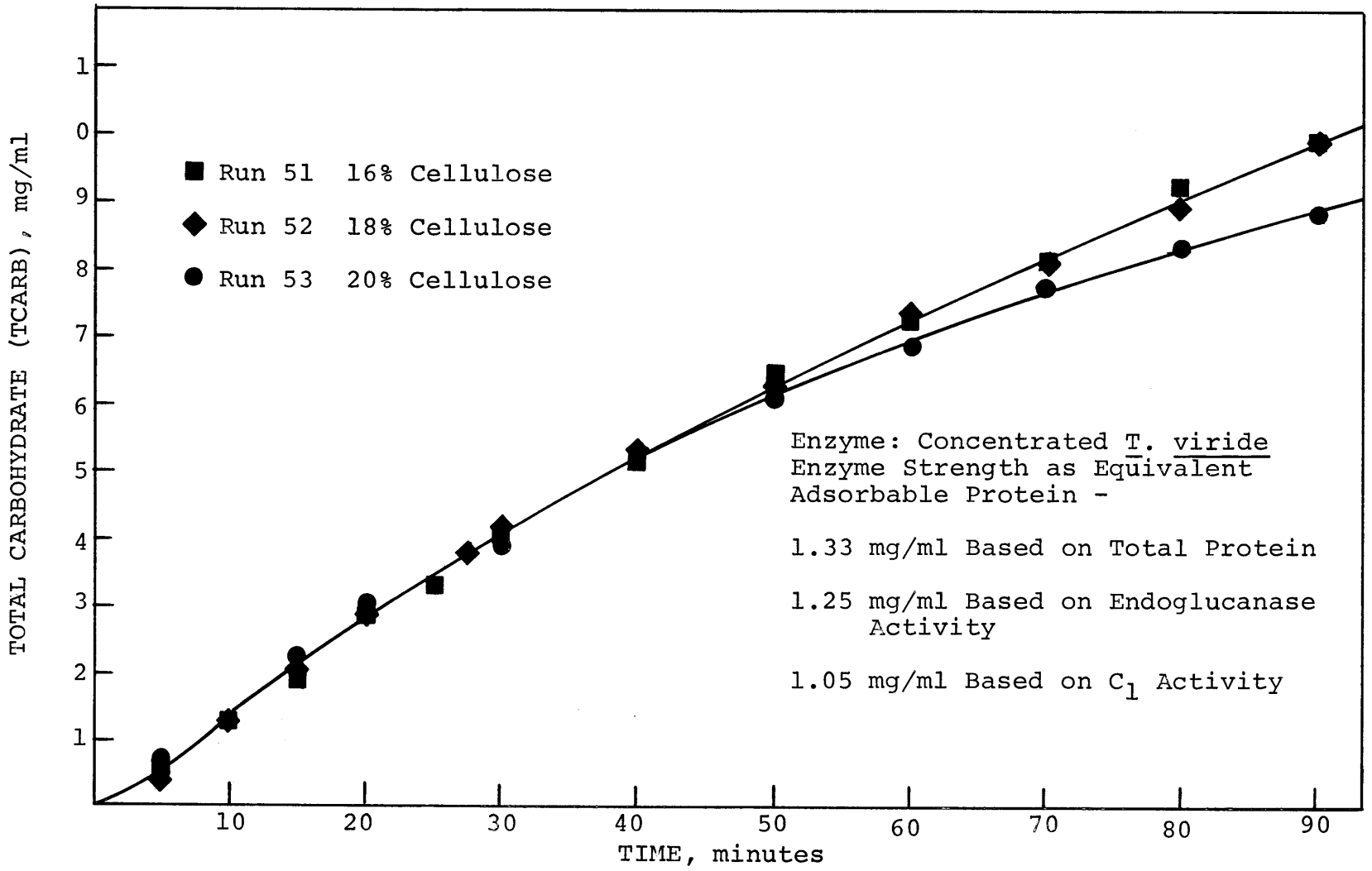

Figure 7-12. Effect of Cellulose Concentration (High Enzyme Strength)

$C<C_{opt}$ (16 wt%) was directly proportional to C/C_{opt}. The rate at $C>C_{opt}$ (18 wt%) was computed from the equations in Chapter VIII. Since the hydrolysis rates for 16 wt% and 18 wt% were relatively equal, the two rate expressions were equated and solved for C_{opt}.

VIII. DISCUSSION OF HYDROLYSIS RESULTS

A. Introduction

A good perspective of the enzymatic hydrolysis of cellulose can be garnered by examining the 1969 review "Cellulases and Their Applications" (27). Much effort has been expended in attempting to understand the hydrolysis mechanism and in particular the role of the various enzymes. The accessibility of the cellulose substrate to the enzyme molecules has also received much attention. Mandels (141-149) has spent a great deal of time developing mutant strains of cellulolytic fungi in order to increase the strength of the natural enzyme complex. Lately she has been looking at hydrolysis by adsorbed enzymes (142). Ghose (73-75) has explored enzyme concentration by ultrafiltration and the use of the concentrated enzyme in continuous saccharification reactors.

Published hydrolysis data, however, are scarce and difficult to utilize for determining kinetic rate constants. In addition little effort has been expended in examining the effects of the major variables (substrate and enzyme concentrations) in order to establish a kinetic model. No data have been published to show the effect of bulk mass transfer on the hydrolysis reaction rate nor have the published data conclusively shown if the enzyme actually diffuses into the cellulose. Finally, although C_1 is thought

to be the rate controlling enzyme little data have been published to varify this hypothesis.

The purpose of these hydrolysis studies was to examine the effect on the hydrolysis reaction rate of 1) agitator speed, hence, bulk mass transfer; 2) substrate concentration, hence, the order of the reaction; and 3) enzyme concentration. The results from the hydrolysis studies have been combined into a kinetic model that elucidates some of the above areas.

B. Bulk Mass Transfer Studies

Figures 7-1 and 7-2 show that agitation has little if any effect on the hydrolysis reaction. The cellulose particles must be kept in suspension, however, as can be seen by the low rate of reaction of the curve representing zero RPM. The minimum RPM to suspend 8 wt% cellulose with the geometry employed was 100. This RPM corresponds to a Reynolds number of 1200. The reynolds number corresponding to transition from a laminar to a turbulent flow pattern for a 3-bladed propeller in a baffled is 1000 (154). Since this geometry is similar to that employed in the hydrolysis studies, an agitator speed of 200 RPM (N_{Re} = 2400) is, therefore, close to the minimum turbulent speed and well within the range of commercial Reynolds numbers (1,000 to 20,000).

Since neither the short-time curve nor the longer-time

curve showed any effect of agitation provided the particles were suspended, bulk transfer to and product transfer from the cellulose particle must be much faster than the rate controlling mechanism.

C. Typical Hydrolysis Curve

A typical carbohydrate production curve, Figure 8-1, plots soluble carbohydrate concentration as a function of time. The literature has repeatedly reported that such measurements are an adequate method of measuring cellulose wieght loss, and hence hydrolysis. The ordinate records either PCARB or TCARB. The former is a measure of all soluble carbohydrate, while the latter is a good measure of glucose and cellobiose.

A reaction time curve with a rapid initial rate followed by a nearly constant rate nay be indicative of a two component reaction in which one fraction is more reactive than the other. The "constant" rate plateau appears to occur when the more reactive species is exhausted and is usually proportional to the quantity of resistant reactant remaining. The carbohydrate production curves (Figures 7-3 to 7-6) were indicative of this multi-substrate behavior.

Since cellulose is composed of amorphous and crystalline fractions, a dual substrate was expected. The nearly constant rate plateaus in Figure 7-3 evidenced by Runs 14

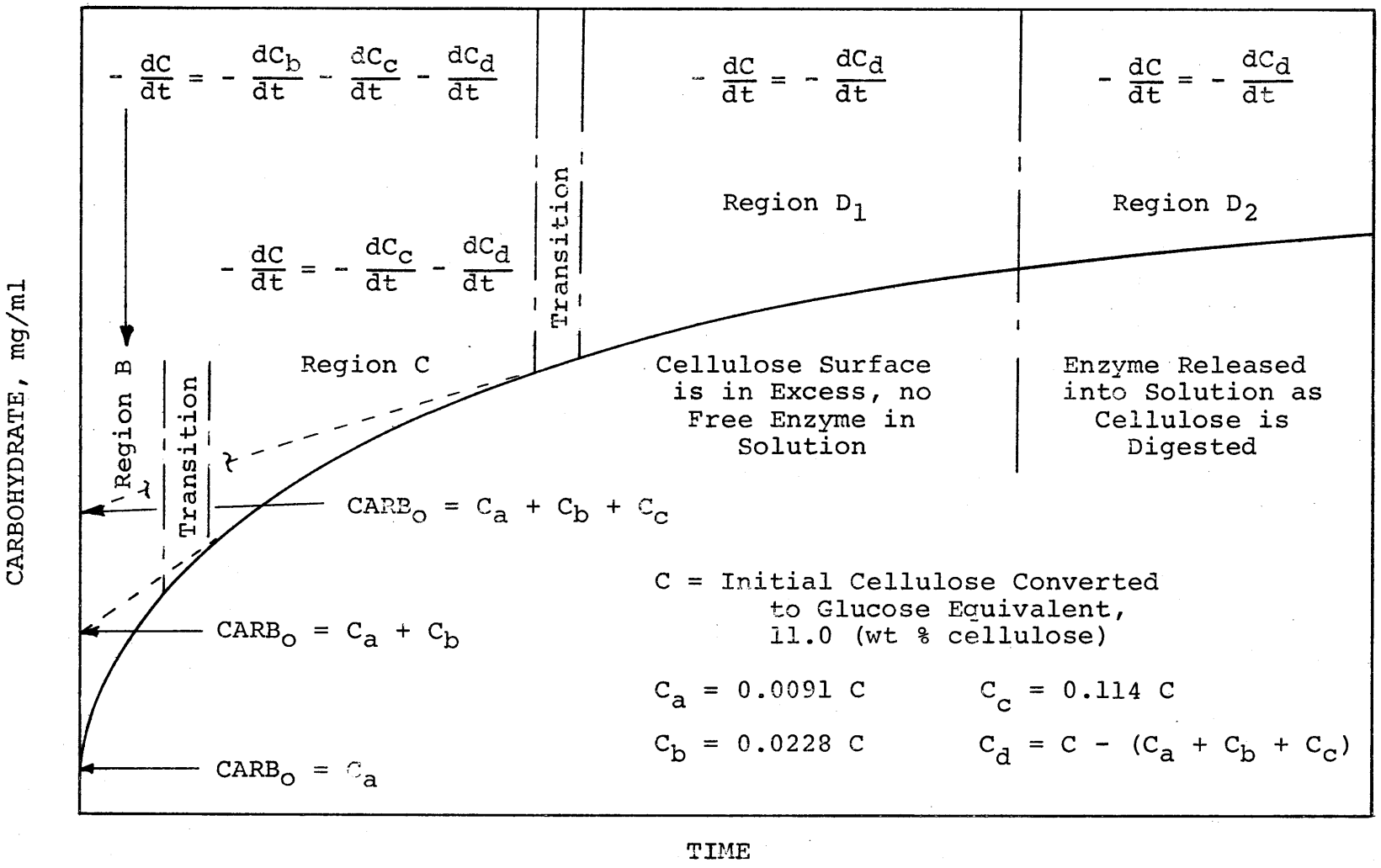

Figure 8-1. Typical Hydrolysis Curve

and 15 occurred after all of the easily hydrolyzed amorphous cellulose had been reacted. The PCARB produced from 30 minutes to 90 minutes with these two runs resulted mainly from the hydrolysis of crystalline cellulose. The curves were extrapolated back to the zero time axis to yield pseudo-curves (dashed lines) similar to ones that might have resulted had there been no amorphous cellulose.

Since PCARB was not zero at time zero, part of this easily hydrolyzed cellulose must have been initially soluble. This soluble material, C_a (0.8 mg/ml or 0.91 wt% C), was probably moderate length cellulose chains (5<DP<200) fragmented during milling. Shorter fragments would have been hydrolyzed to glucose by β-glucosidase and, hence, would have produced $TCARB_o$ values not evident in Figure 7-5; longer fragments are not soluble. As discussed in Appendix A, milling can provide enough energy to break hydrogen bonds which are about 5 kcal/g mole. The remainder of the rapidly hydrolyzed material (2.0 mg/ml or 2.88 wt%) was considered insoluble amorphous cellulose, C_b .

Initially the resistant material was considered one substrate. The rate of reaction after hydrolysis of the amorphous cellulose, therefore, should have been proportional to the cellulose present. The moderate time curves for Runs 14 and 15 (Figure 7-4) however, decreased too rapidly for the hydrolysis to have been the result of only one substrate. The resistant material was consequently

subdivided into crystalline cellulose, C_c , and inaccessible crystalline cellulose C_d .

The cellulose particle as viewed by the author is a spheroid. A fairly porous casing of amorphous and crystalline cellulose surrounds a highly crystalline core containing few, if any, pores large enough to admit an enzyme molecule. The casing is much more accessible to the enzyme than is the core, thus it is hydrolyzed first. Since the enzyme has access to cellulose molecules in the casing the rate of carbohydrate production is proportional to the intrinsic kinetics of the hydrolysis of the amorphous and crystalline fractions. Although the core could contain amorphous cellulose, the overall kinetics is probably limited by the rate at which enzyme molecules can gain access to new cellulose chains, rather than by the hydrolysis itself.

The quantity of crystalline cellulose, C_c , could not be estimated in a similar fashion to the amorphous cellulose, because Run 15 was the only experiment to have completely hydrolyzed the accessible amorphous and crystalline cellulose in the time period studied. (The scope of the experiments was to examine the initial rate; most runs were, therefore, limited to 12 hours.) Since the quantity of crystalline cellulose was calculated by the difference between the initial cellulose and the sum of the other fractions (C_a , C_b , C_c), the inaccessible cellulose, C_d ,

had to be known. For Run 15 assuming that all C_c was hydrolyzed at 10 hours, the cellulose remaining at this time (C_{10}) was determined as the difference between C and $PCARB_{10}$. The observed rate coefficient, k_d, was calculated from

$$-\frac{dC_i}{dt} = k_i C_i \qquad (8\text{-}1)$$

or

$$k_d = -\frac{1}{C_{10}}\frac{dC}{dt} \qquad (8\text{-}2)$$

where dC/ct was the slope of the hydrolysis curve. Integration of equation (8-2) between 0 and 10 hours allowed determination of C_{d_o} as 75.2 mg/ml (85.4 wt% of the glucose equivalent of the initial cellulose concentration). Crystalline cellulose, C_c, was then 10.0 mg/ml (11.4 wt%) since the other three fractions were known.

The major assumptions in the above argument are supported by the latter sections of the Literature Review. Ghose's data (75) tend to support the present findings that Solka Floc contains amorphous and crystalline cellulose. The work of Norkans (172) and Walseth (265) supports the hypothesis of a crystalline core. The inaccessible nature of the core is supported by the small fraction of

pore volume accessible to an enzyme molecule (see Chapter IX, The Solute Exclusion Technique). The absence of a rapid initial rate reported by Selby in the discussion by Ranby (189) is understandable when one realizes that cotton has a median pore diameter one-half that of wood pulp (38). The rapid initial rate is absent because most of the amorphous cellulose is inaccessible to the enzyme.

D. Effect of Substrate Concentration

As discussed in Appendix D the rate of carbohydrate production was expected to increase with an increase in initial cellulose concentration, C_o , until all of the enzyme was adsorbed and participating in hydrolysis. At this point further increase in C_o was not expected to effect the rate of hydrolysis. TCARB was chosen to portray this effect because initially there is no cellobiose or glucose present, whereas the varying $PCARB_o$ values would obscure the effect. The results differed significantly from those expected. As can be seen in Figure 7-10 the rate of hydrolysis did increase as the cellulose weight per cent increased from 2 wt% to 4 wt%. The rate of hydrolysis then proceeded to fall drastically as C_o was increased from 4 wt% to 12 wt%. Similar behavior was exhibited for other enzyme concentrations and by PCARB.

The initial cellulose concentration, C_{opt} , was defined as that C_o yielding the maximum hydrolysis rate

for a given enzyme concentration. The cellulose concentration is given as weight per cent of the total solution because it is the dimension most often found in the literature and to differentiate it from C , the glucose equivalent of the cellulose concentration (mg/ml). C_{opt} , plotted as a function of the enzyme concentration in Figure 8-2, can be expressed

$$C_{opt} = 14.1\ [E] \qquad (8\text{-}3)$$

where [E] is the adsorbable enzyme protein. The data up to and including [E] of 0.78 mg/ml were obtained with the T. viride mixture.

A special batch of enzyme was prepared which was more concentrated than the enzyme used during most of this study. This allowed extension of equation (8-3) to high enzyme levels. The concentrated T. viride enzyme was obtained from Dr. Mary Mandels of the U.S. Army Research Laboratory, Natick, Massachusetts. This was originally a fermentation broth similar to that used for most of the hydrolysis studies. It was concentrated by passage through an ultrafiltration unit that deactivated some of the endoglucanase and nearly one-half of the C_1 enzyme. The concentrate, therefore, had a ratio of C_1 : endoglucanase : total protein different from the standard T. viride mixture. The difference in enzyme activities between the standard

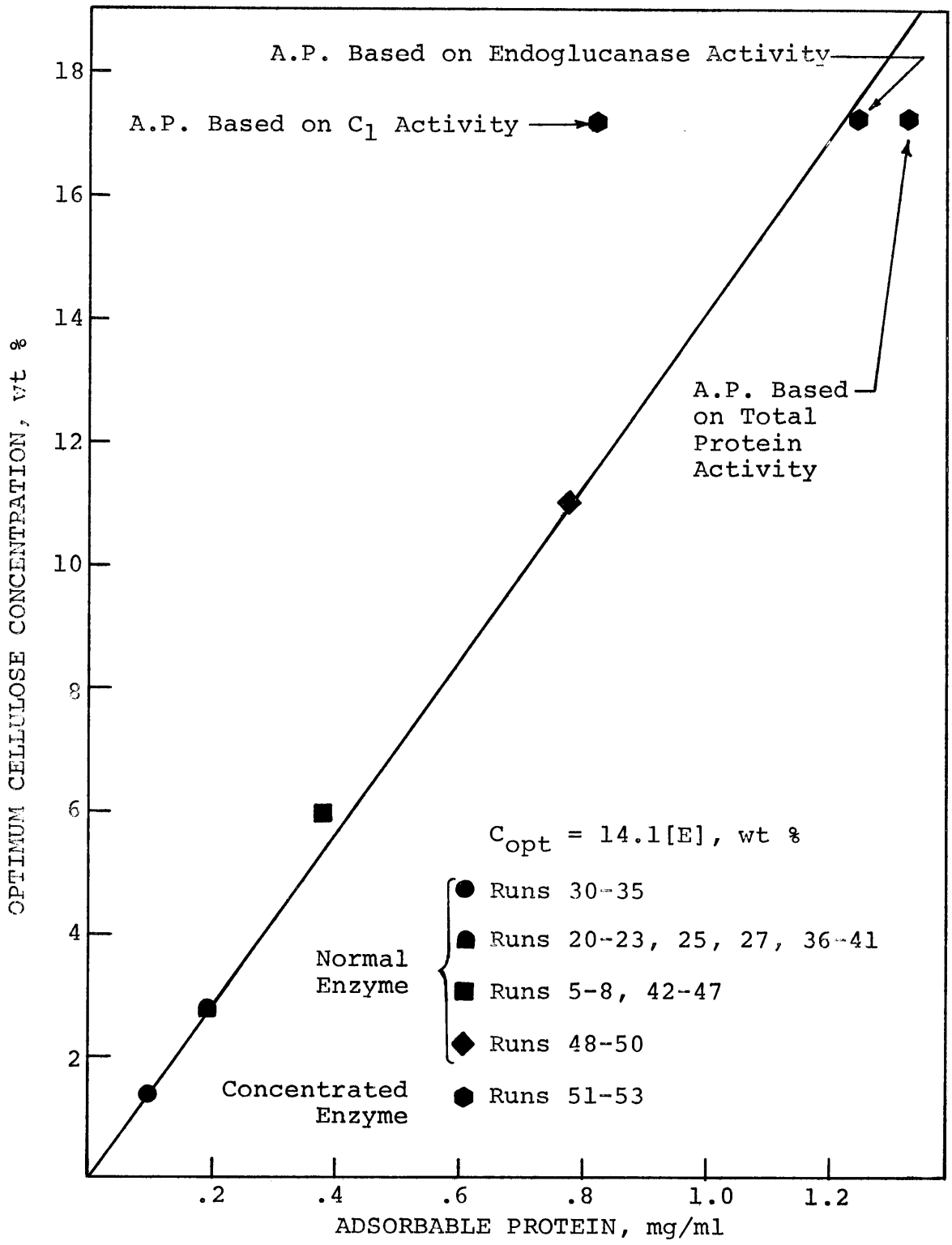

Figure 8-2. Optimum Cellulose Concentration

enzyme and the concentrated batch was important in determining which enzyme governed the optimum cellulose concentration.

Since the maximum stirrable cellulose concentration was 20 wt%, the concentrated enzyme was diluted 1:2 with buffer so that the expected optimum cellulose concentration would be below 20 wt%. This dilution gave a protein, endoglucanase activity, and C_1 activity of 1.7, 1.6, and 1.05 times the corresponding values of the normal enzyme mixture used in most of the studies. The optimum cellulose concentration for the diluted concentrate was 17.2 wt%. Multiplying the adsorbable protein value of the mixture by the various activities the abscissa value would have been 0.82 mg/ml, 1.25 mg/ml, or 1.33 mg/ml based on C_1 activity, endoglucanase activity, or total protein respectively. It is evident from Figure 8-2 that the abscissa value based on comparative endoglucanase activity yields the best correlation. It appears that endoglucanase is the controlling enzyme under conditions of excess cellulose. Perhaps even more significant is the finding that C_{opt} is definitely not based on C_1 activity.

The optimum cellulose concentration can also be expresses as a dimensionless group, θ, the enzyme adsorbed per unit cellulose:

$$\theta = \frac{[E]}{10.0\ C_o} \qquad (8\text{-}4)$$

At the optimum cellulose concentration this group would be

$$\theta = \frac{[E]}{10.0\ C_{opt}} = 0.0071 \qquad (8\text{-}5)$$

A similar θ group could be formed for any adsorbing system. A θ_{opt} probably exists for other enzyme-cellulose systems and possibly even for noncellulosic systems. It should be noted that this group is similar to catalyst loading factors often employed in heterogeneous catalysis.

E. Development of the Kinetic Model

A kinetic expression was developed to relate the initial enzyme and cellulose concentrations to the observed rate coefficient, k_i , and hence to the intrinsic kinetic rate constant, k_i^* . The model was based on the division of the substrate into the four fractions, i . The carbohydrate produced, PCARB, was assumed to be the sum of that resulting from the hydrolysis of each fraction. The hydrolysis of each substrate was considered first order with respect to the amount of that material remaining according to equation (8-1).

The assumptions implicit in the model are:

1. The substrate (cellulose) is composed of various fractions, C_i , decreasing in reactivity

$$C = \Sigma C_i = C_a + C_b + C_c + C_d \qquad (8\text{-}6)$$

where C is given as glucose equivalent (mg/ml) for ease in comparison with the products of reaction.

2. The hydrolysis rate of substrate i is proportional to C_i

$$-\frac{dC_i}{dt} = k_i C_i \tag{8-1}$$

3. The magnitude of the observed rate coefficients is

$$k_a > k_b > k_c > k_d \tag{8-7}$$

4. The composite hydrolysis expression is

$$-\frac{dC}{dt} = \frac{dPCARB}{dt} = \sum_{i=a}^{d} -\frac{dC_i}{dt} = \Sigma k_i C_i \tag{8-8}$$

5. The rate of hydrolysis if initially at the optimum cellulose concentration is proportional to C_{opt}

$$-\frac{dC}{dt} = (\text{Constant})C_{opt} \tag{8-9}$$

6. As the cellulose is hydrolyzed below C_{opt} the surface available for enzyme adsorption will become deficient and enzyme will be released into solution. This should occur in Region d and yields the transition from

d_1 to d_2 . At this point the enzyme will not be a constant quantity but will be proportional to C_{d_2}

$$[E] = \text{Constant } C_{d_2}{}^{n} \tag{8-10}$$

Since $[E]_{d_2}$ is less than $[E]_{d_1}$, k_{d_2} should be less than k_{d_1} .

The basis for assumption one has already been discussed. Extrapolation of the curves in Figures 7-3 and 7-4 and other similar curves to the zero time axis allowed determination of the various substrate fractions as a function of cellulose concentration. These fractions and the initial cellulose concentration can be calculated as equivalent glucose from C_o , the initial wt% cellulose

$$C = 11.0\ C_o \tag{8-11}$$

$$C_{a_o} = 0.0091\ C \tag{8-12}$$

$$C_{b_o} = 0.0228\ C \tag{8-13}$$

$$C_{c_o} = 0.114 \tag{8-14}$$

$$C_{d_o} = C - (C_a + C_b + C_c)_o \tag{8-15}$$

Assumption two and equation (8-1) can be restated

$$-\frac{dC_i}{C_i} = -d(\ln C_i) = k_i dt \qquad (8\text{-}16)$$

the general solution of which is

$$-\ln(C_i/C_{i_o}) = k_i \Delta t \qquad (8\text{-}17)$$

A graph of $-\ln(C_i/C_{i_o})$ versus time should, therefore, be linear with a slope equal to the observed rate coefficient k_i. As can be seen in Figures 7-7 to 7-9, equation (8-17) does hold for the initial rate in each area, thus varifying assumption two.

The quantities plotted in Figures 7-7 to 7-9 required calculation of C_i. Employing assumption three the PCARB at the beginning of Region i was normalized to zero to determine the net production of carbohydrate within the region. Thus,

$$C_i = C_{i_o} - (\text{PCARB} - \Sigma C_j) \qquad (8\text{-}18)$$

where the C_j's are the cellulose fractions already hydrolyzed. The time, t_i, signifying the beginning of Region i was assumed to occur when

$$\text{PCARB} = \Sigma C_j \qquad (8\text{-}19)$$

Equation (8-18) can therefore be rewritten

$$C_i = \left(\sum_{i=a}^{i} C_{i_o} \right) - \text{PCARB} \qquad (8\text{-}20)$$

Assumption three was verified by examining the observed rate coefficients k_i for a typical run. These were determined for Run 15 from Figures 7-7 to 7-9:

$$k_a \simeq \infty$$

$$k_b = 12.6 \text{ hr}^{-1}$$

$$k_c = 0.8 \text{ hr}^{-1}$$

$$k_d = 0.0112 \text{ hr}^{-1}$$

The transition from Region d_1 to d_2 occurred at a PCARB of 19 mg/ml, thus C_{d_2} was about 69 mg/ml. A k_{d_2} value equivalent to k_{d_1} is obtained by multiplying the observed value of k_{d_1} by $C_{d_2}/(C_{opt} \times 11.0)$ to give k_d (0.0100 hr^{-1}). Assumptions three and six are therefore verified because

$$12.6 > 0.80 > 0.0112 > 0.0100$$

In addition, the value of C_d at the transition is approximately the same as would have been predicted from the

amount of enzyme present (0.488 mg/ml) and the amount of cellulose to adsorb 1.0 mg/ml of adsorbable protein (14.1 wt%) by equation (8-3).

The verification of assumptions one, two, three, and six provided encouragement for further development of the model. Since the rate of hydrolysis appeared to depend on the initial concentration of enzyme and cellulose, the observed rate coefficient in equation (8-1) was expressed

$$k_i = k_i^* [E]^{\sigma} C_o^{\rho_i} \qquad (8\text{-}21)$$

These units (mg/ml, enzyme, and wt% cellulose) were again chosen because of their prevalence in the literature.

The rate coefficients were determined from the hydrolysis curves using the values of C_i (discussed previously). Since k_d could only be determined for Run 15, the ratio of k_c/k_d for this run was assumed constant for all of the runs. (C_c and C_d were assumed to be crystalline cellulose and the intrinsic kinetics should be similar for both fractions.) Using equation (8-8) the values of k_c were then calculated from the slopes of the hydrolysis curves after sufficient time for all of the amorphous cellulose to have been hydrolyzed. The k_b values were determined from the initial slopes of the hydrolysis curves. The results of these calculations are presented in Table 8-1. The coefficients from Runs 20-23, 25 and 27 were used to

TABLE 8-1. FIRST ORDER KINETIC RATE CONSTANTS

Run	C_o	[E] mg/ml	k_b hr^{-1}	k_c hr^{-1}	k_d hr^{-1}
Opt A	8	0.566	7.35	0.675	0.0140
12	8	0.0975	0.55	0.049	
27	8	0.195	1.49	0.136	
13	8	0.293	2.9	0.26	
14	8	0.390	4.35	0.39	
15	8	0.488	6.25	0.55	0.01125
Opt B	2.75	0.195	4.50	1.45	
21	4	0.195	2.90	0.63	
22	6	0.195	2.13	0.25	
27	8	0.195	1.49	0.136	
23	10	0.195	1.21	0.088	
25	12	0.195	1.07	0.059	

Intrinsic Rate Constants, k_i^* :

$k_b^* = 144$ $(mg/ml)^{-1.5}hr^{-1}$ $\quad \rho_b = -1.0$

$k_c^* = 102$ $(mg/ml)^{-1.5}hr^{-1}$ $\quad \rho_c = -2.5$

$k_d^* = 2.1$ $(mg/ml)^{-1.5}hr^{-1}$ $\quad \rho_d = -2.5$

determine the effect of the initial cellulose concentration on the observed rate coefficient as shown in Figure 8-3. The slopes of the curves are the exponents ρ_i (also given in Table 8-1).

This effect is both physical and apparent. The apparent effect results from a definition of the observed rate coefficient k_i (see equation 8-1). Since $k_i C_i$ must be constant if the hydrolysis rate is constant, a change in C_i would cause an opposite change in k_i without necessarily affecting the rate itself. The physical effect is caused by the distribution of endoglucanase on the surface of the cellulose. Increased initial surface decreases the effective endoglucanase concentration on the surface, without decreasing the total endoglucanase adsorbed.

Assuming that the hydrolysis of crystalline cellulose requires concurrent action on the same chain by an endoglucanase and a C_1 molecule, a "dual adsorption" theory provides a possible explanation. Surface in excess of that proportional to C_{opt} would decrease the probability that an endoglucanase molecule and a C_1 molecule would concurrently bind to the same chain. If C_1 initiates the hydrolysis (a hypothesis supported by the literature) and endoglucanase is in excess at the reaction site, the overall rate of hydrolysis would be proportional to C_1. If, however, endoglucanase is not in excess, the overall rate would become proportional to the endoglucanase at the

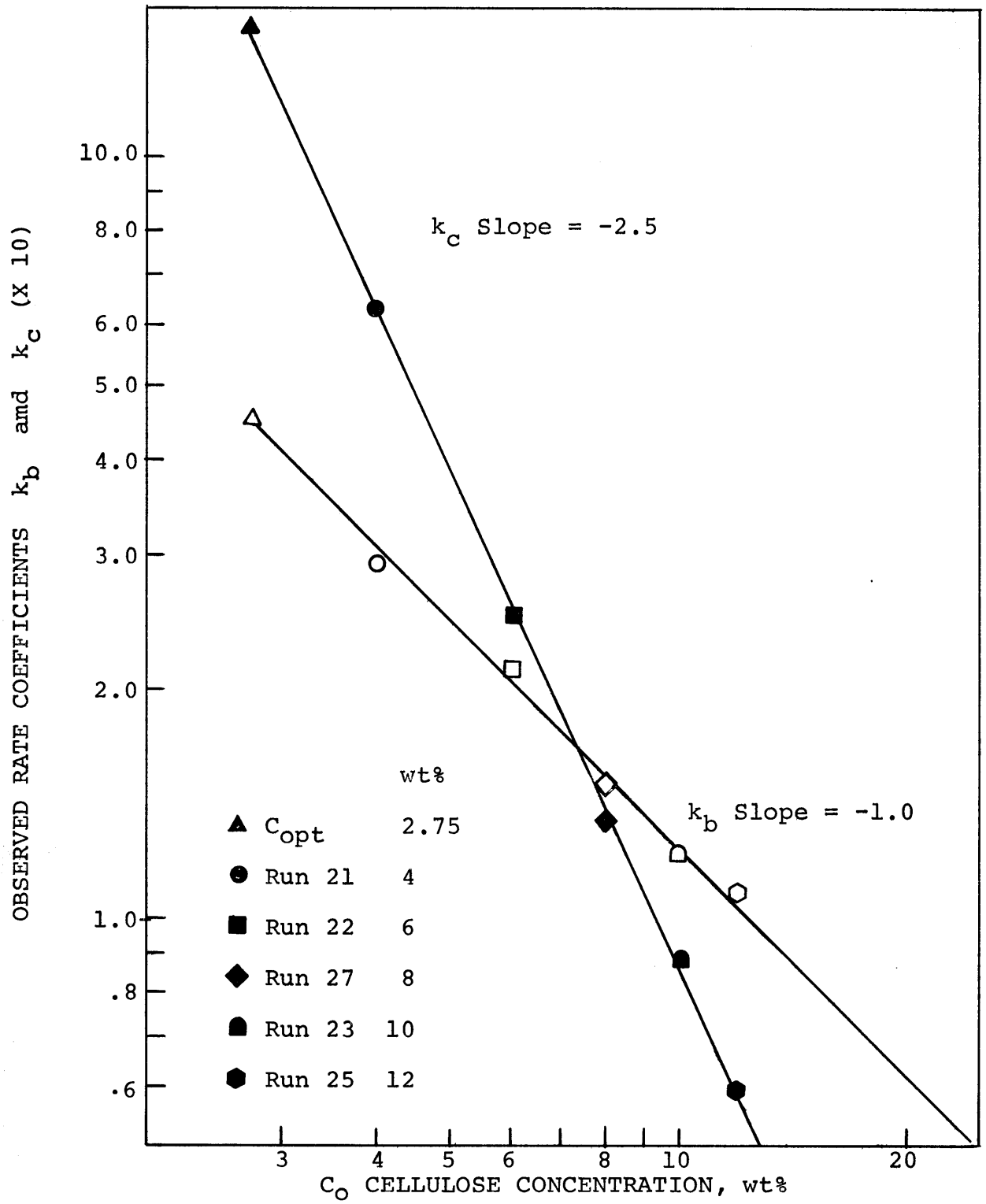

Figure 8-3. Effect of Initial Cellulose Concentration on Rate Coefficients

reaction site. The hydrolysis rate would be controlled by C_1 at cellulose concentrations less than or equal to C_{opt}. Since excess surface decreases the effective endoglucanase at the site of C_1 initiation, the overall rate would become endoglucanase limited at cellulose concentrations in excess of C_{opt}. The optimum cellulose concentration could then be considered the maximum cellulose concentration that does not so reduce the effective endoglucanase concentration at the initiation site as to cause a reduction in the rate of reaction.

This effect should be less pronounced on the hydrolysis of C_b (hence on k_b) because amorphous cellulose has fewer interchain hydrogen bonds than crystalline cellulose. All interchain hydrogen bonds must be broken for a fragment to be free to diffuse away from the reaction site. Release of an amorphous fragment, therefore, would require fewer C_1 - endoglucanase interactions than a similar length crystalline chain. A fragment that is not completely released can reorient with other chains and reform previously broken hydrogen bonds.

The dual adsorption hypothesis is supported by the evidence that C_{opt} is dependent on the endoglucanase concentration as observed from runs with the concentrated enzyme. Evidence (discussed later) that the overall hydrolysis is proportional to C_1 also strengthens the hypothesis.

The next step in refining the kinetic model was to determine the effect of [E] on the apparent rate coefficient. Figure 8-4, a logarithnic plot of k_i versus [E], was constructed from the data for Runs 12-15 and 27. The curves can be expressed

$$k_i \alpha [E]^{\sigma} \tag{8-22}$$

where σ (=1.5) is the slope of the curves. Since the function f[E] is the same for both b and c, amorphous and crystalline cellulose are probably hydrolyzed by the same mechanism.

Incorporating the effects of [E] and C_o, the complete expression for the observed rate coefficient is

$$k_i = k_i^*[E]^{1.5} C_o^{\rho_i} \tag{8-23}$$

The hydrolysis of each component is

$$\text{Hydrolysis Rate} = \begin{bmatrix}\text{Intrinsic Rate Constant}\end{bmatrix}\begin{bmatrix}\text{Effective Enzyme Conc.}\end{bmatrix}\begin{bmatrix}\text{Fraction } C_i \text{ Remaining}\end{bmatrix} \tag{8-24}$$

$$-\frac{dC_b}{dt} = k_b^*[E]^{1.5}\frac{C_b}{C_o} \tag{8-25}$$

$$-\frac{dC_c}{dt} = k_c^*\left(\frac{[E]}{C_o}\right)^{1.5}\frac{C_c}{C_o} \tag{8-26}$$

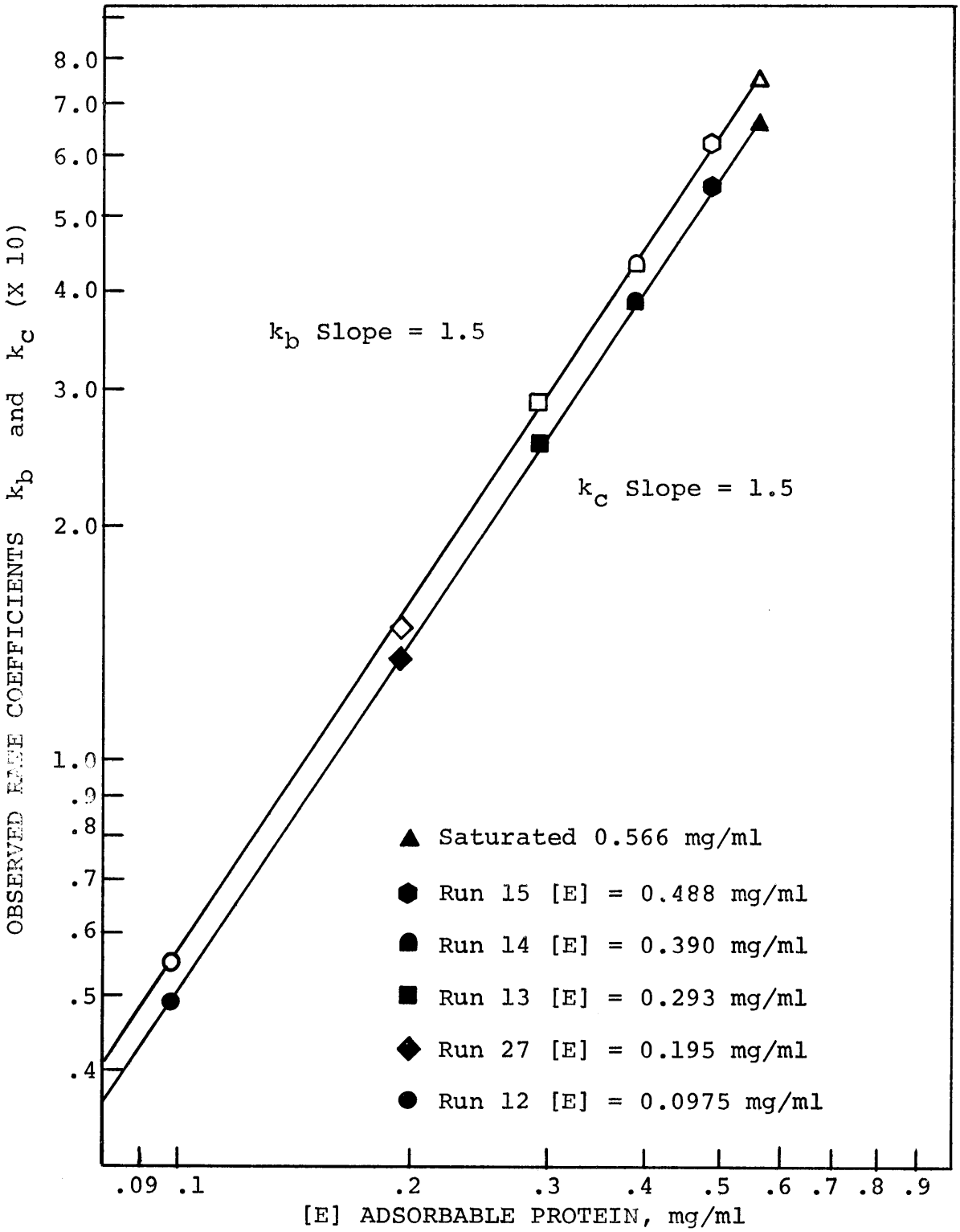

Figure 8-4. Effect of Enzyme Concentration

$$- \frac{dC_d}{dt} = k_d^* \left(\frac{[E]}{C_o}\right)^{1.5} \frac{C_c}{C_o} \qquad (8\text{-}27)$$

The complete rate equation is

$$- \frac{dC}{dt} = \frac{dPCARB}{dt} = - \sum_{i=b}^{d} \frac{dC_i}{dt} \qquad (8\text{-}8)$$

$$= - \sum_{i=b}^{d} k_i^* [E]^{1.5} C_o^{\rho_i} C_i \qquad (8\text{-}28)$$

Note: The form of equation (8-27) was assumed from the similarity of C_d and C_c. The normalized cellulose concentration corrects for the apparent effect of C_o discussed in the previous section.

Substitution of the θ for $[E]/(10C_o)$ results in

$$- \frac{dC_c}{dt} = k_c^* (10\theta)^{1.5} \frac{C_c}{C_o} \qquad (8\text{-}29)$$

and

$$- \frac{dC_d}{dt} = k_d^* (10\theta)^{1.5} \frac{C_d}{C_o} \qquad (8\text{-}30)$$

The hydrolysis of crystalline cellulose is, therefore, proportional to the (enzyme per unit cellulose)$^{1.5}$ and to the crystalline cellulose concentration. An enzyme exponent of unity would have been indicative of monatomic reaction;

an exponent of two would have indicated a diatomic (enzyme-enzyme) interaction. A power of 1.5 is somewhere in between; i.e., one C_1 interaction with two endoglucanase molecules could possibly liberate two soluble fragments.

This expression holds only as long as C is greater than C_{opt} so that all the enzyme is adsorbed and participating in hydrolysis. When C is less than C_{opt} there will be insufficient surface for total enzyme adsorption. The enzyme initially participating in the reaction can be calculated from equation (8-3). As hydrolysis proceeds the normalized cellulose concentration must be superseded by C raised to a fractional power. Some evidence indicates that this power approaches 0.78 at extended hydrolysis. A power of 0.67 would imply that adsorbed enzyme was proportional to the external surface of shperical particles, whereas a power of 1.0 implies a volumetric relationship. (The volume, hence weight, of a sphere is proportional to r^3, whereas the external surface is proportional to r^2. As a sphere decreases in weight the radius decreases proportional to $wt^{1/3}$. The external surface, therefore, becomes proportional to $(wt^{1/3})^2$ or $wt^{0.67}$.)

F. Arrhenius Plot

An Arrhenius plot (Figure 8-5) was constructed from the data of Runs 18, 26, 54, and 55 to determine the activation energies of the hydrolysis reaction. The activation

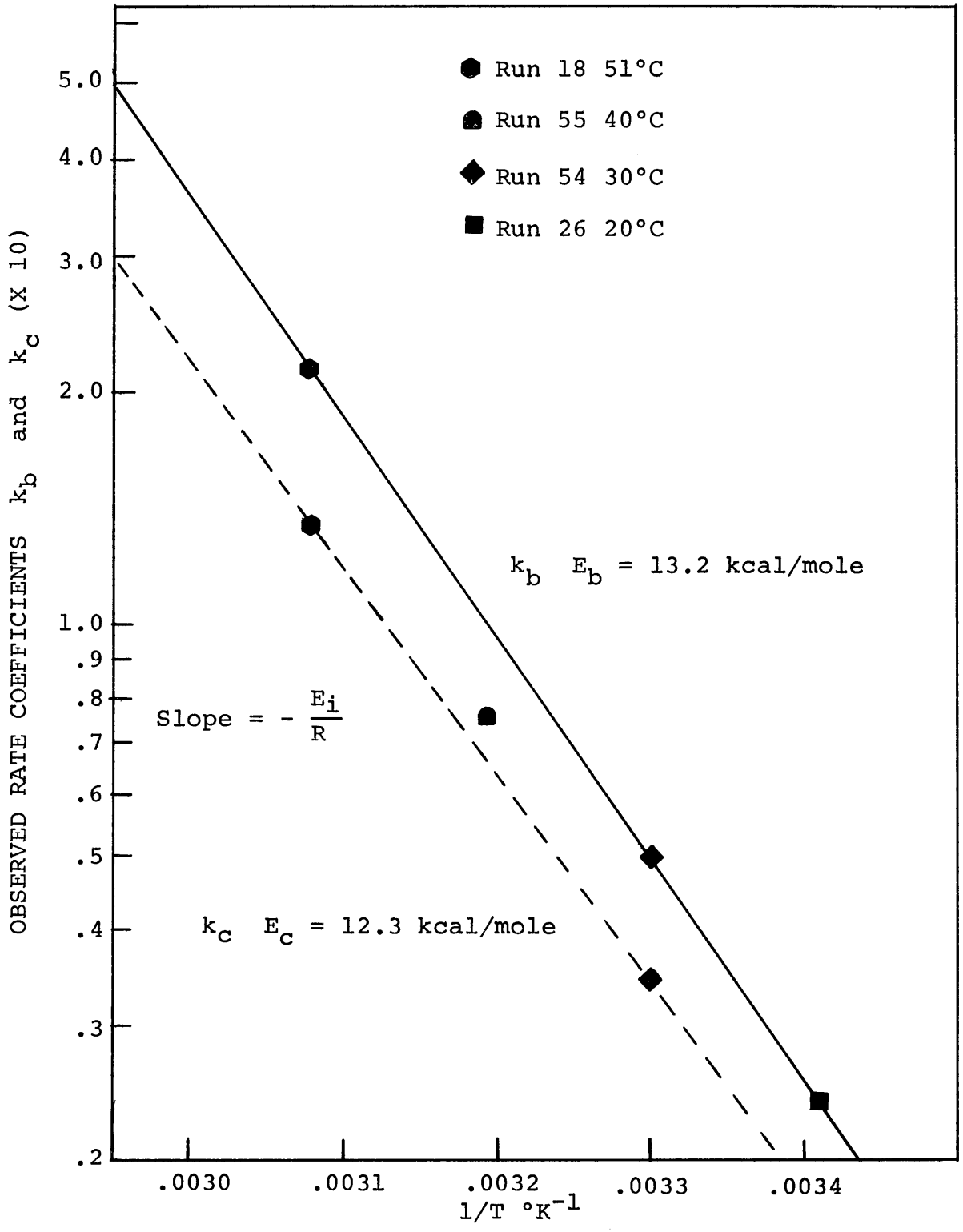

Figure 8-5. Arrhenius Plot

energies were 13.2 kcal/mole for the hydrolysis of C_b and 12.3 kcal/mole for C_c . The energies are close enough that one could assume that the same reactions are involved. Making the assumption that k_d has the same activation energy as k_c , the Arrhenius expression can be utilized to adjust the intrinsic rate constants for changes in temperature.

G. Test of the Kinetic Model

The data for Runs 14 and 15 are presented along with the curves predicted by equation (8-28) in Figure 8-6. The equation tends to predict slightly high values in the initial stages of hydrolysis because it assumes hydrolysis of all three substrates (C_b , C_c , and C_d) from time zero. In reality there is probably a slight time lag that the equation does not consider; this time lag is evident in Figures 7-3 and 7-5.

Total carbohydrate production both measured and predicted by equation (8-28) and solution enzyme concentration are plotted in Figure 8-7. Protein appears to adsorb much faster than enzyme activity decreases. This is caused by adsorption to soluble long chain fragments. The enzyme adsorbed on these fragments can still participate in hydrolysis and, hence, show activity. In this adsorbed state, however, the enzyme protein can not react with the Lowry reagent to yield protein optical density. As these frag-

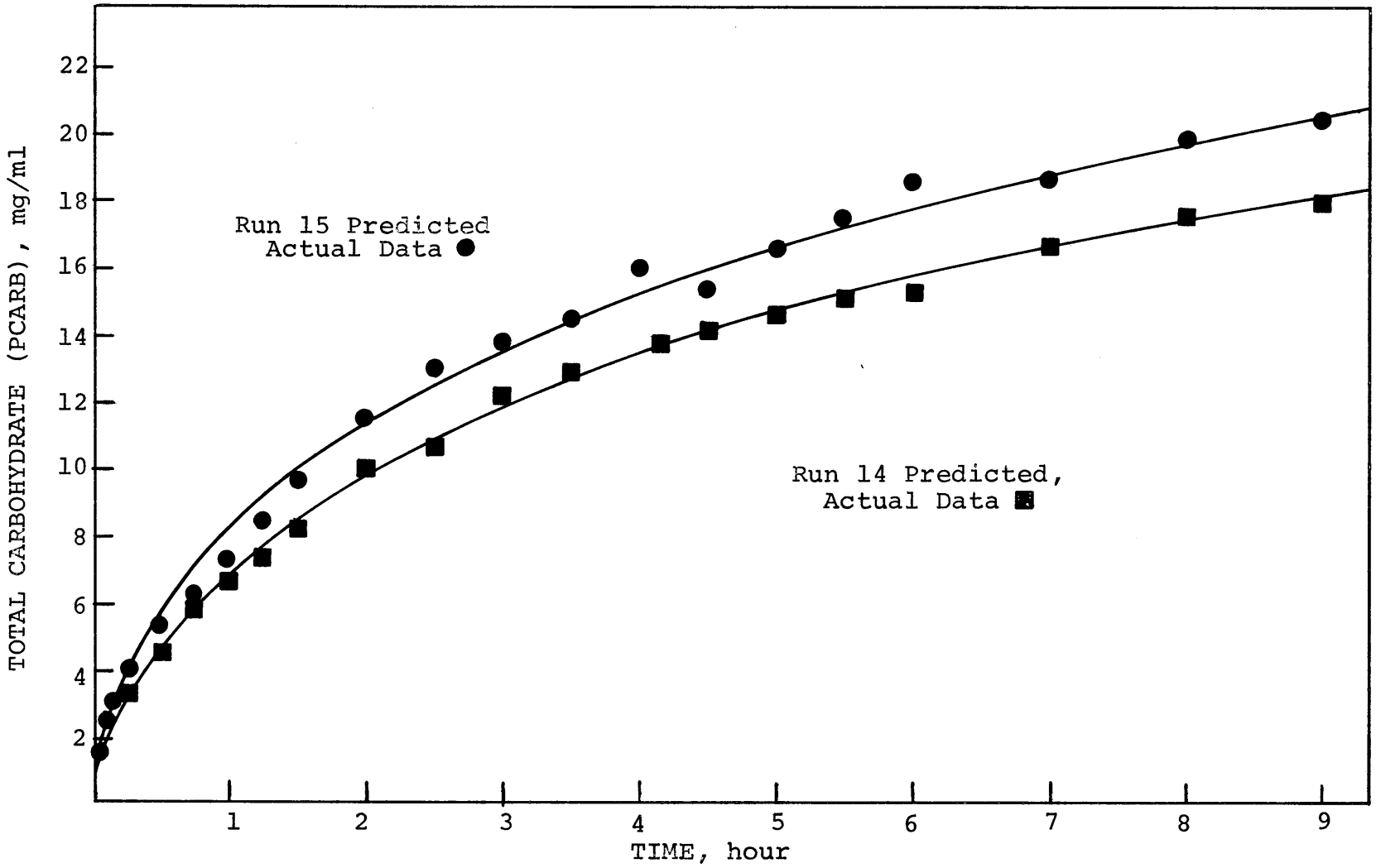

Figure 8-6. Comparison of Actual and Predicted Data

ments are hydrolyzed the enzyme adsorbs onto the solid cellulose particle.

At high enzyme concentrations the external surface of these particles is rapidly saturated forcing the remaining unadsorbed enzyme to diffuse into the pore structure to find surface on which to adsorb. The restricted diffusion into the "pores" is much slower than adsorption onto the external surface as is evidenced by the slow reduction in enzyme activity shown in Figure 8-7. This behavior is only evident at high enzyme concentrations. Adsorption of enzyme onto the external surface and the surface of the gross capillaries near the external boundary is nearly instantaneous as long as this surface is in excess of that required for complete enzyme adsorption.

H. Evidence That C_1 is the Rate Controlling Enzyme

Development of the kinetic model and review of the hydrolysis studies have provided some evidence that C_1 is the rate controlling enzyme. As mentioned previously, a special concentrated batch of *T. viride* enzyme was used for some of the hydrolysis studies (Runs 11, 51-53). Run 11 employed the concentrate diluted with buffer to give total protein, endoglucanase and C_1 activities 0.425, 0.40 and 0.263 respectively times those of the *T. viride* mixture employed for most of the hydrolysis studies. This allowed comparison of the hydrolytic action of the concen-

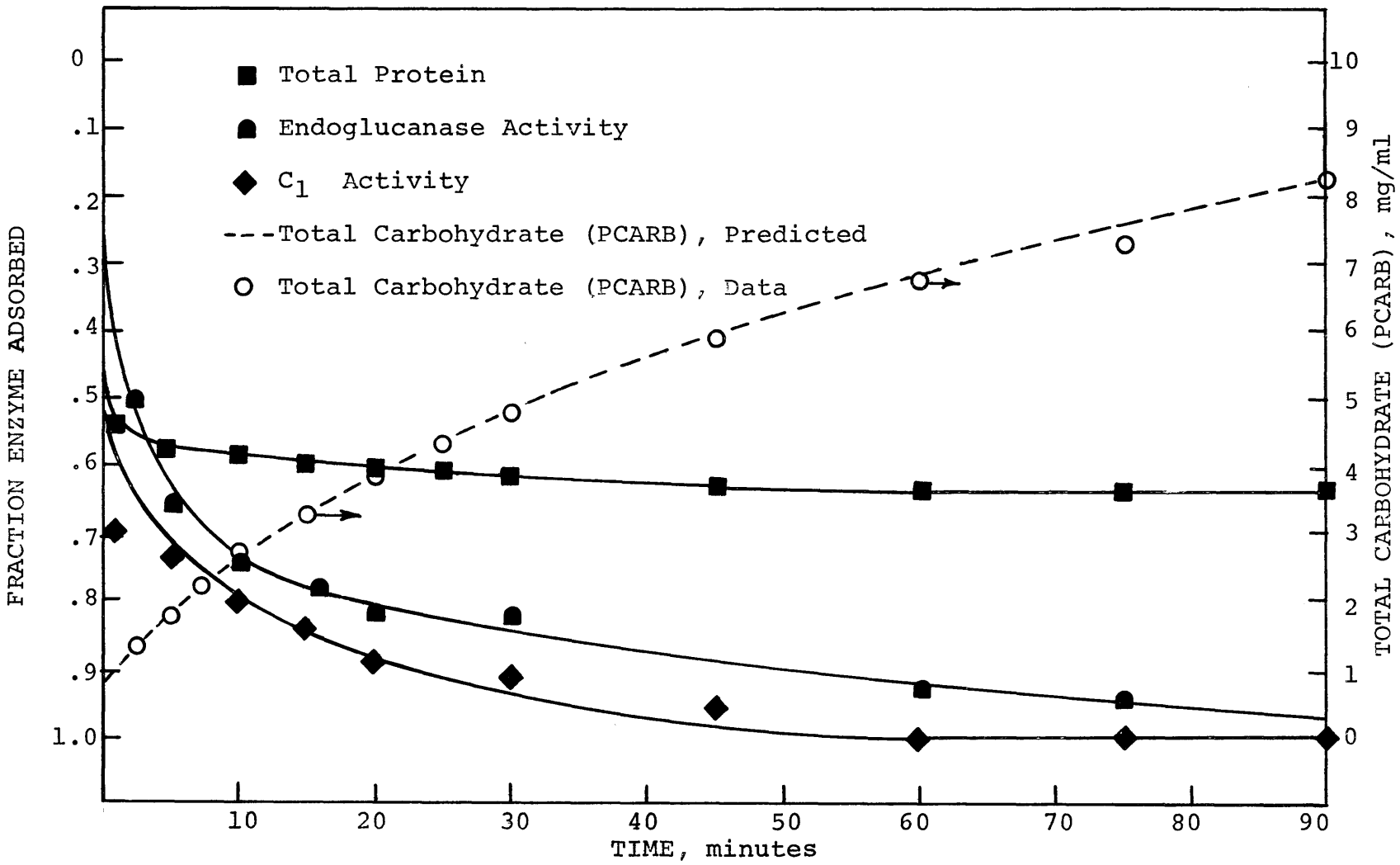

Figure 8-7. Reaction Progress Curves, Run 14

trate as compared with runs employing various dilutions of the mixture. Since the rate of reaction is proportional to $[E]^{1.5}$, the hydrolysis of Run 11 should be predicted by the kinetic model with suitably chosen values of $[E]$. The value of $[E]$ for the T. viride mixture was 0.78 mg/ml adsorbable protein. The endoglucanase and C_1 activities are proportional to the adsorbable protein, and hence, $[E]$ should be proportional to the enzyme activities. The enzyme concentrations used in Figure 8-8 to predict the hydrolysis of Run 11 were

$$[E]_{C_1} = \frac{(C_1)_{\text{Run 11}}}{(C_1)_{\text{mix}}} [E]_{\text{mix}} \qquad (8\text{-}31)$$

$$= 0.263(0.78 \text{ mg/ml})$$

$$= 0.205 \text{ mg/ml}$$

and

$$[E]_{EN} = \frac{(ENDO)_{\text{Run 11}}}{(ENDO)_{\text{mix}}} [E]_{\text{mix}} \qquad (8\text{-}32)$$

$$= 0.40(0.78 \text{ mg/ml})$$

$$= 0.312 \text{ mg/ml}$$

Although these may not be the actual adsorbable protein

concentrations they should be adequate representations of C_1 and endoglucanase. Equation (8-19) was used with equations (8-31) and (8-32) to predict the hydrolysis of Run 11. The predicted behavior based on the C_1 activity yielded a much better prediction than did the endoglucanase activity. The kinetic model based on C_1 activity tended to underpredict the initial hydrolysis of amorphous cellulose, but not nearly as much as the model based on endoglucanase would have over predicted hydrolysis. The amorphous cellulose C_b, therefore, requires some C_1 enzyme for hydrolysis although it is not as dependent on C_1 as is cellulose C_c.

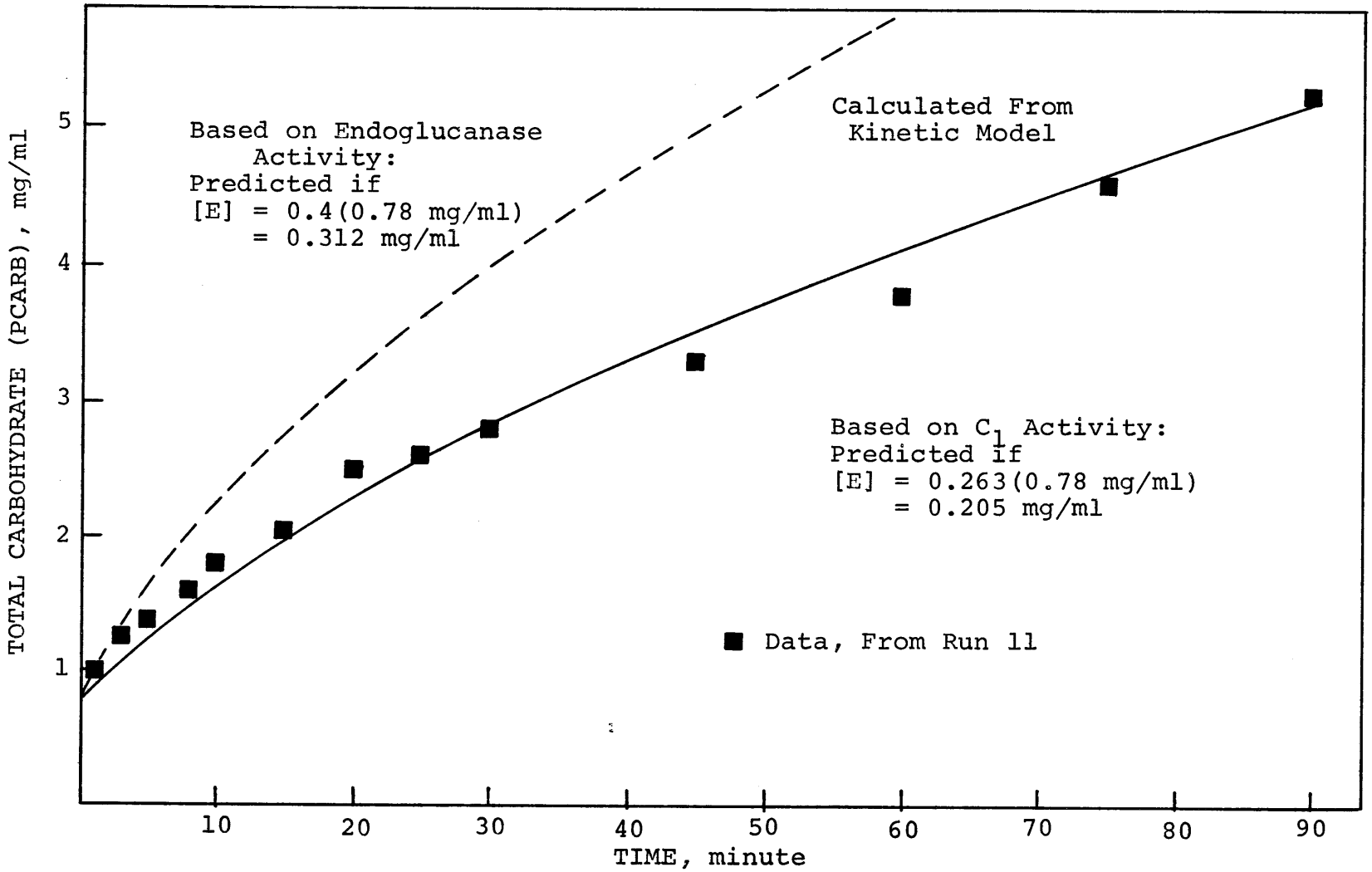

Figure 8-8. Verification That C_1 is the Rate Controlling Enzyme

IX. SOLUTE EXCLUSION TECHNIQUE

A. Introduction

In order to determine if the enzyme molecules diffused into the cellulose pore structure, the nature of the pore structure itself had to be determined. For this reason the solute exclusion technique was developed.

A similar technique was employed by Stone et al. (238-242) and Tarkow et al. (254 and 255) to obtain pore size distributions of water swollen cellulosic materials. Nelson and Oliver (169) employed these methods to characterize acetic acid swollen cellulose. None of these researchers, however, published a clearly defined experimental procedure. The purpose of this portion of the thesis was to develop such a procedure, and to employ it to characterize the cellulose substrate.

B. Theory

A porous body (possibly immersed in water) has added to it a known weight of solute dissolved in water. The system is then thoroughly mixed. If all of the pores are accessible to the solute molecules, the solute concentration of the bulk solution will not change (Case A). If a solution of larger solute molecules is used (Case B) so that the smaller pores in the porous material are inaccessible to the solute molecules, then the water in these

smaller pores is unavailable for dilution, and the solution after mixing will be slightly less diluted than in Case A. When the solute molecule is so large that it can not enter the porous body at all (Case C) the inaccessible water equals the total water of swelling or fiber saturation point, a useful quantity that is often difficult to measure by other means.

Consider a sample of porous material consisting of p grams of dry solid and q grams of water. Let Δ_s be the total weight of water inaccessible to a given solute molecule. The total amount of water available for dilution of an added solute solution, therefore, is $q - \Delta_s$. The final solute concentration is

$$C_f = \frac{W\ C_i}{W + q - \Delta_s} \tag{9-1}$$

where W and C_i are the weight of solution added and the initial solute concentration respectively. This expression can easily be solved for δ_s, the inaccessible water per unit weight dry solid or

$$\delta_s = \frac{\Delta s}{p} = \frac{W + q}{p} - \frac{WC_i}{pC_f} \tag{9-2}$$

The water inaccessible to a given solute molecule can therefore be determined from knowledge of the sample weight

and water content, the weight and initial solute concentration of solution added, and the final solute concentration. When a series of solute molecules of progressively larger diameters is employed with this technique a cumulative pore volume curve (often termed an accessibility curve) is obtained. The fiber saturation point corresponds to the plateau formed with very large diameter solute molecules while the median pore size is that solute diameter above and below which is one-half of the total pore volume.

$$\text{Accessible water} = \text{fiber saturation point} - \text{inaccessible water} \qquad (9\text{-}3)$$

C. Size and Shape of Molecular Probes

The ability of the technique to determine an absolute pore size distribution is dependent upon the size and shape of the molecules employed. An excellent review on polyethylene polymers is presented by Stone and Stratta (237), and molecular dimensions of polyethylene glucol (PEG) are given by Nelson and Oliver (169). Equivalent sphere dimensions for dextrans and related materials are presented by Stone et al. (242). Colton (33) has presented an excellent review of the dimensions of various molecules in solution.

Stone et al. employed dextrans and related sugars

and, based on the review by Grotte (81), assumed that the molecules could be considered solvated spheres. They often assumed that the diameters of these solvated molecules could be calculated from their diffusion coefficients according to the Stokes-Einstein equation (discussed in Appendix E). The diameters of the dextrans employed by Stone et al. were found by interpolation of the data given by Granath (70), and the diameters of the sugars were calculated from the diffusion coefficients of Longworth (138).

Dextran molecules are probably not hydrated spheres. Colton (33) has reported that Dextran 15 (mw = 16,000) has an axial ratio of 6.9 with a minor axis 20 Å in diameter. Stone and Scallan would have used an equivalent sphere diameter of 56 Å. Since molecular seives exclude molecules by their minor axis, this dimension was employed to characterize the ability of a molecule to penetrate a porous material.

The volume of a prolate ellipsoid is given by

$$V = 4/3\pi ab^2 \qquad (9\text{-}4)$$

where a and b are the major and minor axes respectively. The minor axis can be calculated from knowledge of the equivalent sphere diameter d_e by equating the spherical and elliptical volumes

$$1/6\pi d_e^{\,3} = 1/6\pi ab^2 \qquad (9\text{-}5)$$

and hence

$$b = (6.9)^{-0.33} d_e = 0.525\ d_e \qquad (9\text{-}6)$$

D. Experimental Procedure

The basic experimental technique is quite simple. This simplicity, however, is deceiving since the solute exclusion technique depends upon accurate measurements of very small changes in solution concentration. Considerable care must be taken at each step to avoid any possibility of sample contamination or solvent evaporation.

The initial step was the preparation of the cellulose substrate to be characterized. Cellulose wood pulp (Solka Floc BW-300) was soaked in distilled water for at least a week prior to use. The cellulose was then rinsed several times to remove microscopic and soluble cellulose fragments. The water content of the substrate was then determined in duplicate by recording the weight of the sample before and after drying. Drying at 110°C for 3 hours was sufficient for a 5 gram wet sample. Extended drying at this temperature caused charring. (Note that dry cellulose is quite hydroscopic; the hot dry samples should, therefore, be cooled and stored in a desiccator prior to reweighing.)

Identical samples of the wet cellulose sufficient to contain 1.0 to 1.5 grams of dry cellulose were then weighed into clean weighing bottles which were quickly covered to prevent evaporation. Triplicate samples were prepared for each molecular probe. (To prevent extensive evaporation and hence variance in water content during transfer to the bottles, only 40 samples were removed from any batch. Every tenth sample was used to monitor the batch water content.) A constant volume (10 ml) of polymer solution (3.0% to 4.0% in distilled water) was then pipetted into each weighing bottle. An equal volume of distilled water was added to one triplicate set to produce a concentration "blank". This blank was used to correct the measured concentrations (C_f) for soluble material which remained in the smaple even with extensive rinsing. An aliquot of each polymer solution was preserved for determination of C_i. (Note that the amount of liquid used was the minimum to both cover the sample in the weighing bottle, and to provide sufficient liquid sample for determination of C_f.)

The solutions contacted the cellulose for 16 to 40 hours, after which approximately 2.0 ml of liquid was withdrawn. This was accomplished by suction filtration. This step was the most difficult because the ultimate results depended upon the filtration technique. Extensive suction until a cake formed caused random, nonreproducible results. If the filtration were halted while the mixture was still

in a slurried state, the ultimate results were quite reproducible. (Rapid withdrawl of liquid may cause a chromatographic effect, thus, stranding the large solute molecules.)

The concentration of each sample filtrate and of the original solution aliquots were then determined by their refractive indices as measured by a Brice-Pheonix differential refractometer. The refractive indices were found to be linear with respect to solution concentration (weight fraction) to well above the maximum employed in these studies.

The inaccessible water was determined from equation (9-2) and the ratio of the initial solution concentration to the final concentration (C_i/C_f). Since the solution concentrations were used as a ratio, the refractometer readings were employed without intermediate conversion to actual concentrations. C_f was the average reading of the sample filtrate less the average "blank" concentration.

E. Discussion of Procedure

The major sources of error are a result of errors in concentration measurement rather than of errors in sample size or water content. Random errors caused by weighing and pipetting could be tolerated by increasing the number of replicate samples employed for each molecular probe. The contamination of a probe solution resulting in an inaccurate δ_s value was not even a major catas-

trophe because the δ_s values of the other molecular probes helped smooth the overall accessibility curve.

Systematic errors, however, were much more severe since they tended to shift the entire spectrum of results. For this reason the initial rinsing of the cellulose batch and the accurate determination of the blank concentration were performed with the ultimate care. Thorough rinsing resulted in a three fold decrease in blank concentration from 0.16% to 0.05%.

A 1% difference in the final concentration C_f produced a 10% variance in inaccessible water. Similar variation in sample weight, p, water content, q, or solution weight, w, respectively caused 1.5%, 4.2%, and 2.6% deviation in inaccessible water. Clearly the determination of concentration was the major source of error.

One other source of error was adsorption of the solute. Glass apparatus was employed with dextran solutes and was initially employed with PEG. The PEG results were an order of magnitude below those for dextran indicating a significantly reduced C_f. One run with PEG E20,000 produced inaccessible water values of 0.023, 0.096, 0.023, and 0.131 ml/g. A run with dextran 2000 produced an average δ_s of 0.5 ml/g. Since polyethylene glycol is known to adsorb on glass, polyproplyene apparatus was substituted for glass and the PEG E20,000 run repeated. The resulting values of δ_s were 0.5 to 0.6 ml/g. It is believed,

although not conclusively proved, that the polyethylene glycol did adsorb onto the glassware. Clearly the later results established that PEG E20,000 did not sufficiently adsorb on cellulose to cause the results exhibited by the series using glassware.

F. Results

A series of dextran and of polyethylene glycol molecules (donated by Dow Chemical Company, Midland, Michigan) were employed to determine the pore volume distribution of the cellulose used in the hydrolysis studies. The molecular porbes with their weights and dimensions are tabluated in Tables 9-1 and 9-2. Also tabulated are the inaccessible water values. These have been plotted in Figure 9-1. The characteristic diameter used for the dextran molecules was the minor axis of a prolate ellipsoid. This is also the dimension assumed to characterize the enzyme molecules.

The dextran series definitely yielded a fiber saturation point less than that of the PEG series. An explanation of this is that the dextran fractions probably contained a higher quantity of lower molecular weight portions than did the PEG fractions. Since the low molecular weight molecules can diffuse into the cellulose more easily than larger molecules, a fraction with small molecules would have a lower final concentration than without.

A pore size distribution curve was computed from the

TABLE 9-1. MOLCEULAR WEIGHTS AND SOLUTION DIAMETERS OF THE POLYETHYLENE GLYCOL SERIES

Molecule	Molecular Weight	Diameter in Solution, Å[a]	Total Pore Volume, cc/g
PEG E200	200	13	.26
PEG E300	300	16	.46
PEG E400	400	18	.47
PEG E500M	500	20*	.49
PEG E1450	1,450	33*	.54
PEG E4000	4,000	54	.58
PEG E6000	6,000	70*	.62
PEG E9000	9,000	90	.64
PEG E20000	20,000	130	.66

*Interpolated value
[a]Nelson and Oliver (169)

TABLE 9-2. MOLECULAR WEIGHTS AND SOLUTION DIAMETERS OF

Molecule	Molecular Weight	Diameter in Solution, Å: Diameter of Equivalent Sphere	Diameter in Solution, Å: Minor Axis of Prolate Ellipsoid	Total Pore Volume, cc/g
Sucrose	342	10[c]	10	.12
Raffinose	504	12[c]	12	.14
Inulin	5,200	40[a,d]	13.5	.39
Dextran 10	10,000	51[c]	27	.43
Dextran 15	20,000	68[c]	36	.40
Dextran 40	40,000	90[c]	47	.42
Dextran 80	77,500	125*[c]	66	.50
Dextran 100C	150,000	165[c]	87	.46
Dextran 200C	252,000	222*[c]	117	.47
Dextran 500	500,000	295*[c]	207	.45
Dextran 2000	2,000,000	560[c]	294	.46

[a]Value is for major axis
*Interpolated value
[b]Calculated from an axial ratio of 6.9
[c]Stone et al. (242)
[d]Colton (33)

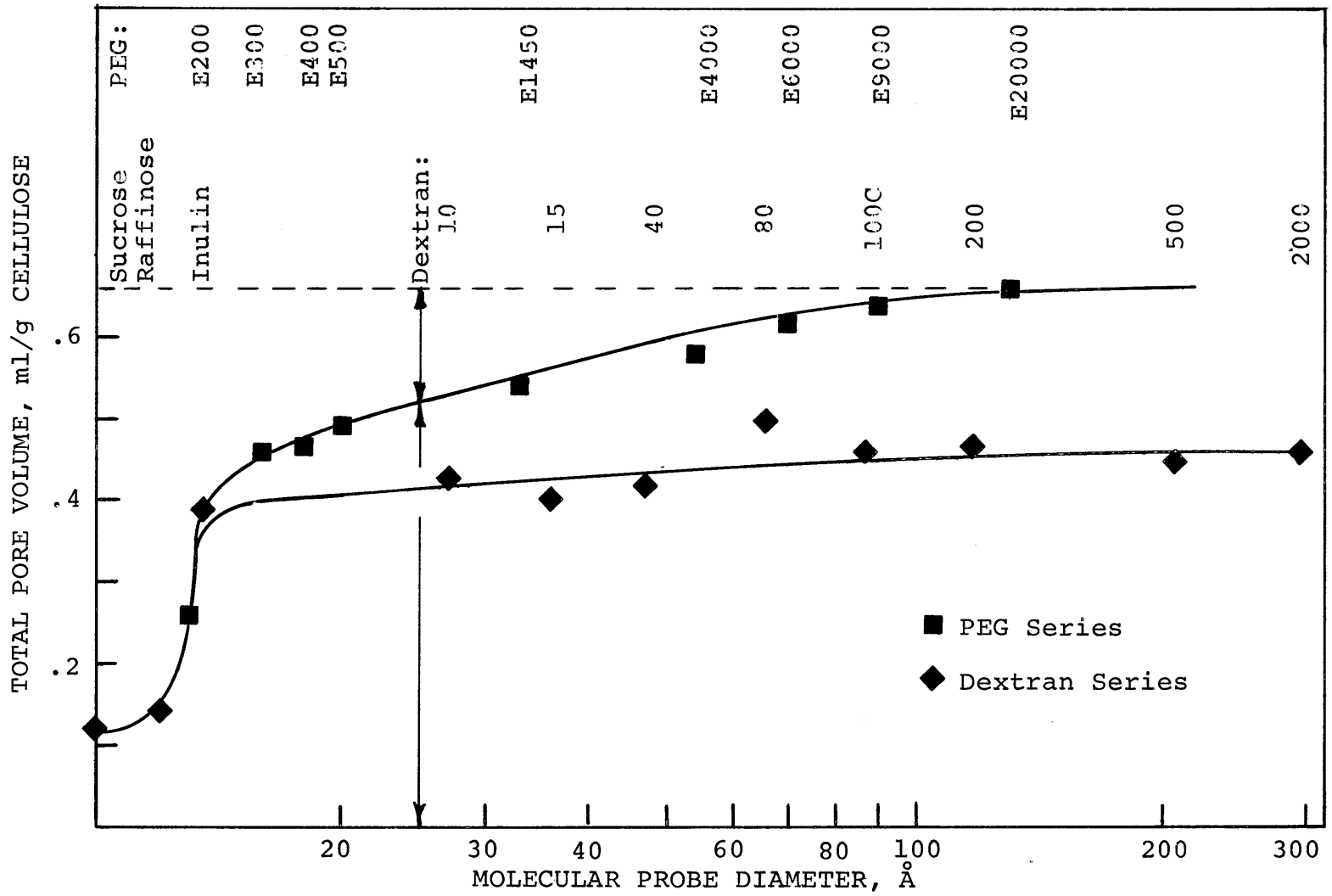

Figure 9-1. Cumulative Pore Volume Curve

cumulative pore volume curve for the PEG series. The cumulative curve was differentiated by division into intervals of increasing pore diameters. The change in pore volume per angstrom, $\Delta V/\Delta pd$, was computed for each interval. This quantity was then plotted as a function of the median pore diameter in each interval to yield Figure 9-2. The fractional pore volume inaccessible to a molecule larger than 35 Å (the minimum enzyme dimension) was 85%. The pore volume accessible to an enzyme molecule was 0.1 cc/g cellulose. The shaded area under the curve is the pore volume accessible to the enzyme.

Stone et al. (242) have reasoned that the most feasible intrafibrillar shape is that of lamellae or sheets of microfibrils. The pores would then be the slit-like spaces between these sheets. The characteristic pore width would be the space between the sheets w . The pore area for each characteristic "diameter" would then be

$$A = \frac{2\Delta V}{w} \qquad (9\text{-}7)$$

where ΔV is the differential volume associated with each median pore "diameter" w .

Employing 10 Å intervals for each median pore diameter from 130 Å to 50 Å and 5 Å intervals from 50 Å to 35 Å, the accessible area calculated from equation (9-7) was 35 m^2/g cellulose. The external surface area based on

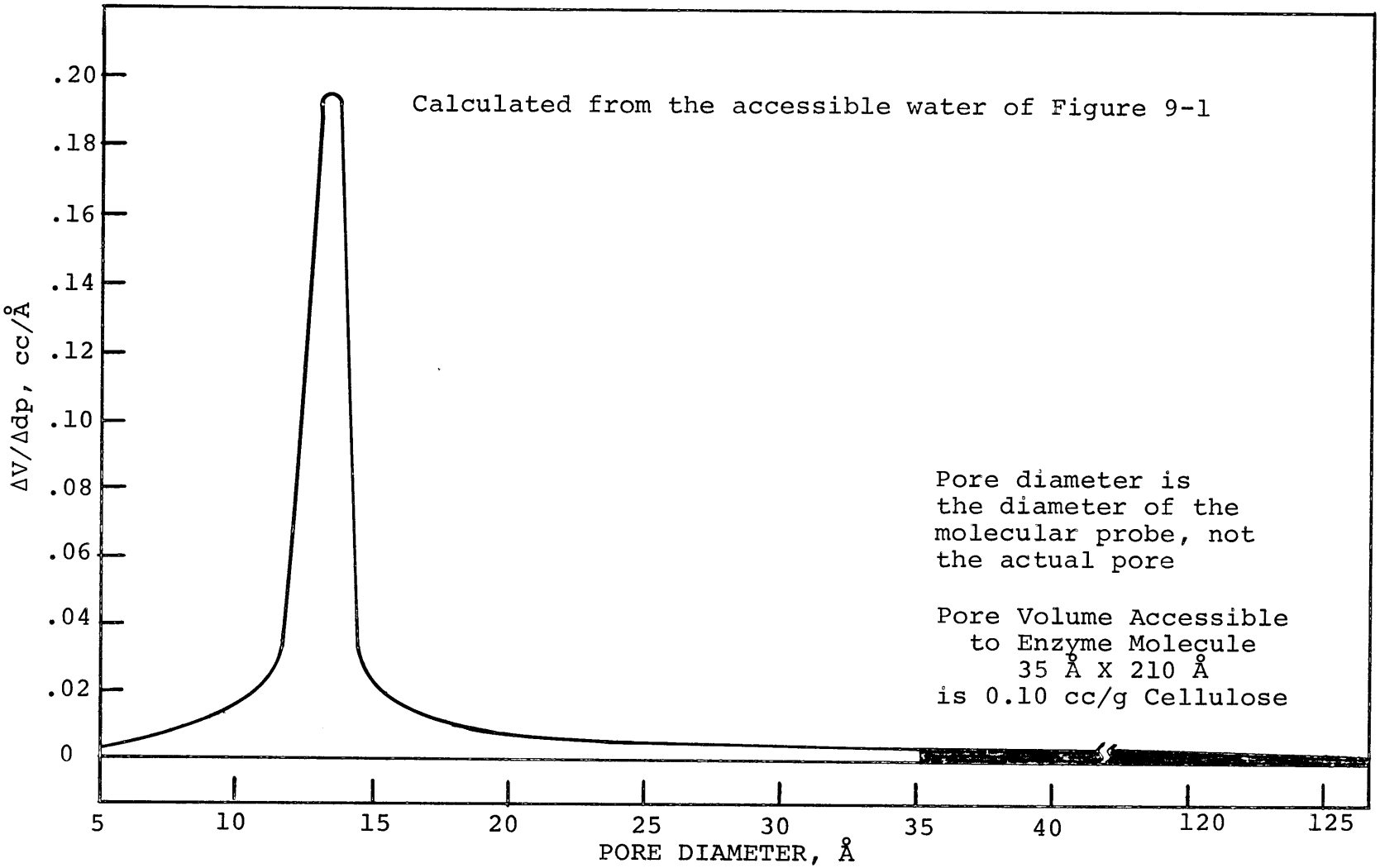

Figure 9-2. Pore Size Distribution Curve for Solka Floc

swollen 16μ spherical cellulose particles was only 0.5 m^2/g cellulose. The external surface is therefore, only 2% of the total area accessible to the enzyme molecules. The surface required to adsorb the enzyme measured during the hydrolysis studies was calculated to be 25 m^2/g, which agreed with the total available surface and is 50 times greater than that available only from the external surface.

Although the available pore surface is only 10% of the total pore area, it is extremely important to the hydrolysis reaction. It is upon this surface that most of the hydrolysis occurs. This accessible pore structure probably forms the "casing" around the core. The inaccessible crystalline core contains 85% of the total pore volume and 90% of the total pore area. The rate of hydrolysis could be significantly increased if these pores can be made accessible to the enzyme molecules.

Rough calculations employing the Faxen equation indicate that the effective diffusivity for enzyme molecules diffusing into pores between 35 Å and 40 Å (approximately 23% of the accessible pore volume) is reduced nearly 100 fold over the bulk diffusivity. The adsorption data for Run 15 was used with classical solutions of the pore diffusion equation to again determine the effective diffusivity; a 100 fold reduction in diffusivity was apparent. Albeit rough, these calculations also support the hypothesis that the enzyme can and does diffuse into the cellu-

lose particle.

G. Discussion of Results

The solute exclusion technique has been developed into a usable procedure for determining relative pore volumes. Previous work was extended by elaborating the experimental technique and defining the major sources of error. The technique, however, can not be used to determine an absolute pore size distribution. Such a determination would require firm knowledge of the actual configuration of the solute molecules within the pores. At present this is unknown and is, therefore, dependent upon assumptions. In addition detailed studies of the possibility of solute adsorption on the porous surface of the substrate have not been accomplished. Nelson and Oliver (169) reported that solutions of PEG ranging in concentration from 0.5 to 10% gave the same values of δ_s , but they made no mention of adsorption on glass and employed acetic acid, not water, as a solvent. In addition, no effort has been made to correct the results for polydispersity of solute molecular weight.

Employment of a test substrate that would not swell in water and upon which the solute molecules would not adsorb would prove an invaluable tool. Such a substrate would permit determination of pore volume and size distribution via the standard techniques of heterogeneous catalysis:

B.E.T. adsorption and mercury porosimetry. Comparison of the data with that of the solute exclusion technique using various water soluble probes including dextran and PEG would allow determination of the actual configuration of the molecular probes in solution. This data would eliminate the need for many of the assumptions presently required.

The adsorption phenomenon should be studied with each solute series and each substrate to be characterized. Variation in solute concentration should not change the values of inaccessible water unless adsorption occurs (see Appendix F). A relatively constant value of δ_s with different solute concentrations would imply the absence of adsorption.

The dextran series has one advantage over the PEG series: it can easily be fractionated on chromatograph columns. Such fractionation would give nearly monodisperse polymer fractions around each average molecular weight and would provide additional average molecular weights that are not commercially available.

Polyethylene glucols, unfortunately, are difficult to fractionate at molecular weights over 5000 (237). Various authors report that PEG is narrowly dispersed because they have attained a molecular weight (number based) agreeing with the manufacturer (254). They failed to realize, however, that the manufacturers have based their molecular weight on a number average, not a weight average

technique (126 and 245). Comparison of experimentally determined molecular weights with manufacturer's molecular weight does not yield mw/mn, a quantity which when unity signifies a narrow molecular weight distribution.

The solute exclusion technique as employed in this study provided an indication that cellulose has a pore structure, a small fraction of which is accessible to the enzyme. Although porviding a small surface area by catalytic standards (35 m^2/g versus 300 m^2/g) this area is extremely important to the enzymatic hydrolysis of cellulose because it determines the quantity of enzyme that can adsorb and hence participate in hydrolysis.

X. CONCLUSIONS AND RECOMMENDATIONS

A. Conclusions

The major goals of this thisis were to elucidate the mass transfer resistances involved in hydrolysis, to develop a kinetic model for the hydrolysis reaction, to verify that C_1 is the rate controlling enzyme, and to determine if the enzyme diffuses into the cellulose pore structure. In order to accomplish these objectives a complete set of procedures had to be developed to assay for the different hydrolysis products and for the concentrations of the enzymes in soltuion. In addition, the solute exclusion technique had to be developed and employed to characterize the cellulose pore structure.

The assay procedures developed provided easily reproducible mehtods for differentiating between soluble long chain cellulose fragments and the short fragments, cellobiose and glucose. In addition the latter could also be differentiated through calculation. The enzyme assays were reproducible and fairly easy to employ. The Lowry protein procedure yielded the surprising evidence that carbohydrate enhances the resulting optical density. (This information was not apparently available in the literature.)

The hydrolysis studies revealed that bulk mass transfer of the enzyme to the cellulose surface is not a factor in the reaction as long as the cellulose particles are sus-

pended in the solution. The bulk mass transfer of reaction products from the particle to the bulk solution also had little if any effect on the rate of reaction. The superposition of the data points for these studies was indicative of a high degree of reproducibility.

The wood pulp employed as a substrate yielded a rapid hydrolysis followed by a slower rate similar to the hydrolysis of amorphous and crystalline cellulose. For this reason the cellulose was subdivided into different fractions according to susceptibility to hydrolysis. The initial portion C_a was thought to be soluble long chains fragmented from the particles during milling. The next fraction C_b was considered the amorphous cellulose accessible to the enzyme. C_c was, therefore, the crystalline cellulose initally accessible to the enzyme. The final fraction C_d was the crystalline (and amorphous) cellulose initially inaccessible to the enzyme. Hydrolysis of C_d is probably controlled by the ability of the enzyme to gain access to the cellulose molecules rather than by the intrinsic kinetics that would depend upon the type of cellulose present.

Initial analysis of the hydrolysis curves (represented as the production of total carbohydrate with time) supported the hypothesis that the reaction was first order with respect to C_b , C_c , and C_d separately. Apparent first order kinetic coefficients were calculated for two series

of studies. The first established the effect of varying the cellulose concentration while holding enzyme constant. The second elucidated the effect of varying the enzyme concentration while holding the cellulose concentration constant.

The effect of substrate concentration indicated that the rate of reaction increased with initial cellulose concentration until a point at which the rate decreased with further increase of C_o . This point was defined as C_{opt} and was proportional to the enzyme concentration. A hypothesis was proposed that C_{opt} is the minimum cellulose concentration for complete adsorption of the enzyme present. Further, the extra surface provided by cellulose concentrations greater than C_{opt} decreased the probability that an endoglucanase and a C_1 molecule would concurrently bind to the same cellulose chain, thus decreasing the rate of reaction. Studies with a special concentrated enzyme revealed that C_{opt} was proportional to the endoglucanase activity rather than to the total protein or to C_1 activity.

The effects of substrate and enzyme concentration were combined into a complete kinetic expression. Each cellulose fraction (C_b , C_c , and C_d) was treated as a separate entity with the total carbohydrate being the sum of that liberated from each reaction. Each reaction was first order with respect to the quantity of the corre-

sponding fraction remaining, and proportional to the effective enzyme concentration to the 1.5 power. Since this was the same for both b and c , amorphous and crystalline cellulose were probably hydrolyzed by the same mechanism. The hydrolysis of amorphous cellulose was independent of surface in excess of C_{opt} ; hence, the effective enzyme concentration was the adsorbed enzyme concentration. The hydrolysis of crystalline cellulose was proportional to $C_o^{-1.5}$ indicating that the effective enzyme concentration was the enzyme concentration per unit cellulose as expressed by the θ group.

At cellulose concentrations less than C_{opt} , the initial rate of hydrolysis was proportional to C_o/C_{opt} . The order of the reaction decreased during hydrolysis from unity to 0.78 at moderately extended periods. An order of 0.67 would imply that hydrolysis was proportional to the surface of decreasing spheres.

Comparison of data obtained with an enzyme ratio (C_1 : endoglucanase) different from that used to develop the kinetic model indicated that the rate of hydrolysis is proportional to the amount of C_1 enzyme present, rather than to the endoglucanase concentration. Although not absolutely conclusive, this evidence does support the theory that C_1 is the rate controlling enzyme.

The solute exclusion technique was developed and its disadvantages elucidated. The technique was employed to

characterize the pore size distribution of the Solka Floc employed in the hydrolysis studies. The cellulose definitely is porous although 85% of the pore volume is inaccessible to a molecule the size of the minimum dimension of an enzyme molecule. Assuming a rectangular pore shape the accessible pore volume provides 98% of the surface available to the enzyme. The enzyme must diffuse into the accessible pores because the corresponding surface is required for complete adsorption of the enzyme protein.

Observation of the enzyme sorption data indicated nearly instantaneous adsorption of enzyme at high cellulose to enzyme ratios. As the cellulose concentration approached C_{opt} the rate of enzyme adsorption decreased. Rough calculations indicated that this decrease was proportional to a 100 fold decrease in effective diffusivity, approximately what would be predicted by diffusion into pores roughly the same size as the enzyme molecule. This supports the previous conclusion that the enzyme diffuses into the cellulose particles.

B. Recommendations

The work should be extended by exploring the effect of altering the C_1 : endoglucanase ratio. This would require fractionation of the enzyme complex on a chromatograph column. In addition the T. viride enzyme employed in this series of studies contained little if any exoglu-

canase or β-glucosidase. Glucose was, therefore, a small portion of the reaction products. Addition of exoglucanase and β-glucosidase should be examined for their effects on the overall hydrolysis reaction. It might prove feasible to employ a second reactor containing exoglucanase and β-glucosidase to hydrolyze the reaction products separate from the hydrolysis of the cellulose.

The model itself should be further verified by extending the hydrolysis into concentrations where cellulose is definitely the limiting reagent. Although the enzyme participating in hydrolysis at these conditions appeared equal to θ_{sat}, and the order of extended reaction appeared to be 0.78, this functionality should be investigated in more detail.

Although some researchers believe that increasing the strength of the enzyme complex is of paramount importance, the reaction appears limited by the available cellulose surface. Research efforts should therefore, be redirected into increasing the accessible surface.

The substrate should also be varied. Wood pulp is too ideal to be a feasible substrate for a commercial system becuase its preparation is too expensive. Milled newspaper and wood chips would be a much more difficult material to hydrolyze but would be a cheaper substrate for commercial conversion to glucose.

The solute exclusion technique should also be improved

by employing a substrate that will not swell in water. Mercury porosimetry and B.E.T. studies could then be used to verify the assumptions of molecular configuration employed by the solute exclusion technique. In addition the adsorption of dextran and polyethylene glycol on cellulose should be explored. Fractionation of the molecular probes prior to employing them in the technique would serve to narrow the molecular weight distribution around each average molecular weight chosen. Fractionation would also yield more average molecular weight portions than are available commercially, thus improving the results.

XI. APPENDIX

APPENDIX A

Cellulose Literature Review

1. The Chemistry and Physics of Cellulose

The chemical nature of cellulose was established more than 40 years ago. It is a carbohydrate consisting of polymerized glucose residues with a degree of polymerization (DP) as high as 14,000. The supramolecular structure of natural cellulosic material consists of cellulose chains ordered into microfibrils which are then ordered along with non-cellulosic material into the easily recognized forms of wood, cotton, etc.

The individual glucose residues display minimum free energy in the chair configuration. Each residue is joined by a β-1→4 glucoside bond as shown in Figure A-1. Infrared measurements of Liang and Marchessault (130) suggested that the cellulose molecule is stabilized by intrachain hydrogen bonding between the OH^3 in one unit and the O^5 in another and also by interchain hydrogen bonding as shown by the dotted lines in Figure A-1. Sumi, Hale, and Ranby (246) and Ranby (189) showed that all OH groups are involved in hydrogen bonding.

The cellulose crystal lattice, therefore, consists of parallel chains of cellulose bonded together in layers by intrachain hydrogen bonding, and between layers by van der Waals forces and weaker interchain hydrogen

bonds. Figure A-2 shows the unit cell of cellulose II (regenerated cellulose) (177). The strongest hydrogen bonds (between the O^5 and OH^3 groups) occur along with the primary valence groups in the "002" paratropic plane. The combined bond energy of the 002 hydrogen bonds and the primary valence bonds is about 50 kcal/mole. Individual cellulose chains or "ribbons" are bound together in sheets by interchain hydrogen bonds in the $10\bar{1}$ plane. The sheets are then held together by weaker interchain hydrogen bonds and van der Waals forces in the 101 planes. The 101 and $10\bar{1}$ bonds have about 15 kcal/mole and 8 kcal/mole respectively (177).

In electron micrographs the native cellulose microfibrils are usually seen as bundles of lamellae containing an indefinite number of fibrillar units. The microfibrils are about 30Å-40Å wide and have an indefinite length. The surface layers are shown to be areas of sufficient disorder to be hydrolyzed into rod-like particles (micelles) by aqueous, non-swelling strong acid. The preparation of microcrystalline cellulose by acid hydrolysis of native and regenerated fibers has been extensively studied by Battista et al. (10,11). The process aspects of wood chemistry have been reviewed by Oshima (176).

"It is evident from a study of x-ray diffraction diagrams that the major part of native cellulose has a crystalline arrangement. These diffraction patterns, which consist principally of clearly defined rings or arcs, also

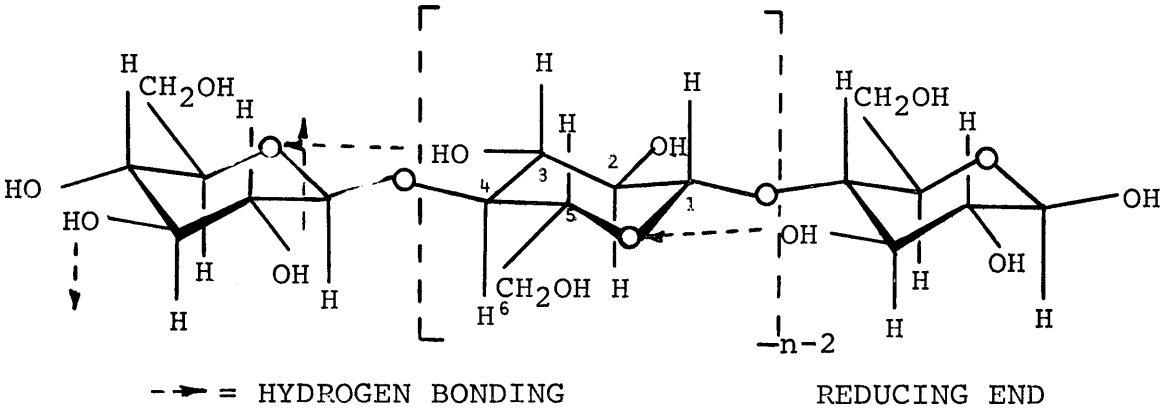

Figure A-1. Diagramatic Model of the Cellulose Molecule

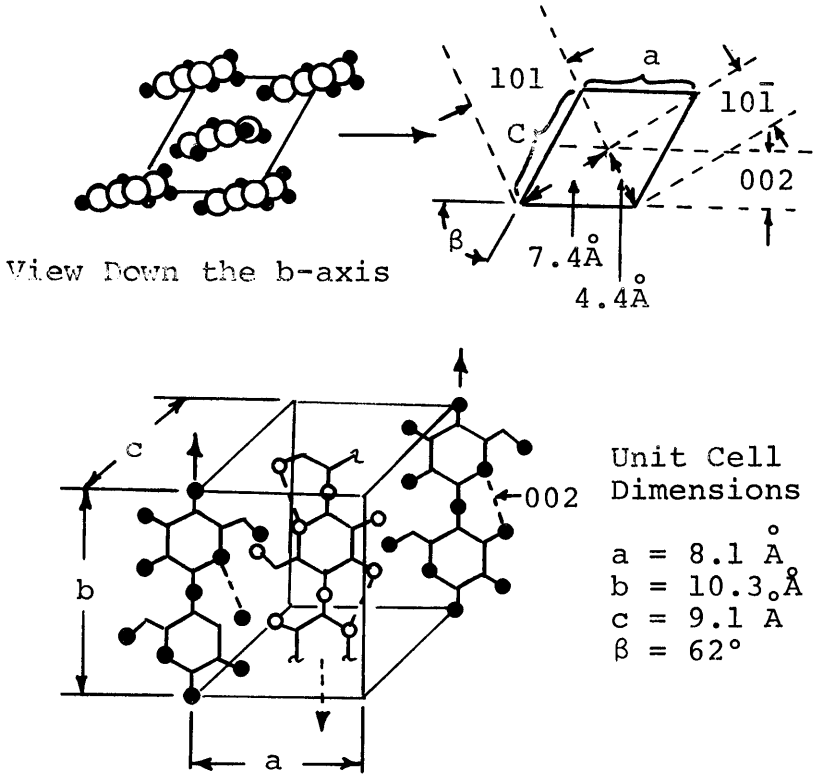

Figure A-2. Unit Cell of Cellulose II (Regenerated Cellulose)

show a diffuse halo from which it is concluded that amorphous (or non-crystalline) areas are interspersed among the imperfectly arranged crystalline regions" (70). This interspersion of crystalline types has complicated the modeling of cellulose structures. Muhlethaler (167) summarized five early models of cellulose structures as shown in Figure A-3. The earliest models consisted of (a) cellulose chains hydrogen bonded together into random crystalline areas and (b) extended chains of crystalline and paracrystalline cellulose. Later investigators tried to extend to cellulose the finding that most crystalline polymers exist in the folded configuration (c, d, e). Later work, however, revealed that crystallinity increased when wood cell walls were strained under tension in contrast to crystalline polymers that lose crystallinity upon stretching. Crystalline cellulose, therefore, must exist initially in an extended condition.

Based on x-ray studies of polymers, Statton (236) proposed a modification of the old fringe micelle model as shown in Figure A-4. In polymers where a crystalline state with a nearly perfect lattice can be obtained, disorders can be caused by dislocations. These defects, which contribute to diffuse scattering, are caused by the end of a molecule. If a molecule stops, a screw dislocation is caused which continues on through the lattice until it is stopped by meeting a similar chain end. These disturbances in well ordered crystals may contribute to diffuse

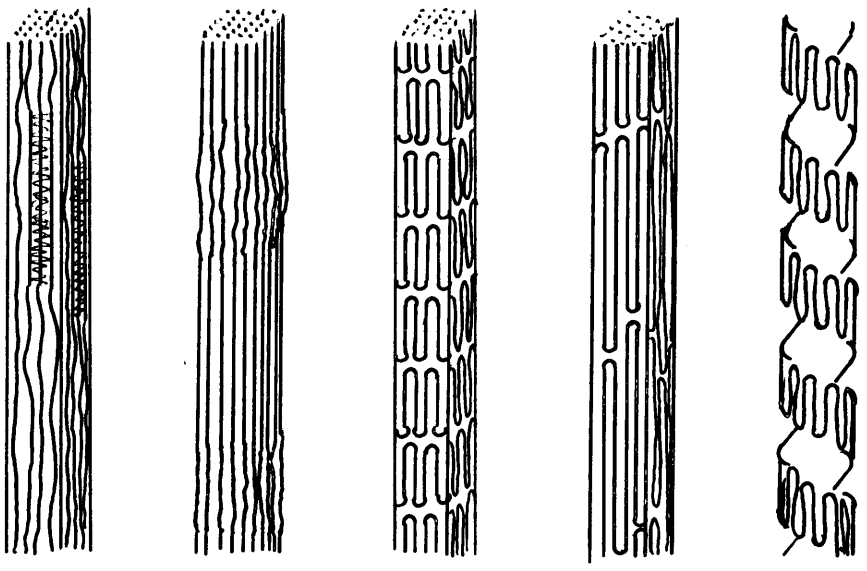

Figure A-3. Early Models of Elementary Cellulose Structure

Figure A-4. Statton's Model of the Microfibril

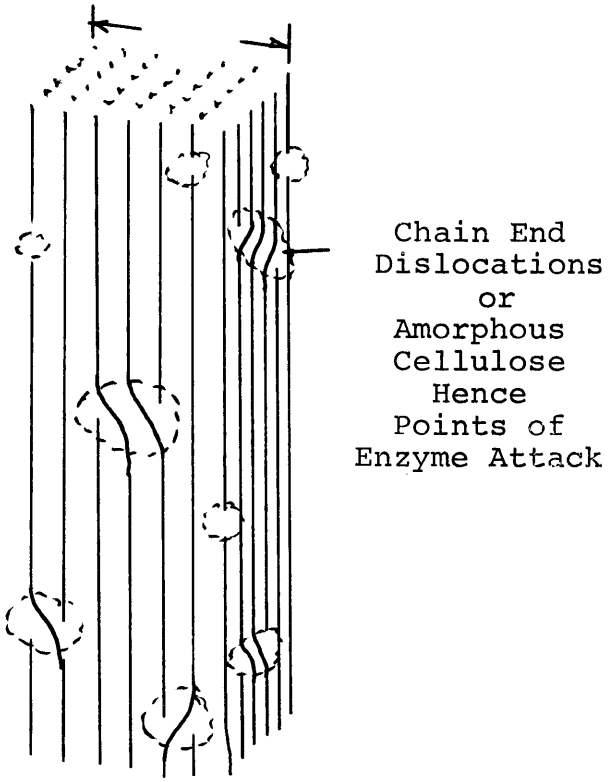

scattering to the same extent as an entangled region. His results showed that fiber density is related to crystal perfection (236). Statton's model of chain end dislocations agrees closely with Ranby's cross section model (88) and with Warwicker et al. (266): The cellulose fiber consists primarily of crystalline microfibrils containing about 100 cellulose chains.

Cellulose exists in various states of purity in plant cell walls. Native cotton and wood are 90% and 45% cellulose respectively. Cotton fibers are single-celled hairs that cover the surface of the cotton seed. They are formed independently and thus contain no intercellular substance. The outermost layer of cotton, the cuticle, corresponds to the middle lamella of wood. Both cotton and wood have a thin primary wall consisting of a loose fibrillar network surrounding the relatively thick secondary wall. In the wood cell this secondary wall usually consists of three layers, S_1, S_2, and S_3. The S_1 and S_3 layers are usually thin and are deposited in a flat helix with respect to the fiber axis, while those of the S_2 layer form the bulk of the cell wall and are nearly parallel with the axis. The S_3 layer is prominent in wood cells but not always in cotton fibers. In cotton the S_2 layer is deposited in a series of concentric zones. The cellulose microfibrils are held together by non-cellulosic material (38).

The chemical constituents of wood and cotton fibers include cellulose, several hemicelluloses, lignin (dis-

cussed in 2. Non-cellulosic Components of Wood), a wide variety of extraneous material including certain nitrogenous substances and a small amount of inorganic matter (38). Covalent bonds between lignin and certain of the polysaccharides in wood cell walls have been suggested for many years. Evidence for this remains in doubt because the possibility of physical entanglement can not be excluded. Whether or not a true covalent linkage does occur, the lignin and wood polysaccharides form a mutually interpenetrating system of polymers. As will be discussed later this intimate association with lignin accounts for much of the resistance of wood to many organisms that readily degrade cotton fibers. The lignin apparently prevents the cellulase and hemicellulase enzymes of these organisms from contacting a sufficient number of glycosidic bonds to permit significant hydrolysis (38).

Although cotton and wood form the major sources of cellulose, the bast fibers such as flax, hemp, ramie, and jute should not be ignored. Whereas the cotton fiber is a single cell, bast fibers as used in textiles and rope are composed of many cells. These fibers are composed of fibrils arranged in alternating spiral layers around a central axis.

Regenerated and substituted celluloses are also of interest. Rayon and cellophane are good examples of the former. Cellulose is treated with carbon disulfide in aqueous sodium hydroxide to form cellulose xanthate which

dissolves in the alkali to form a viscous colloidal dispersion called viscose. When the viscose is forced through a spinnerette into an acid bath, cellulose is regenerated in the form of fine filaments which yield threads of the material known as rayon. If a narrow slit is used in place of the spinnerette, cellulose is regenerated as thin sheets which, when softened by glycerol, yield cellophane. Although these compounds are considered regenerated cellulose, they consist of much shorter chains than the original cellulose because of degradation by the alkali treatment (177).

Substituted cellulose is formed by the dehydrolysis reactions of various acids with the free hydroxyl groups on the glucosyl residues. The degree of substitution (DS) is the number of these hydroxyl groups reacted per residue. Cellulose nitrate and cellulose acetate are formed from reactions of cellulose with a mixture of nitric and sulfuric acids and a mixture of acetic acid, acetic anhydride, and sulfuric acid respectively. Carboxymethylcellulose is formed by the action of formic acid and the sixth hydroxyl group to give a repeating unit of

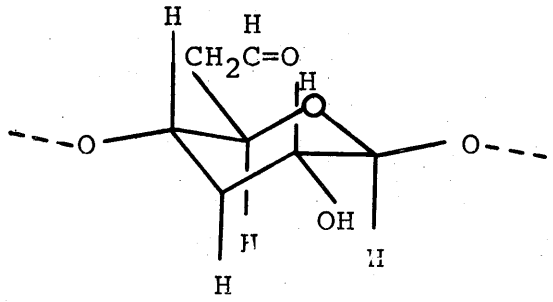

This ether is soluble in water and is used as a non-nutritive food filler, thickner, and as a substrate for the assay of cellulase enzyme (177).

Several excellent reviews have been published recently to update the work of Ott et al. (177): Hamby (85), and Warwicker et al. (266) on cotton, and the volumes edited by Zimmerman (275) and Côté (36) on wood.

2. Non-cellulosic Components of Wood

As mentioned previously wood cellulose occurs naturally in close association with many other substances such as the hemicelluloses, pectin, and lignin. The hemicelluloses and lignin together approach the cellulose content in amount. The hemicelluloses include all of the cell wall polysaccharides "which are removable from untreated tissues by extraction with hot or cold dilute alkali, and which can be hydrolyzed with dilute acids to give the constituent monosaccharide units" (174). The hemicelluloses can be subdivided into (a) the polyuronides, containing uronic acid groups and (b) the cellulosans, which do not characteristically contain hexuronic acid units. The polyuronides are composed of the pentoses xylose and arabinose, and the hexoses glucose and galactose. They are amorphous and appear to be part of the system which penetrates and covers the cellulose matrix. The cellulosans, xylan, mannan, and the glucans are to some degree oriented in the micellar structure and form the pulp fractions

known as β- and γ-cellulose. "The hemicelluloses are thought to be linked to lignin, at least to some extent, probably by a glysodic linkage" (71).

Pectins are almost exclusively composed of galacturonic acid and its methyl ester. These substances are found in all young plant tissues and are characteristic tissues of fruits and fleshy roots. In tissues that become lignified and in which secondary thickening of the cell wall occurs, the pectic content diminishes, though some calcium or calcium magnesium pectate may persist to maturity in the middle lamella (173).

Lignin may be defined as a "system of (thermoplastic) tridimentional polymers (derived from coniferyl alcohol or other guaiacylpropane monomers), which permeates the membranous polysaccharides and the spaces between the cells (of wood plants), thereby strengthening them" (179). The chemical characterization of lignin emanates from an idealized representation for which spruce lignin is the model. It is insoluble in water, in most organic solvents, and in strong sulfuric acid. Lignin has a varying composition and a molecular weight ranging from 4,000 to 100,000. It has a characteristic ultraviolet absorption spectrum giving a maximum at a wave length of 280 nm, and gives characteristic color reactions with many phenols and aromatic amines. Lignin reacts readily with sodium bisulfire (pulping) or thioglycolic acid to form soluble products.

3. Pulping: Delignification

Pulping is the removal of lignin from wood chips to leave a nearly pure cellulose residue. In the sulfite process wood chips are digested in an aqueous solution containing sulfur dioxide and a sulfurous acid salt such as calcium or sodium bisulfite. Essentially lignin dissolution occurs in two stages: (1) solid phase sulfonation of the lignin producing a solid lignosulfonic acid and (2) solution of this acid giving water soluble lignosulfonic acids which leave the solid phase. These are separated from the residual cellulosic pulp by filtration and washing (and are then often dumped into a handy body of water). Products such as Solka Floc and Alpha Cellulose are nearly pure cellulose pulps. Most paper is made from wood pulps; newspaper, however, is mostly made from ground softwood (spruce or pine) and, hence, contains lignin and hemicellulose (179).

4. Degradation of Cellulose

The four major types of cellulolytic degradation as summarized by McBurney (152) are (1) hydrolytic, (2) oxidative, (3) mechanical, and (4) microbiological.

Hydrolytic Degradation

The cellulose molecule is sensitive to acids because it is bound together by acetal linkages. The acid rapidly penetrates the amorphous regions of the cellulose where it causes chain scission. Once all of the amorphous

regions have been hydrolyzed, the reaction becomes extremely slow because penetration of the acid into the crystallites is difficult. Several processes involving dilute and concentrated sulfuric acid, concentrated hydrochloric acid and hydrochloride gas have been developed; these are well summarized by Oshima (176).

Hydrolysis of wood proceeds quantitatively with very little degradation of sugar when sufficiently large quantities of sulfuric acid are used to insure intimate acid cellulose contact. Recovery of the acid is diffucult and expensive. The process has become more successful by development of ingeneous equipment to intimately contact the wood with small quantities of the concentrated acid and to recover this acid.

The dilute sulfuric acid process was devised to surmount the difficulties of sulfuric acid recovery. The trend was to operate at elevated temperatures to boost the catalytic activity of the dilute acid. The product was a dilute sugar solution, utilizable only for the growth of yeast and, thereby, the production of alcohol.

Hydrochloric acid is more easily recovered than sulfuric acid, but it is also much more corrosive. Consequently, the development of this process has been dependent upon the development of corrosion resistant materials and equipment. Although the initial product was a dilute sugar solution, later hydrochloric acid processes have concentrated the broth by distillation in order to

provide an adequate solution for crystallization of the sugar product. The hydrochloric gas process is a refinement that can utilize most HCl containing gas streams as an acid source. The high cost of corrosion resistant equipment has been the main disadvantage with this process.

Oxidative Degradation

Cellulose, because of its polyhedric alcohol structure, is very sensitive to oxidizing media such as hypochlorite, potassium permanganate, chlorine, and oxygen. The reactions are extremely sensitive to pH. Little chain scission occurs as a result of oxidation, but chemically labile groups are formed that are then sensitive to alkaline cleavage. Bleaching reactions, which are utilized in the manufacture of all types of cellulose, are oxidative reactions. Heating in the presence of air and water produces severe reduction in tensil strength. The consumption of oxygen is accelerated by moisture and the loss in strength follows the consumption of oxygen.

Mechanical Degradation

Grinding, milling, and cutting are common unit processes in the chemical industry employed to achieve both size reduction and an increase in surface area. Application of these processes does not usually cause any deep-seated chemical or physical changes. When these operations are applied to polymers, however, size reduction is also accompanied by physical and chemical alterations in

the polymer. These alterations occur in the form of crystal lattice deformation and concurrent reduction in degree of polymerization.

Milling produces two distinct products. Initially the fibers undergo fibrillation into very fine fibrils. Further milling (about 30 min total) produces cellulose powder with a maximum dimension of 10μ. The powdery modification of cellulose has undergone extensive changes in its physical and chemical properties. The x-ray diffraction pattern, for example, has changed from that of mainly crystalline cellulose to a broad diffuse band corresponding to amorphous cellulose. This crystal lattice deformation is accompanied by an increase in fluidity (solubility, solution viscosity), moisture regain, and carboxyl content as shown in Figure A-5. The fluidity time curve is indicative of major chain scission, whereas the moisture absorption increase is the result of reduction in crystallinity. These powdery celluloses will not retain their amorphous structure unless they are protected from moisture (152) which causes hydrogen bonding, and hence, recrystallization. The advantage of milling will be shown in Effect of Substrate Pretreatment on Enzyme Action.

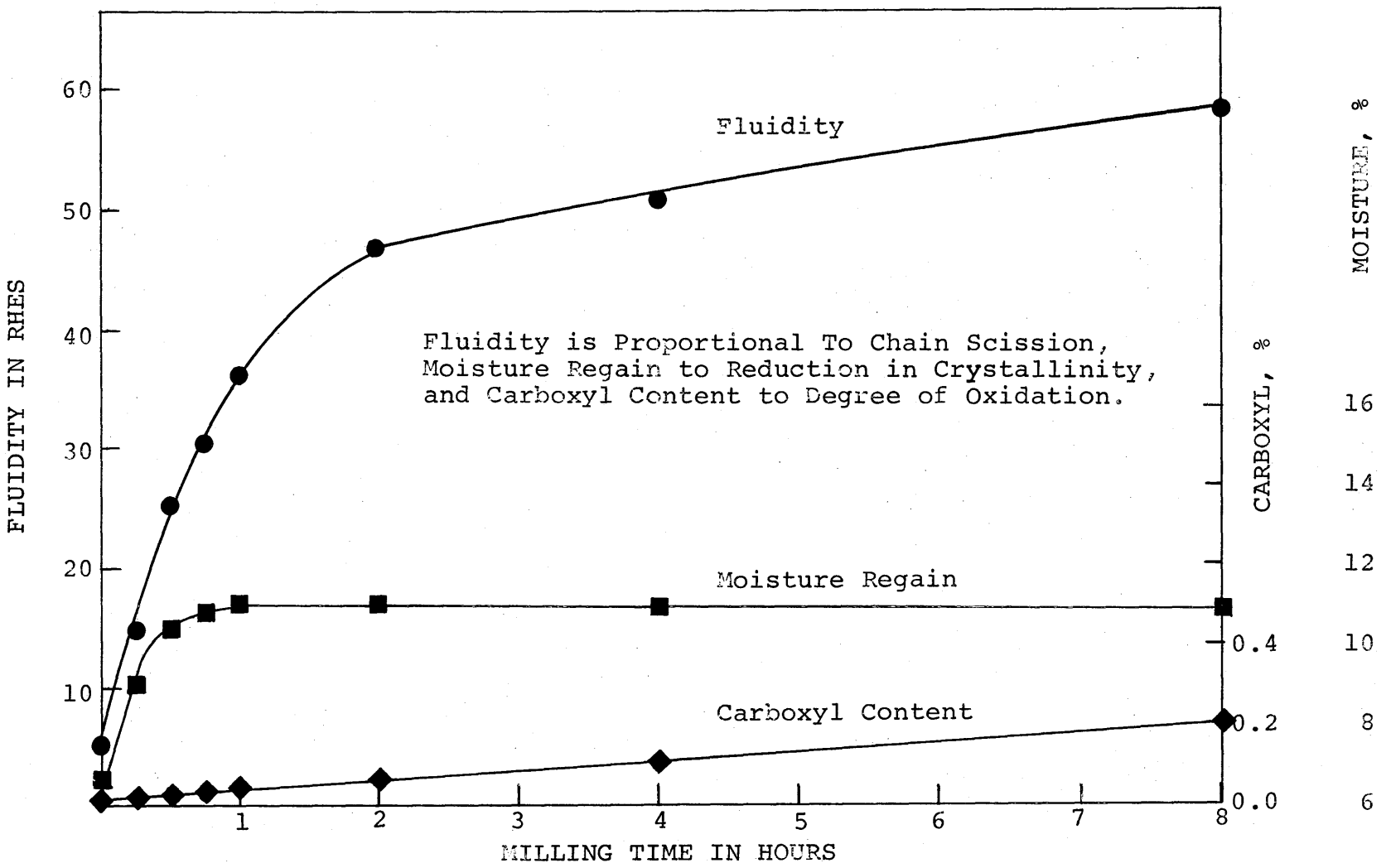

Figure A-5. Results of Cellulose Milling (152)

APPENDIX B

Cellulase Enzyme Literature Review

1. The Enzyme and Its Mode of Action

In enzymology degradative enzymes are often named by adding -ase to the compound or substrate they degrade. Cellulases then are enzymes that degrade (in this case hydrolyze) cellulose. Cellulase is an extracellular enzyme complex produced by all cellulolytic fungi. It degrades cellulose chains by hydrolyzing the β-1→4 glucoside bonds. King and Vessal (108)reported that the Trichoderma viride cellulase complex is a true cellulase in the most rigid sense, capable of hydrolyzing crystalline, amorphous, and chemically derived cellulose quantitatively to glucose. It has been established that (a) the system is multi-enzymatic, (b) at least three enzyme components are both physically and enzymatically distinct, and (c) all three components are essential to the overall hydrolysis of cellulose to glucose. The action of the complex is summarized below by King and Vessal and diagramed in Figure B-1.

> "As currently understood, the cellulase complex contains the following components (listed in the order in which their action on cellulose occurs);
>
> 1. C_1 is an enzyme whose action is unspecified. It is required for the hydrolysis of highly oriented solid cellulose (Cotton, Avicel, etc.) by β-1→4 glucanases.
>
> 2. β-1→4 Glucanases (often referred to as C_x) are the hydrolytic enzymes. In his book, Eriksson (48) uses cellulase as synony-

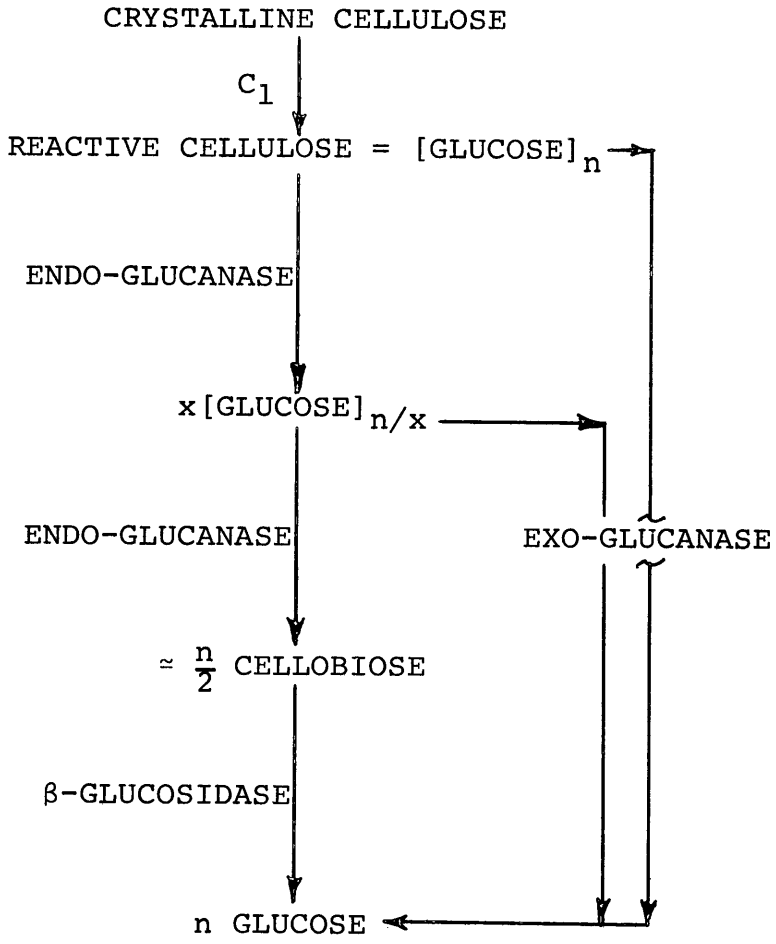

Figure B-1. Action of the Cellulase Complex (141)

mous with β-1→4 glucanase. It is preferable to reserve the term cellulase for the C_1-C_x complex. C_x is an earlier synonym which can be discarded. β-1→4 Glucanase is usually measured by action on soluble cellulose derivatives, usually carboxymethylcellulose. The "x" in C_x emphasizes the multi-component nature of this reaction.

The β-1→4 glucanases are clearly of two types:

(a) exo-β-1→4 glucanase, sucessively removing single glucose units from the non-reducing end of the cellulose chain;

(b) endo-β-1→4 glucanases with action of a random nature, the terminal linkages generally being less susceptible to hydrolysis than internal linkages.

3. β-Glucosidases vary in their specificities. Those that act primarily on aryl-β-glucosides are not involved in cellulase action. The β-glucosidases that are involved in cellulose breakdown are those highly active on the β-dimers of glucose, including cellobiose. "Cellobiase" is the most descriptive designation for this group (to cellulase workers) but a more accurate name might be "β-glucodimerase," indicating the ability to act on all of the β-dimers of glucose.

β-Glucosidases and exo-β-1→4 glucanases have substrates in common, cellobiose to cellohexaose. β-Glucosidases hydrolyze the smaller oligomers most rapidly; exo-glucanases, the larger ones. β-Glucosidases act by retention of configuration; exo-glucanases by inversion. β-Glucosidases are strongly inhibited by gluconolactone, exo-glucanases much less so. Finally there is a difference in linkage specificity, the exo-enzyme generally being more specific; the β-glucosidase less specific," (109)

The C_1 enzyme is required for attack on crystalline cellulose. Iwasaki, Hayashi, and Funatsu (100) used a hydroxyapatite chromatograph column to separate the complex into C_1 and C_x components. They reported a molecular weight of about 50,000 for the component active on cotton. Selby (216) considered the C_1 a glycoprotein with

a carbohydrate ratio of about 1:1, apparent molecular weights by gel-filtration of about 57,000, and isoelectric pH values of approximately 4.05. He proposed an extension of the hydrogen-bondase concept proposed by Siu (227), i.e., that C_1 breaks interchain hydrogen bonds enabling C_x to reach the individual cellulose chains. Based on new theories of the supramolecular structure of cotton (see Appendix A: The Chemistry and Physics of Cellulose) Selby claimed that the disturbance of the regular molecular chains by the occurence of chain ends could cause sufficient disruption in interchain hydrogen bonding to enable C_x acting alone to detatch soluble sugars. C_1 might further disturb the hydrogen bonding, loosening a length of surface chain which could be attacked by C_x. Chain ends occur at intervals of approximately 200 glucose units which would explain both the occurrence of 200 degree of polymerization fragments and the difficulty in detecting the effect of C_1 or C_x acting alone by measurements of swelling, loss of weight, or loss of wet strength.

The C_x components attack amorphous cellulose and cellulose derivatives. These are the actual hydrolytic enzymes and include endo-β-1→4 glucanase(s) and exo-β-1→4 glucanase(s). King and Vessal (108) reported that physically the endo- and exo-glucanases differ markedly in amino acid composition, molecular weight, and thermal stability. Enzymologically they differ only slightly in activation energies for hydrolysis of both cellulodextrins

and carboxymethylcellulose, but are significantly different in mode of action, Km values for the cellulodextrin series (Table B-1) (108), optimum substrate chain length, and pH optimum. The Michaelis-Menton constant (Km) (discussed in Appendix D: Enzyme Kinetics) is in essence the substrate concentration required to give one-half the maximum rate of hydrolysis. A strong enzyme usually has a low Km and a weak enzyme a high Km. As can be seen in Table B-1, endoglucanase has a preference for longer chain substrates while exoglucanase prefers either cellotetrose or cellopentose.

The endoglucanase is essentially random in its action, while the exoglucanase acts endwise, removing single β-glucosic units from the non-reducing end of the chain. The exoglucanase has a high affinity for oligosaccharides (short chain glucose polymers) and acts by inversion producing α-glucose. According to a verbal commumication from Mary Mandels the enzyme will hydrolyze a chain of mixed α- and β-glucans. It apparently acts by binding to the β-linkage and hydrolyzing an adjacent linkage, either α or β.

Selby and Maitland (217) separated a filtrate from T. viride on Sephadex G-75. A low molecular weight carboxymethylcellulase was removed after the first separation. The remaining components were unresolved, but there was evidence for the existence of separate peaks of C_1, β-1→4 glucanase, and β-glucosidase. The C_1 component was sepa-

rated from the latter C_x components by gradient elution on DEAE-Sephadex. The β-glucosidase(s) and β-glucanase(s) were subsequently resolved on SE-Sephadex. Recombination experiments (Table B-2) illustrate the synergistic action of the various components acting on crystalline cellulose: (1) C_1 is virtually without activity in the absence of C_x; (2) There is no synergism between the components of C_x; and (3) Synergism between C_1 and the individual components of C_x is limited. All three must be present to account for the activity toward cotton.

The multienzyme nature of this complex increases the difficulty of discerning and modeling the mechanism of hydrolysis. Cellulase researchers have concentrated on discovering and developing potent cellulase complexes and in investigating the hydrolysis mechanism.

2. Physical Properties of Cellulases

The cellulolytic enzymes are water soluble protein molecules of high molecular weight. The most complete physio-chemical characterization of a cellulolytic enzyme was performed by Whitaker, Colvin and Cook (272) on the cellulase of Myrothecium verrucaria. No mention was made concerning which enzyme of the complex was characterized. Their data indicate that this molecule is an asymmetric globular protein with a molecular weight of about 63,000. In their words, "it corresponds to a cigar-shaped molecule roughly 200 Å long and 33 Å wide at the broadest point."

TABLE B-1. MICHAELIS CONSTANTS FOR CELLULOSE POLYMER SERIES: ENDO- AND EXOGLUCANASES OF TRICHODERMA VIRIDE*

Substrate	Michaelis Constants: Endoglucanase	Exoglucanase
Cellobiose	190 X 10^{-4}M[a]	220 X 10^{-5}M[a]
Cellotriose	31 X 10^{-4}M	18 X 10^{-5}M[a]
Cellotetraose	28 X 10^{-4}M	6.5 X 10^{-5}M[a]
Cellopentose	7.0 X 10^{-4}M	6.0 X 10^{-5}M
Cellohexose	1.0 X 10^{-4}M[a]	16.0 X 10^{-5}M[a]

[a]These Lineweaver-Burk plots showed apparent substrate inhibition at concentrations greater than 0.05M.
* King and Vessel (108)

TABLE B-2. SYNERGISM OF C_1 AND C_x COMPONENTS OF T. VIRIDE CELLULASE*

Component	Relative Cellulase Activity (%)
Original solution	100
C_1	1
C_x	5
C_1 + C_x	102
CMC-ase	4
Cellobiase	1
CMC-ase + cellobiase	2
C_1 + CMC-ase	35
C_1 + cellobiase	20
C_1 + CMC-ase + cellobiase	104

*Selby and Maitland (217)

Their judgement of the shape of the cellulase molecule was substantiated by comparison of hydrodynamic parameters (Table B-3) and estimates of size and shape derived from available viscosity and diffusion data for a well characterized globular protein, serum albumin, and an elongated, rod-shaped protein, tropomysin (Table B-4) (272).

Estimates of the diameters of the other cellulolytic enzymes are given in Table B-5 (38). In some cases (marked GF) the dimensions given were calculated by the method of Laurent and Killander (124) from available gel-filtration data on the enzymes. In other cases (marked MW) the dimensions were obtained by interpolating a logarithmic plot of molecular radius versus molecular weight using data summarized by Tanford (253). (A curve plotted from this source is presented in Appendix E: Diffusion Theory.) A considerable range of dimensions is shown for the various cellulose preparations. If the enzymes are considered spherical they range from 25 Å to 80 Å in diameter, with an average of 60 Å. If the enzymes are ellipsoids with an axial ratio of about six, as demonstrated for M. verrucaria enzyme, they range from 15 Å by 80 Å to 40 Å by 250 Å with an average of 35 Å by 200 Å. As can be seen from Table B-5 there is a large variation in data. It is not known whether different microorganisms produce different sized enzymes; whether the same microorganisms produce different sized enzymes depending upon the inducer; or whether the variation in data results from differences

TABLE B-3. COMPARISON OF HYDRODYNAMIC PARAMETERS FOR A CELLULOLYTIC ENZYME FROM MYROTHRECIUM VERRUCARIA, A GLOBULAR PROTEIN, SERUM ALBUMIN, AND AN ELONGATED ROD-SHAPED PROTEIN, TROPOMYOSIN

Protein	Molecular Weight M_{sD}[a]	Sedimentation Coefficient $S_0 \times 10^{13}$	Diffusion Coefficient $D_0 \times 10^7$	Frictional Ratio[b] f/fmin	Intrinsic Viscosity (η) ml/g
Cellulase	63,000	3.72	5.61	1.44	8.70
Serum albumin	65,000	4.31	5.94	1.35	3.70
Tropomyosin	93,000	-	2.24	3.22	52

[a]Based on sedimentation diffusion data
[b]fmin refers to the frictional factor for the hydrodynamically equivalent sphere.
Whitaker et. al. (272)

TABLE B-4. ESTIMATES OF SIZE AND SHAPE OF A CELLULOLYTIC ENZYME FROM MYOTHRECIUM VERRUCARIA, A GLOBULAR PROTEIN, SERUM ALBUMIN, AND AN ELONGATED ROD-SHAPED PROTEIN, TROPOMYOSIN (Whitaker et. al. (272)

	Fully Solvated Equivalent Sphere		Unsolvated Equivalent Ellipsoid	Partially Solvated Equivalent Ellipsoid
	Water of Solvation g/g	Diameter Å.	Length X Width Å.	Length X Width Å.
Derived from Viscosity Data				
Cellulase	2.8	90	380 X 40	300 X 50
Serum Albumin	0.8	70	250 X 40	230 X 45
Tropomyosin	20.0	180	1700 X 60	-
Derived from Diffusion Data				
Cellulase	1.5	80	300 X 40	250 X 40
Serum Albumin	1.1	70	250 X 40	210 X 40
Tropomyosin	23.0	190	3000 X 50	-

TABLE B-5. ESTIMATED SIZE OF CELLULASES OF VARIOUS FUNGI*

	Molecular Weight	Equivalent Sphere Diameter, Å.	Equivalent Ellipsoid W X L, Å.	Method of Estimation
Aspergillus niger	-	60	30 X 190	GF
Aspergillus niger (Rohm and Haas Cellulose 36)	-	30	15 X 100	GF
	-	25	15 X 85	GF
Myothrecium verrucaria	63,000	40	25 X 140	GF
		40	20 X 130	GF
Myothrecium verrucaria	49,000	80	40 X 250	MW
Myothrecium verrucaria	55,000	65	35 X 210	MW
	30,000	70	35 X 220	MW
	30,000	50	30 X 170	MW
	5,300	55	30 X 190	GF
Penicillum notatum	35,000	25	15 X 80	MW
Penicillum notatum	35,000	65	35 X 210	GF
Polyporus versicolor	51,000	55	30 X 180	MW
	11,400	65	35 X 210	MW
Stereum sanguinolentum	20,500	35	20 X 110	MW
Trichoderma koningi	50,000	35	20 X 120	GF
	26,000	65	35 X 210	MW
Trichoderma viride	76,000	45	25 X 150	MW
	49,000	75	40 X 250	MW
Trichoderma viride	61,000	65	35 X 210	MW
	12,000	70	40 X 230	MW
	39,000	35	20 X 210	MW

*Calculated values are from available gel filtration or molecular weight data. The deminsions given are for hydrodynamically equivalent spheres of ellipsoids with an axial ratio of six as demonstrated for the cellulase of Myothrecium verrucaria (38).

between various enzymes (C_1 and the C_x's) of the cellulase complex. Although the data is obscure, it at least provides an estimate of molecular dimensions.

3. Enzyme Inhibition

Minerals are often necessary for enzymatic reaction. Pidgen and Heaney (181) reported that molybdenum, sulfur, phosphorus, iron, magnesium, and calcium have stimulated cellulolytic activity, whereas copper, cobalt, zinc, and boron are inhibitors. Mandels and Reese (147) reported that hydrolysis proceeds better in phosphate buffer than in citrate buffer.

Mandels and Reese summarized the results of various inhibition studies in Table B-6 (147). The values shown give the lowest concentrations required to give a cellulase inhibition of approximately 50%. The inhibition may be greatly affected by using different enzyme preparations or experimental conditions.

Substrate inhibition has also been reported by Mandels and Reese (147). For Trichoderma viride cellulase acting on soluble CMC, the optimum substrate concentration is 10 mg/ml, above which inhibition seems to occur. For the same cellulase acting on cellolose sulfate, however, the optimum substrate concentration is over 20 mg/ml. Some enzymes bind their substrate at two different sites. As the substrate concentration increases, the likelihood of the enzyme binding with two different substrate mole-

TABLE B-6. INHIBITION OF CELLULASE--SUMMARY*

Adsorbants	Charcoal, clay 0.1%
Heat	100°, 10-20 min
Acid	pH 2 or below
Alkali	pH 8.5 or above
Irradiation	2-5 megarads
Urea	4M at pH 5.0
	Concentration Required for 50% Inhibition
Metals	
Ag	10^{-4}M
Hg	10^{-3}M
Cu, Cr, Fe, Pb	No Effect
Mn	10^{-3}M
Halogens	10^{-3}M
Halogenators	10^{-4}M
Ethylene Bisdithiocarbamate	10^{-4}M
Phenyl Mercuric acetate NO_3	Saturated
Dibutyl Mercury	Saturated
Octyl Gallate	Saturated
2-3-Dichloronaphthoquinone	Saturated
Nitroso Pyrazoles	Saturated
Substituted Phenols (Pentachlorophenol)	10^{-3}M
Quebracho Tannin	0.0078%
Bayberry Inhibitor	0.00018%
Persimmon Leucoanthocyanin	0.00005%

*Mandels and Reese (147)

cules increases, resulting in inhibition. The action of β-1→4 glucanases acting on soluble substrates such as carboxymethylcellulose could be such a case.

Ghose (73) has reported glucose inhibition. Reese and Mandels (196) reported inhibition by other sugars (Table B-7). This form of inhibition is unfortunate since cellobiose and glucose are the major products of hydrolysis. Product inhibition is usually the competative type in which the product competes with the substrate for the active site. The reaction, however, may be reversible, in which case increasing product concentration would tend to force the equilibrium toward dehydrolysis.

4. Effect of pH

The optimum pH for hydrolysis by Trichoderma viride cellulase on Solka Floc and Alpha Cellulose is shown in Figure B-2 to be between 4.8 and 5.2 (148). Figure B-3 shows that pH optimum varies with the enzyme (147). The effect on the hydrolysis rate should have about the same dependence on pH as does the extent of hydrolysis. The enzymes tend to deactivate at extremes of pH as temperature increases. Heating at pH 2.0 or 10.0 at 80°C for one hour will completely deactivate the enzyme.

5. Effect of Temperature

Ghose and Kostick (75) showed that temperature has little effect on the pH optimum of hydrolysis. The hy-

TABLE B-7. INHIBITION OF PENICILLIUM PUSILLUM CELLULASE BY SUGARS*

	INHIBITION OF HYDROLYSIS			
	CMC visc.	Swollen Cellulose Weight Loss	Ball-milled Cotton Weight Loss	Cotton Swelling
Cellobiose	48	46	72	52
Lactose	88[a]	44	60	54
Maltose	5	4	1 stim.	NT
Glucose	5	NT	NT	37

[a]Lactose (0.1%) gave 52% inhibition
*Reese and Mandels (196)

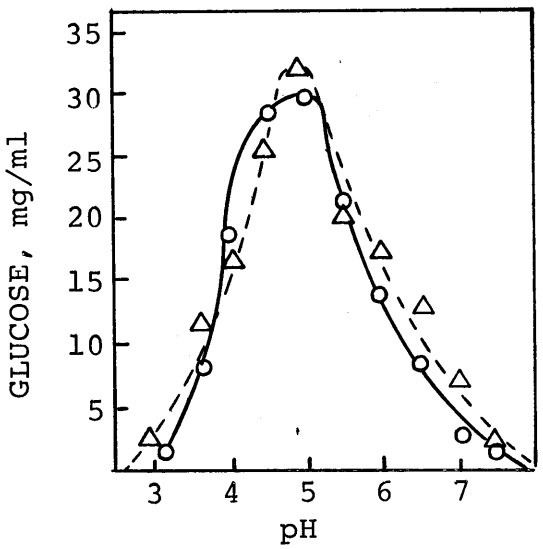

o Solka Floc
△ Alpha Cellulose

5% Suspension Incubated 10 Days at 50°C, Unshaken

Figure B-2. Effect of pH on Extended Hydrolysis by T. viride Cellulase (148)

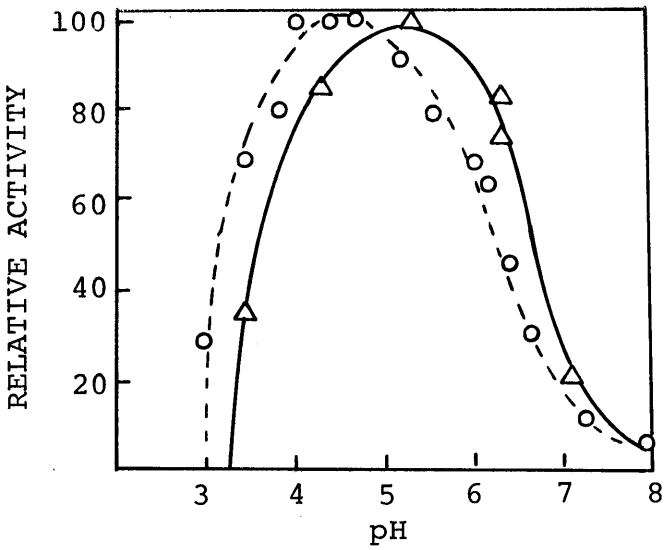

△ Cellulase of T. viride
o Cellulase of Basidiomycete
50°C; 0.05 M buffer

Figure B-3. Effect of pH on Cellulase Activity (147)

drolytic rate appears to increase with temperature up to 60°C at which point long term inactivation of the enzyme becomes important (Figure B-4) (147). Enzyme denaturation is a problem especially at temperatures over 50°C. A typical Arrhenius plot is shown by Li, Flora, and King (128) in Figure B-5. The break in the CMC curve occurs because this material forms a viscous gel at temperatures below 37°C increasing the resistance to diffusion of the enzyme into the gel and of glucose from the gel.

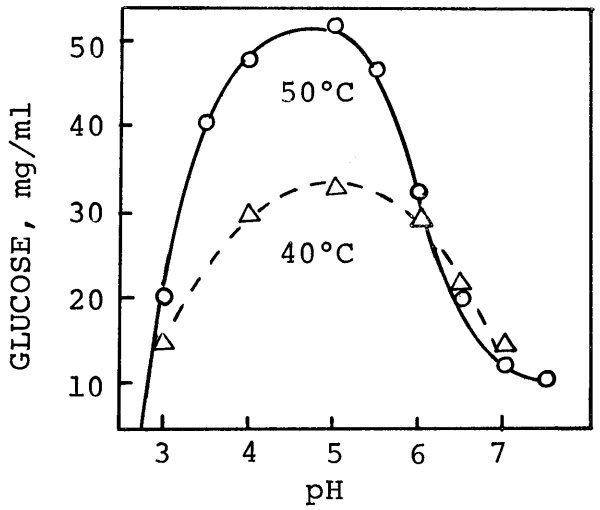

Cellulose activity - 1.26 FP units;
Substrate concentration - 10%:
Time - 10 hours;
0.5 liter glass stirred tank reactor

Figure B-4. Effect of Temperature on pH Optimum (75)

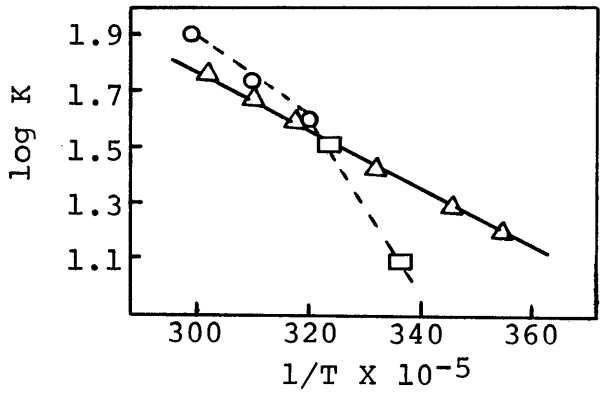

△ Cellulose 5.1 kcal/mole
○ CMC 6.4 kcal/mole
□ CMC 16.7 kcal/mole

Figure B-5. Arrhenius Plot for Cellulase Hydrolysis (128)

APPENDIX C

Saccharification Processes Literature Review

A few attempts have been made at continuous enzymatic saccharification of cellulose, the most notable of which have been by Ghose (73) and Ghose and Kostick (74, 75). They employed Solka Floc, a spruce wood pulp widely used as a filter aid, as a substrate. The pH and temperature optima proved to be 5.0 and 50°C respectively. Pretreatment of the cellulose proved necessary to increase the bulk density of the substrate slurry and to increase the rate of hydrolysis. Simultaneous heating and milling to the smallest possible size appeared to yield the best results. The rate of hydrolysis stabilized, independent of pretreatment, as amorphous cellulose was hydrolyzed. Ghose and Kostick (75) investigated the possibility of recycling these crystallites through wet milling and found that milling of the digestion residue greatly increased its susceptibility to further hydrolysis. Only a small loss of enzyme activity during the wet milling occurred. A solids feeder injected dry cellulose into the reactor and an ultrafiltration membrane separated the glucose solution from the enzyme.

A comparison of acid and enzyme hydrolysis was presented by Gascoigne and Gascoigne (72) as shown in Table C-1. Enzymatic hydrolysis was much more extensive than the acid hydrolysis, but resulted in residues having

TABLE C-1. COMPARISON OF ACID AND ENZYME HYDROLYSIS (72)

Sample	Type of Cellulose and D.P.	Acid Hydrolysis: Weight Loss at Level-off %	Acid Hydrolysis: D.P. After Reaction	Enzyme Hydrolysis: Weight Loss at Level-off %	Enzyme Hydrolysis: D.P. After Reaction
A	Kiered Cotton 4970	4	225	25	4200
B	Mercerized 5040	6.5	138	35	3040
C	Decrystallized 4670	7	133	35	3100
D	Decrystallized 3920	8.9	112	65	1630

Sample	Type of Cellulose	Acid Hydrolysis: Time of Reaction hr.	Acid Hydrolysis: Weight Loss %	Acid Hydrolysis: D.P. of Residue	Enzyme Hydrolysis: Time of Reaction hr.	Enzyme Hydrolysis: Weight Loss %	Enzyme Hydrolysis: D.P. of Residue
W	Cotton Linters 1140	48	6.34	105	48	5.35	-
					144	6.68	1105
X	H_3PO_4-swollen cotton Linters 1120	48	8.3	80	144	37.6	1080
Y	H_3PO_4-swollen Cotten Linters 740	48	13.9	40	48	62.7	270
					82	70.5	295
					144	79.3	-

higher degrees of polymerization.

> "The large enzyme molecules, unable to diffuse into the cellulose readily, catalyze the hydrolysis of the regions accessible to them to soluble products rapidly and completely; the reaction then proceeds slowly only at the surfaces of crystalline areas with the rapid dissolution of each chain as it becomes exposed to the surface. In this way hydrolysis would continue with only a transient existence of dextrins of intermediate chain length. The much smaller acid molecules are able to penetrate deeply into the structure, hydrolyzing many more glucosidic bonds, giving rise to shorter chains before extensive solubilization occurs, and without completing their rapid hydrolysis to glucose. Acid hydrolysis is further characterized by an increase in the fluidity of a solution of the fiber due to the fall in chain length and this is accompanied by a loss in fiber tensile strength. There is a linear relationship between fluidity and strength changes, indicating relatively uniform attack by acid, as opposed to the enzymatic or microbial degradation where loss of strength is not accompanied by a large change in fluidity; the latter attack is therefore regarded as localized." (72)

Updegraff (261) has investigated the enzymatic hydrolysis of newspaper as a carbon source for the production of protein from the cellulolytic fungus Myothrecium verrucaria. He milled the newspaper to increase susceptibility in a manner similar to Ghose and Kostick. The final product was the protein harvested from disruption of the fungus cells. Yield was approximately 1.5 g of protein from the consumption of 15 g of cellulose or about 10%. The fermentation process was modeled by Ross and Updegraff (204).

Srinivason and Han (235) and Callihan et al. (24) at the Louisiana State University used sugar cane residue,

bagasse, as a substrate for the production of a cellulolytic bacterium, Cellulomonas, to be used also for single cell protein. They reported a cell yield of 35 to 40% by weight of the baggase consumed. Since 23% of the cell is utilizable as protein, overall protein yield was again about 10%. The reported United States cost would be $.12 per pound of protein which compares favorably with other commercially available proteins as shown in Table C-2.

These latter two processes differ from other enzymatic hydrolysis schemes in that the protein of the cellulolytic fungi is the desired product. The traditional scheme was to utilize the fungi to produce cellulases which would then hydrolyze cellulose to glucose, the desired product.

The A. E. Staley Company is commercially producing glucose by enzymatically hydrolyzing starch (226). The Staley process produces 100 million pounds per year of dextrose crystals and syrup. Starch pretreatment is required: a 30 to 40% purified starch slurry is 20% predigested by acid or by the enzyme, α-amylase, which thins the slurry. This reduces evaporation costs by permiting high initial starch concentrations. Before entering the main digesters the slurry is centrifuged to remove oil and protein by-products which are processed for animal feed. The slurry is then reacted for 72 hours at 60°C at pH 4.0 to 4.5. Approximately 97% conversion to dextrose is achieved. The syrup is then passed through car-

TABLE C-2. COMPARISON OF THE COST OF SCP WITH COMMERCIALLY AVAILABLE PROTEINS IN U.S.*

Product	Price per lb. U.S. $	Protein Content	Price per lb. Protein U.S. $
Peanut Flour	0.07	59%	0.12
Soy Flour	0.05	43%	0.12
Cotton Seed Flour	0.05	50%	0.10
Skim Milk Powder	0.15	36%	0.41
Torula Yeast (Food Grade)	0.17	48%	0.36
Casein (Food Grade)	0.40	100%	0.40
Single Cell Protein			
(I) From Hydrocarbons	-	-	0.35[a]
(II) From Bagasse	-	-	0.12[a]

[a]Estimated cost
*Callihan et. al. (24)

bon decolorizers and staged evaporators and into a final crystallization stage.

Smiley (228) discussed the development of a process similar to the Staley Company's. His work used immobilized enzymes and, hence required a soluble starch substrate. This work provides useful insights for those doing similar work.

ofler (260) discussed the development of a commercial process for producing glucoamylase from the initial conception through commercialization. The approach used and equipment sizes mentioned provide a valuable insight into industrial development practices.

APPENDIX D

Enzyme Kinetics

The factors determining the course of an enzyme reaction are usually the concentrations of the enzyme and its substrate, pH, temperature, and the presence of activators or inhibitors, if any (44).

1. Enzyme Concentration

Under normal conditions the initial reaction velocity, v, is proportional to the enzyme concentration, $[E]$, as shown below and in Figure D-1.

$$v = k[E] \qquad (D\text{-}1)$$

As $[E]$ increases, the reaction rate may appear to level off or even to fall. This could be a result of experimental or substrate limitations, or of the depletion of an essential reactant. The physical apparatus can also become limiting at excessive rates. In series reactions the second enzyme may become limiting as the concentration of the first enzyme is increased. This situation can arise if one of the enzymes preferentially adsorbs on the cellulose. For example the filter paper activity assay is a measure of C_1 activity. Results assume that C_1 and not C_x is the limiting enzyme. If C_x is not in excess, however, the test will actually be measuring C_x and not

C_1 activity. A reactant essential for the activity of the second enzyme, a coenzyme, may preferentially associate with the test enzyme causing a depletion of the coenzyme concentration and hence the reaction rate will begin to decrease when increasing the test enzyme concentration. Finally the available substrate can become saturated with enzyme causing v to level off upon further addition of the test enzyme.

Rarely will the reaction velocity curve show little or no reaction until a certain amount of enzyme E* has been added. This indicates the presence of small amounts of some highly toxic impurity in one of the components other than the enzyme solution itself. An initial enzyme concentration [E*] is required to scavenge out this impurity. The velocity curve should appear linear upon the addition of enzyme beyond [E*] .

If the enzyme preparation contains a reversible inhibitor the free enzyme will be less than expected because some will be complexed with the inhibitor I :

$$E + I \rightleftarrows EI \qquad \text{(D-2)}$$

$$[E] = [E_o] - [EI] \qquad \text{(D-3)}$$

where [E] , $[E_o]$, and EI are the free enzyme, initial amount of enzyme, and enzyme complex respectively. Upon addition of E (plus I) the actual velocity curve will

drop increasingly below the expected linear curve. Since equation (D-2) is bimolecular, [EI] should increase with [E][I] so that more of the enzyme is in the inactive complex at higher $[E_o]$. If the enzyme preparation contains a dissociable activator or coenzyme the velocity curve will rise increasingly above the expected linear curve as the enzyme is added.

2. Substrate Concentration and the Michaelis-Menten Equation

Substrate concentration is one of the most important factors determining the velocity of enzyme reactions. In nearly all cases when the initial reaction velocity is plotted against substrate concentration [S] , a section of a rectangular hyperbola (Figure D-2) is obtained. The equation of the curve is

$$(a - v)(b + s) = \text{constant} \qquad \text{(D-4)}$$

This equation holds whenever a process depends upon a simple dissociation

$$XY \rightleftarrows X + Y \qquad \text{(D-5)}$$

If [Y] is held constant, a plot of [XY] versus [X] should yield a curve similar to Figure D-2.

A theory involving a dissociation of this type was

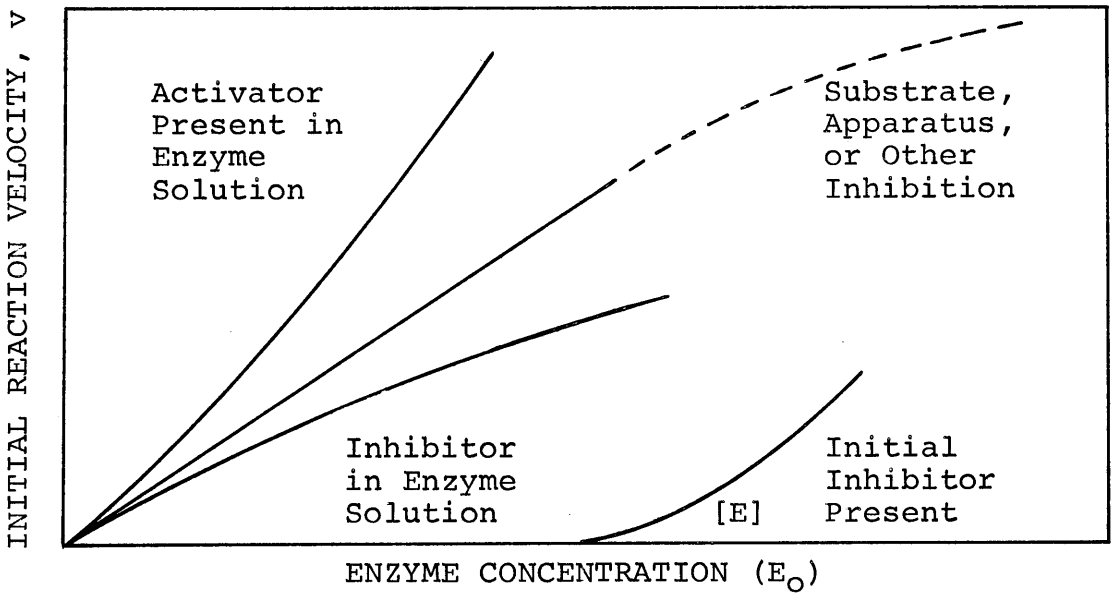

Figure D-1. Typical Initial Reaction Velocity vs. Enzyme Concentration Curves

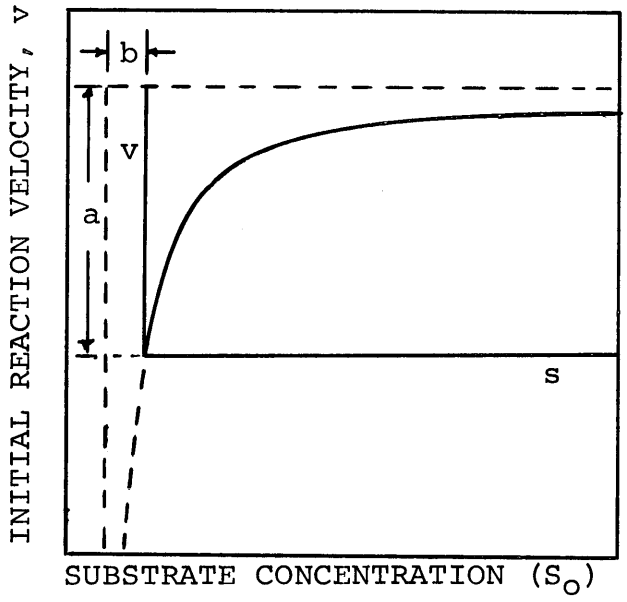

Figure D-2. Hyperbolic Form of Typical Initial Reaction Velocity vs. Substrate Concentration Curve (44)

proposed in 1913 by Michaelis and Menten (44). This was based on the earlier suggestion of Henri (88) that the enzyme first forms a complex with its substrate that later dissociates to yield the free enzyme and the products of reaction. The process can be written

$$E + S \rightleftarrows ES \tag{D-6}$$

$$ES + (\text{any second reactant}) \rightarrow E + PROD \tag{D-7}$$

$$[E] = [E_o] - [ES] \tag{D-8}$$

Let K_s be the dissociation constant for reaction (D-7) then

$$K_s = \frac{[E][S]}{[ES]} = \frac{[E_o][S]}{[ES]} - [S] \tag{D-9}$$

and

$$[ES] = \frac{[E_o][S]}{K_s + [S]} \tag{D-10}$$

The rate of the reaction is given by

$$v = k[ES] = \frac{k[E_o]}{1 + K_s/[S]} \tag{D-11}$$

When [S] is much larger than K_s, v will equal $k[E_o]$ which is often called the maximum velocity V. The Michaelis-Menten equation is, therefore

$$v = \frac{V}{1 + K_s/[S]} \tag{D-12}$$

It can be rearranged similar to (D-4) as

$$(V - v)(K_s - [S]) = VK_s \tag{D-13}$$

When [S] is large, v equals V, and when small

$$v = V[S]/K_s \tag{D-14}$$

When [S] is equal to K_s, v is equal to V/2. The value of K_s is the Michaelis constant written K_m. This depends upon the validity of the assumption implicit in equation (D-10) that equilibrium is maintained between ES, E, and S.

Although equation (D-12) fits experimental facts it is not necessarily the correct model. Langmuir adsorption isotherm and chain reaction mechanisms also form similar equations. Whatever the theoretical interpretation, the Michaelis-Menten equation does hold for the vast majority of enzyme reactions.

Five methods of plotting initial rate data are shown

in Figure D-3. Curve (a) is a plot of equation (D-13) where K_m and K_s are equal. Another method is shown in (b), a plot of v versus pS (the negative log of [S]) corresponding to the logarithmic form of the Michaelis Menten equation.

$$pS = pK_m + \log \frac{V - v}{v} \qquad \text{(D-15)}$$

Here a change in K_m only displaces the curve along the abscissa. Note that setting $v = V/2$ allows determination of K_m with both curves (a) and (b). The only difficulty is in obtaining data of high enough values of [S] to insure the accuracy of V.

The Lineweaver and Burk plot, curve (c), avoids this difficulty by plotting the reciprocal form of the equation

$$\frac{1}{v} = \frac{K_m}{V} \cdot \frac{1}{[S]} + \frac{1}{[V]} \qquad \text{(D-16)}$$

This plot is the most common. Curve (d) is obtained by multiplying equation (D-16) by [S]. Curve (e) is a rearrangement of equation (D-12) to give

$$v = V - K_m \frac{V}{s} \qquad \text{(D-17)}$$

It is not uncommon to find that while equation (D-12) is obeyed at low substrate concentrations, the velocity

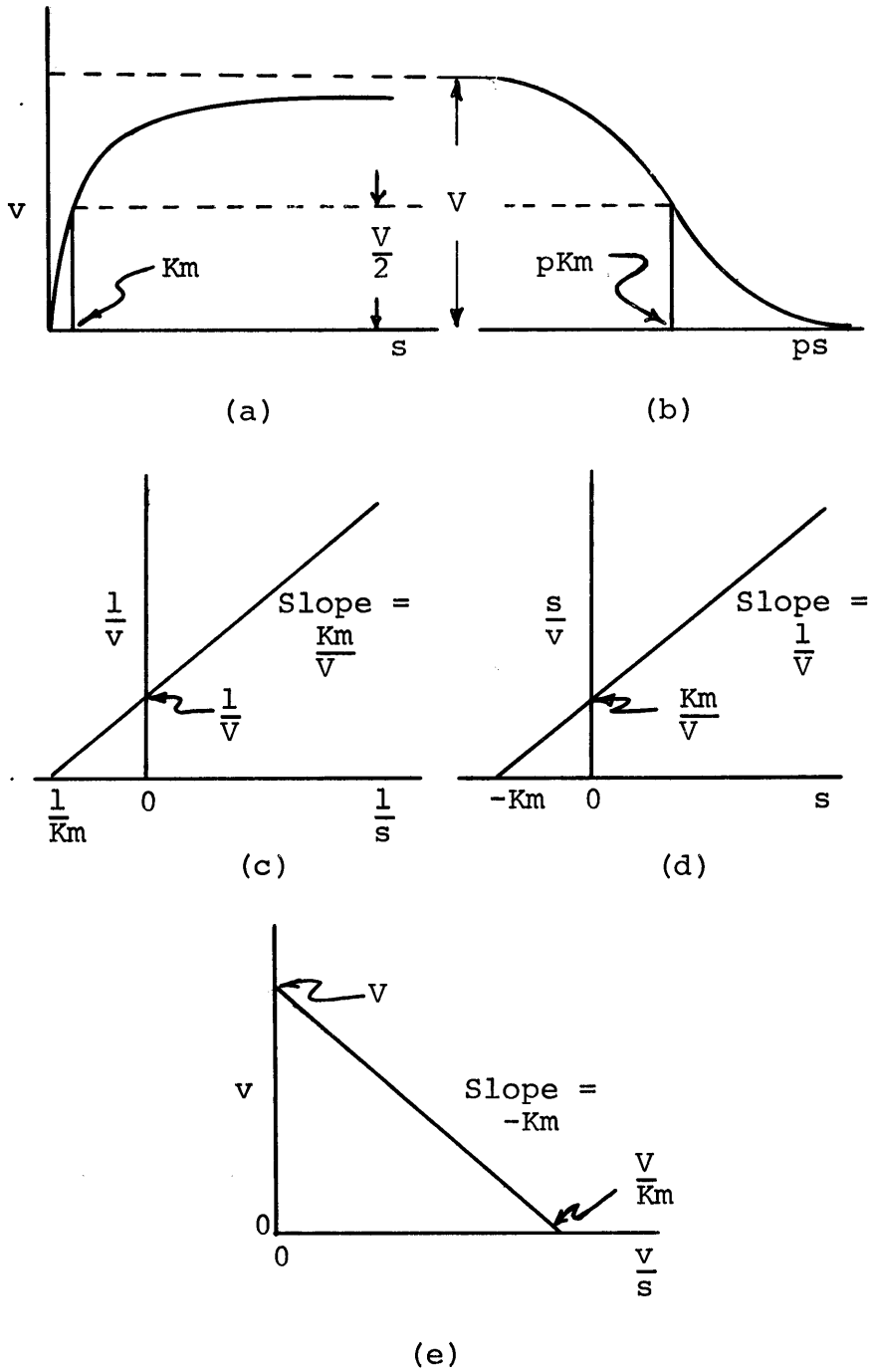

Figure D-3. Five Ways of Plotting the Initial Reaction Velocity, v vs. Substrate Concentration to Determine Km and V (44)

tends to decrease at high [S] . This is commonly called substrate inhibition. Several causes for this, reviewed in Dixon and Webb (44) are summarized below.

Competative Inhibition by the Substrate Itself

A great many enzymes must bind to the substrate molecule at more than one point. As [S] increases the probability of the enzyme binding to multiple substrate molecules and hence forming inactive complexes increases.

Reduction in the Free Concentration of an Essential Reactant

This could be caused by physical exclusion of the reactant from the enzyme by the excess substrate molecules or adsorption or reaction of the reactant with the substrate apart from the enzyme molecules.

A Lineweaver-Burk plot curbing up and away from the expected linear curve as [S] is decreased indicates that the substrate is also acting as an activator. This case also reviewed by Dixon and Webb, however, is rare.

3. The Effect of pH

The hydrogen ion concentration as expressed by pH (a) causes a true reversible effect of V itself, (b) affects the affinity of the enzyme for the substrate, or (c) affects the stability of the enzyme. The latter effect can be reversible or irreversible. All three effects can occur simultaneously, but each can easily be distinguished experimentally. Irreversible destruction can be tested

by exposing the enzyme to a range of pH values for a limited time (about five minutes) and testing the activity at some standard value (usually near the optimum pH). Note that pH deactivation increases with temperature increase and length of time exposed to the test pH. The effect of pH on the affinity can be eliminated by using a sufficiently high substrate concentration to saturate the enzyme at all pH's used. Since large variations in affinity can occur with changes in pH, it should not be assumed that a substrate concentration which is sufficient to saturate an enzyme at one pH will do so at others. To properly define the effect of pH on enzyme activity, enough data should be taken to evaluate V and K_m at each pH by one of the graphical methods previously described.

4. The Effect of Temperature

Increasing temperature may affect (a) the stability of the enzyme, (b) the actual dissociation of the enzyme-substrate complex determined by the heat of activation of the reaction, (c) the pH functions discussed above, (d) the affinity of the enzyme for activators or inhibitors, if any, and (e) the transfer of the rate limiting function from one enzyme to another in any system involving two or more enzymes with different activation energies. These can readily be analyzed experimentally. Effects on stability can be studied similarly to pH effects. The effects on affinity can be eliminated as discussed

above. Thus data at various temperatures allows graphical determination of V and K_m. In a multi-enzyme system each enzyme may usually be studied separately so as to avoid the limiting effects of the other enzymes. Finally, most subsidiary effects can be eliminated by a proper attention to details of technique (44).

APPENDIX E

Diffusion Theory

Often the student initially approaching the subject of diffusion has little understanding of the "physics" of the process. The following paragraphs, adapted from Tanford (253) may help provide the understanding. The latter portions of this section show the improved estimation of diffusion coefficients of proteins in liquids obtained by employing solvation and asymmetry parameters in addition to molecular weight.

Diffusion is the flow of material occurring whenever a concentration gradient exists which tends to equalize the concentration everywhere. Fick deduced that

$$J = - D(dC/dx)_t \qquad \text{(E-1)}$$

where

J = molar flux = moles/cm^2-sec

D = diffusion coefficient = cm^2/sec

C = solute concentration, moles/cm^3

x = length of the diffusion path = cm

The equation of continuity states that

$$\left(\frac{dC}{dt}\right)_x = - \frac{1}{A} \left(\frac{d(AJ)}{dx}\right)_t \qquad \text{(E-2)}$$

where A equals the area perpendicular to diffusion in

cm^2. If the area is constant, combination of the above equations results in Fick's second law

$$\frac{dC}{dt}_x = \frac{d}{dx}\left(D\frac{dC}{dx}\right)_t \qquad \text{(E-3)}$$

which, if D is independent of C, yields

$$\frac{dC}{dt}_x = D\left(\frac{d^2C}{dx^2}\right)_t \qquad \text{(E-4)}$$

The molar flux can be expressed in a mechanical analog as

$$J = \sum_k L_k F_k - \sum_k L_j \left(\frac{d\mu_j}{dx}\right)_t \qquad \text{(E-5)}$$

F_k = external forces, k acting along the x distance (other forces are balanced)

L_{jk} = phenomenological coefficient

μ_j = chemical potential

Consider each macromolecular particle in the solution as a discrete entity moving under an applied force F. Since F equals Ma and a equals du/dt where u is the velocity of the particle, and since a particle moving through a continuum will be opposed by a "frictional force" f proportional to the velocity,

$$M\frac{du}{dt} = F - fu \qquad \text{(E-6)}$$

At steady state

$$F = fu \text{ , or } u = \frac{F}{f} \qquad \text{(E-7)}$$

Since transport processes in macromolecular solutions involve only small forces relative to f, u is small and steady state will apply almost instantly from the application of the force F. If N equals the number of particles per cm^3

$$J = uN = \frac{F}{f} N \tag{E-8}$$

and on a molar basis

$$J = \frac{F}{(N_{av}f)} \frac{N}{(N_{av})} = \frac{C}{(N_{av}f)} F = L_k F \tag{E-9}$$

where N_{av} is Avagadro's number.

In a two component system, isolated from external forces

$$J = - \frac{C}{N_{av}f} \left(\frac{d\mu}{dx}\right)_t \tag{E-10}$$

From thermodynamics

$$\mu = \mu^0 + RT \ln a \tag{E-11}$$

where a equals the activity of the solute in the solvent. Letting γ equal the activity coefficient referred to the concentration in moles per liter,

$$a = 1000\ C\gamma \tag{E-12}$$

for a solute in the solvent. Thus

$$\left(\frac{d\mu}{dx}\right)_t = \left(\frac{RT}{C}\right) \left(1 + \left(\frac{d\ln\ \gamma}{dC}\right)_{T,P}\right) \left(\frac{dC}{dx}\right)_t \tag{E-13}$$

thus

$$J = -\left(\frac{RT}{N_{av}f}\right)\left(1 + C\left(\frac{d\ln\gamma}{dC}\right)_{,P}\right)\left(\frac{dC}{dx}\right)_t \qquad \text{(E-14)}$$

and

$$D = \left(\frac{RT}{N_{av}f}\right)\left(1 + C\left(\frac{d\ln\gamma}{dC}\right)_{T,P}\right)\left(\frac{dC}{dx}\right)_t \qquad \text{(E-15)}$$

The diffusion coefficient can be measured at several different concentrations and extrapolated to zero concentration

$$D^0 = \frac{RT}{N_{av}f} = \frac{kT}{f} \qquad \text{(E-16)}$$

where k equals Boltzman's constant which equals R/N_{av}.

The derivation is based on the assumption that a mechanical force equal to the gradient of the chemical potential provides the driving force for the diffusion process. Note that Fick's law holds only for two-component systems with a nonelectrolyte solute. In multi-component systems interactions between solute molecules affect the diffusion coefficients and the overall transport rates. In all practical applications of diffusion to macromolecular solutions, however, the macromolecules are assumed to act as discrete particles in a two-component system of solute and homogenous solvent, so that Fick's law applies. If an electrolyte is present in sufficiently high ionic strength, its concentration is assumed to remain uniform

throughout the solvent. In reality interactions between the solute and the electrolyte set up an electrostatic potential Ψ. Although Ψ is initially uniform throughout the solvent, it will not remain so as diffusion proceeds. Since no quantitative estimate of the error resulting from this potential is available, Tanford recommended following Fick's law with the realization of probable error.

Protein molecules in soltuion bear electrostatic charges. Even at the isoelectric point where the protein molecule is regarded as "neutral" local charges will exist along the molecule. These charges will interact with the solvent. The addition of a moderately large concentration of a low molecular weight electrolyte such as magnesium chloride should eliminate any such influence.

The derivation (E-16) assumed the particles to act as rigid spheres. Proteins, however, are not spheres, but coils that can possibly entrap solvent within the molecule. The diffusion must therefore be corrected for solvation and non-sphericity. The total volume of the particle is

$$v_h = \frac{Mw}{N_{av}} (v_p + \sigma_s v_s) \qquad \text{(E-17)}$$

where v_p is the average dry specific volume of the protein as cubic centimeters per gram; σ_s is the solvation factor for the solvent in the solute and is approximately

0.2 g/g of protein; and v_s is the specific volume of the solvent. The radius of a sphere with volume v_h (equals 4/3 R_o^3) would be

$$R_o = \frac{3Mw}{4\pi N_{av}} (v_p + \sigma_s v_s)^{1/3} \qquad \text{(E-18)}$$

and the Stokes law frictional coefficient of this hypothetical sphere would be

$$f_o = 6\pi\eta R_o \qquad \text{(E-19)}$$

where η is the viscosity. The actual frictional coefficient f can be expresses in terms of f_o as

$$f = \frac{f}{f_o} \cdot 6\pi\eta R_o \qquad \text{(E-20)}$$

The ratio f/f_o would be 1.0 for a sphere.

We can write for the diffusion coefficient extrapolated to zero concentration

$$f = \frac{kT}{D^o} = 6\pi\eta \frac{f}{f_o} \left(\frac{3Mw(v_p + \sigma_s v_s)}{4\pi N_{av}} \right)^{1/3} \qquad \text{(E-21)}$$

The minimum drag, fmin , and hence the maximum diffusion coefficient, D^omax , can be calculated by letting f/f_o equal one and by assuming no solvation (σ_s equals zero):

$$\text{fmin} = \frac{kT}{D^o\text{max}} = 6\pi\eta \left(\frac{3Mw\ v_p}{4\pi N_{av}} \right)^{1/3} \qquad \text{(E-22)}$$

The ratio of the observed diffusion coefficient i then

$$\frac{D^{o}max}{D^{o}} = \frac{f}{fmin} = \frac{f}{f_o}\left(\frac{v_p + \sigma_s v_s}{v_p}\right)^{1/3} \qquad \text{(E-23)}$$

Typical experimental data for a number of proteins are shown in Table E-1 with f/fmin calculated from the data. Note that proteins can be classified into globular and randomly coiled molecules. The former exhibit hydrodynamic behavior close to that for the hypothetical spheres for which fmin was calculated. Larger values of f/fmin indicate hydrodynamic behavior greatly different from that of unsolvated spheres.

The ratio of f/min depends on two physical properties; solvation as represented by σ_s and asymmetry which is represented by f/f_o. If the disparity between measured and hypothetical diffusion coefficients resulted only from solvation, the ratio f/f_o can be assumed unity and a maximum value of σ_s and the radius Re of the resulting hypothetical sphere can be calculated from equation (E-23). Conversely, if the disparity can be attributed entirely to asymmetry, σ_s will be zero, and $(f/f_o)max$ can be similarly calculated from Figure E-1. The results of these calculations are shown in Table E-2. Use of the oblate ellipsoid model would slightly reduce the values of $(a/b)_{max}$.

Since it is highly unlikely that a protein hydrodynamic particle is either unsolvated or a perfect sphere, a compromise situation must exist. Using a reasonable solvation of 0.2 g solvent per gram of protein, values

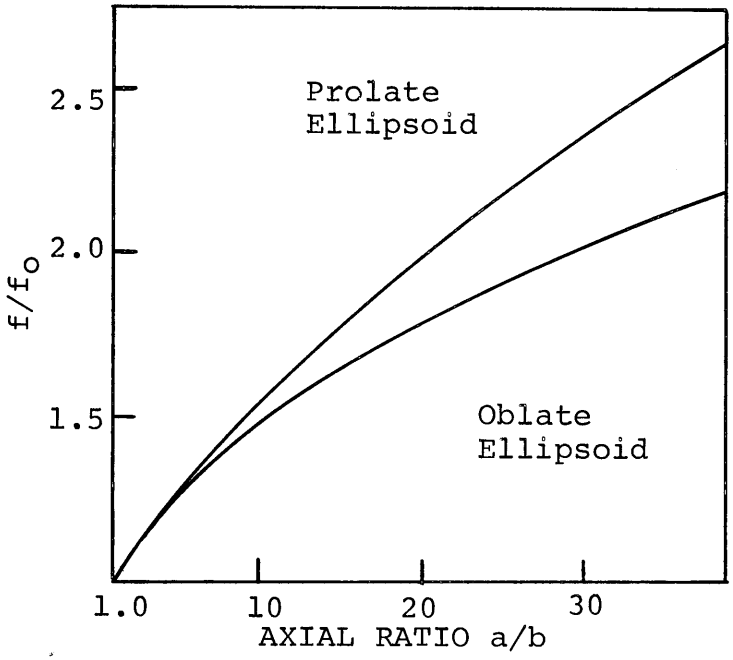

(c) Low Ratio

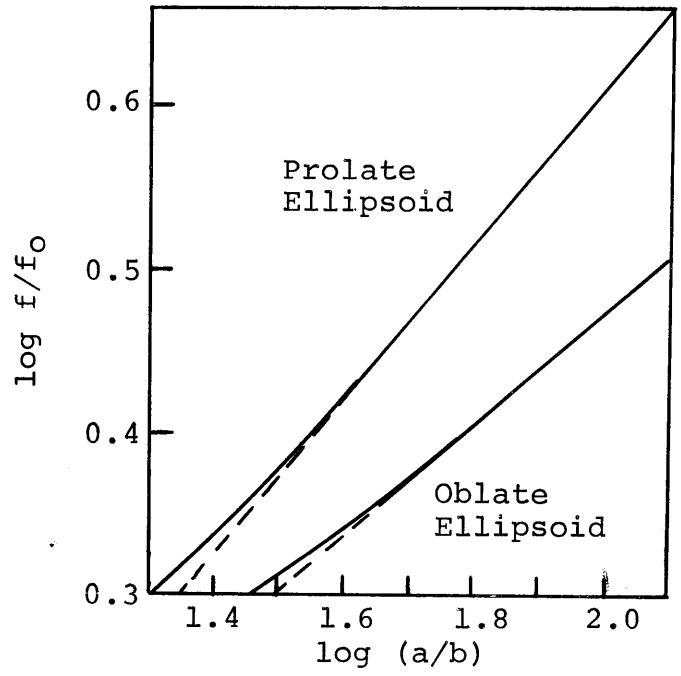

(b) Large Ratio

Figure E-1. Perrin's Factor for the Frictional Coefficient of Ellipsoids (253)

TABLE E-1. DIFFUSION COEFFICIENTS OF PROTEINS IN AQUEOUS SOLUTIONS (20°C)*

	Mw	v_p	$D^o \times 10^7$	f/f_{min}
Ribonuclease	13,683	0.728	11.9	1.14
Lysozyme	14,100	0.688	10.4	1.32
Chymotrypsinogen	23,200	0.721	9.5	1.20
β-Lactoglobulin	35,000	0.751	7.82	1.25
Ovalbumin	45,000	0.748	7.76	1.17
Cellulase[b]	63,000	0.740	5.61	1.44
Serum Albumin	65,000	0.734	5.94	1.35
Hemoglobin	68,000	0.749	6.9	1.14
Catalase	250,000	0.730	4.1	1.25
Urease	480,000	0.730	3.46	1.20
Tropomyosin	93,000	0.710	2.24	3.22
Fibrinogen	330,000	0.710	2.02	2.34
Collagen	345,000	0.695	0.69[a]	6.8
Myosin	493,000	0.728	1.16[a]	3.53

[a]This value was calculated from the sedimentation coefficient using a molecular weight determined by light scattering

[b]From Whitaker et. al. (272)

*Tanford (253)

TABLE E-2. SOLVATION AND/OR ASYMMETRY CALCULATED FROM THE DIFFUSION COEFFICIENTS OF TABLE E-1*

	Maximum Solvation		Maximum Asymmetry	Compromise	
	$(\sigma_s)_{max}$ grams/gram	R_e Å.	a/b of Prolate Ellipsoid	$\frac{f}{f_o}$	a/b of Prolate Ellipsoid
Ribonuclease	0.35	18.0	3.4	1.05	2.1
Lysozyme	0.89	20.6	6.1	1.21	4.3
Chymotrypsinogen	0.52	22.5	4.2	1.11	3.0
β-Lactoglobulin	o.72	27.4	4.9	1.16	3.7
Ovalbumin	0.45	27.6	3.8	1.08	2.5
Cellulase	1.50	80.0	7.5	1.33	6.3[a]
Serum Albumin	1.07	36.1	6.5	1.25	4.9
Hemoglobin	0.36	31.0	3.4	1.05	2.1
Catalase	0.70	52.2	4.9	1.15	3.6
Urease	0.53	61.9	4.2	1.11	3.0
Tropomyosin	23.0	96	62		
Fibrinogen	8.4	106	31		
Collagen	218	310	300		
Myosin	49	215	100		

Maximum Solvation: $f/f_o = 1$, calculate $(\sigma_s)_{max}$
Maximum Asymmetry: $\sigma_s = 0$, $f/f_o = f/f_{min}$
Compromise: $\sigma_s = 0.2$
[a]Corresponds to 250 Å X 40 Å
*Tanford (253)

of f/f_o and a/b have been calculated from equation (E-23). Note that proteins do not actually form ellipsoidal hydrodynamic particles. In fact, their overall shape may be quite irregular. This model, however, is the only one available for interpreting f/f_o .

The data from Tables E-1 and E-2 have been plotted in Figure E-2. Note that the diffusion coefficient can be estimated from knowledge of molecular weight alone. Knowledge of solvation, σ_s , and asymmetry, however, improve the estimation. Since these values are very rarely known, values for molecules similar in function or physical and chemical properties can be assumed.

Note that the diffusion coefficients reported in the literature are often given at a standard condition of 20°C in water. The conditions can be changed by

$$D^o_B = D^o_{20°,w} \cdot \frac{T}{T_{20°}} \cdot \frac{\eta_{20°}}{\eta} \qquad \text{(E-24)}$$

where $T_{20°} = 293.2°K$ and $\eta = 0.01$ poise. A more important caveat, however, is that the experiments upon which protein diffusion constants are based are often carried out in varied buffered solutions differing markedly in pH and ionic strength. Since these have a strong effect on portein conformation in solution, the data (diffusion coefficient, molecular size and shape) should be verified experimentally before extension to other solvents.

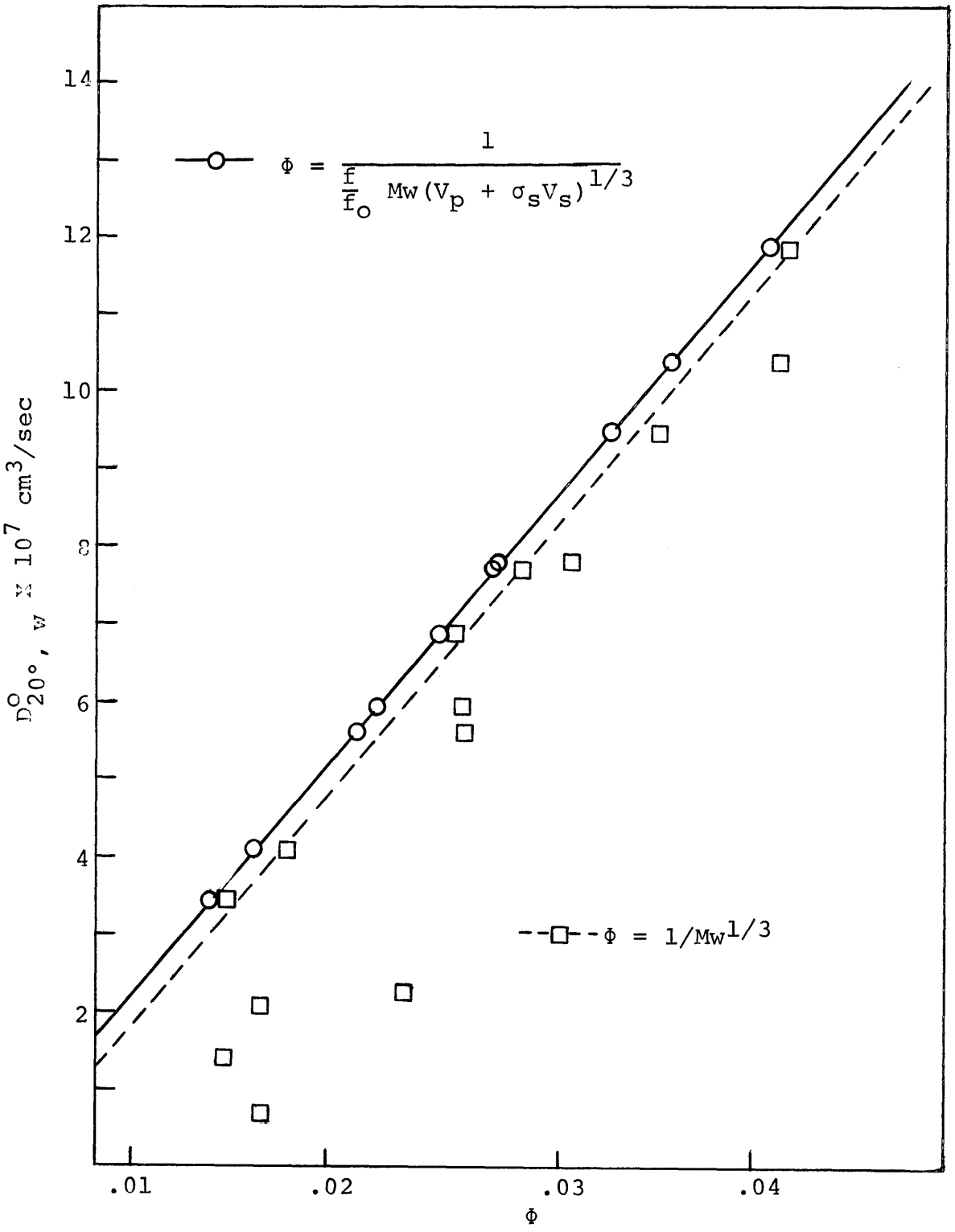

Figure E-2. Correlations for Estimating the Diffusivity of Globular Proteins

APPENDIX F

Adsorption at the Liquid-Solid Interface

Early adsorption studies at the liquid-solid interface are summarized by Freundlich (59). Measurements, mainly of adsorption isotherms, were made with diltue solutions and had the shape of Figure F-1 (a). If an asymptote were approached these isotherms could possibly be described by the Langmuir equation

$$\frac{C_a}{C_{a\infty}} = \frac{bC}{1 + bC} \qquad \text{(F-1)}$$

where C_a is the amount adsorbed at concentration C, and $C_{a\infty}$ is the limiting or maximum possible adsorption, b being a constant (110). When the isotherms did not approach an assymptote another equation could be fitted:

$$\frac{G}{M} = \alpha C^{1/n} \qquad \text{(F-2)}$$

where G is the weight of solute taken up by a weight M of adsorbent, C is the equilibrium solute concentration and α and n are constants. Equation (F-1) has a theoretical basis in the kinetic theory of gases; equation (F-2) initially had no theoretical basis although Henry (89) later tried to give it some basis for adsorption from dilute solutions. Equation (F-2) is usually known as the Freundlich equation.

Isotherms such as Figure F-1 (b) and (c) were observed

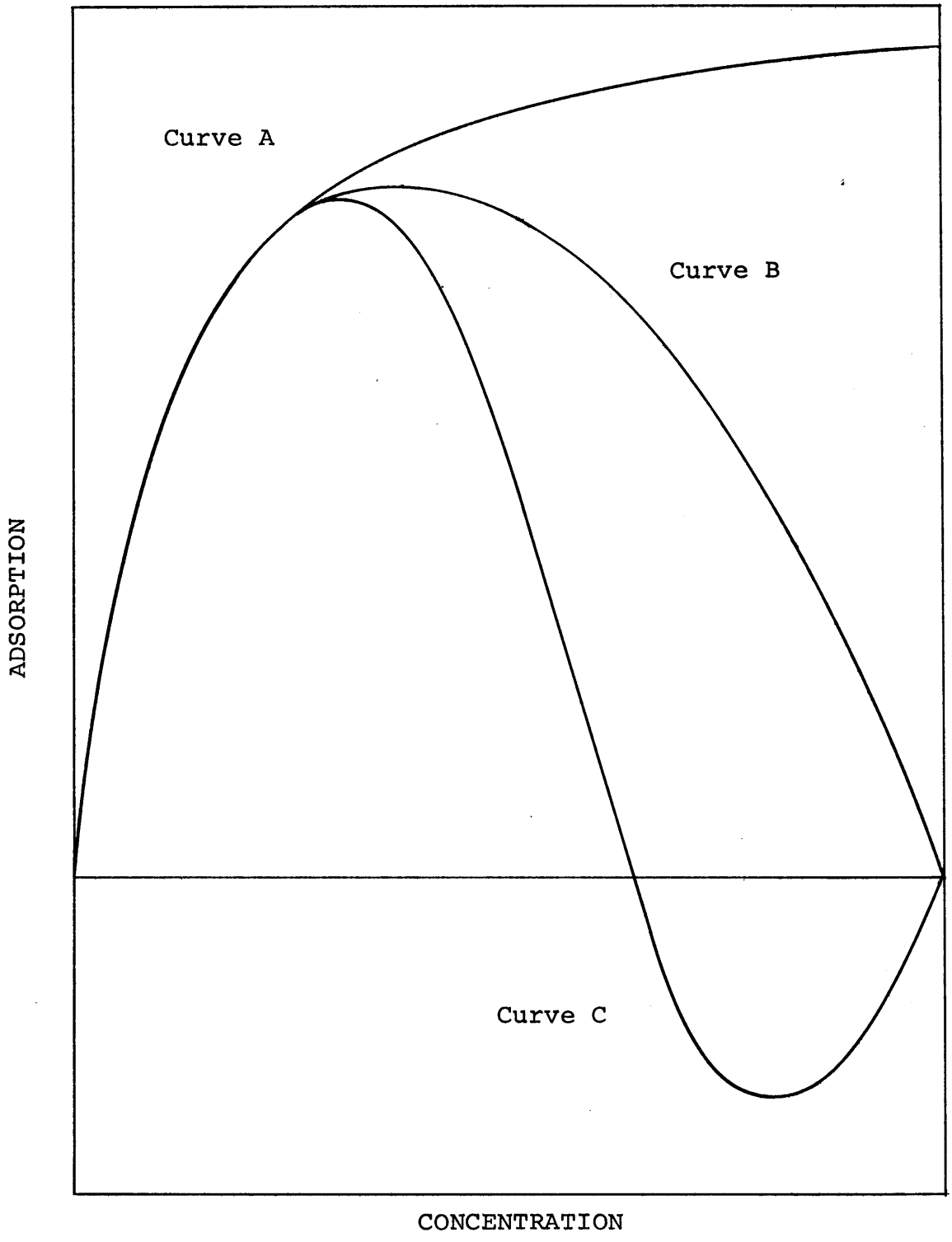

Figure F-1. Three Types of Adsorption Isotherms (110)

during this time, but were left unexplained.

> "These results seem strange only because adsorption by solids from solution has habitually been treated as though it were analogous with adsorption of single gases. The data which are plotted as isotherms, however, are different in principle. The isotherm for adsorption of a single gas by a solid represents directly the quantity of gas adsorbed by unit weight of the solid. The experimental measurement in adsorption from solution is the change in concentration of the solution which results from adsorption. The fact that a change in concentration is measured emphasizes that there are at least two components in the solution." (111)

Previously it was assumed that only the solute was adsorbed. Thus, the extent of adsorption was given by multiplying the change in concentration by the weight of solution used. This assumption is approximately valid only for systems in which the "solute" has very limited solubility in the "solvent" and sometimes for very dilute solutions.

It is now possible to qualitatively understand isotherms (b) and (c). Figure F-1 (b) represents an isotherm for completely miscible liquids. This isotherm must fall to zero at each end of the concentration range because no change in composition at these points (i.e., of the pure liquids) is possible. Figure F-1 (c) indicates that over the first part of the concentration range one component is adsorbed preferentially to the other. This means that at equilibrium this component is present in the adsorbed layer in greater proportion than in the bulk liquid. "Negative" adsorption of component one thus means preferential

adsorption of component two (110).

Two concepts of adsorption must be distinguished when applied to mixtures. The first, preferential adsorption, is given by the experimental measurements just described. This is again the measure of the decrease of the bulk concentration of one component because the surface layer is correspondingly enriched. The second concept is absolute adsorption or adsorption of an individual component. This refers to the actual quantity of that component present in the adsorbed phase (110).

1. The Composite Isotherm

The term adsorption isotherm refers to preferential adsorption. Kipling preferred to call this the "composite isotherm" because it is the result of combining the "true" or individual isotherms for the adsorption of each component. The significance of the composite isotherm is shown by deriving an equation to relate the preferential adsorption from a two-component mixture to the actual adsorption of each component.

When a weight of M of solid is brought into contact with N_o moles of liquid the mole fraction of liquid decreases by ΔX with respect to component one. N_1^s and N_2^s moles of components one and two are transferred from the liquid to a unit weight of the solid during adsorption. At equilibrium N_1 and N_2 moles of components one and two remain in the liquid phase. The initial mole fraction

of component one was X_o .

Then

$$N_o = N_1 + N_2 + N_1{}^{s}M + N_2{}^{s}M \tag{F-3}$$

$$X_o = \frac{N_1 + N_1{}^{s}M}{N_o} \tag{F-4}$$

$$X = \frac{N_1}{(N_1 + N_2)} \tag{F-5}$$

$$(1 - X) = \frac{N_2}{(N_1 + N_2)} \tag{F-6}$$

and

$$\Delta X = X_o - X \tag{F-7}$$

$$\Delta X = \frac{N_1 + N_1{}^{s}M}{N_1 + N_2 + N_1{}^{s}M + N_2{}^{s}M} - \frac{N_1}{N_1 + N_2} \tag{F-8}$$

$$\Delta X = \frac{N_2N_1{}^{s}M - N_1N_2{}^{s}M}{(N_1 + N_2)N_o} \tag{F-9}$$

therefore

$$\frac{N_o\Delta X}{M} = N_1{}^{s}(1 - X) - N_2{}^{s}X \tag{F-10}$$

or

$$\frac{N_o\Delta X_1}{M} = N_1{}^{s}X_2 - N_2{}^{s}X_1 \tag{F-11}$$

where X_1 and X_2 refer to the mole fractions of components one and two respectively in the liquid phase.

The function $N_o\Delta X/M$ is (when moles and mole fractions are used) what has actually been plotted as adsorption to give what is properly the composite isotherm. An equation analogous to (F-10) can be derived in terms of weights and weight fractions

$$\frac{W_o\Delta C}{M} = W_1^s(1 - C) - W_2^s C \qquad \text{(F-12)}$$

where W_o is the initial weight of liquid brought in contact with a weight M of adsorbant, the equilibrium weight fraction of the solution is C, and W_1^s and W_2^s are the weights of the two components, respectively, adsorbed by unit weight of adsorbant. Note that

$$\frac{N_o\Delta X}{M} = \frac{W_o\Delta C}{M}\left[\frac{X}{M_2} + \frac{1 - X}{M_1}\right] \qquad \text{(F-13)}$$

$$\frac{N_o\Delta X}{M} = \frac{W_o\Delta C}{M} \cdot \frac{1}{M_2C + M_1(1 - C)} \qquad \text{(F-14)}$$

where M_1 and M_2 are the molecular weights of components one and two respectively.

2. Resolution of the Composite Isotherms into Individual Isotherms

The composite isotherm can not be resolved into in-

dividual isotherms without knowledge of N_1^s and N_2^s. For very dilute solutions (X less than 0.01) it follows from equation (F-10)

$$N_1^s \simeq \frac{N_o \Delta X}{M} \qquad \text{(F-15)}$$

In such cases, even if N_2^s is considerable, the term $N_2^s X$ can be neglected for a first approximation. Similarly, the term $N_1^s(1 - X)$ approximates to N_1^s because $(1 - X)$ is nearly equal to 1.0. This situation often applies to solutions of solids in liquids because the solubility limit in terms of mole fractions is usually low. In this case the composite isotherm gives a good approximation for the adsorption of the solute even with considerable adsorption of the solvent. Another equation is really needed for more concentrated solutions and for determining the adsorption of the solvent.

One approach is to assume that adsorption occurs only in a mono-layer. It follows that

$$N_1^s \bar{A}_1 + N_2^s \bar{A}_2 = A^* \qquad \text{(F-16)}$$

where $\bar{A}_1$ and $\bar{A}_2$ are the partial molar areas of each component when adsorbed on the surface and A^* is the surface area of a unit weight of solid. A further assumption is that the same area of the solid is available to each component. Kipling and Tester (113) proposed an alternate form based on the same assumptions:

$$\frac{N_1^s}{(N_1^s)M} + \frac{N_2^s}{(N_2^s)M} = 1 \qquad \text{(F-17)}$$

where $(N_1^s)M$ and $(N_2^s)M$ are the numbers of moles of the individual components required to cover the surface of a unit weight of the solid.

A second approach is the pore filling model in which the available volume of the pores is the controlling factor (110). Equation (F-16) is then replaced by

$$N_1^s \bar{V}_1 + N_2^s \bar{V}_2 = V_p^* \qquad \text{(F-18)}$$

where $\bar{V}_1$ and $\bar{V}_2$ are the respective partial molar volumes of the adsorbates, and V_p^* is the pore volume of a unit weight of adsorbent. This approach again assumes equal pore accessibility to the adsorbents. A special case of this model is presented by molecular seives that exclude one of the components. For such a situation equation (F-10) becomes

$$\frac{N_o \Delta X}{M} = N_1^s (1 - X) \qquad \text{(F-19)}$$

because N_2^s is always zero. Furthermore N_1^s is a constant for all values of X. A plot of this equation, therefore, yields a straight line which can be extrapolated to X equals zero to give N_1^s the pore volume of the solid for the component in question.

3. Adsorption of Solids

In the adsorption of solids from solution the isotherms shown in Figure F-2 can (a) approach an asymptote, (b) approach a plateau and then continue to rise, (c) never approach a limiting value, and (d) approach a maximum and then decrease sharply. Curve (a) has often been described by a Langmuir-type equation with the plateau representing complete coverage of the surface by the solute. Unfortunately the solubility limit of the solute is often reached before the plateau appears. These systems can, however, be fitted by a Langmuir-type equation

$$\frac{X}{M} = \frac{kK\ X}{1 + kK} \qquad \text{(F-20)}$$

The application of a Langmuir-type equation is, therefore, not always an indication of complete mono-layer coverage of the surface. Isotherm (b) indicates the possibility of mono-layer coverage followed by either reorientation of the solute, allowing further adsorption in the mono-layer, or adsorption in a second layer. Curve (c) indicates nonsaturation of the mono-layer or easy multi-layer adsorption. The last isotherm (d) indicates continuing adsorption of the solvent at higher solute concentrations, or that the mono-layer is formed at a relatively low concentration of solute with respect to the solubility limit. In this case, equation (F-15) is inadequate and must be replaced with (F-19). Thus, after a complete mono-layer

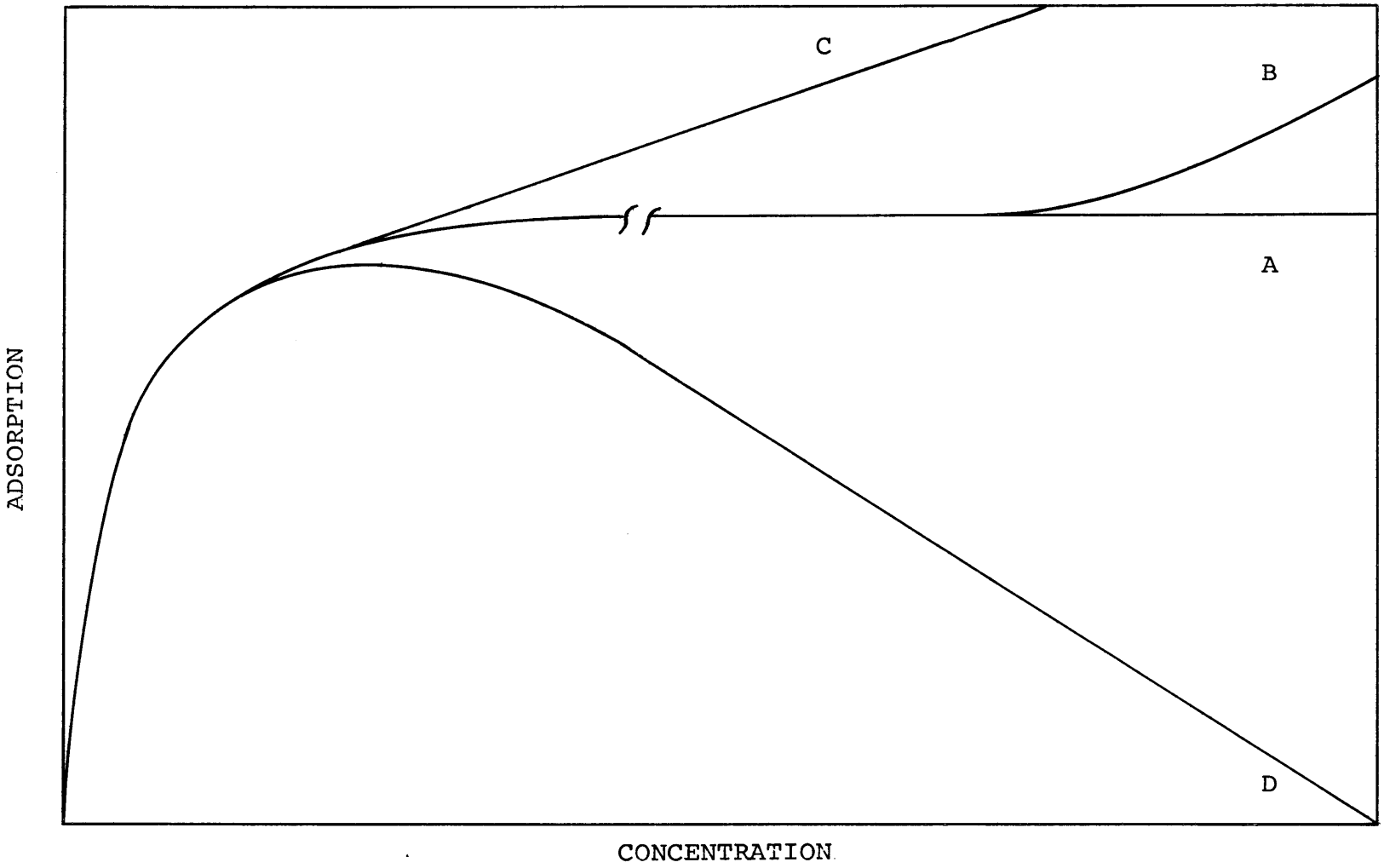

Figure F-2. Typical Adsorption Isotherms for the Adsorption of Solids from Solution

is formed, the composite isotherm must fall linearly with concentration. Extrapolation of the linear section to X equals zero gives the value of N_1^s corresponding to a complete mono-layer. Note that in this case extrapolation to X equals zero should give a value of zero for $N_o\Delta X/M$. If the isotherm reaches zero before X equals one, a mixed mono-layer of constant composition is formed, i.e. the adsorbed phase contains solvent.

4. Increasing Temperature

The effect of temperature on the adsorption of solids from solution is to lower the isotherm, particularly at low concentrations. This corresponds to a weakening of the attractive forces between the solute and the solid surface (and between adjacent adsorbed solute molecules) with increasing temperature, and a corresponding increase in solubility of the solute in the solvent. Thus, if the solvent is regarded as partitioned between the adsorbed layer and the solution, increasing temperature displaces the equilibrium in favor of the solution.

5. Adsorption of Polymers

The adsorption of polymers is a special case of the adsorption of solids, differing mainly in that each molecule has a large number of groups, each of which can potentially be adsorbed at the surface. Moreover, each molecule often has so many degrees of freedom that these

groups have a high degree of mutual independence, subject to the important overriding consideration that the adsorption of any group increases the probability of the adsorption of other, especially neighboring, groups in the molecules.

The main features to be investigated in the adsorption of polymers are the effects of molecular weight and dispersity, of temperature, of the nature of the adsorbent and the solvent, and of the type of monomer unit in the polymer. The most important matter of interpretation is the configuration of the adsorbed molecules (110). Adsorption usually increases with molecular weight, the effect being more obvious with poor solvents and at lower molecular weights. Adsorption that decreases with molecular weight probably indicates a porous adsorbent that tends to exclude increasingly large molecules. The adsorption of polymers is markedly dependent upon the solvent, being much easier with poor solvents.

The effect of temperature is more complex. As with the adsorption of simple solutes adsorption tends to decrease with increasing temperature. The solubility of the polymer, however, tends to increase with temperature. These two effects are opposed and either one can predominate. Increasing adsorption with temperature indicates that the process is endothermic. For the free energy of the system to decrease, the change in entropy must be positive. This may occur because the solvent molecules dis-

placed from the surface by the solute molecules gain more translational entropy than is lost by the polymer molecules. Some solvent molecules could also be released from solvation with the polymer molecule as it adsorbs, again gaining translational entropy.

Three properties of the adsorbent are important; the chemical nature of the surface, the specific surface area, and the extent of porosity. A good adsorbent competing with the solvent has more and stronger active adsorbent sites than a poor adsorbent. These active sites could be crystalline irregularities or even molecular groups chemically bonded to the surface. Since adsorption is a surface phenomenon a good adsorbent must have a high surface to weight ratio. Note, however, that adsorption by a unit weight of adsorbent is only proportional to the specific area for adsorbents having the same chemical nature. The effect of porosity has been discussed before. It is more pronounced, however, the larger the difference in molecular volumes between the solvent and solute molecules.

When estimating the number of polymer molecules required to cover a given surface, assumptions must be made as to the nature of the adsorbed phase. With fairly rigid polymer molecules, or molecules having a defined shape, these assumptions are rather easy to make. With randomly coiled molecules, however, the adsorbed molecules can have many varied configurations. The limiting configurations are the partially-deposited and the totally-

deposited molecule. In the partially-deposited model the molecule is thought to be adsorbed to the solid at only one or a few sites, the remaining parts of the molecule looping out into the solvent. The points of attachment being called anchor segments. In the totally-deposited molecule most of the polymer is actually adsorbed on the solid, and very few loops extend into the solvent. The partially-deposited model obviously permits the adsorption of more molecules per mono-layer than does the totally-deposited model.

6. Adsorption Isotherm for Polymer Adsorption

Various equations have been proposed to fit the adsorption isotherms for polymer adsorption. The Langmuir and Freundlich equations, (F-1) and (F-2), have sometimes been used. Equation (F-1), however, does not consider the adsorption of the solvent. It would be misleading, therefore, to assume that the composite isotherm is equivalent to the individual isotherm for the polymer adsorption because even with dilute solutions, randomly coiled polymers tend to associate with large numbers of solvent molecules. The Freundlich equation does not level off and, hence, is inapplicable to most polymer adsorption isotherms.

A model for the adsorption of flexible polymers from dilute solutions has been developed by Frisch et al. (60-65, 225). They assumed

"that the polymer forms a localized monolayer on the surface of the solid, that it is extremely unlikely that each segment of the polymer chain (which is probably coiled to varying extents when the polymer is in solution) is attached to the surface, and that there is a Gaussian distribution of end-to-end distances in the polymer. The remainder of the polymer chain forms loops or bridges which extend into the solution. Interaction between the chains near the surface is neglected. The probability that a given segment of the chain is adsorbed by the surface is small. In the limiting case, in which this probability tends to zero, the following equation is observed:

$$\frac{\theta}{1 - \theta} \cdot \varepsilon^{2K_1} = (KC)^{1/\langle v \rangle} \qquad \text{(F-21)}$$

which for the limiting case ($K_1 \simeq 0$) approximates to:

$$\frac{(KC)^{1/\langle v \rangle}}{1 + (KC)^{1/\langle v \rangle}} = \theta \qquad \text{(F-22)}$$

where θ $(=a/a_\infty)$ is the fraction of the surface covered by adsorbed segments at a concentration C, $\langle v \rangle$ is the average number of segments adsorbed on the surface per chain, K is a proportionality constant and K_1 expresses the interaction in the bulk liquid. This equation requires a steep rise in the isotherm at low concentrations, after which θ depends only slightly on C and for a considerable range of C remains below the value which would be given by a Langmuir equation.

"For a long flexible chain and low surface coverage $\langle v \rangle$ is proportional to $t^{1/2}$ where t is the number of adsorbable segments in the chain. Thus the extent (and heat) of adsorption should be proportional to the square root of the molecular weight of the polymer. At higher surface coverages, interaction between adsorbed segments becomes important, and adsorption tends to become more nearly a linear function of molecular weight. The value of $\langle v \rangle$ should also increase with increasing chain flexibility which, resulting from increasing temperatures could outweigh other factors and explain observed cases of increased adsorption with increase in temperature.

"An alternate approach is to consider a kinetic picture in which the following equilibria

exist:

1 adsorbed polymer molecule with γ anchor sites → γ "free" sites + 1 polymer molecule in solution

1 adsorbed solvent molecule → 1 "free site" + 1 solvent molecule in solution

Application of the law of Mass Action leads to:

$$\frac{\theta}{\gamma(1-\theta)^{\gamma}} = KC \cdot \qquad \text{(F-23)}$$

"The above equations all have one important limitation - the assumption that γ , the number of anchor segments per chain is independent of θ the surface coverage. This is unlikely to be the case (91), and more adequate equations for the adsorption isotherm should take account of the variation." (112)

APPENDIX G

KINETICS OF ADSORPTION FROM SOLUTION

1. Introduction

Adsorption is normally considered the process by which a molecule or atom in a fluid is attached to an interface, and it is implied that the molecule or atom is in the same location as the adsorption site. The problem, however, is more complex than this. The consideration of adsorption as a point process (one occurring at a fixed site) would require measurement of data at the site, a nearly impossible task. The results of adsorption are, therefore, usually measured in terms of concentration of the adsorbate in the bulk fluid. The whole process must then be divided into the space process by which the adsorbate is transported to the site, and the point process of the actual adsorption on the site. The distinguishing feature is whether the process involves movement of the adsorbate. As stated by Smith (231):

> "What is needed are rate equations which express the kinetics of adsorption in terms of properties of bulk fluid adjacent to the solid particle - space or global kinetics in contrast to point kinetics, which express the rate in terms of properties at the adsorption site. Space processes are significant to the extent that variables such as fluid velocity and particle size affect the global kinetics equations.
>
> "From this point of view the proper approach to design adsorption equipment is a two step procedure:
>
> (1) Establish the point kinetics and equilibrium isotherm for the adsorption step at the site, and the rate coefficients for the various

> space processes. These are the two types of data required for design. The coefficients for the space processes can be estimated to some extent.
>
> (2) By applying the conservation equations (mass, energy) and the data from (1), calculate the concentration as a function of time and position in the adsorption apparatus."

The sequential steps which together form the process of global adsorption are:

(1) Bulk diffusion: transfer of the adsorbate from the bulk fluid to the outer surface of the particle by molecular and convective diffusion.

(2) Pore diffusion: transfer of the adsorbate from the particle surface to the interior site by molecular diffusion through the porous structure and by surface migration.

(3) Adsorption on the interior site: for aqueous adsorption this is usually classified by either ionic or chemical steps, chemisorption, or by a relatively loose physical adsorption. Chemisorption involves stronger molecular interactions than does physical adsorption, and therefore, usually displays higher heats of adsorption.

(4) In replacement or reaction operations, where a product is produced, the above steps occur for the products, only in reverse.

Heats of adsorption or chemical reaction can be significant. Temperature gradients are generally less for liquid systems than for gaseous systems since the heat capacity of the former is an order of magnitude higher

than for the latter. The steps for heat transfer from the adsorption site to the bulk fluid, or from the bulk fluid to the adsorption site, are:

(1) Heat release or adsorption caused by adsorption and reaction if any.

(2) Internal transfer: transfer of energy to or from the outer surface of the solid particle. This is usually considered as conduction through a homogeneous particle with a single effective thermal conductivity.

(3) External transfer: transfer of energy between the particle and the external fluid stream. The properties of flowing fluids are such that the resistance to heat transfer can be larger than that for mass transfer, so that a negligible concentration difference may exist between the bulk fluid and the particle surface and yet the corresponding temperature difference will be significant.

(4) Axial dispersion of energy along the fluid stream: the importance of this process is determined by the reciprocal of the Peclet number for heat transfer (230).

2. Bulk Diffusion

The diffusion process in a stirred tank reactor, STR, is set forth by Satterfield (210). Transfer of a solute from the bulk of a solution to the external surface of a particle or bubble is termed bulk diffusion. Resistance

to mass transfer between the fluid and the outer pellet surface is markedly reduced as the fluid velocity is increased with respect to the pellet. If a concurrent increase in reaction rate is observed, bulk diffusion could be a controlling factor in the overall rate process.

For discussion purposes the reactor will be considered a slurry reactor with the enzyme molecules diffusing into cellulose particles. These particles will be considered spherical for ease in analysis.

Assume that sorption is first order with respect to the enzyme and that it is a function of the external surface of the particle. The concentration of the enzyme in the bulk solution and at the particle surface is C_b and C_s (gm/cm^3) respectively. The initial rate equations (i.e., assuming steady state approximation that C_i, the concentration within the particle, remains much less than C_s for the time under consideration) are:

$$G_v = K_c A_p^* (C_b - C_s) \quad \text{(bulk liquid to surface)} \quad \text{(G-1)}$$

$$G_v = K_s A_p^* C_s \quad \text{(disappearance at surface)} \quad \text{(G-2)}$$

where

G_v = solute fulx, gm/sec

A_p^* = total external particle area

K_c = bulk mass transfer coefficient, cm/sec

K_s = intrinsic sorption rate constant, cm/sec

Hence

$$\frac{C_l}{G_v} = \frac{1}{A_p^*}\left(\frac{1}{K_c} + \frac{1}{K_s}\right) \qquad \text{(G-3)}$$

In a series of tests varying only the particle loading, $\bar{M}$, (hence A_p^*) the reciprocal of the rate should be linear in $1/A_p^*$.

The diffusion rate at the surface of the particle can be equated to the rate of diffusion through a shell of radius r ($\bar{G}$ = diffusion flux = gm/cm^2-sec, and is positive in the direction of decreasing r). Therefore

$$\bar{G}(\pi d_p^2) = D^o(4\pi r^2)\frac{dC}{dr} \qquad \text{(G-4)}$$

$$\frac{Gd_p^2}{4\left(\frac{2}{d_p} - \frac{1}{r}\right)} = - D^o(C_s - C) = D^o(C - C_s) \qquad \text{(G-5)}$$

If $C = C_b$ at $r >> d_p (1/r \simeq 0)$

$$\bar{G} = \frac{2D^o}{d_p(C_b - C_s)} = K_c(C_b - C_s) \qquad \text{(G-6)}$$

Therefore

$$K_c = \frac{2D^o}{d_p} \qquad \text{(G-7)}$$

If, however, $C = C_b$ at $r \simeq d_p$

$$\bar{G} = \frac{4D^o}{d_p}(C_b - C_s) = K_c(C_b - C_s) \qquad (G\text{-}8)$$

and

$$K_c = \frac{4D^o}{d_p} \qquad (G\text{-}9)$$

The actual value of K_c approaches ∞ as r approaches $d_p/2$. Increasing fluid velocity by increasing agitation serves to decrease the effective r thereby increasing the effective mass transfer coefficient.

Brian and Hales (19) correlated K_c with the power input to the slurry. Power input can be calculated from curves presented by Rushton et al. (206) which is reviewed by McCabe and Smith (154). The tip Reynolds number is a measure of the degree of agitation and is useful in determining the flow regime in the reactor. This quantity is defined

$$N_{Re} = \frac{d_a^2 \rho}{60\mu} \qquad (G\text{-}10)$$

where d_a is the impeller tip in inches, N is the agitator RPM, and ρ and μ are the slurry density and

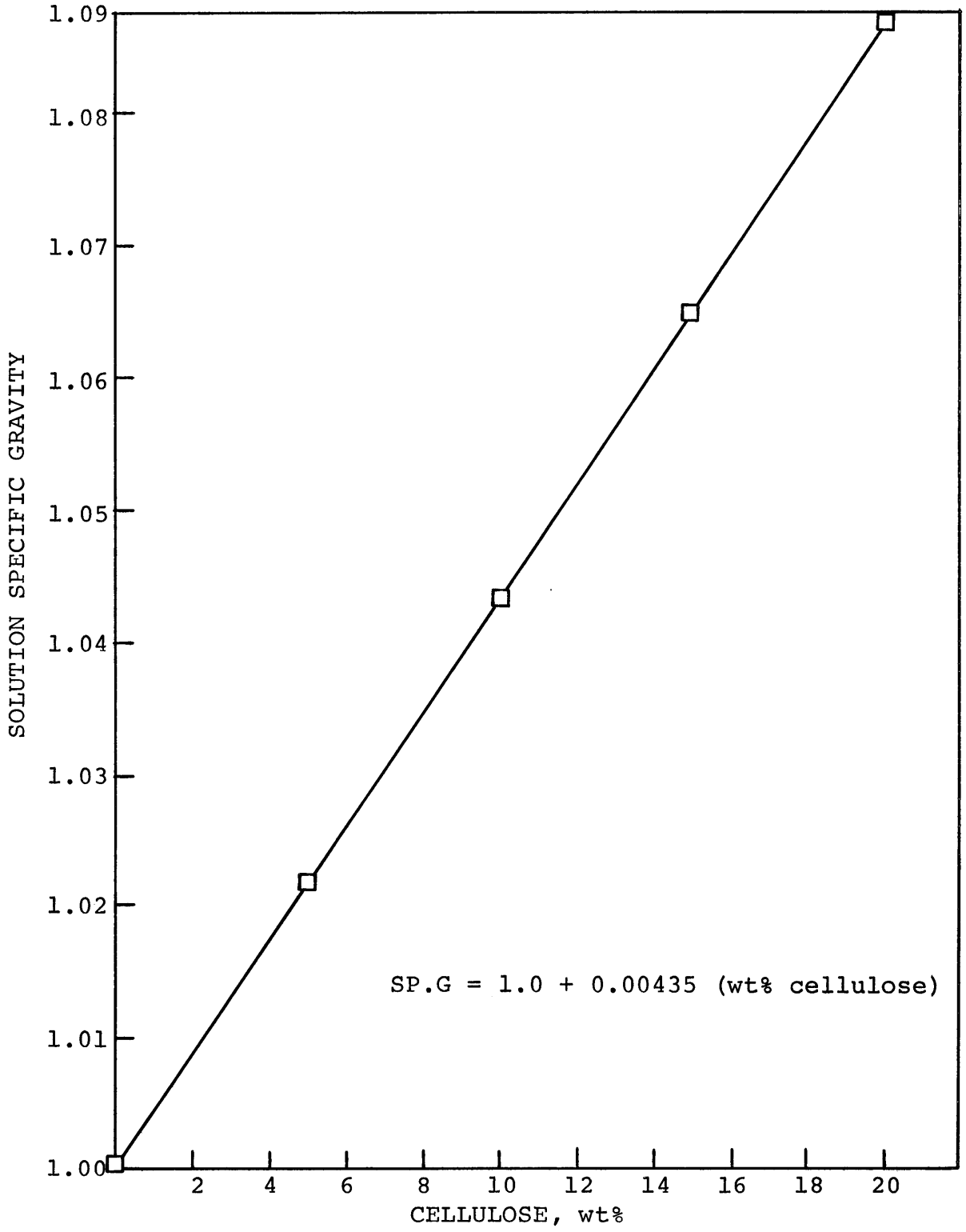

Figure G-1. Density of Cellulose Solutions

viscosity respectively. Figure G-1 allows determination of cellulose slurry density for use in equation (G-10). The viscosity dependence on cellulose was not determined, so a value of 2.0 cp was assumed for an eight per cent cellulose concentration.

Equation (G-1) can be further developed by replacing G_v with $V_b(dC_b/dt)$

$$(V_b)\frac{dC_b}{dt} = K_c A_p^*(C_b - C_s) \qquad \text{(G-11)}$$

where V_b is the total volume of liquid accessible to the enzyme, and therefore

$$C_s = C_b - \left(\frac{V_b}{K_c A_p^*}\right)\frac{dC_b}{dt} \qquad \text{(G-12)}$$

Note that dC_b/dt is the slope of a plot of C_b versus time.

3. Pore Diffusion

Diffusion in porous particles can occur by ordinary (or bulk) diffusion and surface diffusion as discussed by Satterfield (210). If the pores are large with respect to the diffusing molecule (solute) bulk diffusion will predominate. The mean free cross-section of the porous mass is ξ_p, which is identical with the volume fraction voids. If the pores are considered an array of cylinders parallel to the diffusion path, the diffusion flux per unit total

cross section of the porous solid would be the fraction ξ_p of the flux under similar conditions with no solid present. The length of the tortuous diffusion path in real pores, however, is greater than the distance along a straight line in the mean direction of diffusion. Moreover, the actual channels through which diffusion occurs are of irregular shape and varying cross section. The effective diffusivity D_e is therefore

$$D_e = \frac{D^o \xi_p}{L'S'} = \frac{D^o \xi_p}{\tau_p} \qquad \text{(G-13)}$$

Sorption processes are non-steady state and are described by Fick's second law (see Appendix E for derrivation)

$$D_e \nabla^2 C = \frac{dC}{dt} \qquad \text{(G-14)}$$

when the process also involves removal of solute from the mobile assembly, either by adsorption or reaction, the equations used must formally recognize the physical meaning of Fick's second law. The left side of equation (G-14) is still concerned with that portion of solute molecules that remains in the mobile state or creates the driving gradient ∇C for statistical motion. The right side, however, deals with the variation of the total count of mobile (C_i) and immobilized (C_a) molecules. Thus equation (G-14)

becomes

$$D_e \nabla^2 C = \frac{d(C_i + C_a)}{dt} \qquad \text{(G-15)}$$

Since (G-15) contains one more variable than (G-14) an additional equation, an expression relating C_a to C_i, is needed. The adsorption isotherm furnishes this information.

Assuming that the Langmuir isotherm is applicable we have

$$\theta = \frac{C_a}{C_{a\infty}} = \frac{\frac{C_i}{C_i^*}}{1 + \frac{C_i}{C_i^*}} \qquad \text{(G-16)}$$

where C_i^* is the concentration of the mobile species at which half the maximum adsorption $C_{a\infty}$ occurs ($C_i = C_i^*$ at $\theta = 0.5$). Equation (G-14) subject to (G-16) has been solved by Weisz and Hicks (269) for various geometries and constant bulk concentration.

Weisz (268) has approximated the Langmuir isotherm by limits he terms "weak" and "strong" adsorption. Weak adsorption can be described by a linear approximation for concentrations $C_i = 0 \ldots C_i^*/3$.

$$C_a = K_a C_i \qquad \text{(G-17)}$$

Strong adsorption, sometimes referred to as irreversible adsorption can be described

$$C_a = C_{a\infty} \quad C > 0 \tag{G-18}$$

An intermediate adsorption can often be described for concentrations of $C_i = C_i^*(0.33...2.0)$ by

$$\theta = K_a C_i^m \tag{G-19}$$

When $m < 1.0$ equation (G-19) is called the Freundlich isotherm.

The case of weak sorption, i.e. of a linear isotherm, has been solved by Crank (41). Equation (G-14) becomes

$$\frac{dC}{dt} = \left(\frac{D_e}{K_a + 1}\right)\nabla^2 C_i \tag{G-20}$$

Classic solutions can then be used, substituting $D_e/(K_a + 1)$ for D_e .

APPENDIX H

DETAILED ASSAY PROCEDURES

1. Total Carbohydrate - PSOD

   a. Method: Phenol Sulfuric Acid

   b. Range: 0.01 - 1.5 mg/ml carbohydrate

   c. Reagents:

      1) Dilute Phenol Solution - 2.63%: 3 ml of 88% phenol, made to 100 ml with dixtilled water

      2) Concentrated Sulfuric Acid

   d. Procedure:

      1) Add 1.9 ml of phenol reagent to 0.1 ml of sample

      2) Add 5.0 ml of concentrated sulfuric acid and mix immediately

      3) Let stand at least 30 min

      4) Read at 485 nm against a distilled water blank

   Note: Sulfuric acid must be added to the center of the liquid surface to promote mixing. This method hydrolyzes all soluble cellulose fragments to glucose equivalent.

2. Glucose - GLOD

   a. Method: Glucostat (Worthington Biochemical Corp.)

   b. Range: 0.1 - 3.0 mg/ml carbohydrate

   c. Reagents:

      1) Tris Buffer, 0.1 M, pH 7.0 -
         Tris base - 3.03 g
         Maleic anhydride - 2.45 g
         NaOH - 9.5 g
         Make to 1.0 l with distilled water and adjust the pH with HCl or NaOH.

2) Glucostat: Make per manufacturer's instructions

3) 4 N Hydrochloric Acid

d. Procedure:

1) Add 0.1 ml of sample to 2.0 ml of Tris buffer

2) Add 2.0 ml of Glucostat reagent, mix

3) Place in a water bath at 50°C for 45 min

4) Add 2 drops of 4 N HCl, mix

5) Determine optical density at 415 nm against distilled water as a blank

Note: Glucostat is a lyophilized reagent that must be reconstituted immediately prior to use because it darkens upon exposure to light. This procedure is reasonably specific for glucose.

3. Total Carbohydrate - TCOD Short

a. Method: Incubation with β-glucosidase to convert cellobiose to glucose followed by Glucostat to yield optical density

b. Range: 0.3 - 4.0 mg/ml carbohydrate for linearity. If Figure 4-2 is used instead of equation (4-2) the range can be extended to 10 mg/ml

c. Reagents:

1) Phosphate Buffer - 0.05 M, pH 4.9

KH_2PO_4	6.753 g
$Na_2HPO_4 \cdot 2H_2O$	0.0712 g

Make to 1.0 l with distilled water and adjust the pH with HCl or NaOH.

2) 10 mg/ml β-Glucosidase (Sigma Chemical Co., St. Louis, Mo.) - dissolve desired amount in 0.05 M phosphate buffer immediately prior to use

d. Procedure:

1) Place a 0.1 ml sample in a test tube

2) Add 0.2 ml of β-glucosidase reagent

3) Add 0.7 ml of phosphate buffer

4) Incubate at 50°C for 1 hour

5) Remove 0.1 ml sample and determine carbohydrate with the Glucostat procedure

Note: Actual carbohydrate is 10 times the carbohydrate from the Glucostat because of the dilution caused by the addition of reagents.

4. Total Carbohydrate - TCOD Extended

a. Method: Same as for TCOD Short

b. Range: 1 - 10 mg/ml

c. Reagents: Same as for TCOD Short

d. Procedure:

1) Place a 0.1 ml sample in a test tube

2) Add 0.4 ml of β-glucosidase reagent

3) Add 2.0 ml of phosphate buffer

4) Incubate at 50°C for 1 hour

5) Remove 0.1 ml sample and determine carbohydrate with the Glucostat procedure

Note: Actual carbohydrate in the sample is 25 times the carbohydrate from the Glucostat because of the dilution caused by the addition of reagents.

5. Protein Determination - PTOD

a. Method: Lowry (Folin Phenol Reagent)

b. Range: 0.01 - 1.0 mg/ml

c. Reagents:

1) 2.0% Na_2CO_3 in 0.1 N NaOH

2) 0.5% $CuSO_4 \cdot 5H_2O$ in a 1% solution of Rochelle salt

3) 50 ml of Reagent (1) plus 1 ml of Reagent (2) to be mixed daily

4) 1.0 N Folin Phenol Reagent (Fisher Scientific, diluted from 2 N with distilled water)

d. Procedure:

1) Place a 0.2 ml sample in a test tube

2) Add 3.0 ml of Reagent (3), mix well

3) Let stand 30 min at room temperature

4) Add 0.3 ml of 1.0 N Folin Phenol Reagent and mix rapidly

5) Let stand 30 min at room temperature

6) Promptly determine the optical density (PTOD) at 500 nm against a distilled water blank.

Note: Carbohydrate, Tris buffer and other materials interfere with this procedure. Standards must, therefore, be in the same solvents as the unknown.

6. C_1 Assay - FPOD

a. Method: Determination of total carbohydrate liberated from a strip of filter paper

b. Substrate: Whatman No. 1 filter paper cut into 1 X 6 cm strips and rolled into a tight cylinder

c. Reagents:

1) Phosphate Buffer, 0.05 M, pH 4.9 (as described in Total Carbohydrate procedure)

2) β-Glucosidase, 10 mg/ml (as described in Total Carbohydrate procedure)

d. Procedure:

1) Place a 0.2 ml sample into a test tube

2) Add 0.2 ml of β-glucosidase reagent

3) Add 2.0 ml of phosphate buffer

4) Place in an ice bath

5) Add a piece of the rolled filter paper and mix

6) Immediately incubate at 50°C for 1 hour

7) Immediately remove from the 50°C bath and place in an ice bath, agitate for 30 sec

8) Remove filter paper

9) Use normal Glucostat procedure to determine FPOD, except use a 0.2 ml rather than a 0.1 ml sample.

Note: As many as 24 samples can be run if care and speed in manipulation are employed.

7. Endoglucanase Assay - ENOD

a. Method: Measure TCOD produced during incubation with carboxymethylcellulose (CMC) and β-glucosidase

b. Substrate: 1% CMC (DS = 0.4, Hercules Powder Co.) in phosphate buffer, 0.05 M, pH 4.9

c. Reagents:

1) Phosphate buffer, 0.05 M, pH 4.9 (as described in Total Carbohydrate procedure)

2) β-Glucosidase, 10 mg/ml (as described in Total Carbohydrate Procedure)

3) Tris buffer, 0.1 M, pH 7.0 (as described in Glucostat procedure)

d. Procedure:

1) Place a 0.1 ml sample in a test tube

2) Add 0.2 ml of β-glucosidase reagent

3) Place in an ice bath

4) Add 2.0 ml of cold CMC reagent

5) Immediately place in a 50°C water bath for 30 min

6) Remove from 50°C bath and immediately place in an ice bath, agitate for 30 sec

7) Immediately transfer 0.1 ml sample to another test tube containing 2.0 ml of Tris buffer (these tubes should also be in an ice bath)

8) Follow remaining steps of the Glucostat procedure

Note: As many as 24 samples can be run simultaneously if care and speed in manipulation are employed.

APPENDIX I

ENZYME PRODUCTION

1. Introduction

The enzyme solution employed for the hydrolysis experiments was a mixture of enzyme obtained from Dr. Mary Mandels at the U.S. Army Research Laboratory, Natick, Massachusetts, and of enzyme produced in this laboratory. Both enzyme solutions were culture filtrates obtained by the submerged fermentation of the earth fungus Trichoderma viride strain QM 9123. The Natick batch was the strongest in C_1 activity that they had produced. The local enzyme was only 80% as strong, and was equivalent to previous batches produced at Natick. A batch of T. viride concentrate was also obtained from Natick. This enzyme was concentrated by passage through an ultrafiltration cell as will be discussed later. The general fermentation procedure is reviewed by Mandels et al. (143-149).

2. Apparatus

The fermenter was basically a sealed stirred tank reactor. The jar was a 15 liter pyrex cylinder compressed between neoprene gaskets and polycarbonate flanges. The top flange contained 7 1/2 in. stainless steel Swagelok connectors. These were capped or provided with Teflon sleeves. The sleeves were drilled to accomodate various

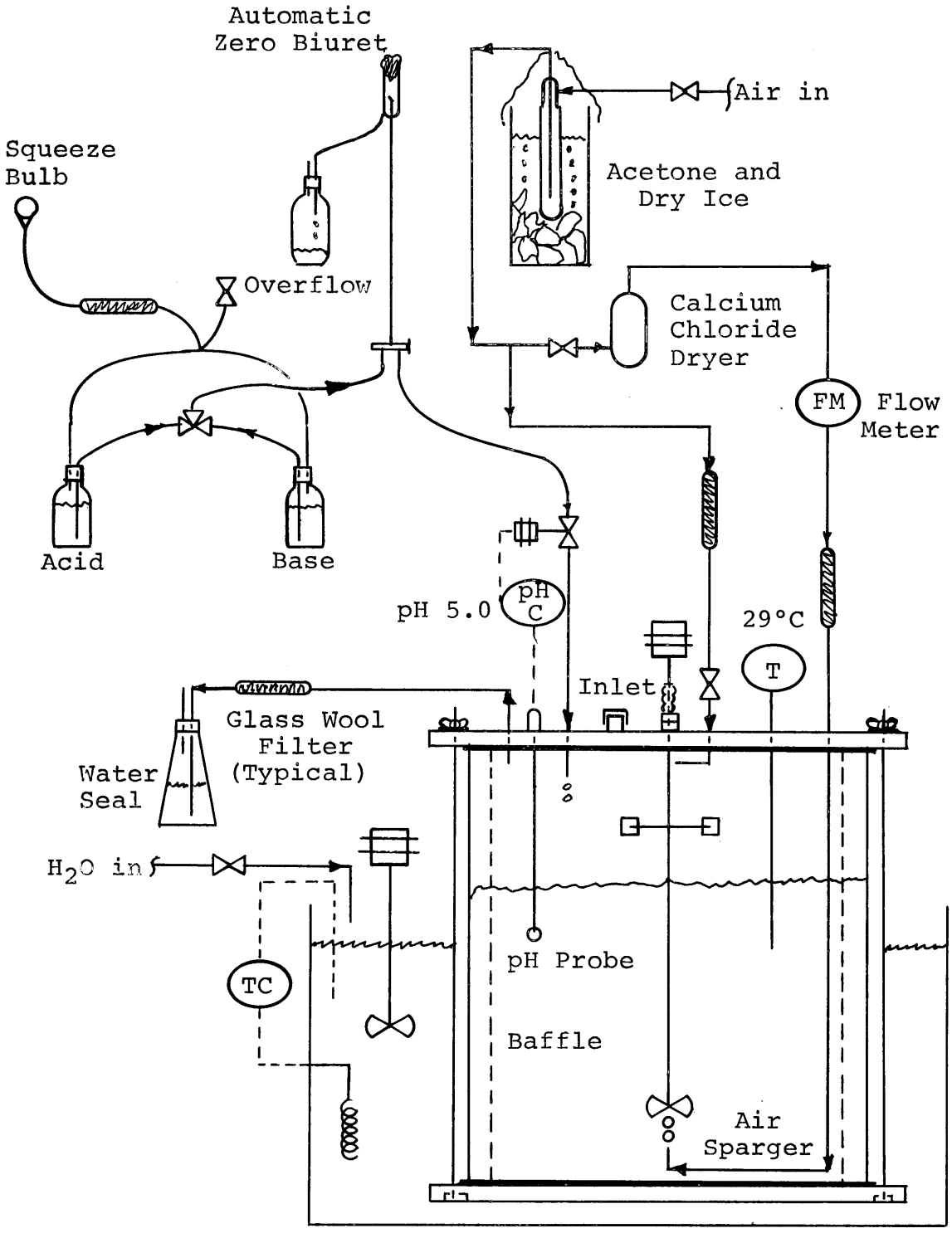

Figure I-1. Fermenter Apparatus

connectors or probes as desired. The capped 3/4 in. connector was used as an inlet port. A similar connector was used to support the agitator seal bearing.

The impeller seal was a Teflon on Teflon bearing. The lower bearing was a Teflon sleeve bored slightly larger than the shaft and wedged into a Swagelok conncetor. The upper bearing was a similar sleeve set in a metal bellows. The bellows was clamped to the shaft. When the shaft was clamped onto the agitator motor, the upper bearing was compressed against the lower. The spring bellows allowed for wear in the bearing surfaces which become incredibly smooth as the Teflon surfaces polished each other. This system was capable of sealing against several inches of water pressure.

The entire fermenter apparatus is presented in Figure I-1. Air was dried by passage through glass bayonet heat exchangers placed in a dry ice-acetone bath. Some of the dry air was further dried and passed through a rotameter and a glass wool filter into a sparger that delivered it beneath the agitator blade. A second stream of air was directed at the base of the impeller shaft. This provided positive pressure through the bearing seal without requiring the passage of excessive air through the liquid. Excessive sparged air could deactivate enzyme by creating an air/water interface (foaming). Waste air was removed through a glass wool filter and bubble chamber (for visual confirmation of air flow rate).

A probe was provided to continuously monitor pH and to adjust it by controlling a titrator. The titrator would activate a magnetic valve to admit acid or base as desired. (Although provided, pH control was not utilized in this series.) Temperature was maintained at 29°C by placing the fermenter into a water bath as shown.

3. Procedure

The fermenter was prepared by adding 12 liters of basal media to the fermenter jar. The basal media was prepared as a 10 fold concentration without peptone, Tween 80, or cellulose added. The peptone provided initial nutrient for the fungus, along with necessary amino acids. The Tween 80 enhanced release of the enzyme into solution. The cellulose induced enzyme production and provided a carbon source for fungal metabolic activity. The final basal media composition is given in Table I-1.

The jar was then covered and all hoses and probes attached. All connections open to the atmosphere were stoppered with glass wool and covered with aliminum foil. The air sparger and seal air lines were clamped at the cover to prevent the liquid in the fernenter from flowing through the tubes into the glass wool air filters. The outlet air connection was left unclamped to allow for expansion and contraction of the material within the fermenter. The complete fermentation apparatus was then placed in an autoclave.

TABLE I-1. BASAL TRICHODERMA VIRIDE FERMENTATION MEDIA

Component	Grams per liter
$(NH_4)_2SO_4$	1.400
KH_2PO_4	2.042
$(NH_2)_2CO$	0.300
$CaCl_2$	0.300
$MgSO_4 \cdot 7H_2O$	0.300
$FeSO_4 \cdot 7H_2O$	0.00500
$MnSO_4 \cdot H_2O$	0.00156
$ZnSO_4 \cdot 7H_2O$	0.00140
$CoCl_2$	0.00366
Tween 80	0.5
Proteose Peptone	0.5
Cellulose	7.5
Distilled Water	Make to 1.0 liter

(The apparatus did not include the water bath, magnetic valve, agitator motor, or input air apparatus upstream of the glass wool filters.) The bolts were then loosened so that differential expansion of the steel bolts and glass jar would not crack the jar. (Contact of the system with the atmosphere must be prevented except through glass wool filters. If acid or base is to be injected, these must be sterilized as well. In addition, all of the hoses connecting the acid and base reservoirs to the fermenter must remain connected. This creates quite a logistical problem.)

The autoclave was slowly pressured to 15 psig with saturated steam. Constant pressure was maintained for 45 min and then slowly reduced. When the pressure was zero, the autovlave was opened. As the fermenter cooled the bolts were hand tightened to maintain an air tight seal but prevent over compression. Air entered the apparatus through the open (except for glass wool filter) waste air connection. When cool enough so that the bolts could be tightened sufficiently, the apparatus was transferred to the water bath. The air inlet system was then connected, and air admitted through the sparger to aid in cooling the media.

During sterilization a tube of distilled water was also included. This was added to a tube of fungus spores grown on potato dextrose agar (Difco, St. Louis, Missouri). The mouths of each tube were flamed to maintain sterility. The spores were transferred into the water by rubbing the agar

surface with a steril wire loop. When the fermenter was cool, air was switched entirely to the seal-air connection. The inlet port was unclamped and flamed and the spores added. The cap was then replaced and the air flow reduced. The high air flow presurized the fermenter even with the inlet uncapped thus helping prevent contamination. The air flow through the sparger was adjusted to 0.1 to 0.3 vol/vol/min.

The pH was adjusted to 5.0 by manual addition of acid or base for the first several days after which no further adjustments were made. Fermentation was complete after 10 days. The fermenter was disconnected and the broth filtered through glass wool. The pH of the filtrate was then adjusted to 5.0 to yield the enzyme solution. Such solutions have maintained activity for a year if kept at 2°C (193).

4. Enzyme Concentration

Some batches of enzyme solution were concentrated by Mandels et al. by passing the broth through an Amicon TCIS ultrafiltration unit equipped with a PM-30 membrane. The ratio of enzyme activities to each other and to total protein is altered by the concentration procedure. Assuming that no protein is lost through the membrane, total protein provides a measure of the concentration factor (approximately 3.4 to 1). The endoglucanase activity of the same sample was only increased 3.2 to 1 indicating apparent deactivation of 6% of the endoglucanase. The C_1 activity was only 2.1

times the original, indicating apparent deactivation of 38% of the C_1 enzyme. The ultimate concentration point is that at which increase in activity caused by water removal is balanced by deactivation of the enzyme itself.

Concentration studies in this laboratory were attempted with a polymeric membrane on a cellulosic support (Millipore Corporation, Bedford, Massachusetts). The throughput was reduced by an order of magnitude after only 15 minutes of ultrafiltration. Filtration of the enzyme solution through Millipore filters caused rapid plugging of the filter. A hypothesis was developed to explain these results which ultimately halted concentration efforts.

The fermenter broth contained Tween 80, (polyoxy ethylene sorbitan monooleate) an extremely large molecular wetting agent. This is thought to bind to the cellulose support of the membrane with long branches extending into the pores. These then attach to material passing through the membrane, gradually forming a bridge that effectively blocks the pore. The totally polymeric Amicon membranes were not affected in this manner.

APPENDIX J

SAMPLE CALCULATIONS

1. Data from Run 15, time, 30 minutes:

PSOD* = 0.675	PTOD* = 0.207	PSK = 8.0
GLOD* = 0.237	ENOD* = 0.150	GLK = 8.0
TCOD* = 0.410	FPOD* = 0.645	TCK = 10.0

2. Correction of carbohydrate optical densities by subtracting blank optical densities

PSOD = 0.675 - 0.010 = 0.665
GLOD = 0.237 - 0.025 = 0.212
TCOD = 0.410 - 0.048 = 0.362

3. Calculation of enzyme blanks and activities

NBOD = [0.36(TCK/9.6)(TCOD*)/ENK] + 0.010
= [0.36(10.0/9.6)(0.410)/3.3] + 0.010
= 0.603 + 0.010
= <u>0.057</u>

FBOD = [(TCK/FPDIL)(FPK/0.05)(TCOD)] + 0.035
= [10.0/24.0)(0.20/0.05)(0.362)] + 0.035
= 0.603 + 0.035
= <u>0.638</u>

ENOD = ENOD* - NBOD
= 0.150 - 0.057
= <u>0.093</u>

FPOD = FPOD* - FBOD
= 0.645 - 0.638
= <u>0.007</u>

ENFRC = ENK(ENOD - 0.072)/1.41
= 3.3(0.093 - 0.072)/1.41
= <u>0.049</u>

FPACT = [(FPOD - 0.046)/0.897](0.2/FPK)
= [(-0.039)/0.897](0.2/0.2)
= <u>0</u>

Fraction of the enzyme adsorbed on solid cellulose

$ENFRC_o$ = 0.625
FRACT Adsorbed = 1 - (0.049/0.625)
= <u>0.922</u>

$FPFRC_o = 0.625$

$FPFRC_o Adsorbed = 1 - (0.0/0.625)$

$= \underline{1.0}$

4. Calculation of Carbohydrate

Total Carbohydrate

$$PCARB = PSK(PSOD - 0.010)$$
$$= 8.0(0.665)$$
$$= \underline{5.32}$$

Cellobiose and Glucose

$$TCARB = TCK[(TCOD - 0.048)/1.275]^{0.91}$$
$$= 10.0(0.317)$$
$$= \underline{3.17}$$

5. Differentiation between glucose and cellobiose

TCK(TCOD) = O.D. Glucose + O.D. Converted Cellobiose

GLK(GLOD) = O.D. Glucose + O.D. Unconverted Cellobiose

TCOD - [GLOD(GLK/TCK)] = O.D. Converted Cellobiose - O.D. Unconverted Cellobiose

= Diff

$$Diff = (1.31 \times CELOB)^{1.1} - (0.145 \times CELOB)^{1.1}$$

where the equations are from Figure 4-2

For first approximation assume O.D. from unconverted C_2 is 0. Therefore,

$$Diff = (1.31 \times CELOB)^{1.1}$$

This provides a starting value for CELOB'. Increment CELOB' by varying amounts until calculated value of Diff is close to the measured value.

$CELOB' \simeq \underline{0.18}$

$$GLUCO = TCK\{(TCOD/1.275) - [1.05(0.18)]^{1.1}\}^{0.91}$$
$$= 10.0\{(0.362/1.275) - [1.05(0.18)]^{1.1}\}^{0.91}$$
$$= 10.0\{0.284 - 0.162\}^{0.91}$$
$$= \underline{1.37}$$

CELOB = 10.0(0.18)
= 1.80

TCARB = CELOB + GLUCO $\overset{?}{=}$ 3.17
= 1.37 + 1.80 = 3.17

6. Calculation of Protein Concentration

PTFRC = (PTOD - INCEP)/SLOPE

where INCEP and SLOPE are the intercepts and slopes of the curves in Figure 4-7.

If TCARB $\leq$ 1.0
SLOPE = 0.605 + 0.011(TCARB)
INCEP = 0.025 + 0.017(TCARB)

If 1.0 < TCARB $\leq$ 3.0
VABLE = (TCARB - 1.0)/2.0
SLOPE = 0.616 + 0.025(VABLE)
INCEP = 0.042 + 0.015(VABLE)

If 3.0 < TCARB $\leq$ 5.0
VABLE = (TCARB - 3.0)/2.0
SLOPE = 0.641 + 0.059(VABLE)
INCEP = 0.057 + 0.008(VABLE)

If 5.0 < TCARB $\leq$ 7.0
VABLE = (TCARB - 5.0)/2.0
SLOPE = 0.700 + 0.040(VABLE)
INCEP = 0.065 + 0.008(VABLE)

If 7.0 < TCARB $\leq$ 10.0
VABLE = (TCARB - 7.0)/3.0
SLOPE = 0.740 + 0.054(VABLE)
INCEP = 0.073 + 0.007(VABLE)

If 10.0 < TCARB $\leq$ 15.0
VABLE = (TCARB - 10.0)/5.0
SLOPE = 0.794 + 0.058(VABLE)
INCEP = 0.080 + 0.011(VABLE)

If 15.0 < TCARB $\leq$ 20.0
VABLE = (TCARB - 15.0)/5.0
SLOPE = 0.852 + 0.065(VABLE)
INCEP = 0.091 + 0.011(VABLE)

If TCARB 20.0, abort the calculation because standard curves were not produced above 20.0 mg/ml.

Since TCARB = 3.17

VABLE = (3.17 - 3.0)/2.0
= 0.085

SLOPE = 0.641 + 0.059(0.085)
= 0.064

INCEP = 0.057 + 0.008(0.085)
= 0.058

PTFRC = (0.207 - 0.058)/0.646
= 0.231

Initial PTFRC = 0.625
Therefore adsorbed fraction = 1 - (0.231/0.625)
= 0.63

Total adsorbable protein was assumed to be 64% of the total protein, therefore, all protein that is going to adsorb has adsorbed.

7. Calculation of Rate Coefficients and Cellulose Concentrations

Hydrolysis rate was determined from tangents to the PCARB curves. From Figure 7-3 $C_a + C_b = 2.8$ when the plateau rate is extrapolated to zero time. Since the curves start at PCARB = 0.8, $C_a = 0.8$ and, therefore,

$C_b = (C_a + C_b) - C_a$
$= 2.8 - 0.8$
$= 2.0$

Calculation of k_d

At 12 hours PCARB = 23.8 mg/ml, therefore,

$C = (C)_o - PCARB = (88 - 23.8)/1.1 = 57.8$ mg/ml

The 1.1 converts cellulose from glucose equivalent to mg/ml cellulose.

Surface required for saturation = C_{opt}

$C_{opt} = 14.1[E]\ 10.0$
$= 14.1\ (0.488)\ 10.0$
$= 68.8$ mg/ml

$$[E]_{12} \simeq (57.8/68.8)[E]_o$$
$$= 0.841[E]_o$$

$$k_{d12} = 0.841\ k_d \Rightarrow k_d = 1.18\ k_{d12}$$

Rate at 12 hr is $\underline{0.65}$ mg/ml/hr

$C_{12} = 88 - 23.8 = 64.2$ mg/ml

$$0.65 \text{ mg/ml/hr} = k_{d12}(64.2)$$
$$k_{d12} = 0.65/64.2 = 0.0103 \text{ hr}^{-1}$$
$$k_{d12} = 1.18(0.0103) = \underline{0.0121 \text{ hr}^{-1}}$$

which agrees with the constant determined from Figure 7-9 (0.0112 hr^{-1}) which was computed from a plot of $-\ln (C_d/C_{d_o})$ vs. time.

Calculation of C_{d_o}

Since $k_d = 0.0111 \text{ hr}^{-1}$

$$-\frac{dC_d}{dt} = k_d C_d$$

Integration from 0 to 10 hours resulted in

$$-\ln C_d \Big|_0^{10} = k_d\ (10 \text{ hr})$$

$$-\ln (66.7/C_{d_o}) = 0.121$$

$$C_{d_o} = 66.7/0.886 = \underline{75.2 \text{ mg/ml}}$$

The 10 hr value was chosen because it is the midpoint of the linear part of the curve in Figure 7-9.

Calculation of C_{c_o}

Since $C_a + C_b = 2.8$ and $C_d = 75.2$ mg/ml

$$C_c = 88.0 - (75.2 + 2.8)$$
$$= \underline{10.0 \text{ mg/ml}}$$

Calcualtion of k_c

At 60 minutes assume that all C_a and C_b have been hydrolyzed. PCARB = 7.4 mg/ml Rate = 4.4 mg/ml/hr

$$-\frac{dC_d}{dt} = 0.0121(75.2) = 0.91 \text{ mg/ml}$$

After 1 hr $C_d = 74.1$ and

$$k_d C_d = 0.0121(74.1) = 0.90 \text{ mg/ml/hr}$$

$$C_c = 10.0 - [7.4 - (2.8 + 0.90)] = 6.3 \text{ mg/ml}$$

$$-\frac{dC}{dt} = -\frac{dC_c}{dt} - \frac{dC_d}{dt} \Rightarrow 4.4 = -\frac{dC_c}{dt} + 0.90$$

$$-\frac{dC_c}{dt} = 3.5 \text{ mg/ml/hr} = k_c C_c$$

$$k_c = 3.5/6.3 = \underline{0.550 \text{ hr}^{-1}}$$

Calculation of k_b

At $t = 0$ Rate = 18.9 mg/ml/hr

$$-\frac{dC}{dt} = -\frac{dC_b}{dt} - \frac{dC_c}{dt} - \frac{dC_d}{dt}$$

$$18.9 = 2k_b + 0.55(10.0) + 0.012(75.2)$$

$$2k_b = 18.9 - (5.5 + 0.91) = 12.5$$

$$k_b = \underline{6.25 \text{ hr}^{-1}}$$

Summary:

$C_a = 0.8$ mg/ml $= 0.0091$ C
$C_b = 2.0$ mg/ml $= 0.0227$ C
$C_c = 10.0$ mg/ml $= 0.114$ C
$C_d = 75.2$ mg/ml $= 0.854$ C

$$C = C_a + C_b + C_c + C_d = 88 \text{ mg/ml}$$

$k_b = 6.25 \text{ hr}^{-1}$
$k_c = 0.55 \text{ hr}^{-1}$
$k_d = 0.0121 \text{ hr}^{-1}$

8. Calculation of Reaction Order (n) for Extended Hydrolysis

Assume θ_{sat} is dependent only on temperature, pH, and type of surface. At extended hydrolysis ($C < C_{opt}$)

$$-\frac{dC}{dt} = k_d^* [\theta]^{1.5} C_d^n \quad \text{and} \quad \theta = \theta_{sat}$$

Run 20 at 8 hr, Rate = 0.18 mg/ml/hr
C = 22.0 - 9.5 = 12 mg/ml

$$-\frac{dC}{dt} = k_d^* (\theta_{20})^{1.5} (12.5)^n = 0.18$$

Run 15 at 12 hr, Rate = 0.65 mg/ml/hr
C = 64.2 mg/ml

$$-\frac{dC}{dt} = k_d^* (\theta_{15})^{1.5}(64.2)^n = 0.65$$

$$\left(\frac{64.2}{12.5}\right)^n = \left(\frac{\theta_{20}}{\theta_{15}}\right)^{1.5} \frac{0.65}{0.18}$$

$$(5.15)^n = 3.6$$
$$n \ln 5.15 = \ln 3.6$$
$$n\ (1.64) = 1.28$$
$$n = 1.28/1.64$$
$$= \underline{0.78}$$

9. Calculation of Swollen Particle Density

Add 2 g of cellulose and 8 g of water to a test tube and measure the final volume

g cellulose	2.0
g H_2O	8.0
Final volume (cc)	9.2
Cellulose density (g/cc)	1.53
Cellulose volume	1.3
Water uptake (g/g cellu)	0.66
Water uptake	1.32
Volume free water (cc)	6.68
Particle volume (cc)	2.52
Particle density (g/cc) = (2 + 1.32)/2.52	1.32

1 g Cellulose takes up 0.66 g H_2O
1.66 g Particles = 1.255 cc

Void volume of cellulose particle is equal to the volume of water

$$\varepsilon_p = 0.66/1.255 = 0.525$$

Density of 8 wt% Cellulose Solution

Basis: 100 g solution
Free water = 92 - 8(0.66) = 86.7 cc
Particle wt = 13.3 g
Particle vol = 13.3 g/(1.33 g/cc) = 10 cc
Total vol = 96.7 cc
Density = 100/96.7 = 1.03 g/cc

10. Reynolds Number Calculation

200 RPM, 8 wt% cellulose

$$N_{Re} = \frac{d_a^2 \, n\rho}{\mu}$$

d_a = impeller diameter = 1 in. = 0.083 ft
n = RPM = 200 = 3.3 RPS
ρ = 1.03 g/cc
μ = 2 cp (assumed)

$$N_{Re} = \frac{(0.083)^2(3.3)(1.03)(62.4)}{2(0.67 \times 10^{-3})}$$
$$= 2400$$

11. Optimum Cellulose Concentration

Runs 51-53 were for 90 min, therefore, k_c is a good basis for calculating C_{opt} because C_b will be hydrolyzed and C_d will be nearly constant.

$$- dC/dt \; \alpha \; [E]^{1.5} C_o^{-2.5}$$

From the kinetic model, at $C < C_{opt}$ where $C = 16$ mg/ml $[E] < [E]_{opt}$ and

$$(RATE)/(RATE)_{opt} = ([E]/[E]_{opt})^{1.5}$$
$$= (C/C_{opt})^{1.5}$$

At $C > C_{opt}$ where $C = 18$ mg/ml

$$(RATE)/(RATE)_{opt} = (C/C_{opt})^{-2.5}$$

Since RATE 16 $\simeq$ 18,

$$(RATE)_{16}/(RATE)_{opt} \simeq (RATE)_{18}/(RATE)_{opt}$$
$$- 2.5 \ln 18 + 2.5 \ln C_{opt} = 1.5 \ln 16 - 1.5 \ln C_{opt}$$
$$4.0 \ln C_{opt} = 4.15 + 7.23 = 11.38$$
$$\ln C_{opt} = 2.84 \Rightarrow C_{opt} = \underline{17.2 \text{ wt\%}}$$

12. Adsorbable Protein

From Runs 12-15 and 27, adsorbable protein fraction equals 0.08 per 1/8 enzyme fraction or 64% of the total

protein for an enzyme fraction of 1.0. Since the enzyme fraction equals 1.22 mg/ml of the total protein, adsorbable protein equals 0.78 mg/ml for an enzyme fraction of 1.0. C_{opt} for 0.195 mg/ml adsorbable protein was 2.75 wt%.

$$C_{opt} = \chi[E] = 2.75$$
$$\chi = 2.75/0.195 = 14.1$$
$$\underline{C_{opt} = 14.1[E]}$$

13. Adsorption Calculations

Assume that the particle equals a 16μ sphere, swollen

$$V_p = 4/3\pi r^3 = 4/3\pi(8 \times 16^{-6})^3 = 2.14 \times 10^{-15} m^3 = 2.14 \times 10^{-9} \text{ cc}$$
$$A_p = 4\pi r^2 = 4\pi(64 \times 10^{-12}) = 8 \times 10^{-10} \text{ m}^2$$

A cellulose particle sorbes 0.66 g H_2O/g cellulose

$$P_{cellulose} = 1.53 \text{ g/cc}$$

Basis: 1 cc particle = χg cellulose $P_{H_2O} = 1$ g/cc

$$1 \text{ cc} = (\chi/1.53) + 0.66\chi$$
$$= 1.31\chi$$
$$= 0.773 \text{ g cellulose}$$

$$\varepsilon_p = 0.5 = \text{porosity}$$

1 cc of particles contains 0.773 g cellulose and 1 g cellulose equals 1.29 cc.

$$\frac{\text{No. of particles}}{\text{g cellulose}} = \frac{1.29}{2.14 \times 10^{-9}} = 6.05 \times 10^8$$

$$\frac{\text{AREA}}{\text{g cellulose}} = 6.05 \times 10^8 \times 8 \times 10^{-10} = 0.5 \text{ m}^2/\text{g}$$

$$C_{opt} = 14.1[E]$$

To adsorb 1 mg/ml, 14.1 wt% of cellulose is required or 141 mg/ml, therefore

$$\frac{\text{Enzyme adsorbed}}{\text{mg cellulose}} = 1/141 = 7.1 \times 10^{-3} \text{ mg/mg}$$

Assuming an enzyme molecular weight of 60,000

$$7.1 \times 10^{-6}\text{g}/60000 \times 6 \times 10^{23} = 7.1 \times 10^{13} \frac{\text{molecules}}{\text{mg cellulose}}$$

$$= 7.1 \times 10^{16} \frac{\text{molecules}}{\text{g cellulose}}$$

One enzyme moleucle is 35 Å by 210 Å or $7.4 \times 10^{-17} m^2$/mole. The area for adsorption of 7.1×10^{16} molecules is

$$7.1 \times 10^{16} \times 7.1 \times 10^{-17} = \underline{5.3\ m^2/\ g}\ \text{cellulose}$$

If the area required per enzyme molecule is that required for it to rotate freely, $(\pi/4)(\text{major axis})^2$ would be a better estimate of required area per molecule, or $(44.4 \times 10^{-17} m^2/\text{molecule})$. The area required for the adsorption of 7.1×10^{16} molecules is, therefore,

$$7.1 \times 10^{16}(44.4 \times 10^{-17}) = \underline{24.8\ m^2}.$$

APPENDIX K

NOMENCLATURE

a	Activity of solution
a	Radius of a sphere
a	Major axis of prolate ellipsoid
A	Area
A*	Surface area of a unit weight of solid
$\bar{A}_i$	Partial molar areas of component i when adsorbed
A_p	Total pore surface area
A_p*	Total particle external surface area
b	Constant in Langmuir equation
b	Minor axis of prolate ellipsoid
b	Partition coefficient, C_s/C_l
C	Concentration
$\underline{C}$	Cellulose concentration, mg/ml, 10.0 C_o
C_a	Concentration of adsorbed solute
C_a	Soluble moderate length cellulose fragments, (GE), mg/ml
$C_{a\infty}$	Maximum possible concentration of adsorbed solute
C_b	Amorphous cellulose, (GE), mg/ml
C_b	Concentration of solute in bulk solution
C_c	Crystalline cellulose, (GE), mg/ml
C_d	Inaccessible crystalline cellulose, (GE), mg/ml
C_f	Final concentration
C_i	Initial concentration
C_i	Species i concentration

C_o	Initial cellulose concentration, wt%
C_{opt}	Optimum C_o
C_s	Concentration of solute at surface of particle
C_x	Collective term for enzymes active on soluble cellulose
C_1	Hydrogenbondase enzyme
C_2	Cellobiose
CELOB	Cellobiose concentration, mg/ml
CMC	Carboxymethylcellulose
D	Bulk diffusivity
d_a	Diameter of impeller, in.
d_e	Stokes-Einstein equivalent sphere diameter
dp	Particle diameter
DP	Degree of polymerization
DS	Degree of substitution
[E]	Enzyme concentration
[E]	T. viride concentration, adsorbable protein, mg/ml
[EI]	Concentration of enzyme-inhibitor complex
[ES]	Concentration of enzyme-substrate complex
ENACT	Endoglucanase activity
ENFRC	[E] based on ENACT
ENK	Endoglucanase assay dilution factor
ENOD	Endoglucanase assay optical density
f	Particle friction in solution
F	Force on particle
f_o	Stokes law friction factor
FBOD	Filter paper assay blank optical density

FPACT	Filter paper activity
FPFRC	[E] based on FPACT
FPK	Filter paper assay dilution factor
FPOD	Filter paper assay optical density
G	Weight of solute taken up
$\bar{G}$	Diffusion flux, g/cm^2-sec
G_v	Solute flux, g/sec
GE	Glucose equivalent, cellobiose X 1.05, cellulose X 1.10
GLK	Unconverted cellobiose dilution factor
GLOD	Unconverted cellobiose optical density
[I]	Inhibitor concentration
J	Molar flux, moles/cm^2-sec
k	Boltzman's constant
k_{ij}	Rate constant of component i in reaction j
K	Constant
K_a	Adsorption rate constant
K_c	Bulk mass transfer constant, cm/sec
k_d	Deactivation rate constant
k_i	Observed rate coefficient
k_i*	Intrinsic rate constant
K_i	Constant for component i
Km	Michaelis-Menten constant
k_r	Recrystallization rate constant
K_s	Intrinsic first order rate constant
K_s	Substrate concentration giving 1/2 the maximum rate of reaction

L'	Pore length factor
L_{jk}	Phenomonological coefficient
m	Constant
M	Particle weight
M	Weight of adsorbent
Mw	Molecular weight, also M
n	Constant or index
n	Impeller speed, RPS
n	Order of reaction
N_{av}	Avogadro's number
NBOD	Endoglucanase blank optical density
n_p	Total number of particles
N_{Re}	Reynolds number
N_{sc}	Schmidt number
O.D.	Optical density
p	Dry solid, g
p	Power input to STR
PCARB	Total soluble carbohydrate, mg/ml
pd	Pore diameter
PEG	Polyethylene glycol
pK	- log Km
PLK	PCARB dilution factor
pS	- log (substrate concentration)
PSOD	PCARB optical density
PTFRC	Enzyme concentration determined from protein
PTOD	Lowry protein optical density

q	Water associated with p, g
r	Radius
R	Gas constant
R_o	Stokes law radius of solute particle (also R_e)
[S]	Substrate concentration
S'	Pore shape factor
STR	Stirred tank reactor
t	Time
t	Number of adsorbable segments in a polymer chain
T	Temperature
T.v.	Trichoderma viride
TCARB	Glucose and cellobiose concentration, mg/ml
TCK	TCARB dilution factor
TCOD	TCARB optical density
u	Velocity of particle
v	Initial velocity of enzyme reaction
V	Maximum velocity of reaction
V	Volume
v_h	Volume of solvated protein
v_s	Specific volume of solvent
<v>	Number of anchor segments adsorbed on surface per chain
V_b	Total volume of liquid accessible to solute
$\bar{V}_i$	Partial mole volume of component i
v_p	Volume of a molecule or particle
V_p*	Pore folume of a unit weight of solute

$\bar{w}$ Width of pore, Å

W Initial weight of liquid

X_i Mole fraction of component i

Greek Symbols

α Constant

γ Activity coefficient

γ Number of anchor segments per polymer chain

δ Inaccessible water ml/g cellulose

Δ_s Total δ_s

ε_p Porosity

η Intrinsic viscosity

θ Fraction of maximum adsorption

θ Effective surface concentration of enzyme, g enzyme/g cellulose

θ_{opt} θ corresponding to C_{opt}

θ_{sat} Maximum θ corresponding to saturation

μ Viscosity

μ_i Chemical potential of component

ν Same as <v>

ρ Density

ρ_i Exponential effect of C_o

σ Exponential effect of [E]

σ Relative substrate concentration

σ_s Solvation parameter

τ_p Tortuosity factor

ϕ Relative reaction velocity

APPENDIX L

LITERATURE CITATIONS

1. Ables, F. B., "Abscission: Role of Cellulose," Plant Physiol., 44, 447 (1969).

2. Ackerman, E., "Biophysical Science," p. 415, Prentice Hall, Englewood, New Jersey (1962).

3. Aggerbrandt, L. C. and L. J. Samuelson, "Penetration of Water Soluble Polymers into Cellulose Fibers," J. Appl. Polymer Sci., 8, 2801 (1964).

4. Alberty, R. A. and G. G. Hammer, "Application of the Theory of Diffusion-Controlled Reactions to Enzyme Kinetics," J. Phys. Chem., 62, 154 (1958).

5. Alexander, J. K., "Characterization of Cellobiose Phosphorylation," J. Bacteriol., 81, 903 (1961).

6. Almin, K. E. and K. E. Eriksson, "Influence of Carboxymethylcellulose Properties on the Determination of Cellulose Activity in Absolute Terms," Biochem. Biophys. Acta, 139, 238 (1967).

7. Almin, K. E., K. E. Eriksson, and C. Jansson, "Enzyme Degradation of Polymers II: Viscometric Determination of Cellulase Activity in Absolute Terms," Biochem. Biophys. Acta, 139, 248 (1967).

8. Antonini, E. and M. Brunori, "Hemoglobin and Myoglobin in Their Reactions with Ligands," pp. 98-101, American Elsevier Publishing Co., New York (1971).

9. Balls, A. K. and S. J. Schwimmer, "Digestion of Raw Starch," J. Biol Chem., 156, 203 (1944).

10. Battista, O. A., S. Coppick, J. A. Howsman, F. F. Morehead, and W. A. Sisson, "Level-off Degree of Polymerization - Relation to Polyphase Structure of Cellulose Fibers," Ind. and Eng. Chem., 48, 333 (1956).

11. Battista, O. A. and P. A. Smith, "Level Degree of Polymerization Cellulose Products," U.S. Patent 2,978,446 (1961).

12. -----, "Beta Glucosidase (Almond)," in "Worthington

Enzyme Manual - Enzymes, Enzyme Reagents, Related Biochemicals," p. 104, Worthington Biochemical Corporation, Freehold, New Jersey (1972).

13. Bhattacharjee, S. S. and A. S. Perlin, "Enzymatic Degradation of Carboxymethylcellulose and Other Cellulose Derivatives," in "Proceedings of the Seventh Cellulose Conference," loc. cit., p. 509 (1971).

14. Bird, R. B., W. E. Stewart, and E. N. Lightfoot, "Transport Phenomena," pp. 542-547, John Wiley and Sons, New York (1963).

15. Blatt, W. F., "Membrane Partition Chromatography: A Tool for Fractionation of Protein Mixtures," Agric. and Food Chem., 19, 589 (1971).

16. Blatt, W. F., S. M. Robinson, and H. J. Bixler, "Membrane Ultrafiltration: The Diafiltration Technique and Its Application to Microsolute Exchange and Binding Phenomena," Analy. Biochem., 26, 151 (1968).

17. Bowski, L., R. Saini, D. Y. Ryu, and W. R. Vieth, "Kinetic Modelling of the Hydrolysis of Sucrose by Invertase," Department of Chemical Engineering, Rutgers University, The State University of New Jersey, New Brunswick, New Jersey (1971).

18. Brew, K., T. C. Vanaman, and R. L. Hill, "Role of α-Lactalbumin and the A Protein in Lactose Synthetase -- Unique Mechanism for the Control of a Biological Reaction," Proc. Natl. Acad. Sci., 59, 491 (1968).

19. Brian, P. L. T. and H. B. Hales, "Transport of Heat and Mass Between Liquids and Spherical Particles in an Agitated Tank," A.I.Ch.E.J., 15, 727 (1969).

20. Britton, R. A., "A Study of the Reaction of Ethyleneimine with Cellulose," Ph.D. thesis, Massachusetts Institute of Technology, Cambridge, Massachusetts (1967).

21. Bucht, B. and K. E. Eriksson, "Extracellular Enzyme System Used by the Rot Fungus, Steseum sanguinolentum, for the Breakdown of Cellulose," Arch. Biochem. Biophys., 124, 135 (1968).

22. Burrous, S. E. and W. A. Wood, "Enzyme Distribution in Membrane, Cytoplasm, and Nuclear Fractions of Pseudomonas fluorescens," J. Bacteriol., 84, 364 (1962)

23. Callihan, C. D., "How Engineers are Putting Microbes to Work," Chem. Eng., 77, 160 (1970).

24. Callihan, C. D., V. R. Srinivason, S. P. Yang, R. W. Pike, W. F. McKnight, C. E. Dunlap, and Y. W. Han, "Single Cell Protein and Cellulosic Wastes," Proposal, Louisiana State University, Baton Rouge, Louisiana (1970).

25. Cayle, T., "Action of a Microbial Cellulase Complex," U.S. Patent 3,075,886 (1963).

26. -----, "Cellulase (Trichoderma viride)," in "Worthington Enzyme Manual - Enzymes, Enzyme Reagents, Related Biochemicals, p. 96, Worthington Biochemical Corporation, Freehold, New Jersey (1972).

27. -----, "Cellulases and Their Applications," G. J. Hajny and E. T. Reese, ed., Advances in Chemistry Series No. 95, American Chemical Society, Washington (1969).

28. Chang, M., "Folding Chain Model and Annealing of Cellulose," in "Proceedings of the Seventh Cellulose Conference," loc. cit., p. 343-362.

29. Chitumbo, K. and W. Brown, "The Separation of Oligosaccharides on Cellulose Gels," in "Proceedings of the Seventh Cellulose Conference," loc. cit., pp. 279-292.

30. -----, "Cleaning our Environment: The Chemical Basis for Action," p. 163, Committee on Public Affairs, Subcommittee on Environment, American Chemical Society, Washington (1969).

31. Cole, F. E. and K. W. King, "Site of Hydrolysis of Cellulodextrins and Reduced Cellulodextrins by Purified Cellulase Components," Biochem. Biophys. Acta, 81, 122 (1964).

32. Collins, F. C. and G. E. Kimbell, "Diffusion-Controlled Reaction Rates," J. Colloid. Sci., 4, 1425 (1949).

33. Colton, C. K., "Permeability and Transport Studies in Batch and Flow Dialyzers with Applications to Hemodialysis," Ph.D. thesis, Massachusetts Institute of Technology, Cambridge, Massachysetts (1969).

34. Colton, C. K., K. A. Smith, E. W. Merrill, and P. C.

Farrell, "Permeability Studies with Cellulosic Membranes," J. Biomed. Mater Res., 5, 459 (1971).

35. Colvin. J. R., "The Size and Shape of Lysozyme," Can. J. Chem., 30, 831-834 (1952).

36. Côté, W. A., Jr., ed., "Cellular Ultrastructure of Woody Plants," p. 603, Syracuse University Press, Syracuse, New York (1961).

37. Cowling, E. B., U.S. Dept. Agr. Tech. Bull. No. 1258, p. 79 (1961).

38. Cowling, E. B. and W. Brown, "Structural Features of Cellulosic Materials in Relation to Enzymatic Hydrolysis," in "Cellulases and Their Applications," loc. cit., pp. 152-187.

39. Ibid., p. 184

40. Cowling, E. B. and A. J. Stamm, "An Approach to the Measurement of Solid-Solution Structures in Wood and Other Cellulosic Materials," in "Proceedings of the Fourth Cellulose Conference," loc. cit., pp. 243-252.

41. Crank, J., "The Mathematics of Diffusion," The Clarendon Press, Oxford, England (1964).

42. Dean, G. R. and J. B. Gottfried, "The Commercial Production of Crystalline Dextrose," in "Advances in Carbohydrate Chemistry," C. S. Hudson and S. M. Cantor, ed., Vol. 5, pp. 127-143, Academic Press, Inc., New York (1950).

43. Determan, H., "Gel Chromatography," Springer-Verlag, New York (1969).

44. Dixon, M. and E. C. Webb, "Enzymes," pp. 54-166, Academic Press, Inc., New York (1964).

45. Dubois, M., K. A. Gilles, J. K. Hamilton, P. A. Rebers, and F. Smith, Anal. Chem., 28, 350 (1956).

46. DuPont, I., "Cellulase Degradation of Cellulose," B.S. thesis, Massachusetts Institute of Technology, Cambridge, Massachusetts (1971).

47. -----, "Enzymatic Hydrolysis of Cellulose and Related Materials (Advances in)," E. T. Reese, ed., Pergamon Press, London (1963).

48. Eriksson, K. E., "New Methods for the Investigations

of Cellulose," in "Cellulases and Their Applications," loc. cit., pp. 83-104.

49. Etheridge, D. E. and M. Jubbes, "Basis for Selection of Heartwood Fungi in Balsam Fir," Can. J. of Bot., 35, 615 (1957).

50. Fagan, R. D., H. E. Crethlein, A. Converse, and A. Porteous, "Kinetics of the Acid Hydrolysis of Cellulose Found in Paper Refuse," Environmental Science and Tech., 5, 545 (1971).

51. Fengel, D., "Ideas on the Ultrastructure Organization of Cell Wall Components, in "Proceedings of the Seventh Cellulose Conference," op. cit., pp. 383-392.

52. Flodin, P. E., B. Gelotte, and J. Porath, "Concentrating Solutes of High Molecular Weight," Nature, 188, 493 (1961).

53. Flora, R. M., "The Enzymatic Solubilization of Crystalline Cellulose," Ph.D. thesis, Virginia Polytechnic Institute, Blacksburg, Virginia (1965).

54. Forss, K. and K. E. Fremer, "Repeating Unit in Spruce Lignin," Paperi Puu., 47, 443 (1965).

55. Forss, K., K. E. Fremer, and B. Stendlund, "Spruce Lignin and Its Reactions in Sulfite Cooking: I. Structure of Lignin," Tappi, 47, 485 (1967).

56. Forziati, F. H., J. W. Rowen, and E. K. Plyler, "Spectrophotometric Determination of Carboxyl in Cellulose," J. Research Natl. Bur. Std., 46, 288 (1951).

57. Freudenberg, K., "Lignin. Its Constitution and Formation From ρ-Hydroxycinnamyl Alcohols," Science, 148, 595 (1965).

58. Freudenberg, K. and J. M. Harkin, "Supplement to the Constitutional Scheme for Spruce Lignin," Chem. Ber., 93, 2814 (1960).

59. Freundlich, H., "Colloid and Capillary Chemistry," Methuen, London (1926).

60. Frisch, H. L., "Polymer Chain Configuration Near a Boundary Exerting Forces," J. Phys. Chem., 59, 633 (1954).

61. Frisch, H. L., M. Y. Hellman, and J. L. Lundberg, "Ad-

sorption of Polymers: Polystyrene on Carbon," J. Polymer Sci., 38, 441 (1959).

62. Frisch, H. L. and R. Simha, "The Adsorption of Flexible Macromolecules," J. Phys. Chem., 58, 507 (1956).

63. Frisch, H. L. and R. Simha, "Monolayers of Linear Macromolecules," J. Chem. Phys., 24, 652 (1956).

64. Frisch, H. L. and R. Simha, "Statistical Mechanics of Flexible High Polymers at Surfaces," J. Chem. Phys., 27, 702 (1957).

65. Frisch, H. L., R. Simha, and F. R. Eirich, "Statistical Mechanics of Polymer Adsorption," J. Chem. Phys., 21, 365 (1953).

66. Fuwa, H. J., "Microdetermination of Amylase Activity Using Amylose as the Substrate," J. Biochem. (Japan), 41, 583 (1954).

67. Galambos, J. T., "The Reaction of Carbazol with Carbohydrates: 1. Effect of Borate and Sulfamate on the Carbazole Color of Sugars," Anal. Biochem., 19, 119-132 (1967).

68. Gardner, K. H. and J. Blackwell, "The Substructure of Crystalline Cellulose and Chitin Microfibrils," in "Proceedings of the Seventh Cellulose Conference," loc. cit., pp. 327-340.

69. Gascoigne, J. A. and M. M. Gascoign, "Biological Degradation of Cellulose," Butterworths, London (1961).

70. Ibid., p. 14.

71. Ibid., p. 52.

72. Ibid., p. 181.

73. Ghose, T. K., "Continuous Enzymatic Saccharification of Cellulose with Culture Filtrates of Trichoderma viride QM6a," Biotech. Bioeng., 11, 239 (1969).

74. Ghose, T. K. and J. A. Kostick, "A Model for Continuous Enzymatic Saccharification of Cellulose with Simultaneous Removal of Glucose Syrup," ACS Symposium on Industrial Microbial Enzymes, American Chemical Society, New York (1969).

75. Ghose, T. K. and J. A. Kostick, "Enzymatic Saccharifi-

cation of Cellulose in Semi- and Continuously-Agitated Systems," in "Cellulases and Their Applications," loc. cit., pp. 415-446.

76. Gibson, Q. H., B. E. P. Swoboda, and V. Massey, "Kinetics and Mechanism of Action of Blucose Oxidase," J. Biol. Chem., 239, 3927 (1964).

77. Gilliland, E. R. and E. B. Gutoff, "Rubber-Filler Interactions: Solution Adsorption Studies," J. Appli. Polymer Sci., 3, 26 (1960).

78. -----, "Glucostat," in "Worthington Enzyme Manual - Enzymes, Enzyme Reagents, Related Biochemicals," p. 181, Worthington Biochemical Corporation, Freehold, New Jersey (1972).

79. Granath, K. A. and T. C. Laurent, "Fractionation of Dextran and Ficoll by Chromatography on Sephadex G-200," J. Chromatog., 28, 69 (1967).

80. Gregg, S. J. and K. S. W. Sing, "Adsorption, Surface Areas and Porosity," Academic Press, New York (1967).

81. Grotte, G., "Passage of Dextran Molecules of Various Sizes from Blood to Lymph," Acta Chir. Scand. Suppl., 211, 1 (1956).

82. Guardia, E. J. and G. J. Haas, "Influence of Water Binders on the Activity and Thermal Inactivity of Lipase," J. Agr. Food Chem., 15, 412 (1967).

83. Halliwell, G., "Measurement of Cellulase and Factors Affecting Its Activity," in "Enzymatic Hydrolysis of Cellulose and Related Materials," loc. cit., pp. 71-92.

84. Halliwell, G., "Solubilization of Native and Derived Forms of Cellulose by Cell-free Microbial Enzymes," Biochem. J., 100, 315 (1966).

85. Hamby, D. S., "The American Cotton Handbook," Interscience Publishers, Inc., New York (1945).

86. Hammerstrom, R. A., K. D. Clause, J. W. Coghlan, and R. H. McBee, "Constitutive Nature of Bacterial Cellulases," Arch. Biochem. Biophys., 56, 123 (1956).

87. Hearon, W. M., "Cellulose as a Chemical Raw Material," in "Proceedings of the Fourth Cellulose Conference, loc. cit., pp. 277-278.

88. Henri, V. C. R., Acad. Sci. Paris, 135, 916 (1902).

89. Henry, D. C., "Kinetic Theory of Adsorption," Phil. Mag., 44, 689 (1922).

90. Hicks, J. S. and J. Wei, J. Assoc. Computing Machinery, 14, 549 (1967).

91. Higuchi, W. I. and T. Higuchi, "Theoretical Analysis for Diffusional Movement Through Heterogeneous Barriers," J. Phys. Chem., 65, 487 (1961).

92. Hoeve, C. A. J., "Adsorption Isotherms for Polymer Chains Adsorbed from θ Solvents," J. Chem. Phys., 44, 1505 (1966).

93. Hoeve, C. A. J., "Density Distribution of Polymer Segments in the Vicinity of an Adsorbing Interface," J. Chem. Phys., 43, 3007 (1965).

94. Hoeve, C. A. J., E. A. DiMarzio, and P. Peyser, "Adsorption of Polymer Molecules at Low Surface Coverage," J. Chem. Phys., 42, 2558 (1965).

95. Honeyman, J., "Recent Advances in the Chemistry of Cellulose and Starch," p. 469, Interscience Publishers, Inc., New York (1959).

96. Horton, J. C. and N. T. Keen, "Regulation of Induced Cellulase Synthesis in Pyrenochaeta terrestris by Utilizable Carbon Compounds," Can. J. Microbiol., 12, 209 (1966).

97. Hulcher, F. H. and K. W. King, "Disaccharide Preference of an Aerobic Cellulolytic Bacterium Cellvibrio gilvus," J. Bacteriol., 76, 565 (1958).

98. Hungate, R. E., "Cellulose (III) Culture and Isolation of Cellulose-Decomposing Bacteria from the Rumen of Cattle," Bacteriol. Rev., 14, 1 (1950).

99. Itzhaki, R. F. and D. M. Gill, "A Micro-Biuret Method for Estimating Proteins," Analyt. Biochem., 9, 401 (1964).

100. Iwasaki, T., K. Hayashi, and M. Funatsu, "Biochemical Studies on Cellulase (I) Purification and Characterization of Two Types of Cellulase from Trichoderma koningii," J. Biochem. Tokyo, 55, 209 (1947).

101. Katz, M. and E. T. Reese, "Production of Glucose by Enzymatic Hydrolysis of Cellulose," Applied

Microbiology, 16, 419 (1968).

102. Killander, J., "Separation of Human Heme- and Hemoglobin-Binding Plasma Proteins Ceruloplasm and Albumin by Gel Filtration," Biochim. Biophys. Acta, 93, 1 (1964).

103. King, K. W., in "Advances in Enzymatic Hydrolysis of Cellulose and Related Materials," loc. cit., p. 159.

104. King, K. W., "Endwise Degradation of Cellulose," Virginia Agri. Esp. Sta. Tech. Bull., (Blacksburg, Virginia), 154, 1 (1964).

105. King, K. W., "Enzymatic Degradation of Crystalline Cellulose," J. Fermentation Tech. (Japan), 43, 79 (1965).

106. King, K. W., "Enzymatic Degradation of Crystalline Hydrocellulose," Biochem. Biophys. Res. Comm., 24, 295 (1966).

107. King, K. W. and R. M. Simbert, "Distinctive Properties of β-Glucosidases and Related Enzymes Derrived from a Common Aspergillus niger Cellulase," Appl. Microbiol., 11, 315 (1963).

108. King, K. W. and M. I. Vessal, "Enzymes of the Cellulase Complex," in "Cellulases and Their Applications," loc. cit., pp. 7-25.

109. Ibid., p. 23.

110. Kipling, J. J., "Adsorption from Solutions of Non-Electrolytes," Academic Press, New York (1965).

111. Ibid., p. 26.

112. Ibid., pp. 149-151.

113. Kipling, J. J. and D. A. Tester, "Adsorption from Binary Mixtures Determination of Individual Adsorption Isotherms," J. Chem. Soc., 4123, (1952).

114. Kiselev, N. A., C. L. Shpitzberg, and B. K. Vainstein, "Crystallization of Catalase in the Form of Tubes with Molecular Walls," J. Mol. Biol., 25, 433-441 (1967).

115. Klein, E. and K. Bosarge, "Optical Dispersion and Birefringence of High Tenacity Cellulose Fibers," in "Proceedings of the Fourth Cellulose Confer-

ence," loc. cit., pp. 515-526.

116. Klinkenberg, A., "Isotherms for Preferential Adsorption from Binary Liquid Mixtures Based on Langmuir Equation," Rec. Trav. Chim., 78, 83 (1959).

117. Klop, W. and P. Kooiman, "Action of Cellulolytic Enzymes on Substituted Celluloses," Biochem. Biophys. Acta, 99, 102 (1965).

118. Kozinski, A. A. and E. N. Lightfoot, "Ultrafiltration of Proteins in Stagnation Flow," A.I.Ch.E.J., 17, 81 (1971).

119. Krupnova, A. V. and V. T. Sharkov, "Converting Cellulose to Readily Hydrozable State by Thermomechanical Methods," Gidrolizn. Lesukhim. Prom., U.S.S.R., 16, 8 (1963).

120. Krupnova, A. V. and V. T. Sharkov, "Mechanothermal Degradation of Cellulosic Material into a Readily Hydrolyzable State," Gidrolizn. Lesukhim. Prom., U.S.S.R., 7, 3 (1964).

121. Lamm, O. and A. Polson, "The Determination of Diffusion Constants of Proteins by a Refractometric Method," Biochim. J., 30, 528-541 (1936).

122. Langmuir, I., "The Adsorption of Gases on Plane Surfaces of Glass, Mica, and Platinum," J. Am. Chem. Soc., 40, 1361 (1918).

123. Lauer, O., "Grain Size Measurements on Commercial Powders - A Guide for Experts," issued by Alpine AG Augsburg, Mayer-Druck, Augsburg, Giggenbachstrasse 2 (1966).

124. Laurent, T. C. and J. Killander, "Theory of Gel-Filtration and Its Verification," J. Chromatog., 14, 317 (1964).

125. Lee, G. F., Jr., "Physical Factors Affecting Enzymatic Hydrolysis of Cellulose," M. S. theses, State University College of Forestry at Syracuse University, Syracuse, New York (1966).

126. Lellek, B. Personal Communication, Dow Chemical Corporation, Midland, Michigan (June 1, 1972).

127. Leopold, B. and J. S. Fujii, "Degradation by Mechanical Action as a Means of Studying Cellulose-Water Interaction," in "Proceedings of the Fifth Cellulose Conference," loc. cit., pp. 149-160.

128. Li, L. H., R. M. Flora, and K. W. King, "Individual Roles of Cellulase Components Derived from Trichoderma viride," Arch. Biochem. Biophys., 111, 439 (1965).

129. Li, L. H. and K. W. King, "Fractionation of β-Glucosidases and Related Extracellular Enzymes from Aspergillus niger," Appl. Microbiol., 11, 320 (1963).

130. Liang, L. Y. and R. H. Marchessault, "Infrared Spectra of Crystalline Poly-saccharides: I Hydrogen Bonds in Native Cellulose," J. Polymer Sci., 37, 385 (1959).

131. Lifson, S., "Partition Functions of Linear-Chain Molecules," J. Chem. Physics, 40, 3705 (1964).

132. Lifson, S., "Theory of the Helix-Coil Transition in DNA Considered as a Copolymer," Biopolymers, 1, 25 (1963).

133. Lifson, S. and B. H. Zimm, "Simplified Theory of the Helix-Coil Transition in DNA Based on a Grand Partition Function," Biopolymers, 1, 15 (1963).

134. Lineweaver, H. and D. Burk, "Determination of Enzyme Dissociation Constants," J. Amer. Chem. Soc., 56, 658 (1934).

135. Liu, D. L. and C. C. Walden, "A Spectrophotometric Assay for Cellobiose," Anal. Biochem., 31, 211 (1969).

136. Liu, T. H. and K. W. King, "Fragmentation During Enzymatic Degradation of Cellulose," Arch. Biochem. Biophys., 120, 462 (1967).

137. Loeb, G. and H. Scheraga, "Hydrodynamic and Thermodynamic Properties of Bovine Serum Albumin at Low pH," J. Phys. Chem., 60, 1633-1634 (1956).

138. Longsworth, L. G., "Diffusion Measurements of Aqueous Solutions of Amino Acids, Peptides, and Sugars," J. Amer. Chem. Soc., 74, 4155 (1952).

139. Lowry, O. H., N. J. Rosebrough, A. L. Farr, and R. J. Randall, "Protein Measurements with the Folin Phenol Reagent," J. Biol. Chem., 193, 265 (1951).

140. Mackor, E. L. and J. H. Van der Waals, "The Statistics of the Adsorption of Rod Shaped Molecules in Connection with the Stability of Certain Colloidal

Dispersions," J. Colloid Sci., 7, 535 (1952).

141. Mandels, M. and T. K. Ghose, "Enzymatically Hydrolyzed Cellulose as a Substrate for Single Cell Protein," Colloquium on Microbial Protein Production X, International Congress for Microbiology, Mexico City, Mexico (1970).

142. Mandels, M.,J. Kostick, and R. Parizek, "The Use of Adsorbed Cellulase in the Continuous Conversion of Cellulose to Glucose," unpublished paper, U.S. Army Natick Laboratories, Natick, Massachusetts (1971).

143. Mandels, M., F. W. Parrish, and E. T. Reese, "Sophorose as an Inducer of Cellulase in Trichoderma viride," J. Bacteriol., 83, 400 (1962).

144. Mandels, M. and E. T. Reese, "Fungal Cellulases and the Microbial Decomposition of Cellulosic Fabric," Develop. Ind. Microbiol., 5, 5 (1964).

145. Mandels, M. and E. T. Reese, "Induction of Cellulase in Fungi by Cellobiose," J. Bacteriol., 79, 816 (1960).

146. Mandels, M. and E. T. Reese, "Induction of Cellulase in Trichoderma viride as Influenced by Carbon Sources and Metals," J. Bact., 72, 269 (1957).

147. Mandels, M. and E. T. Reese, "Inhibition of Cellulases and β-Glucosidases," in "Advances in Enzymatic Hydrolysis of Cellulose and Related Materials," loc. cit., pp. 115-157.

148. Mandels, M. and J. Weber, "The Production of Cellulases," in "Cellulases and Their Applications," loc. cit., pp. 391-414.

149. Mandels, M., J. Weber, and R. Parizek, "Enhanced Cellulase Production by a Mutant of Trichoderma viride," Appl. Microbiol., 21, 152 (1971).

150. Marechal, L. R., "Isolation and Some Properties of a β-1-3 Oligoglucan Phosphorylase," Biochem. Biophys. Acta, 146, 417 (1967).

151. Mayer, A. M. and Y. Shain, "Activation of Enzymes During Germination. Amylopectin-1,6-Glucosidase in Peas," Science, 162, 1283 (1968).

152. McBurney, L. F., "The Degradation of Cellulose," Ott and Spurlin, loc. cit., pp. 99-196.

153. Ibid., p. 195.

154. McCabe, W. L. and J. C. Smith, "Agitation and Mixing of Liquids," in "Unit Operations of Chemical Engineering," pp. 241-278, McGraw Hill, New York (1967).

155. McLaren, A. D., in "Cell Interface Reactions," H. D. Brown, ed., p. 1, Scholar's Library, New York (1963).

156. McLaren, A. D., "Enzyme Reactions in Structurally Restricted Systems. IV The Digestion of Insoluble Substrates by Hydrolytic Enzymes," Enzymologia, 26, 237 (1963).

157. McLaren, A. D., "Enzyme Reactions in Structurally Restricted Systems. III Yeast β-Fructofuranosidase Activity in Concentrated Sucrose Solutions," Enzymologia, 26, 1 (1963).

158. McLaren, A. D., "Mole Fractions in Enzyme Kinetics," Arch. Biochem. Biophys., 97, 1 (1962).

159. McLaren, A. D. and K. L. Babcock, "Characteristics of Enzyme Reactions at Surfaces," in "Subcellular Particles," T. Hayashi, ed., p. 23, Roland Press, New York (1959).

160. McLaren, A. D. and E. F. Eastman, "Adsorption and Reaction of Enzymes and Proteins on Kaolinite (III) Isolation of Enzyme-Substrate Complexes," Arch. Biochem. Biophys., 61, 158 (1956).

161. McLaren, A. D. and G. H. Peterson, "Montmorillonite as a Caliper for the Size of Protein Molecules," in "Soil Nitrogen," W. V. Bartholomew and F. E. Clark, ed., p. 259, American Society of Agromony, Inc., Madison, Wisconsin (1965).

162. Meier, H., "Cell Walls and the Distribution of the Constituents Across the Walls," Zimmerman, loc. cit., p. 139.

163. -----, "Methods in Carbohydrate Chemistry," Vol. III, R. L. Whistler, ed., Academic Press, New York (1963).

164. Miller, G. L., "Use of Dinitrosalicylic Acid Reagent for Determination of Reducing Sugar," Anal. Chem., 31, 426 (1959).

165. Miller, G. L., R. Slater, R. Birzgalis, and R. Blum,

"Application of Different Colorimetric Tests to Cellodextrins," Anal. Biochem., 2, 521 (1961).

166. Mitchel, P., "Translocation Through Natural Membranes," Advances in Enzymology, 29, 33 (1967).

167. Muhlethaler, K., "Fine Structure of Natural Polysaccharide Systems," in "Proceedings of the Sixth Cellulose Conference," loc. cit., pp. 305-315.

168. Nelson, M. L. and R. T. O'Connor, "A New Infrared Ratio for Estimation of Crystallinity in Cellulose I and II," J. Appl. Polymer Sci., 8, 1325 (1964).

169. Nelson, R. and D. W. Oliver, "Study of Cellulose Structure and Its Relation to Reactivity," in "Proceedings of the Seventh Cellulose Conference," loc. cit., pp. 305-320.

170. Nickerson, R. F., "The Relative Crystallinity of Celluloses," in "Advances in Carbohydrate Chemistry," Vol. 5, C. S. Hudson and S. M. Cantor, ed., pp. 103-126, Academic Press Inc., New York (1950).

171. Niwa, T., S. Inouye, T. Tsurouka, Y. Koaze, and T. Niida, "Nojirimycin as a Potent Inhibitor of Glucosidase," Agr. Biol. Chem., 34, 966 (1970).

172. Norkans, B., "Growth and Cellulolytic Enzymes of Tricholoma," Symbolae Botanicae, Uppsala, Sweden, 11, 126 (1950).

173. Norman, A. G., "Noncellulosic Carbohydrates," in Ott and Spurlin, loc. cit., pp. 459-480.

174. Ibid., p. 461.

175. Okada, G., K. Nisizawa, and H. Suzuki, "Cellulase Components from Trichoderma viride," J. Biochem., 63, 591 (1968).

176. Oshima, M., "Wood Chemistry - Process Engineering Aspects," Nores Development Corp., Pearl River, New York (1965).

177. Ott, E., H. M. Spurlin, and M. W. Grafflin, "Cellulose and Cellulose Derivatives," in "High Polymers," Vol. 5, 2nd ed., Interscience Publishers, Inc., New York (1954).

178. Pazur, J. H. and K. Kleppe, "The Oxidation of Glucose and Related Compounds by Glusoce Oxidase from

Aspergillus niger," *Biochem.*, *3*, 578 (1964).

179. Pearl, I. A., "The Chemistry of Lignin," p. 3, Marcel Dekker, Inc., New York (1967).

180. Peterson, C. and T. K. Kwei, "The Kinetics of Polymer Adsorption Onto Solid Surfaces," *J. Phys. Chem.*, *65*, 1330 (1961).

181. Pigden, W. J. and D. P. Heaney, "Lignocellulose in Ruminant Nutrition," in "Cellulases and Their Applications," *loc. cit.*, pp. 245-261.

182. Pitcher, W. H., Jr., "Restricted Diffusion in Liquids within Fine Pores," Sc.D. thesis, Massachusetts Institute of Technology, Cambridge, Massachusetts (1972).

183. -----, "Proceedings of the Fifth Cellulose Conference," T. E. Timell, ed., *Journal of Polymer Sci.: Part C*, No. 11, Interscience Publishers, Inc., New York (1965).

184. -----, "Proceedings of the Fourth Cellulose Conference," R. H. Marchessault, ed., *Journal of Polymer Sci.: Part C*, No. 2, Interscience Publishers, Inc., New York (1963).

185. -----, "Proceedings of the Seventh Cellulose Conference," E. C. Jahn, ed., *Journal of Polymer Sci.: Part C*, No. 36, Interscience Publishers, Inc., New York (1971).

186. -----, "Proceedings of the Sixth Cellulose Conference," R. H. Marchessault, ed., *Journal of Polymer Sci.: Part C*, No. 28, Interscience Publishers, Inc., New York (1969).

187. Ragnarsson, J. O., "The Solubilization of Fish Protein Concentrate," M.S. thesis, Massachusetts Institute of Technology, Cambridge, Massachusetts (1971).

188. Ranby, B. G., "Fine Structure of Cellulose Fibrils," *Das Papier*, *18*, 593 (1964).

189. Ranby, B. G., "Recent Progress on the Structure and Morphology of Cellulose," in "Cellulases and Their Applications," *loc. cit.*, 139-148.

190. Rautela, G. S., Ph.D. thesis, Virginia Polytechnic Institute, Blacksburg, Virginia, p. 108 (1967).

191. Rautela, G. S. and K. W. King, "Significance of the

Crystal Structure of Cellulose in the Production and Action of Cellulase," Arch. Biochem. Biophys., 123, 589 (1968).

192. Reese, E. T., "Biological Degradation of Cellulose Derrivatives," Ind. Eng. Chem., 49, 89 (1957).

193. Reese, E. T., Personal Communication, U.S. Army Natick Laboratories, Natick, Massachusetts (September 22, 1971).

194. Reese, E. T. and A. Maguire, "Increase in Cellulase Yields by Addition of Surfactants to Cellobiose Cultures of Trichoderma viride," Developments in Industrial Microbiology, 12, 212-224 (1971).

195. Reese, E. T., A. Maguire, and F. W. Parrish, "Glucosidases and Exogludanases," Can. J. Biochem., 46, 25 (1968).

196. Reese, E. T. and M. Mandels, "Chemical Inhibition of Cellulases and β-Glucosidases," Research Report, Pioneering Research Division, Quartermaster Research and Development Center, Natick, Massachusetts, Microbiology Series No. 17.

197. Reese, E. T. and M. Mandels, "Enzymatic Hydrolysis of Cellulose and Its Derivatives," in "Methods of Carbohydrate Chemistry," R. L. Whistlar, ed., Academic Press, New York (1963).

198. Reese, E. T. and M. Mandels, "Marine Boring and Swelling Organisms," D. L. Ray, ed., p. 265, University of Washington Press, Seattle, Washington (1959).

199. Reese, E. T., L. Segal, and V. W. Tripp, "Effect of Cellulase on the Degree of Polymerization of Cellulose and Hydrocellulose," Text Res. J., 27, 626 (1957).

200. Rinaudo, M., F. Barnoud, and J. P. Merle, "Enzymatic Cegradation of Cellulosic Fibers," in "Proceedings of the Sixth Cellulose Conference," loc. cit., pp. 197-207.

201. Robert, L. and P. Samuel, "Mechanism of Elastolysis by Pancreatic Elastase," Experimentia, 13, 167 (1957).

202. Rollins, M. L. and V. W. Tripp, "Electron Microscopy of Cellulose and Cellulose Derivatives," in "Methods of Carbohydrate Chemistry," loc. cit.,

pp. 356-364.

203. Ross, L. W., "Perturbation of Diffusion-Coupled Biochemical Reaction Kinetics," paper 31D, 62nd Annual Meeting A.I.Ch.E., Washington, D. C. (1969).

204. Ross, L. W. and D. M. Updegraff, "Kinetics of Diffusion Coupled Fermentation Processes: The Conversion of Cellulose to Protein," Biotech. Bioeng., 13, 99 (1971).

205. Rowland, F., R. Bulas, E. Rothstein, and F. R. Elrich, "Structure of Macromolecules at Liquid-Solid Interfaces," in "Chemistry and Physics of Interfaces," American Chemical Society, Washington, D. C. (1965).

206. Rushton, J. H., E. W. Costich, and H. J. Everett, "Power Characteristics of Mixing Impellers," Chem. Eng. Prog., 43, 395 (1950).

207. Sarkaner, K. V. and C. H. Ludwig, ed., "Lignins: Occurance, Formation, Structure and Reactions," John Wiley and Sons, Inc., New York (1971).

208. Sarko, A. and R. H. Marchessault, "Supramolecular Structure of Polysaccharides," in "Proceedings of the Sixth Cellulose Conference," loc. cit., pp. 319-331.

209. Sato, S., "Enzymatic Maceration of Plant Tissue," Physiol. Plantorum, 21, 1067 (1968).

210. Satterfield, C. N., "MassTransfer in Heterogeneous Catalysis," M.I.T. Press, Cambridge, Massachusetts (1970).

211. Schafer, M. L. and K. W. King, "Utilization of Cellulose Oligosaccharides by Cellvibrio gilvus," J. Bacteriol., 89, 113 (1965).

212. Schurr, J. M. and A. D. McLaren, "Enzyme Action: Comparison on Soluble and Insoluble Substrate," Science, 152, 1064 (1966).

213. Schurr, J. M. and A. D. McLaren, "Kinetics of Trypsin Hydrolysis of Gelatin Spheres and the Structure of Both Free Solution and Gel-state Gelatin," Enzymologia, 29, 315 (1965).

214. Schwert, G. W., "The Molecular Size and Shape of the Pancreatic Proteases II. Chymotrypsinogen," J. Biol. Chem., 190, 799-806 (1951).

215. Seifter, S., D. Seymour, B. Novic, and E. Muntwyler, "The Estimation of Glycogen with the Anthrone Reagent," Arch. Biochem., 25, 191 (1950).

216. Selby, K., "The Purification and Properties of the C_1 Component of the Cellulase Complex," in "Cellulases and Their Applications," loc. cit., pp. 34-52.

217. Selby, K. and C. C. Maitland, "Cellulase of Trichoderma viride Separation of the Components Involved in the Solubilization of Cotton," Biochem. J., 104, 716 (1967).

218. Selby, K. and C. C. Maitland, "The Fractionation of Myrothecium verrucaria Cellulase by Gel Filtration," Biochem. J., 94, 578 (1965).

219. Selby, K., C. C. Maitland, and K. V. A. Thompson, "The Degradation of Cotton Cellulose by the Extracellular Cellulase of Myrothecium verrucaria," Biochem. J., 88, 288 (1963).

220. -----, "Sephadex - Gel Filtration in Theory and Practice," Pharmacia Fine Chemicals, Inc., Piscataway, New Jersey (1970).

221. Sheth, K. and J. K. Alexander, "Cellodextrin Phosphorylase from Clostridium thermocellum," Biochim. Biophys. Acta, 148, 808 (1967).

222. Silberberg, A., "Adsorption of Flexible Macromolecules III. Generalized Treatment of the Isolated Macromolecule - Effect of Self-Exclusion," J. Chem. Phys., 46, 1105 (1967).

223. Silberberg, A., "The Adsorption of Flexible Macromolecules," J. Phys. Chem., 66, 1872 (1962).

224. Simha, R., "Statistics of Flexible Molecules at Interfaces," J. Polymer Sci., 29, 3 (1958).

225. Simha, R., H. L. Frisch, and F. R. Eirich, "The Adsorption of Flexible Macromolecules," J. Phys. Chem., 57, 584 (1953).

226. Sinclair, P. M., "Enzymes Convert Starch to Dextrose," Chem. Eng., 72, 90-92 (1965).

227. Siu, R. G. H., "Microbial Decomposition of Cellulose," Reinhold, New York (1951).

228. Smiley, K. L., "Continuous Conversion of Starch to

Glucose with Immobilized Glucoamylase," A.S.C. Meeting, Chicago, Illinois (September 13-18, 1970).

229. Smith, J. K., W. J. Kitchen, and D. B. Mutton, "Structural Study of Cellulosic Fibers," in "Proceedings of the Fourth Cellulose Conference," loc. cit., pp. 499-513.

230. Smith, J. M., "Kinetics of Adsorption," in "Adsorption from Aqueous Solutions," Advances in Chemistry Series 79, W. J. Weber, Jr., E. Matijevic, ed., pp. 8-22, American Chemical Society, Washington, D. C. (1968).

231. Ibid., p. 9.

232. Somogyi, M., "Notes on Sugar Determination," J. Biol. Chem., 195, 19 (1952).

233. Sophianopoulos, A. J., C. K. Rhodes, D. N. Halcomb, and K. E. VanHolde, "Physical Studies of Lysozyme I. Characterization," J. Biol. Chem., 237, 1107-1111 (1962).

234. Sophianopoulos, A. J. and K. E. VanHolde, "Physical Studies of Muranidase (Lysozyme) II. pH-Dependent Dimerization," J. Biol. Chem., 239, 2516-2524 (1964).

235. Srinivasan, V. R. and Y. N. Han , "Utilization of Bagasse," in "Cellulases and Their Applications," loc. cit., pp. 447-460.

236. Statton, W. O., "The Meaning of Crystallinity When Judged by X-Rays," J. Polymer Sci. C., 18, 33 (1967).

237. Stone, F. W. and J. J. Stratta, "Ethylene Oxide Polymers," Encyclopedia of Polymer Science and Technology, 6, 103-145 (1967).

238. Stone, J. E. and A. M. Scallan, "Cell Wall Structure Studied by Nitrogen Adsorption," Pulp and Paper Mag. Can., 67, 263 (1966).

239. Stone, J. E. and A. M. Scallan, "Effect of Component Removal upon the Porous Structure of the Cell Wall of Wood," in "Proceedings of the Fifth Cellulose Conference," loc. cit., pp. 13-25.

240. Stone, J. E. and A. M. Scallan, "Effect of Component Removal upon the Porous Structure of the Cell

Walls of Wood II. Swelling in Water and the Fiber Saturation Point," Tappi, 50, 496 (1967).

241. Stone, J. E. and A. M. Scallan, "Effect of Component Removal upon the Porous Structure of the Cell Walls of Wood III. Comparison Between the Sulfite and Kraft Process," Pulp and Paper Mag. Can., 69, 288 (1968).

242. Stone, J. E., A. M. Scallan, E. Dönefer, and E. Ahlgren, "Digestibility as a Simple Function of a Molecule of Similar Size to a Cellulase Enzyme," in "Cellulases and Their Application," loc. cit., pp. 219-241.

243. Storvick, W. O., F. E. Cole, and K. W. King., "Mode of Action of a Cellulase Component from Cellvibrio gilvus," Biochem., 2, 1106 (1963).

244. Storvick, W. O. and K. W. King, "Complexity and Mode of Action of the Cellulase System of Cellvibrio gilvus," J. Biol. Chem., 235, 303 (1960).

245. Stratta, J. J., Personal Communication, Union Carbide Corp., Tarrytown, New York (May 30, 1972).

246. Sumi, Y., R. D. Hale, and B. G. Ranby, "Accessibility of Native Cellulose Microfibrils," Tappi, 46, 126 (1963).

247. Sumner, J. B. and N. Gralen, "The Molecular Weight of Crystalline Catalase," J. Biol. Chem., 125, 33-36 (1938).

248. Sumner, J. B., N. Gralen, I. Eriksson-Quensel, "The Molecular Weight of Urease," J. Biol. Chem., 125, 37-44 (1938).

249. Sumner, J. B. and G. F. Somers, "Laboratory Experiments in Biological Chemistry," Academic Press, Inc., New York (1944).

250. Swenson, H. A., C. A. Schmitt, and N. S. Thompson, "Comparison of the Configuration of β-1,4 Linked Hexosans and Wood Xylan Pentosans by Means of the Eizner-Ptitsyn Viscosity Equations," in "Proceedings of the Fifth Cellulose Conference," loc. cit., pp. 243-252.

251. Swisher, E. J., W. O. Storvick, and K. W. King, "Metabolic Non-equivalence of the Two Glucose Moieties of Cellobiose in Cellvibrio gilvus," J. Bacteriol., 88, 817 (1964).

252. Tanford, C., "Chemical Basis for Antibody Diversity and Specificity," Accounts Chem. Res., 1, 161 (1968).

253. Tanford, C., "Physical Chemistry of Macromolecules," John Wiley and Sons, New York (1967).

254. Tarkow, H., W. C. Feist, and C. F. Southerland, "Interaction of Wood with Polymeric Materials - Penetration Versus Molecular Size," Forest Prod. J., 16, 61 (1966).

255. Tarkow, H. and C. F. Southerland, "Interaction of Wood with Polymeric Materials I. Adsorbing Surfaces," Forest Prod. J., 14, 184 (1964).

256. Thoma, J. A. and D. E. Koshland, Jr., "Stereochemistry of Enzyme, Substrate, and Products During β-Amylase Action," J. Am. Chem. Soc., 82, 2511 (1960).

257. Thomas, D. K. and A. Charlesby, "Viscosity Relationship in Solutions of Polyethylene Glycols," J. Polymer Sci., 42, 195-202 (1960).

258. Toren, E. C., Jr., "Determination of Glucose - A Kinetics Experiment for the Analytical Course," Journal of Chemical Education, 44, 173 (1967).

259. Tusk, A. G. and G. Oster, "Determination of Enzyme Activity by a Linear Measurement," Nature, 190, 721 (1961).

260. Underkofler, L. A., "Development of a Commercial Enzyme Process: Glucoamylase," in "Cellulases and Their Applications," loc. cit., pp. 343-358.

261. Updegraff, D. M., "Utilization of Cellulose from Waste Paper," Biotech. Bioeng., 13, 77 (1971).

262. Vessal, M. I., Ph.D. thesis, Virginia Polytechnic Institute, Blacksburg, Virginia (1967).

263. Wagner, M. L. and H. A. Scheraga, "Gouy Diffusion Studies of Bovine Serum Albumin," J. Phys. Chem., 60, 1066-1076 (1956).

264. Walker, G. J. and P. N. Hope, "The Action of Some α-Amyloses on Starch Granules," Biochem. J., 86, 452 (1963).

265. Walseth, C. S., "Influence of the Fine Structure of Cellulose on the Action of Cellulases," Tappi,

35, 228-233 (1952).

266. Warwicker, J. O., R. Jeffries, R. L. Colbran, and R. N. Robinson, Shirley Institute Pamphlet No. 93, Cotton, Silk and Man-Made Fibers Research Association, Manchester (1966).

267. Weichselbaum, T. E., "Determination of Proteins in Small Amounts of Blood, Serum, and Plasma," Am. J. Clin. Pathol., 7, 40 (1946).

268. Weisz, P. B., "Sorption-Diffusion in Heterogeneous Systems, Part I - General Sorption Behavior and Criteria," Transactions of the Faraday Society, 63, 1801 (1967).

269. Weisz, P. B. and J. S. Hicks, "Sorption-Diffusion in Heterogeneous Systems, Part 2 - Quantitative Solutions for Uptake Rates," Transactions of the Faraday Society, 63, 1807 (1967).

270. Weisz, P. B. and H. Zollinger, "Sorption-Diffusion in Heterogeneous Systems, Part 3 - Experimental Models of Dye Sorption," Transactions of the Faraday Society, 63, 1815 (1967).

271. Weisz, P. B. and H. Zollinger, "Sorption-Diffusion in Heterogeneous Systems, Part 4 - Dyeing Rates in Organic Fibers," Transactions of the Faraday Society, 64, 1639 (1968).

272. Whitaker, D. R., J. R. Colvin, and W. H. Cook, "Molecular Weight and Shape of Myrothecium verrucaria Cellulase," Arch. Biochem. Biophys., 49, 247 (1954).

273. Wilson, E. J. and C. J. Geankoplis, "Liquid Mass Transfer at Very Low Reynolds Numbers in Packed Beds," Ind. Eng. Chem. Fundam., 5, 9 (1966).

274. Wood, T. M., "Cellulolytic Enzyme Systems of Thichoderma koningii. Separation of Components Attacking Native Cotton," Biochem. J., 109, 217 (1968).

275. Zimmerman, M. H., "The Formation of Wood in Forest Trees," Academic Press, New York (1964).

BIOGRAPHICAL NOTE

The author, Bingham H. Van Dyke, Jr., was born on December 16, 1944 in Pittsburgh, Pennsylvania, the first of three children. He attended elementary school and secondary schools in Greensburg and Allentown, Pennsylvania, Scarsdale, New York, and North Palm Beach, Florida.

The author was graduated from the University of Pennsylvania with a B.S. in Chemical Engineering in May, 1966. He then joined the M.W. Kellogg Co. in New York City as an analytical systems engineer. After field experience he was transferred to the Dallas, Texas office where he attained the position of Analytical Job Leader.

In September, 1969, the author entered the Massachusetts Institute of Technology where he was supported by a teaching assistantship and by industrial fellowships. At M.I.T. he authored the first Chemical Engineering Yearbook and was elected to the society of Sigma Xi.

The author married the former Janice Coate of Orlando, Florida, in June, 1967.

As of October, 1972, the author has accepted employment with Westvaco in Charleston, South Carolina.